MONTE CARLO INVESTIGATION OF TRANSIENT ACOUSTIC FIELDS IN PARTIALLY OR COMPLETELY BOUNDED MEDIUM

A Dissertation

Presented to

the Faculty of the School of Engineering and Applied Science

University of Virginia

In Partial Fulfillment

of the Requirements for the Degree

Doctor of Philosophy (Aerospace Engineering)

by

BALAKRISHNA DATTATRAYA THANEDAR

October 1972

MONTE CARLO INVESTIGATION OF TRANSIENT ACOUSTIC FIELDS IN PARTIALLY OR COMPLETELY BOUNDED MEDIUM

ABSTRACT

This dissertation presents a Monte Carlo technique for the determination of the transient radiation fields in partially or completely bounded media. The impetus for the selection of this topic is that the analysis of the radiation in a partially or completely bounded medium presents a problem of common interest in many branches of engineering and physics; yet, at present, no satisfactory method is available for its treatment in the general case.

In this dissertation a more general basic technique is developed with special emphasis on applications to acoustical field solutions. It investigates what happens to the field in terms of signal paths of disturbance

originating from the energy source, and based on the information so collected reconstructs the field as a function of space and time on a statistical basis. For this analysis a suitable model is created from which is developed an algorithm for the estimation of the acoustic pressure variations, as a function of space and time, in the region under investigation.

The validity of the technique and the algorithm thus created is demonstrated with the help of simple physical models, analyzed on the digital computer. The results obtained from the present work are compared with other available analytical data.

At present, the applicability of the proposed Monte Carlo technique is demonstrated when the medium is homogeneous and is enclosed by either rectangular or curved boundaries. Possible future developments are indicated which would, it is believed, make the Monte Carlo method a valuable tool when boundary conditions are complex or when the medium is inhomogeneous.

ACKNOWLEDGMENTS

The research work presented in this dissertation was partly supported by the NASA under Grants NGR 47-005-085, and NGR 47-005-108. Computations were made on the Burroughs 5500 and the CDC 6400 of the Computing Center of the University of Virginia, and were supported by University Computer grants.

My gratitude is expressed to Dr. John Kenneth Haviland, my adviser, for creating broad philosophy behind this dissertation, for a close supervision of the work and for the encouragement throughout the period. The help received from him in both academic and nonacademic matters calls for more profound thanks than could be presented in a formal acknowledgment. The rapid progress during the period has become possible only through some of the very lively and educating discussions with Dr. W. L. Harris, Sr. and Dr. J. E. Mann, Jr., Members of my advisory committee; special thanks are to them.

TABLE OF CONTENTS

TABLE OF CONTENTS (continued)

TABLE OF CONTENTS (continued)

TABLE OF CONTENTS (continued)

TABLE OF CONTENTS (continued)

TABLE OF CONTENTS (continued)

LIST OF TABLE

LIST OF FIGURES

LIST OF FIGURES (continued)

LIST OF FIGURES (continued)

LIST OF FIGURES (continued)

LIST OF FIGURES (continued)

LIST OF FIGURES (continued)

LIST OF FIGURES (continued)

LIST OF FIGURES (continued)

LIST OF SYMBOLS

A	amplitude function; duct radius
$A0^*$, $A1^*$	duct radius
A_M	expansion coefficient
$AREF^*$	reference radius
$ART0^*$	reference ray tube area
B0,B1,B2	side of a triangle
B3	semiperimeter of a triangle
D	function
D^2	variance
DC1,DC2, DC3	direction cosines
$\underline{DCI}$	direction vector of the incident ray

Notes: 1. The underscore (~) denotes the vectorial quantity.

2. The overhead dot ($\dot{}$) denotes the differentiation of the quantity with respect to time.

3. The overhead prime (') denotes the differentiation of the quantity with respect to the argument.

4. The overhead star (*) denotes the variable in the nondimensional form.

LIST OF SYMBOLS (continued)

DCN	direction vector of the inward normal to the boundary surface
DCR	direction vector of the reflected ray
DCTL	duct length
DPHI	elemental length
DPSI	elemental length
E	expected value
F	function
G	Green's function
H	unit step function
I	integer; integral expression
I1	integral expression
J	total integral number of the transient period time cells
J_i	i^{th} order Bessel function of the First Kind
K	integer
K_{ij}	characteristic value
L_j	dimension of the room
	Laplace transform
	inverse Laplace transform
M	integer
M_{ij}	constant
N	integer
N_i, N_k, NR	number of ray tubes; number of pulses

LIST OF SYMBOLS (continued)

N_M	normalizing factor
N_p	total number of pulses
P	total pressure; probability
P_0	constant background pressure
PREF*	pressure at the reference point
Q	rate of introduction of the fluid volume
Q_i	pulse strength; weight of the ray tube
Q_j	function
R, R_m, R_{im}	arcual distance between the receiving point and the source position; radius of a circle
$\mathbb{R}$	random number
$\mathcal{R}e$	real part
S	arbitrary function; phase function
T	function
T_c	total computer time
T_p	time period of the pulse
TREF*	reference time
U	parameter
V	volume of the bounded medium
V'	volume of the fluctuating medium
W_k	statistical weight
WL_n	rectangular room wall designation
X1,X2,X3	Cartesian rectangular coordinates
XC*	point of ray collision with the boundary

LIST OF SYMBOLS (continued)

$\underline{XI}^*$	point on the incident ray
$\underline{XR}^*$	receiving point position
$\underline{XRF}^*$	axial point
$\underline{XS}^*$	source position
a	absorption coefficient; duct radius
a1,a2,a3	direction ratios
a_i	coefficient
b_i	coefficient
c	characteristic wave velocity
c_0	standard wave velocity(constant)
d	lining thickness
f	function
g	constant
g_j	function
i	integer; $(-1)^{\frac{1}{2}}$
j	integer
k	integer
K, k_0, K_M	wave number
l_{21}	labour ratio
m	mass injection per unit volume from the source centre
m_c	number of computer operations per trial
n	integer; generalized refractive index of the medium
p_i, p_{im}	pressure contribution from the i^{th} pulse

LIST OF SYMBOLS (continued)

p_{imj}	pressure contribution from the i^{th} pulse during the j^{th} time interval
p_j	acoustic pressure in the normalized form in the j^{th} time interval
q_j	function
r	reflection coefficient; distance variable in radial direction
s	variable in Laplace transform; arcual distance
$\hat{s}$	unit normal to the wavefront
$\hat{s}_0$	initial direction of the signal path
t	time
t_c	computer time per operation
t_i	time of origin for the i^{th} pulse
t_m	time instant corresponding to the arrival of a propagating disturbance at a receiving point
u	variable
$\underset{\sim}{u}$	particle velocity
u_i, u_r	component of particle velocity
$\underset{\sim}{v}$	particle velocity
v_{zj}	axial component of particle velocity
v_{21}	variance ratio
$\underset{\sim}{x}_r$	receiving point position
$\underset{\sim}{x}_s$	source position
z	specific acoustic impedance; distance variable in axial direction

LIST OF SYMBOLS (continued)

α	angle of incidence; coordinate angle; factor of proportionality
α_{ij}	coefficient
α_M	normal mode coefficient
β	coordinate angle
β_{ij}	coefficient
γ	coordinate angle; ratio of two specific heats of the fluid
δ	Kronecker delta; error of Monte Carlo method
δ_{prob}	probable relative error
ϵ	preassigned elemental quantity
ζ	variable
η	efficiency; variable
θ	angular direction in cylindrical coordinate system; polar angle
κ	elasticity of the medium
λ	wavelength
μ	mean
μ_M	Monte Carlo estimate of ; eigenvalue
ν_M	resonance frequency
ξ	variable
ρ	mass density of the medium
σ	standard deviation
τ	retarded time
ω	circular frequency of the source

LIST OF SYMBOLS (continued)

Δt	elemental time period
Δt_{im}	time spent by the ray into a test cell
ΔR ΔR_{im}	distance of ray penetration into a test cell
ΔV	elemental volume; test cell volume
$\Delta \tau$	elemental time period
$\Delta \Omega$	elemental solid angle
∇	divergence
Ψ	spatial part of the wave function
Ψ_M	eigenfunction

Chapter 1

INTRODUCTION

A Monte Carlo method is suggested for the computation of the time-varying acoustical pressure in a wide variety of problems. The more interesting areas in which the Monte Carlo method is applicable are the boundary value and the initial value problems with linear differential equations as the governing equations.

Broadly speaking the method of determining an action at a distance from the source of the radiation energy is to construct a field of dynamic and thermodynamic quantities and then to study their propagation in the supporting medium, which in general absorbs, emits, and scatters the radiation. In terms of wave motion the analysis of, for example, potential and force fields, electromagnetic and gravitational fields has been possible for considerable time. An acoustical field is a scalar field of similar nature. For the description of the field satisfactory approaches are

known when the medium extends to infinity, but not always so when it is bounded. The suggested Monte Carlo method is in response to the obvious need for a numerical method to supplement analytical methods of solution which are only valid when the boundaries have simple shapes. An alternative method might have been developed from finite element techniques, they have already been applied successfully to some fluid problems, as suggested by Zienkiewicz (1967) and Oden (1969). However, the computer storage requirements for such solutions in three dimensions could well be prohibitive, and computation times excessive. The Monte Carlo method is particularly effective in multidimensional problems.

The generally known wave motion approach that is developed for the description of a field in a bounded medium results in a very lengthy exercise of mathematical analysis as it involves explicit or implicit integrations over a variety of complex surface areas. In contrast, the Monte Carlo technique that is developed here calls for very simple repetitive calculations. It considers the problem under investigation as a statistical problem. It investigates what happens to the field in terms of the signal paths of disturbances originating from the energy source, and based on the information so collected reconstructs the field as a function of space and time on a statistical basis.

The analysis of signal paths, from viewpoint of the Helmholtz wave equation and the Eikonal equation, is included in Appendix 1. Chapter 2 presents a brief survey of the known analytical methods for the description of the radiation field, with a highlight on the need for a more general numerical approach to supplement them.

The problem of radiation field in a bounded medium is viewed in Chapter 3 on the basis of the statistical model; included therein also is a brief description, in general terms, of the Monte Carlo method along with its scope and limitations. This is followed by a systematic development of an algorithm with special emphasis on applications to acoustical field solutions.

The algorithm thus created is verified critically in Chapter 4, and is shown to give the known results. This establishes the validity of the basic technique that is developed. Subsequent is the application of this technique in Chapter 5, to a specific physical model consisting of a nonconducting, isotropic, homogeneous medium enclosed by rectangular walls. Calculations are presented for a pressure field caused by an actuating point source with its strength time history characterized by a double rectangular pulse, single cycle sinusoidal pulse, and a N-shape pulse. The results are grouped in seven different cases for material absorption coefficients ranging from zero to one hundred

percent on different walls, with as many as six different receiving points dispersed in the region.

The Monte Carlo results for Case 1, all walls perfectly reflecting, for the single cycle double rectangular pulse source strength time history, are shown to be in qualitative agreement with those of Mintzer (1950); but the much needed closer quantitative comparison is not possible in this case, mainly, due to the lack of the knowledge of the specific normalizing factor utilized in the Mintzer's results.

With a view of presenting a quantitative comparison, for the case of perfect reflecting walls with sinusoidal shape source strength time history, an analytical solution is sought in Chapter 6 in terms of the normal modes by the application of the Green's Function technique.

The first half of the dissertation , dealing with the development of the basic technique and its applications, is restricted to considerations of the transient acoustic field in rectangular rooms containing no 'sound scattering' obstacles, having each wall uniform absorption, and no absorption in the medium itself. The removal of each of these restrictions will require further study; but the basic analysis appears to be well adapted for these extensions. The latter half of the dissertation presents an extension of the above technique to problems where the boundaries are

nonrectangular.

In order to adapt the Monte Carlo technique, developed in the first half of the dissertation, to the cases of practical importance where the boundaries are not at right angles, certain modifications become essential especially to cover such eventualities as the occurrence of possible focussing effects, the associated singularities, etc. in the region under investigation. Such modifications and the extension of the proposed Monte Carlo technique to cover the cases of curved boundaries, not necessarily of simple geometric shape, are studied in the latter half of the dissertation.

In view of the particular importance of the transmission properties of the axisymmetric duct in engineering applications, the concepts that are developed are then applied to the prediction of the transient acoustic field caused by a sound source inside a cylindrical duct. The results obtained by the application of the Monte Carlo technique in this case are then compared with those from an analytical solution based on the theory cast in terms of the normal modes of oscillation of the duct.

A survey of the literature indicates, as a common technique, the use of superposition of infinite succession of wave motions of monochromatic type, each defined by a single frequency of oscillation, in the study of forced vibrations and sound propagation inside a circular duct.

However, in this dissertation use has been made of somewhat different technique in arriving at the analytical results, the approach is to utilize the time domain instead of the frequency domain to characterize the sound sources as well as the field caused by them. If so desired, this time base resulting field can always be transformed to the frequency base by the use of the Fourier Transforms.

The problem of computing the effects of the propagating signal in a region surrounded by a curved boundary is identified in Chapter 7 and an expression in nondimensional form is presented for a pressure contribution at a receiving point that comes under the influence of the propagating ray tube that is traced in the Monte Carlo processing.

The process of random selection of the source along with the direction of the ray tube, with due consideration of the specific directional characteristics of any particular source, is considered in the most general-terms, with the help of flow diagrams, in Appendix 6. In Chapter 8 is presented a detailed discussion of the processing of the ray tube, and an algorithm is developed there for evaluation of the pressure contribution at a receiving point from the ray tube that is under process. Defining a quantity, termed as 'equivalent distance', as a function of the divergence factor of the ray tube cross-sectional area, this

modified algorithm for the case of curved boundary is shown to be in perfect agreement with that for the case of rectangular boundary, developed in the earlier portion of the dissertation.

In Chapter 9 the problem of the acoustical pressure field inside a rigid duct of constant radius is investigated from the normal mode point of view.

The results from application of these two methods are presented in Chapter 10 for a particular case where the emission is from a single point source with a single cycle sinusoidal shape strength time history. This is followed in Chapter 11 by a general discussion of the developments of the Monte Carlo method.

Chapter 2

RADIATION FIELD

The sound generated at a given position of the source, in a compressible fluid, distributes itself as a scalar material field of radiation. It is a field that is constructed to analyze the problem of action at a distance. Viewed macroscopically the radiation field is an idealized continuous function of space and time describing the dynamic and thermodynamic state of the supporting fluid medium.

The acoustic radiation field, which may be constructed as a solution to the initial and boundary value problem, provides the basis for any systematic approach to noise control, and hence is of considerable technological importance. Depending on the extent of the supporting medium, exterior to the radiating energy source, the radiation field is categorized as unbounded or bounded. In the former case, as the medium extends to infinity, only the diverging waves originating from the radiator (Fig. 1a) are present. A survey

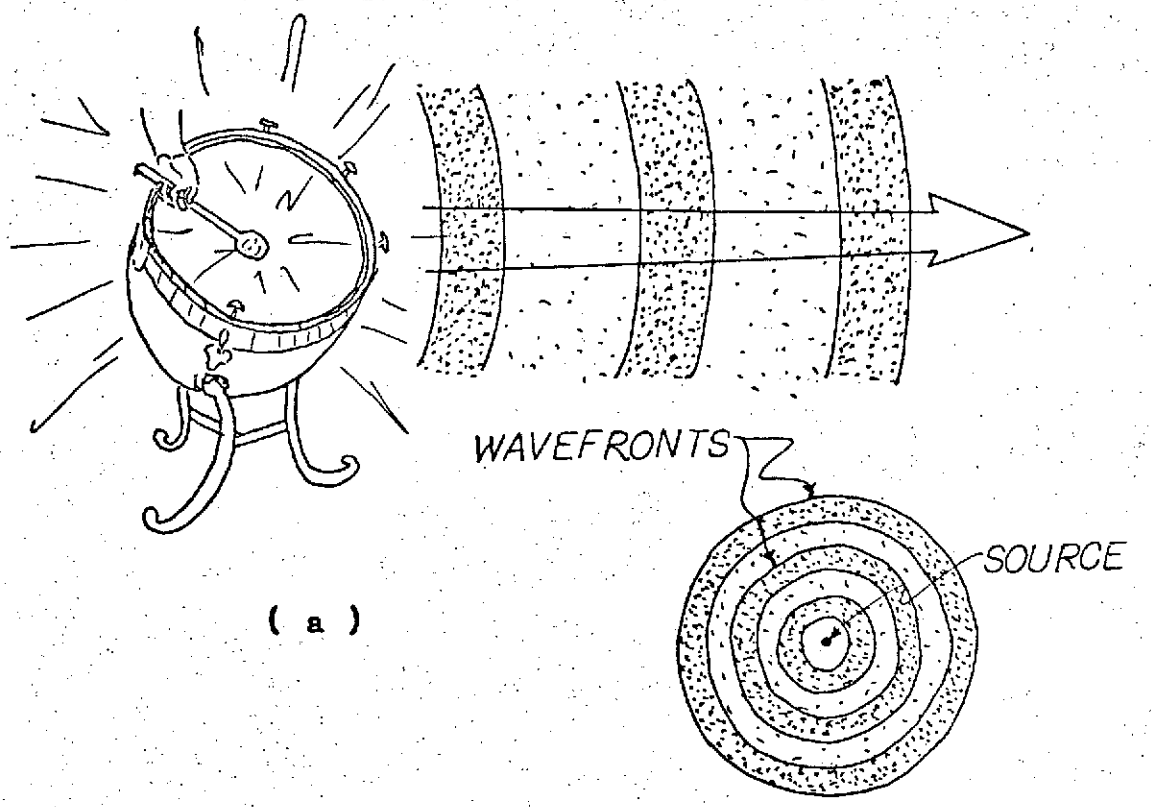

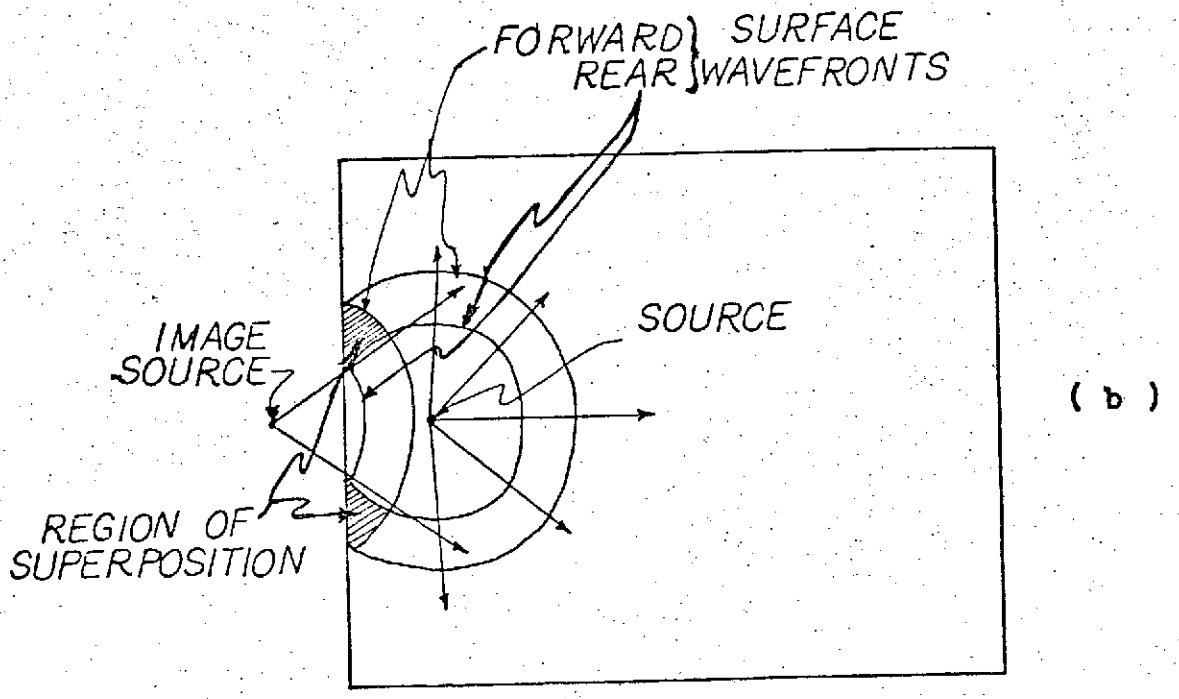

Fig. 1 Source in an Unbounded Medium & a Bounded Medium

of the literature indicates that a large number of satisfactory numerical methods are available for analysis of the radiation field when the medium is unbounded. These can be classified broadly in two groups as

I. Differential Equation Formulation

- Multipoint Boundary Value Problem

II. Integral Equation Formulation

- Extension of Classical Potential Theory.

On the other hand, in a bounded medium, the boundaries are present at finite distances from the source. In acoustics, the physical effects of the boundary are to cause reflections which then must be added to the wave developed by the source to give the resultant field. Figure 1b shows a typical pressure pulse in a bounded medium; also indicated therein is a region of superposition resulting from a wall reflection. The methods that are known and find certain applications in the analysis of a radiation field in a bounded medium are :

1. Separation of Variables

The problem of practical importance involves, in general, complicated cross-sections for which the natural coordinate system becomes extremely complicated and as a result the problem, in general, would not be amenable to the standard method of separation of variables.

2. Conformal Mapping

The method of conformal mapping makes use of a technique of transforming the cross-sectional area into a simpler one, but its success depends heavily on the availability of the proper mapping function. This effectively rules out its application to problems with arbitrary boundaries.

3. Green's Function

Even if it is known that the Green's function does exist for the region under investigation, it is an extremely difficult task to find it; and as such this method is mostly used in the theoretical approach.

4. Method of Images

The method of images finds applications in certain special cases of rigid walls, but in a very few cases the images are the real images of the source. Even in these few special cases it is no simple task to find these images analytically.

5. Method of Normal Modes

In the normal mode method the medium enclosed is considered to be a three dimensional elastic body having its own natural modes of vibration governed by the mechanical constant of the mass of the medium and the boundary conditions on the enclosure surface. Then the sound field in a given

enclosure is expressed as the summation of the normal modes involving various decay constants and normal frequencies. Although this method shares the gain in power afforded by the generalized coordinates in mechanical problems, its applicability is limited to a few specialized cases, as in cases involving geometries other than the separable ones, the procedure inevitably becomes involved and complex.

This clearly brings out the fact that these known analytical methods can be applied only in a very few specialized cases, and there is an obvious need for a more general numerical method to supplement them. This is afforded by the proposed Monte Carlo technique that is developed in this work; the central idea being to follow the propagation of the signals of disturbance originating from the energy source.

At every point in the medium the signal propagates along a direction normal to the wavefront, the locus of the wavefront normal forming the required trajectory that is used in the Monte Carlo method as the propagational path of the acoustic ray. In general this is a function of

a. Initial direction of any particular ray emanating from the energy source
b. Spatial variations of the physical and thermodynamic characteristics of the supporting medium

c. Spatial variations of the geometric shape and the thermodynamic properties of the boundaries that enclose the region under investigation.

When these are specified mathematically the problem of the determination of the ray trajectory becomes determinate, and can be solved completely by formulating a set of equations defining the direction of the ray successively.

In the Monte Carlo method based on the statistical model the requisite initial direction for any particular acoustical ray from the source is selected at random in accordance with the directional characteristics of the acoustical source. Such a selected ray is then traced through multiple reflections from boundaries, and through other events, if applicable. The pressure time histories at receiving points are calculated by accumulating the effects of penetrations of the rays through test cell volumes located at these points, i.e., at the points where the pressure is to be found. In the first half of the dissertation the method is adapted to the problem of the rectangular room, and calculated results are given for comparison with other calculated results, such as those of Mintzer (1950), and those obtained by the normal mode method.

The difficulties to be overcome in adapting the method to more general problems are also discussed, and necessary developments are shown to include adaptation to

curved boundaries, to moving or inhomogeneous media, and to problems involving diffraction. The latter poses the worst problem, because it involves a breakdown in classical ray acoustics. Looking further ahead, it is fascinating to conjecture whether the rays can be treated as trajectories of phonons, and whether, by such an approach, nonlinear acoustical problems can be handled by considering the interactions between such phonons.

Chapter 3

STATISTICAL MODEL AND THE MONTE CARLO TECHNIQUE

PROBLEM IDENTIFICATION

Sound is a dynamic disturbance of equilibrium of the physical characteristics of the supporting fluid medium. The sound generated in one region will propagate away, reflect from nearby walls or structures into different paths, and redistribute itself. The analytical problem associated with such a physical situation is the prediction of the sound field everywhere in the fluid region under investigation from its observable characteristics such as pressure, particle velocity, etc. at the source surface. This requires familiarity with the laws governing the propagation of sound through the supporting medium, and with the relationships between such measures of sound strength as the fluctuating pressure, the energy associated with the fluctuation, etc. In general the distribution of the sound field in the medium depends on the

following factors :

a. Distribution of the sound sources and their strength time histories with any directional properties associated with them

b. Thermodynamic and physical characteristics of the supporting fluid medium

c. Shape and thermodynamic properties of the boundaries enclosing the region that is under investigation.

When these are specified mathematically the problem, which is recognized to be a combination of the initial and the boundary value problem, becomes a determinate and, in principle, can be solved completely; however, in practice the solution remains tractable only in a restricted class of problems involving simple geometric shapes, thereby suggesting an obvious need for a more general numerical method to supplement the known analytical ones. The proposed Monte Carlo technique based on a statistical model and the tracing of the acousticcal rays, whose directions have been selected randomly, through multiple reflections from the boundaries and other events appears to meet this requirement.

DESCRIPTION OF THE MONTE CARLO METHOD

In general the Monte Carlo methods, dealing with the solution of the problems by setting up equivalent 'games' in which choices are made by drawing random numbers, are classified under two types, Probabilistic or Deterministic. The initial and the boundary value problem in acoustics, identified above, is a deterministic problem that can be formulated in theoretical language but can be solved by theoretical means only for very simple geometries. In fact, being deterministic, this problem has no direct association with the random processes; but when its underlying structure is exposed it may perhaps reveal that it also describes some apparently unrelated random processes. Practically all problems in physics and engineering have a statistical basis, being influenced by a large number of factors having approximately equal effects; but one represents these by nonstatistical mathematical models when the samples involved are extremely large. For complex problems the analytical description may be practically impossible; however, the statistical simulation and its successful investigation may be possible with the application of the Monte Carlo method. This permits the solution of the determinstic problem under investigation numerically by Monte Carlo simulation of the

concomitant probabilistic problem. It is expected that in the limiting case of the large number of samples the solution thus obtained will converge to the same limit as the physical process that is represented. In fact one of the most serious limitations imposed on the Monte Carlo method is that a very difficult choice must be made between the desired accuracy and the economy. A general discussion of the error analysis and the probability estimates of the Monte Carlo results is included in Appendix 2. Access to a high speed digital computer is essential in Monte Carlo applications.

Monte Carlo methods are recent innovations, since general programmes are generally unavailable special methods must be created to suit individual problems. Since economic considerations will keep the level of the sample size in any particular solution relatively small, it is expected that the results are subject to random fluctuations and hence can be quoted only in the limits of plus and minus a standard deviation from the statistical mean. Then as shown in Appendix 2 the exact solution of the simulated problem can be estimated to be within the limits of plus and minus one standard deviation about 68 % of the time.

It pays to scrutinize the problem to see whether any part of the experiment could well be replaced by an exact theoretical analysis, since such a replacement will

cause no uncertainty. To escape the formidable or even impractical amount of experimental labour it be essential to change or at least to distort the original problem.

A procedure that can be used to establish the magnitude of the statistical variability is the very simple one of repeating the runs. The root cause for such a variability is the whole set of random numbers that get employed in any Monte Calo application to represent the various processes involved. Usually this simple procedure of repeating the runs, treating these as independent samples until the variability has been reduced to the desired level is not feasible due to the large amount of the computational labour involved to obtain any single sample. The quantity under examination is often highly variable; if not, in fact, its mean value could have been estimated by some deterministic approach. In order to make the Monte Carlo application economically competitive it is highly desirable to implement one or more of the variance reducing techniques, such as, Stratification, Control Variates, Antithetic Variates, etc. What most of these methods have in common is that they do not introduce bias into the estimation and thus they make the results more precise without sacrificing reliability. A judicious use of any of the above methods calls for a deeper thought in the problem. Since no attempt was made to use such sophisticated techniques here, there is no necessity to dwell

on this subject here; Kahn (1954), Tocher (1963), and Hammersley (1965) provide certain discussion on this topic.

APPLICATIONS TO ACOUSTICAL PROBLEMS

The Monte Carlo method defies description beyond that already given in general terms; however, the particular acoustical model that is used in this work here can be described as follows.

A probabilistic model is used, by means of which the pressure time history at any receiving point in the field can be computed by superimposing the effects of many individual 'wavelets', representing the disturbance generated by the source, transported along the rays of propagation. In order to obtain the results within a reasonable computing time, the receiving point is represented by a small elemental test cell surrounding it; and the mean pressure within any small time increment is obtained by summing the times of transit of the rays through the test cell.

The rays are assumed to consist of small tubes or bundles originating with a given elemental solid angle from the acoustical source, having intensities, directions, and times of origin which have been selected at random, in accordance with the spatial, directional, and timewise distributions of these sources. Each ray is

traced taking account of its interaction with boundaries, or with the gradients in the medium through which it is transmitted. Events occuring during the lifetime of any particular ray may be of two kinds; causal, such as when it reflects off a solid boundary; or probabilistic, such as when losses at a wall are accounted for by a 'sudden death' game. Tracing of a particular ray is terminated either when the required solution time is elapsed, or when it has been terminated in a sudden death. During all of this time, the pressure time history is determined at preselected 'receiving points', i.e., points at which the pressure is desired, by using appropriate sampling techniques. For this analysis a suitable model is created from which is developed an algorithm for the estimation of the acoustic pressure variations in the region under investigation.

STATISTICAL MODEL

Any mathematical model of a physical system requires the following three parts :

1. A conceptual, idealized physical model of the actual system
2. A method to solve the equations describing the idealized physical model
3. A computational procedure to implement item 2.

The ultimate measure of a mathematical model is the degree to which it produces satisfaction to its user. This satisfaction can usually be produced when the computed values agree with the reliable experiments. An alternative method of checking the validity of any new technique is the application to a very simple physical model that is amenable to another proven technique, and the subsequent comparison of the two results. When this latter course of comparison is adopted, as is the case in the present work, a proper consideration must be accorded to the fact that the method selected for comparison might not be an exact but an approximate one. Obviously the better verification is afforded by the former course of comparison.

Governing Equation for the Pressure Field

The first step is to formulate a conceptual, idealized physical model of the acoustical system that is to be analyzed. The generated sound in the region under investigation is considered to be a collective effect of a certain distribution of sound sources. In the absence of these sound sources, let the medium be stationary, and its physical state be described by a pressure field with a constant value, say P_0. The introduction of the sound sources causes the pressure in the medium to fluctuate. Let $P(\underset{\sim}{x}_r,t)$ be the total pressure at a receiving point $\underset{\sim}{x}_r$ in the field at time t, the underscore

$(\sim)$ denoting the vectorial quantity. The distribution of the pressure field is governed by the nonhomogeneous wave equation

$$(1 / c^2) (\partial^2 P / \partial t^2) - \nabla^2 P = \text{R.H.S.} \qquad (1)$$

where c is the characteristic wave velocity; it is the velocity at which the pressure disturbance propagates in the supporting fluid medium of characteristic impedance ρc^2, ρ being the mass density of the medium. In Eq. 1 the term 'R.H.S.' is interpretable as a strength distribution of simple acoustic sources per unit volume.

Assumptions

The classical Wave Equation of linear acoustics is expressed as

$$(1 / c^2) (\partial^2 P / \partial t^2) - \nabla^2 P = 0 \qquad (2)$$

This is obtainable from the more general Navier-Stokes equation of fluid motion under certain restrictive assumptions, the more important of them are enumerated below, the less important such as body forces, chemical reactions, etc. are omitted.

I. The fluctuating acoustical pressure $p(\underset{\sim}{x}_r, t)$ given by

$$p(\underset{\sim}{x}_r, t) = P(\underset{\sim}{x}_r, t) - P_0 \qquad (3)$$

is sufficiently small compared to the equilibrium pressure P_0. This implies the proportionality of the deformations and the stresses caused by the perturbation. This approximation will require reexamination when the mean square pressure levels are of the order of 130 dB.

II. Thermo-viscous dissipation is negligibly small. Inclusion of these effects is possible, but the mathematical complexity will obscure the basic problem.

III. In case of the sound generation by the turbulence, the cross-correlation between the sound field and the turbulence is small enough to allow the decoupling of the two equation sets. This permits the examination of the sound field independently of the turbulence field. This assumption is seen to be invalid in the proximity of the sound sources.

These assumptions allow the separation of the wave equation from the equation of motion.

Monopole Field

In the study of transient sound generation in a given acoustic cavity, the notion of the multipole representation of the acoustic sources can be used profitably.

The very useful conception of a monopole, commonly known as a 'point source' was introduced into the subject by Helmholtz. The position of a point source in the field is the location of a 'point singularity'. At such a point, one can imagine, that a fluid is introduced or abstracted at a certain rate. In the presence of certain volume distributed monopoles the pressure field is govrrned by the wave equation

$$(1 / c^2) (\partial^2 P / \partial t^2) - \nabla^2 P = \partial \dot{m} / \partial t \qquad (4)$$

where $\dot{m}$ is the rate of mass injection per unit volume, the overhead dot ($\dot{}$) denotes the differentiation of the quantity with respect to time. In Eq. 4 the R.H.S. term $\partial \dot{m}/\partial t$ represents simple sources of strength $\partial \dot{m}/\partial t$ per unit volume considered as a source for the pressure, and not for the velocity potential.

Let O be the reference point, origin, inside the volume V' (Fig. 2) of the fluctuating medium representing an entity of volume distributed acoustic sources. Within this volume V' consider an elemental volume $dV'(\underset{\sim}{x}_s)$ representing a point source at the position $\underset{\sim}{x}_s$. Let $\underset{\sim}{x}_r$ be a receiving point external to V'; then defining as the retarded time

$$\tau = t - R / c \text{ , where } R = | \underset{\sim}{x}_r - \underset{\sim}{x}_s | \qquad (5)$$

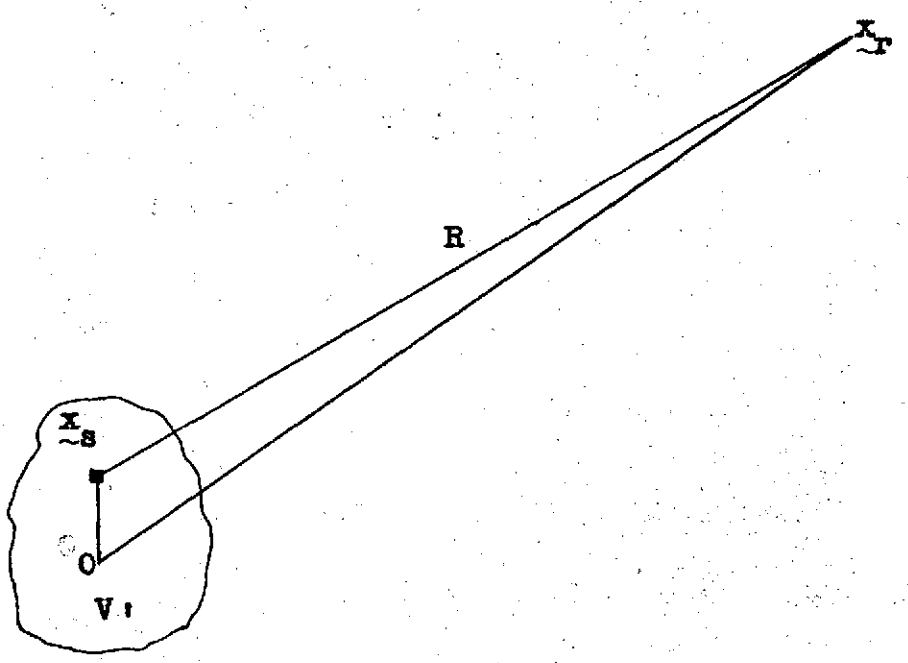

Fig. 2. Volume Distributed Acoustic Sources

it is possible to express the pressure contribution from this entity of the volume distributed acoustic sources at the receiving point $\underset{\sim}{x}_r$ at time t as a solution of Eq. 4 represented by, using Eq. 3,

$$p(\underset{\sim}{x}_r,t) = (1/4\pi) \int_{V'} (1/R)\, \partial \dot{m}(x_s,\tau)/\partial t \; dV'(\underset{\sim}{x}_s) \qquad (6)$$

When the linear dimension of the fluctuating region V' is small compared to the distance R, i.e. when the relation

$$(V')^{1/3} / R <<< 1 \qquad (7)$$

is satisfied, it is possible to approximate Eq. 6 by

$$p(\underset{\sim}{x}_r, t) = (V'/4\pi R) (\partial^2/\partial t^2) m(\underset{\sim}{x}_s, \tau) \qquad (8)$$

In other words, the pressure field at the receiving point $\underset{\sim}{x}_r$, due to the distributed acoustic sources, is <u>equivalent</u> to that due to a concentration of the total sources at a single source point $\underset{\sim}{x}_s$ when the relation given by Eq. 7 is satisfied. An equivalent form of Eq. 8 is

$$p(\underset{\sim}{x}_r, t) = (\rho/4\pi R) \dot{Q}(\underset{\sim}{x}_s, \tau) \qquad (9)$$

where $Q(\underset{\sim}{x}_s, t)$ is the rate at which the fluid material is introduced at $\underset{\sim}{x}_s$ by a point source located there and represents its strength as defined originally by Helmholtz.

When the region is unbounded, Eq. 8 or 9 provides the sufficient information in regards the time history of the pressure contribution at a given receiving point $\underset{\sim}{x}_r$ resulting from the action of a point source located at $\underset{\sim}{x}_s$. It is assumed here that the medium is homogeneous and is at rest initially.

Finite Representation of the Source

As stated earlier, in the present statistical model, the generation of sound in a given acoustic cavity is considered to be a collective effect of distributed sound sources. From a given distribution, now, consider a representative source; if it is not adjacent to the solid boundary, and has no preferred directions as its characteristics, it would emit isotropically in the medium. It is characterized by its spatial location in the cavity, its time of origin, and its strength time history. Figure 3a is a typical strength time history of an acoustical point source. Its time period T_p is divided into a finite number of intervals

$$2 n_p = T_p / \Delta\tau \qquad (10)$$

where $\Delta\tau$ is a width of any individual interval. The strength of the source in each of these intervals is approximated as constant. The use of an equivalent finite number of elementary pulses, as shown in Fig. 3b, then provides the requisite finite representation of the acoustical source. Out of these $2 n_p$ elementary pulses any particular one is defined by

its strength Q_i

and its time of origin $t_i = (i-\frac{1}{2})\Delta\tau$ (11)

where i is an integral index such that

$$1 \leq i \leq 2 n_p$$

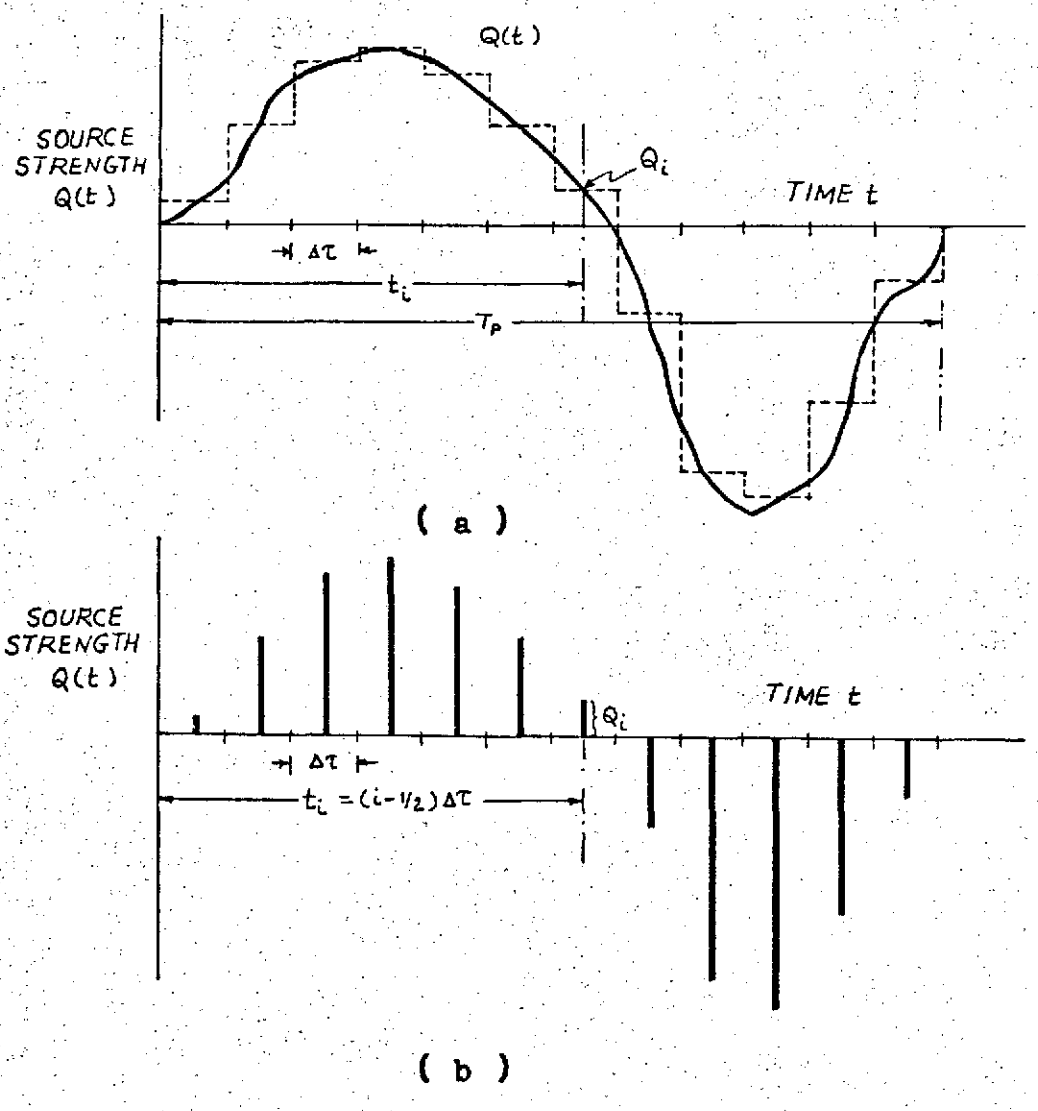

Fig. 3 Typical Source Strength Time History

Random Pulse Selection

Now at this stage an elementary pulse is selected from this aggregation. There are number of ways to accomplish this with varying degree of sophistication, probably the simplest one would be to generate an integer random number and then to pick a corresponding pulse. In computer applications, this needs a generation of string of random numbers, which forms the essential element of any Monte Carlo method.

Generation of Pseudo Random Numbers

It was mentioned above that a source of random numbers is required from which they can be drawn in succession. When a routine is to be checked, it is of great convenience to be able to draw the same set of random numbers each time the calculations are repeated, thereby making the random numbers used in the Monte Carlo application not truly random but 'pseudo' random.

Hull (1962) has presented a rather complete treaties on various random number generators. The so called 'Multiplictive Congruential Method' of generation requires a starting integer y, an integer a as a multiplier, and a modulus m which is greater than a or y. The maximum period of the resulting sequence of numbers is given by m, and this is chosen as a power of two for a binary computation.

Real type random number. The algorithm that is used for the generation of a string of 'pseudo' random numbers in the present work is selected from the 'Collected Algorithm Computer Programs' 266-P-1-0 CACM. This is based on the multiplicative congruential method of generation of random numbers. It utilizes an integer 3125 as a multiplier and 67108864 (= 2 E 26) as a modulus. The exact procedure here is as follows :

```
integer  :  y
real     :  ℝ
            before first use
            set  y = any odd integer such that
            y < 67108864
begin
            y = 3125  x  y
            y = (y - y / 67108864)  x  67108864
            ℝ = y / 67108864
end.                                          ( 12 )
```

This provides $\mathbb{R}$ as a random number of type real such that

$$0 < \mathbb{R} < 1 \qquad (13)$$

An important property that is utilized in the present application is that the continuous random variable $\mathbb{R}$ obtained by this method has a uniform distribution over the interval $[0,1]$. A uniformly distributed random variable

represents the continuous analog to 'equally likely outcomes' in the following sense. For any subinterval $[t, t+\Delta\tau]$ where

$$0 \leq t < t + \Delta\tau \leq T_p \qquad \text{(Fig. 3)}$$

the probability that the random variable $\mathbb{R}$ lies between t and $t + \Delta\tau$ is the <u>same</u> for all subintervals having the same length $\Delta\tau$. That is the probability

$$P(t \leq \mathbb{R} \leq t + \Delta\tau) = \Delta\tau / T_p \qquad (14)$$

and thus depends only on the length of the interval and not on the location of that interval.

<u>Integer type random number</u>. The required integer random number i in Eq. 11 above, for the pulse selection, is obtained as

$$i = \text{INT}\left[(\mathbb{R}) \times (2\, n_p) + 1 \right] \qquad (15)$$

where the real type parameter of the product $(\mathbb{R}) \times (2\, n_p)$ is converted to the integer type. All the integers upto $2\, n_p$ are seen to be equally probable for the value of i given by Eq. 15. A pulse corresponding to this integral index i is the random selected pulse (Fig. 4a). It is defined by its strength Q_i and its time of origin t_i (Eq. 11).

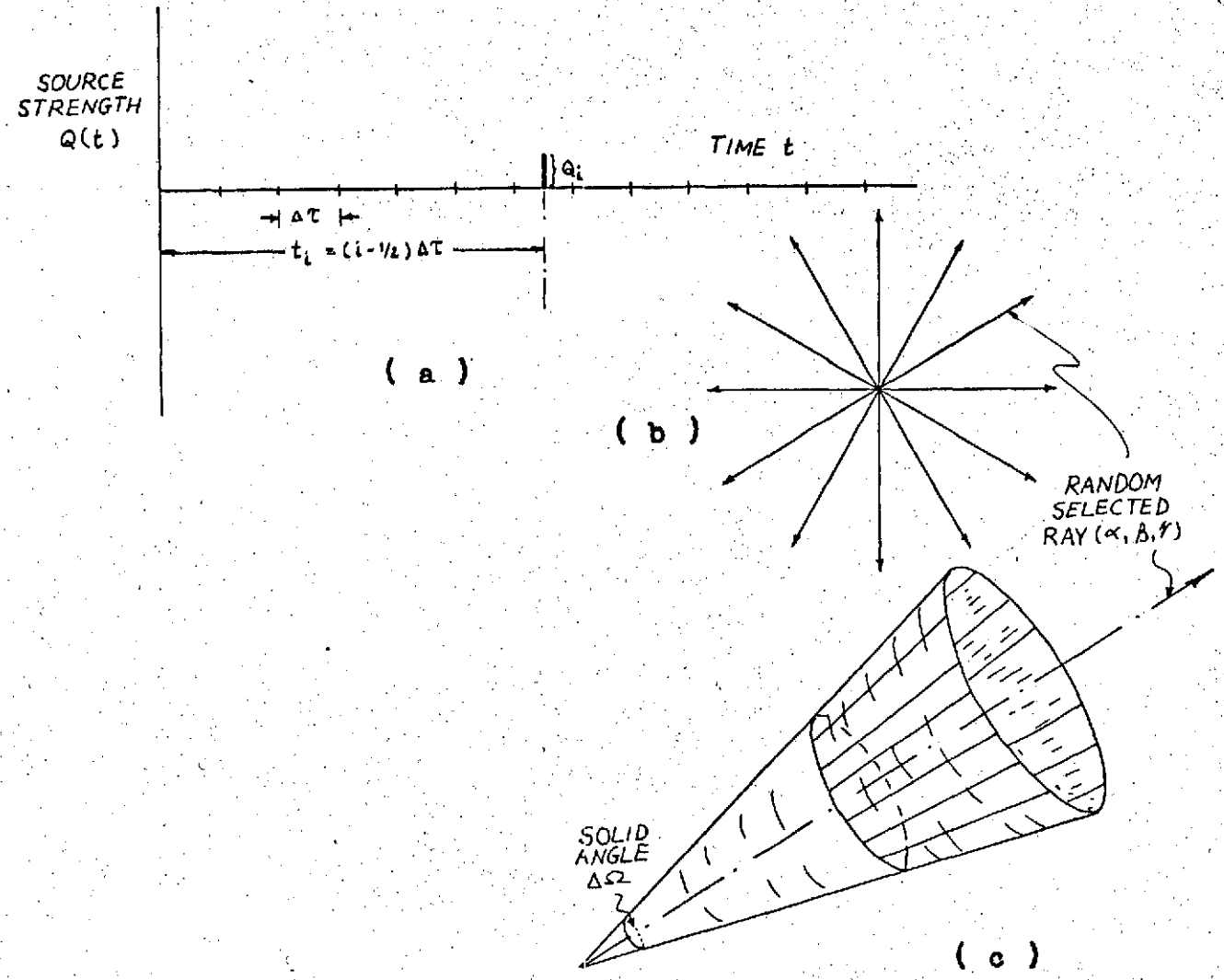

Fig. 4 Random Selected Pulse, Ray, and Ray Tube

Random Ray Selection

At the time of its origin, the selected pulse emits isotropically in the medium. The directions of the emitting rays, which are normal to the disturbance wavefronts, are infinite in number; only a few of these are shown in Fig. 4b. It is necessary to select one of these. The method that is adopted for this, given by Haviland (1965), is to pick a point, say A, at random on a unit circle with polar coordinates, say R, Θ (Fig. A3.1, Appendix 3). This is accomplished by picking two Cartesian coordinates, say X1, X2, at random, both in the range -1 to +1, and rejecting them if the point A lies outside the unit circle. Let $\mathbb{R}1$ and $\mathbb{R}2$ be two random numbers; then

$$\begin{aligned} X1 &= 1 - 2\,\mathbb{R}1 \\ X2 &= 1 - 2\,\mathbb{R}2 \\ R^2 &= X1^2 + X2^2 \end{aligned} \qquad (16)$$

If $R^2 \leq 1$ values of the random numbers $\mathbb{R}1$ and $\mathbb{R}2$ are accepted; otherwise rejected, and a new set of random numbers is tried. Over a long period, $\pi / 4$ tries will be successful, and this defines the 'efficiency' of the method. This is a Monte Carlo method of random direction selection; in Appendix 3 it is examined in more details and also included there is its comparison with an alternative method that is

conceived on pure geometric considerations.

Let DC1($= \cos\alpha$), DC2($= \cos\beta$), DC3($= \cos\gamma$) represent the direction cosines of the unit vector in the direction of the propagating ray, at the source position (Fig. A3.1, Appendix 3); then

$$\begin{aligned} DC1 &= 1 - 2R^2 \\ DC2 &= 2X1\,(1 - R^2)^{\frac{1}{2}} \\ DC3 &= 2X2\,(1 - R^2)^{\frac{1}{2}} \end{aligned} \qquad (17)$$

This completes the specification of the initial direction vector for the ray selected at random.

Rather than following a single ray to represent the signal propagation, it is more convenient to follow a small ray tube (Fig. 4c) consisting of a bundle of rays originating from the energy source within a given elemental solid angle $\Delta\Omega$ centred around this selected ray.

Influence of the Randomly Selected Ray

Consider, now, the influence of the randomly selected pulse with the integral index i, strength Q_i, and time of origin t_i. Further, let its influence be confined to a ray tube, as defined above, centered around the randomly selected ray(α, β, γ). This is traced, taking into account its interaction with boundaries, or with gradients in the medium through which it is transmitted. At any point along

its trajectory, the name of such a ray tube is constituted by its direction, its coordinates, and its weight. A weight of the ray tube represents its intensity. Its original weight is Q_i.

In the absence of physical, or thermodynamical gradients in the supporting fluid medium, the rays originating from the energy source propagate essentially in paths composed of straight lines from one boundary to another. Figure 5 shows first few reflections from the rectangular walls.

Now since the influence of the selected pulse is assumed to be confined within the ray tube that is traced, it is essential to examine whether at any instant during the progress, the receiving point falls within the influence of this ray tube; then and only then there could be a pressure contribution from this pulse at that particular receiving point in the region.

Pressure in an unbounded medium. Consider now the effect of the previously selected pulse of integral index i. At the time of its origin in the short interval of time, say, from t_i to $(t_i + \epsilon)$ it produces a localized disturbance in the immediate neighbourhood of the source position $\underset{\sim}{x}_s$. At a subsequent instant t greater than t_i, its effect is localized in a very thin spherical shell with

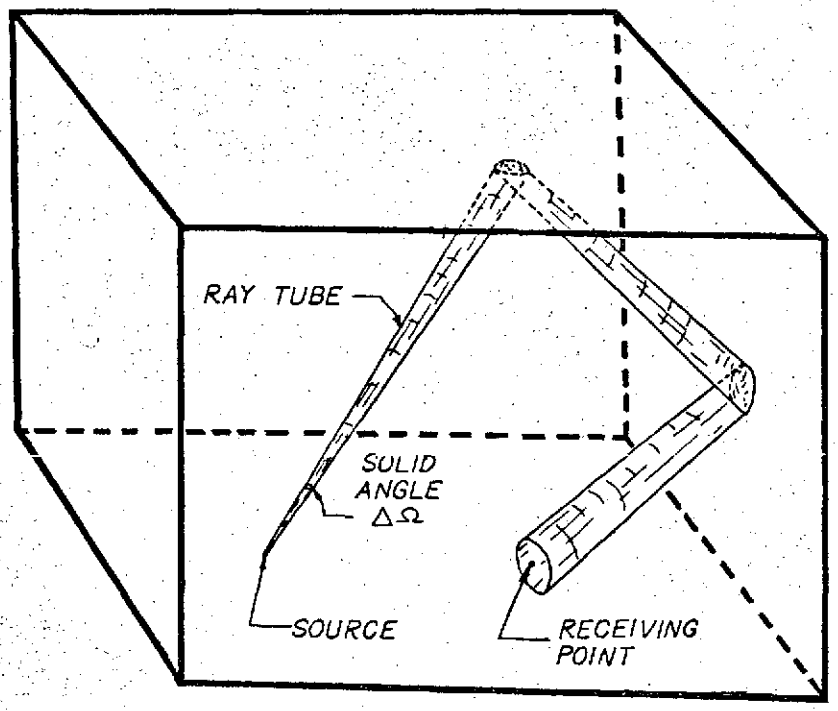

Fig. 5 Rectangular Boundary Problem

centre $\underset{\sim}{x}_s$, and radius $c(t-t_i)$. Now if t_m represents that particular instant at which the propagating disturbance arrives at the point in question, the pressure contribution from this pulse can be expressed, using a δ-function along with Eq. 9, as

$$p_{im}(\underset{\sim}{x}_r,t) = (\rho/4\pi R_m)\,\dot{Q}_i\,\delta(t - t_m - t_i) \qquad (18)$$

where $R_m = |\underset{\sim}{x}_r - \underset{\sim}{x}_s| = c(t-\tau) = c(t - t_i)$

Pressure in a bounded medium. In general, now, if the variable R_m in Eq. 18, or R in Eq. 9, is defined to be the arcual distance along the trajectory of any particular signal originating from the source position upto the point in question, Eqs. 9 and 18 hold even when the medium is bounded, only the difference is that in the case of a bounded medium proper account needs to be taken of the multiple reflections that the ray suffers before arriving at the receiving point.

This effect of multiple reflections can be handled relatively easily when the boundaries enclosing the region form rectangles. It is this case that is treated presently; whilst the situation resulting in the case of nonrectangular boundaries is studied in greater details in the latter half of the dissertation.

Let an infinite set R_{im} , m = 1 to ∞ , represent all of the possible distances travelled by the selected ray (α, β, γ) characterizing the i^{th} pulse, from the source position to the point in question; then using Eq. 18 above, the pressure time history at this point resulting from this i^{th} pulse is

$$p_i(\underset{\sim}{x}_r, t) = \sum_{m=1}^{\infty} p_{im}(\underset{\sim}{x}_r, t)$$

$$= \sum_{m=1}^{\infty} (\rho / 4\pi R_{im}) \dot{Q}_i \, \delta(t - t_m - t_i) \qquad (19)$$

where $t_m = t_i + R_{im} / c$

The concept of the method of images provides a means of visualizing this result more clearly. In this method, as shown in Fig. 6 for the case of perfectly reflecting walls of a rectangular room, an infinite array of image rooms is constructed, each containing an image source. The pressure at the receiving point is the sum of the effects of all of these image sources plus that of the true source.

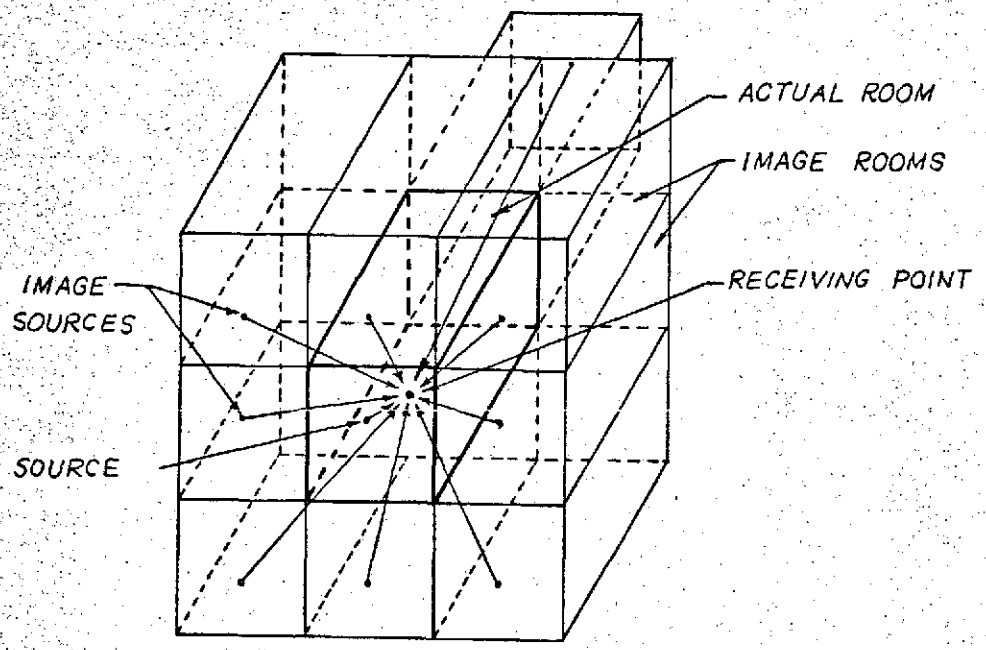

Fig. 6 Array of Image Rooms

Finite cell transient period. The total transient period, for which the solution is sought, is divided up into, say, J time cells, each of duration Δt; and the pressure p_{imj} is considered to be the mean value of the pressure $p_{im}(\underset{\sim}{x}_r,t)$, given by Eq. 18, taken over the j^{th} time interval, resulting in an expression

$$p_{imj}(\underset{\sim}{x}_r) = (1/\Delta t) \int_{j\Delta t - 1}^{j\Delta t} p_{im}(\underset{\sim}{x}_r,t)\, dt$$

$$= \rho\, \Delta\tau\, \dot{Q}_i / 4\pi \Delta t\, R_{im}$$

if the ray passes through the receiving point for the m^{th} time during the j^{th} interval

$$= 0 \quad \text{otherwise.} \qquad (20)$$

Pressure accumulation alternate method. The method just described is further investigated in the latter part of the dissertation, where the Monte Carlo technique of the present part is modified to cover a larger class of cases of practical interest involving boundaries that are not at right angles to each other; however, a simpler alternative method is possible for rectangular boundaries that are

investigated here. This consists of introducing a small parallelepiped test cell of an elemental volume ΔV at the receiving point, and then determining the penetration ΔR of the propagating ray into it, alongwith the travel distance R of this ray tube starting from the source upto the penetration point. The two methods are shown in Fig. 7.

Let ΔR_{im} and R_{im} be the length of penetration and the travel distance, respectively, for the ray tube that is under process; then the time spent by the ray in the test cell is given by

$$\Delta t_{im} = \Delta R_{im} / c \qquad (21)$$

The pressure contribution resulting from such a penetration can then be expressed as

$$p_{imj}(\underset{\sim}{x}_r) = (\dot{Q}_i / 4\pi R_{im}) \cdot (\Delta t_{im} / \Delta t) \cdot (R_{im}^2 \, c \, \Delta\tau \, \Delta\Omega / \Delta V)$$

where $j = t / \Delta t + 1$

$$= (t_i + R_{im} / c) / \Delta t + 1 \qquad (22)$$

The first term on the right hand side of Eq. 22 corresponds to that of Eq. 18, the second term is the sample correction factor which is the ratio of the penetration time interval to the averaging time interval; whereas the third term is the

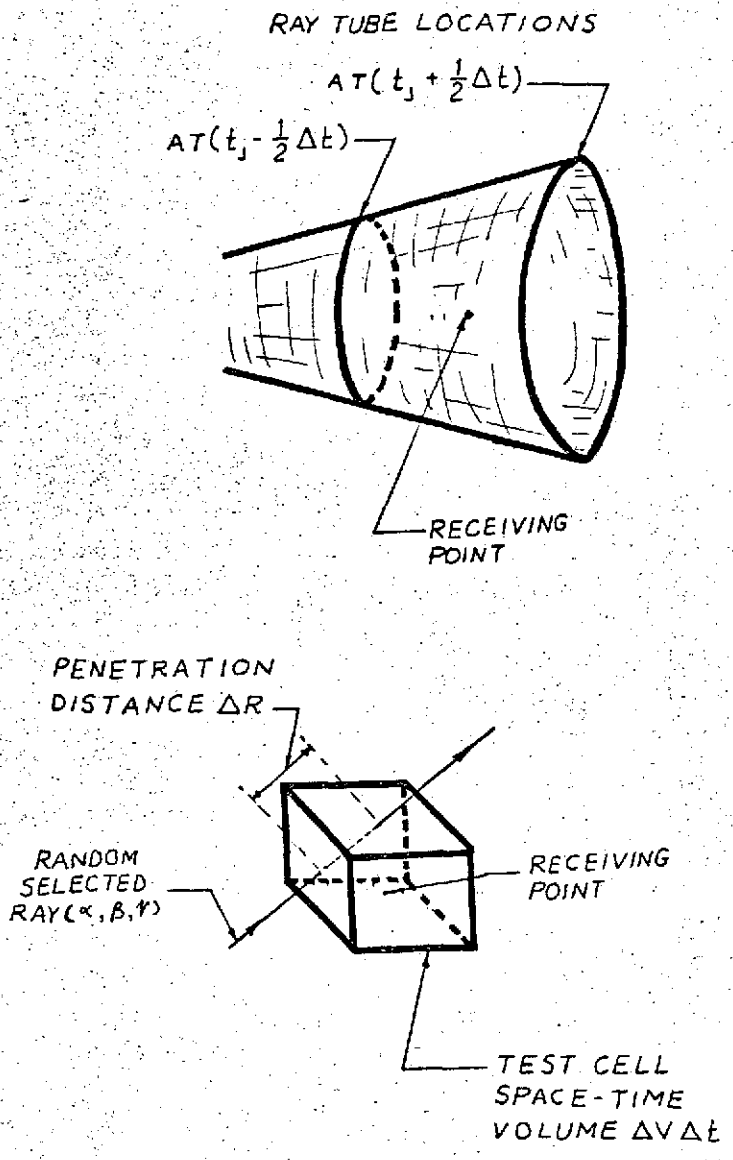

Fig. 7 Alternative Methods of Accumulating Acoustical Pressure Contributions

ratio of the volume occupied by the ray tube to the test cell volume, and covers the probability that the ray will miss the test cell altogether.

Thus goes the processing of any particular ray tube with the accumulation of its influence at a given receiving point in the region under investigation. Either when the time index j exceeds the limiting value J, which corresponds to the total transition period length, or the intensity of of the ray tube drops below a predetermined level, the processing of that particular ray tube is terminated; and the process is repeated for, say, a total of N ray tubes in a particular Monte Carlo run. Each ray tube represents, separately, a randomly selected pulse.

Normalized Pressure Value

It is recalled that the time period T_p of the source was subdivided into $2\,n_p$ equal intervals of width $\Delta\tau$, and that the ray tubes which were used to represent the source strength time history were considered to be centred around a randomly selected ray with a solid angle $\Delta\Omega$; then since 4π represents the total solid angle, the total number of pulses N_p that could have been selected is given by

$$N_p = (4\pi / \Delta\Omega)\, 2\, n_p = 4\pi\, T_p / \Delta\Omega\, \Delta\tau \qquad (23)$$

Finally, the expected pressure is obtained by averaging over all of the N pulses that were followed, and normalizing by multiplication by the total number of pulses N_p. Then the resulting acoustic pressure, in the normalized form, in the j^{th} time interval, can be expressed, using Eqs. 21, 22, and 23 as

$$p_j(\underset{\sim}{x}_r) = (N_p / N) \sum_{i=1}^{N} \sum_{m} p_{imj}(\underset{\sim}{x}_r)$$

$$= (\rho T_p / N \Delta V \Delta t) \sum_{i=1}^{N} \sum_{m} \dot{Q}_i R_{im} \Delta R_{im}$$

$$= (\rho T_p / N \Delta V \Delta t) \sum_{i=1}^{N} \dot{Q}_i R_i \Delta R_i \qquad (24)$$

In the last expression, for simplicity, the index m and its corresponding summation sign have been suppressed with an understanding that in a closed acoustic cavity a particular selected ray, representing a random pulse, can pass through a given receiving point many number of times, thus making pressure contributions there at those instances, as a result of the multiple reflections the ray suffers during its life time trajectory.

The relation given by Eq. 24 is now divided on both sides by ρc^2, the characteristic impedance of the supporting medium, to yield the following expression for the expected pressure in the nondimensional form

$$p_j^*(\underset{\sim}{x}_r) = (T_p / N \; c^2 \Delta V \; \Delta t) \sum_{i=1}^{N} \dot{Q}_i R_i \Delta R_i$$

where $p_j^*(\underset{\sim}{x}_r) = p_j(\underset{\sim}{x}_r) / \rho c^2$ (25)

the overhead star (*) denoting the variable in nondimensional form.

Statistical Fluctuations

As pointed out earlier the economic considerations, in general, keep the sample size N relatively low; and as a consequence, the results obtained from the statistical algorithm of Eq. 24 would obviously show certain random fluctuations. In such circumstances it is essential to have the knowledge of the standard deviation; which is obtained by repeating the calculations leading to Eq. 24 in, say, K different blocks with the sample value in any individual block k, where $1 \leqslant k \leqslant K$, is given by N_k. The results for this can be expressed as

$$\left[p_j^*(x_r)\right]_k = (T_p / N_k\, c^2 \Delta V\, \Delta t) \sum_{i=1}^{N_k} \dot{Q}_i\, R_i\, \Delta R_i \qquad (26)$$

which is just an alternative form of Eq. 25.

Now by assigning equal statistical weight to each selection the required pressure field, which is the statistical mean of all of the samples, is given by

$$p_j^*(\underset{\sim}{x}_r) = \sum_{k=1}^{K} W_k \cdot \left[p_j^*(\underset{\sim}{x}_r)\right]_k \qquad (27)$$

where W_k is the statistical weight defined as

$$W_k = N_k / \sum_{i=1}^{K} N_i \qquad (28)$$

The variance of such a pressure field is given by

$$D^2\left\{p_j^*(\underset{\sim}{x}_r)\right\} = \sum_{k=1}^{K} W_k^2 \cdot \left\{ \left[p_j^*(\underset{\sim}{x}_r)\right]_k - p_j^*(\underset{\sim}{x}_r) \right\}^2$$

$$= \sigma^2_{p_j^*} \qquad (29)$$

where $\sigma_{p_j}^*$ is the required deviation of the predicted acoustical pressure in the j^{th} time interval at a given receiving point $\underset{\sim}{x}_r$.

A flow diagram showing the computer logic necessary to perform these calculations is given in Fig. 8. Before applying the technique thus developed, to a specific problem, it is essential to examine its validity in more detail; this is done in the following chapter.

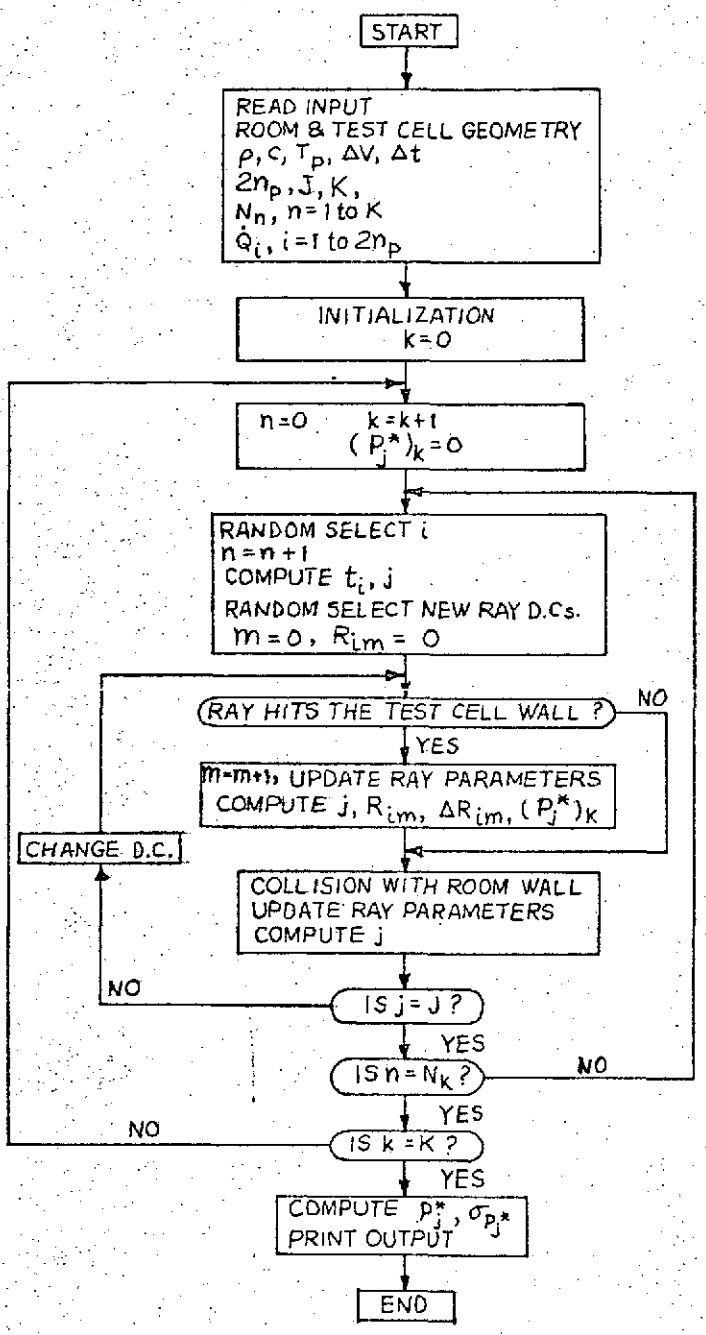

Fig. 8 Flow Diagram of the Monte Carlo Method Applied to Rectangular Problem

Chapter 4

VERIFICATION OF THE ALGORITHM

The proposed Monte Carlo approach for applications to acoustical field solutions being a new one, it is prudent to check its consistency by considering the results that would be obtained by solving a few simple problems. The first solution that is considered here is that of a source in an unbounded medium, whilst the second is that of the ultimate average pressure rise that to be expected in a rectangular room; both are treated in the present chapter by evaluating the algorithm of the Monte Carlo technique, given in Eq. 24 of the preceding chapter, and then comparing with the known solutions.

SOURCE IN UNBOUNDED MEDIUM

The problem is illustrated in Fig. 9. An isotropic point source of strength $Q(t)$, such that the quantity $\dot{Q}(t)$ is constant over its total period $T_p (>>\Delta t)$,

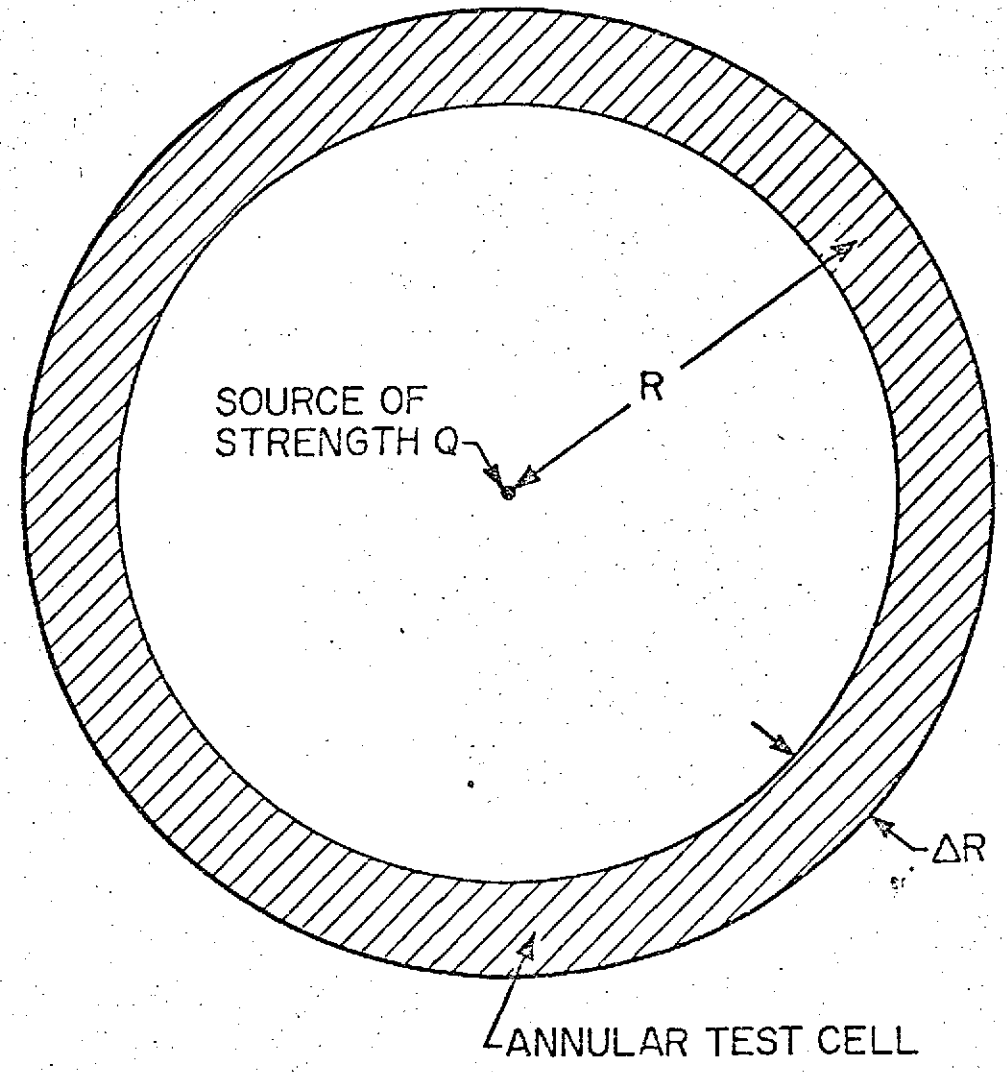

Fig. 9 Point Source in an Unbounded Medium

is surrounded by an annular test cell of mean radius R(=ct), thickness $\Delta R(= c\,\Delta t)$, and thus of volume

$$\Delta V = 4\pi R^2 \Delta R \qquad (1)$$

Let j be the time index corresponding to the time interval from $(t-\Delta t/2)$ to $(t+\Delta t/2)$, and N be the total number of rays selected to characterize the complete strength time history of the source of period T_p; then that corresponding to the elemental time interval Δt is given by

$$n = N\,\Delta t / T_p \qquad (2)$$

During the interval of the j^{th} time cell every selected ray, out of these n, penetrates the test cell volume for a distance

$$\Delta R_{im} = \Delta R \qquad (3)$$

and at a mean distance of travel

$$R_{im} = R \qquad (4)$$

Substitution of these values into Eq. 24 of Chapter 3 results in the following expression for the acoustic pressure during the j^{th} time interval

$$p_j = \dot{Q} / 4\pi R \qquad (5)$$

which is the known analytical solution for the problem.

SOURCE IN BOUNDED MEDIUM

Consider a point source acting in a bounded medium of volume V. The position of the point source, it is recalled, is a point of singularity where the fluid is introduced or abstracted at a certain rate, and the volume Q(t) thus introduced per unit time represents the strength of the source in question. At any time t, the fluid volume introduced by the source then can be expressed as

$$dV(t) = \int_0^t \int_0^\tau \dot{Q}(\mu)\, d\mu\, d\tau$$

$$= \left[\tau \int_0^\tau \dot{Q}(\mu)\, d\mu\right]_0^t - \int_0^t \tau\, \dot{Q}(\tau)\, d\tau \qquad (6)$$

If the source only operates for its period from t=0 to $t=T_p$, and cuts off at $t=T_p$ satisfying the condition

$$\int_0^{T_p} \dot{Q}(t)\, dt = 0 \qquad (7)$$

then the final volume introduced by this source can be expressed as(using Eqs. 6 and 7 above)

$$dV(t > T_p) = dV(T_p)$$
$$= -\int_0^t \tau \, \dot{Q}(\tau) \, d\tau \qquad (8)$$

Consider now the source strength time history of the source to be replaced by its equivalent finite approximation (Fig. 3) consisting of $2n_p$ elementary pulses; then Eq. 8 takes the form

$$dV(t_j) = -\Delta\tau \sum_{i=1}^{2n_p} t_i \, \dot{Q}_i \quad , \text{for } t_j > T_p$$

Since this relation represents the final fluid volume introduced by the source, the total change in the density of the fluid medium, resulting from the activation of the source in question, is given by

$$d\rho(t_j) = \rho \, dV(t_j) / V$$

or in other words,

$$d\rho(t_j) / \rho = dV(t_j) / V$$
$$= -(\Delta\tau / V) \sum_{i=1}^{2n_p} t_i \, \dot{Q}_i \qquad (9)$$

When this is small compared to unity, the pressure changes can be taken proportional to changes in the density, and the resulting acoustical pressure can then be expressed as

$$p(t) = \kappa \cdot d\rho(t) / \rho \qquad (10)$$

where κ is the elasticity of the medium and is given by

$$\kappa = \begin{cases} \rho c^2 & \text{, for isothemal compression} \\ \rho c^2/\gamma & \text{, for adiabatic compression} \end{cases} \qquad (11)$$

γ is the ratio of two specific heats of the fluid, for air $\gamma = 1.402$.

Now consider the expected pressure rise predicted by the Monte Carlo method, using Eq. 24 of Chapter 3. Because the selection of any one of the $2n_p$ pulses is equally possible, it is readily shown that

$$E\{p_j\} = (\rho T_p / N \Delta V \Delta t) \cdot E\left\{ \sum_{i=1}^{N} \sum_{m} \dot{Q}_i R_{im} \Delta R_{im} \right\}$$

$$= (\rho c \Delta\tau / \Delta V \Delta t) \sum_{i=1}^{2n_p} \dot{Q}_i \cdot (t_j - t_i) \cdot E\{R\} \qquad (12)$$

where $E\{\Delta R\}$ is the expected value of the penetration distance. This is most readily obtained, for the case of a rectangular room, by using the method of images as shown in Fig. 10, and considering the effect of all of the image sources. The total number of such images which can influence the pressure p_j is the number in an annular volume of radius $c(t_j-t_i)$ and thickness $c\,\Delta t$. Since there is one source per room of volume V, the total number is

$$4\pi c^3 (t_j-t_i)^2 \Delta t / V$$

This number is actually equal to the number of reflections in the room during the corresponding period. The expected penetration into the test cell ΔV of any one of these is equal to

$$\Delta V / 4\pi c^2 (t_j-t_i)^2$$

Therefore the expected value of the penetration is the product of these, so that

$$E\{\Delta R\} = c\,\Delta V\,\Delta t / V \qquad (13)$$

Substituting into Eq. 12, assuming the cut off condition given by Eq. 7 to hold,

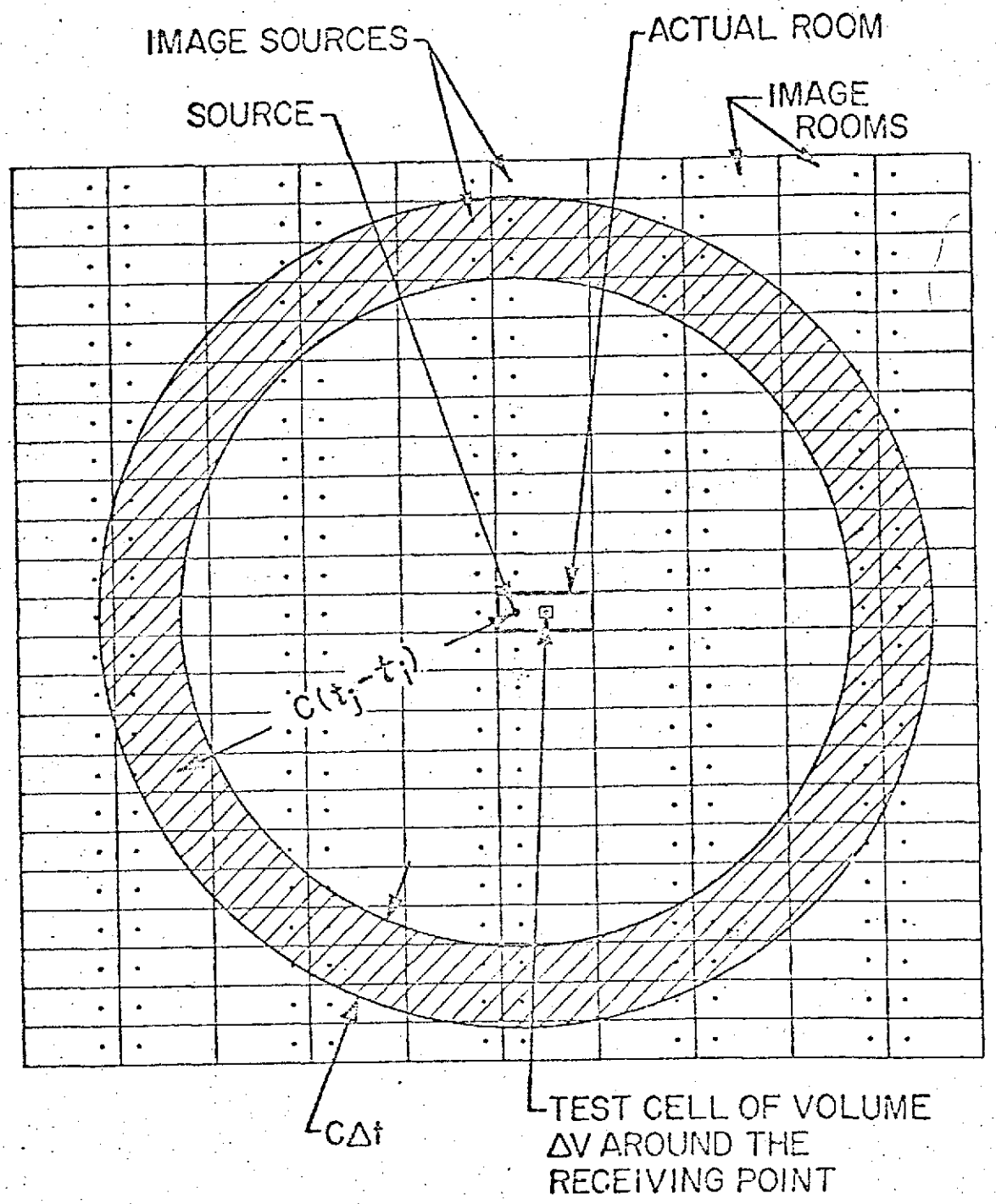

Fig. 10 Average Pressure by Image Method

$$E\left\{p_j\right\} = (\rho c^2 \Delta\tau / V) \sum_{i=1}^{2n_p} \dot{Q}_i \cdot (t_j - t_i)$$

$$- (\rho c^2 \Delta\tau / V) \sum_{i=1}^{2n_p} t_i \cdot \dot{Q}_i \quad , \text{for} \quad t_j > t_i \qquad (14)$$

which is in agreement with Eq. 10, in the light of Eqs. 9 and 11.

This provides the requisite verification of the Monte Carlo technique, and thereby confirms the algorithm that is given in Eq. 24 of the preceding chapter.

Chapter 5

CALCULATIONS FOR RECTANGULAR ROOM

RECTANGULAR ROOM PROBLEM

The sound received at one point from any other point in the same room has two parts; that received directly and that received along a number of indirect paths involving reflections at the boundary walls. It has been realized for a long time that the reflection pattern in a room, the background noise, and certain characteristics of hearing are the major factors that govern the room acoustics; but exactly how these factors combine to give the ultimate results has not been very clearly understood. Nevertheless the quality of speech and music, for example, in a room is a function of the reflection pattern.

In general a sound source can be represented as pulsed wave trains. Most sounds of speech and music can

be classified as pulsed wavetrains whose amplitudes and frequency components fluctuate sufficiently within the time intervals shorter than the time constant of a given room so that the room seldom reaches the steady state. Thus the transient response of the room to transient sounds of this general type is an especially important physical problem of room acoustics. The task of describing mathematically the response of a room to an arbitrary transient, and of studying the roles of room geometry and distribution of absorbing materials in this response is extremely complicated (Morse, 1968). The Monte Carlo technique developed in the preceding chapter appears to be well-suited for this purpose, the object of this chapter is to demonstrate this with the help of a simple physical model.

An important aspect of architectural acoustics is to get a clearer picture of the relation between the reflection patterns and the subjective quality. The proper control of the distribution of sound energy throught a room and of the growth and decay of the transient sounds are the prime objectives of good acoustical design. Any attempt to this end on quantitative basis calls for a systematic interpretation of the reflection patterns by the hearing mechanisms. It is anticipated that the proposed Monte Carlo technique will prove very helpful here by providing the quantitative prediction of the reflection patterns.

The specific physical model that is considered for the application of the Monte Carlo technique consists of a nonconducting, isotropic, homogeneous medium enclosed by rectangular walls. The essential dimensions of the room are :

length 110 ft. , width 66 ft. , height 44 ft. Calculations are presented for a pressure field caused by an actuating point source characterized by a single cycle double rectangular pulse, sinusoidal pulse, and N-shape pulse as shown in Fig. 11; the mathematical representation of the source in each of these three cases being given by

Double Rectangular Pulse

$$\dot{Q}(t) = (4/\pi)\left[1 - H(t)\right] \cdot \sum_{n=1}^{\infty} \left\{ \sin\left[2(2n-1)\pi\, t/T_p\right] \right\} /(2n-1) \qquad (1)$$

Sinusoidal Pulse

$$\dot{Q}(t) = \left[1 - H(t)\right] \left\{ \sin\left[2\pi\, t/T_p\right] \right\} \qquad (2)$$

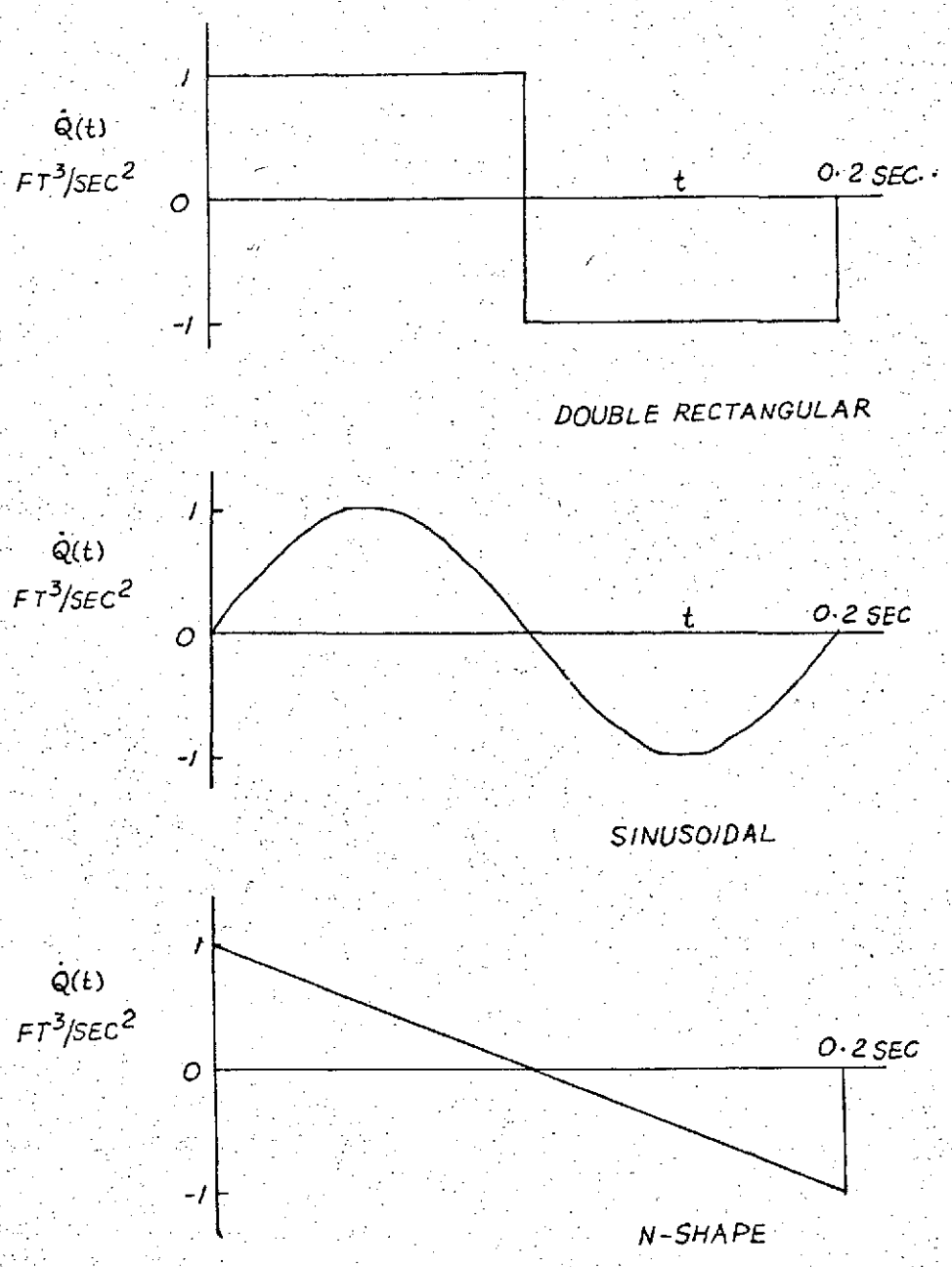

Fig. 11 Point Source Pulse Configuration

N-shape Pulse

$$\dot{Q}(t) = (2/\pi)\,[1 - H(t)] \sum_{n=1}^{\infty} \left\{ \sin [2n\pi t/T_p] \right\} /n \qquad (3)$$

where $H(t)$ is the unit step function defined as

$$H(t) = \begin{cases} 0 \;, & t < T_p \\ 1 \;, & t > T_p \end{cases}$$

$T_p = 0.2$ secs., is the source time period.

The results are grouped in seven different cases for material absorption coefficient ranging from zero to one hundred percent on different walls, with as many as six different receiving points dispersed in the region.

GEOMETRICAL SPECIFICATION

The selected Cartesian coordinate system (X1, X2, X3) is shown in Fig. 12. To facilitate further discussion, each wall is designated by a symbol WLn(n=1 to 6), and is shown in Fig. 12 along with an equation of its defining coordinate plane. The number of receiving points chosen for the evaluation of the acoustical field is six; the individual locations of these receiving points with their specific symbolic designations : D, E, F, G, H, I are shown

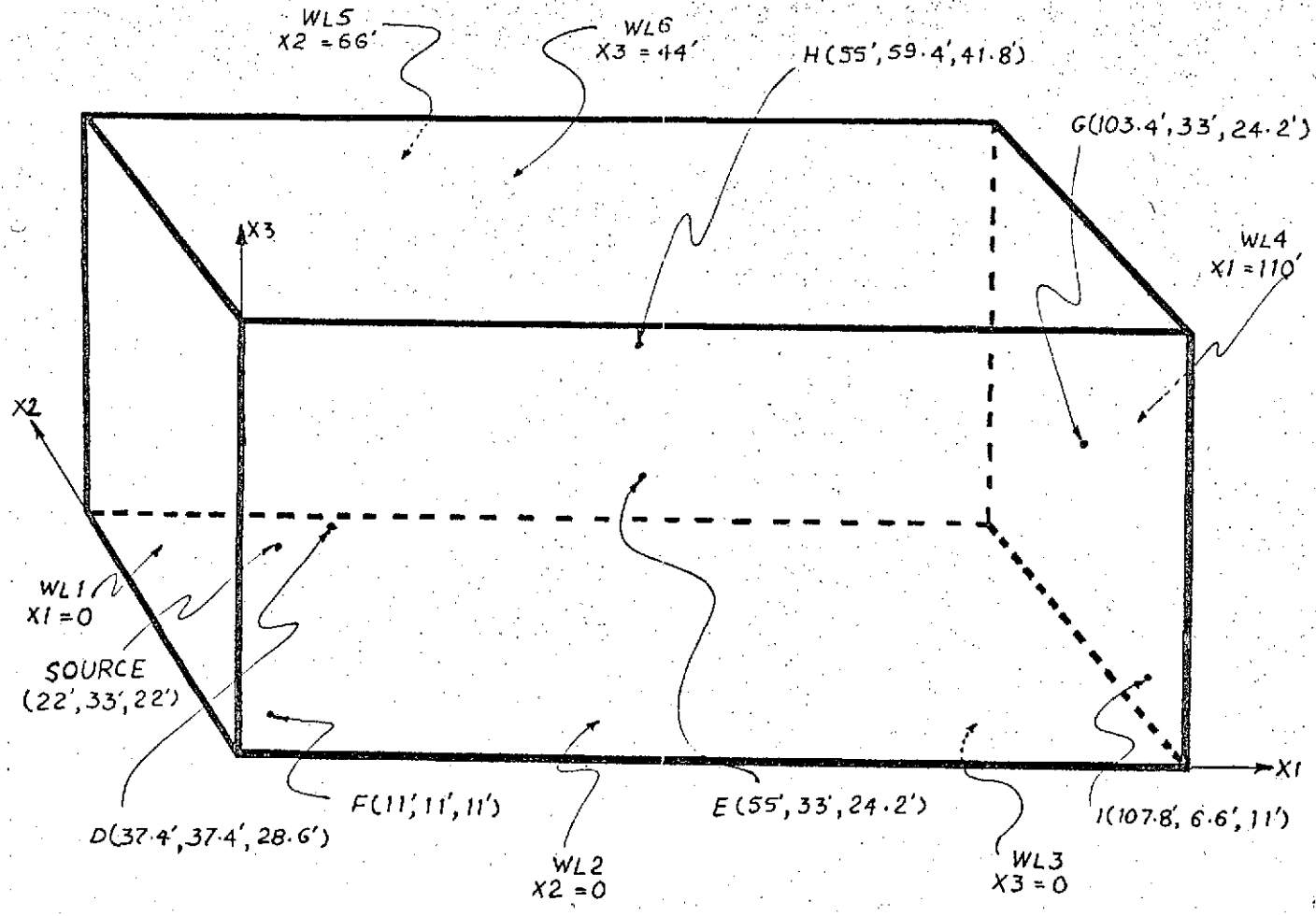

Fig. 12 Geometrical Specification Rectangular Room Problem

in Fig. 12, also seen there is the position of the point source.

MATERIAL SPECIFICATION

In order to study the effect of the variations in the material properties of the bounding walls on the field, the material absorption coefficient was varied from zero to one hundred percent on different walls. The results are grouped into the following seven different cases:

Case 1 All walls perfectly reflecting

Case 2 The wall represented by X1 = 0 , i.e. WL1, is 100 % absorptive; and all other walls perfectly reflecting

Case 3 The wall represented by X3 = 44', i.e. WL6, is 100 % absorptive; and all other walls perfectly reflecting

Case 4 The wall represented by X3 = 0 , i.e. WL3, is 10 % absorptive; and all other walls perfectly reflecting

Case 5 The wall represented by X1 = 110', i.e. WL4, is 20 % absorptive; and all other walls perfectly reflecting

Case 6 The wall represented by X2 = 66', i.e. WL5, is 40 % absorptive; and all other walls perfectly reflecting

Case 7 The wall represented by $X2 = 0$, i.e. WL2, is 60 % absorptive; and all other walls perfectly reflecting.

GENERAL DESCRIPTION OF THE MONTE CARLO RESULTS

The supporting medium was considered to be air with a mass density ρ equal to 0.002378 slugs/ft^3, and a velocity of sound c equal to 1100 ft/sec. Taking the space-time volume (i.e. $\Delta V \ \Delta t$) of the test cell to be 0.4259 ft^3-sec., in each of the above mentioned seven cases, at an individual receiving point, ten blocks of data were collected including a total of 50000 selected signal pulses. The results from these Monte Carlo calculations are presented in the form of the overall mean values with plus and minus one standard deviation in Appendix 4.

In order to study the variations in the pressure values, as a function of the spatial location in the region and the material properties of the bounding surfaces, it was found more convenient to regroup the above results and present only the overall mean values as shown in the following figures:

Double Rectangular Pulse	Figures 13, 14, and 15
Sinusoidal Pulse	Figures 16 to 28

N-shape Pulse Figures 29 to 41.

For these calculations the transition period length of 0.4 seconds, twice the pulse duration, was considered.

The nature of the diffused field can be studied by observing the variations in the pressure values for a longer duration of time at any one receiving point in the region. This is accomplished by accumulating the pressure values at the receiving point E, the one that is in the vicinity of the centre of the rectangular room, for a duration of 0.8 seconds, four times the pulse duration. These results are shown in the following figures :

Double Rectangular Pulse	Figure 42
Sinusoidal Pulse	Figures 43 to 49
N-shape Pulse	Figure 50.

For a case with perfect reflecting walls, i.e. for Case 1, it is possible to make an estimate of the adiabatic pressure rise in the room. The nondimensional pressure values, obtained for the three different source configurations under investigation by the use of Eqs. 9, 10, and 11 of Chapter 4 are

Double Rectangular Pulse	2.80387 E -6
Sinusoidal Pulse	1.785 E -6
N-shape Pulse	1.669 E -6

These levels are marked in Figures 13, 16, 29, 42, 43, and 50.

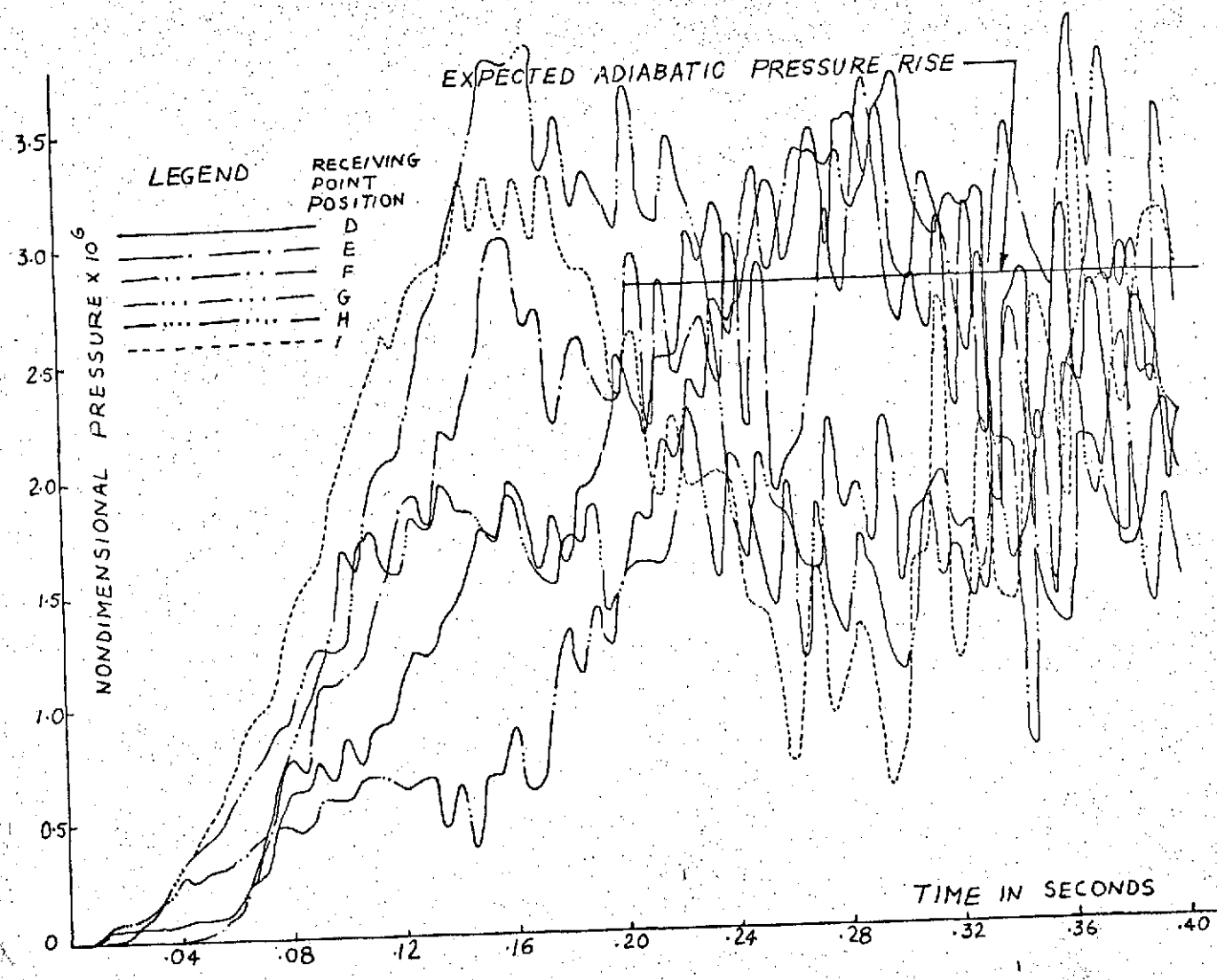

Fig. 13 Pressure Time History at Six Different Receiving Points for Single Cycle Double Rectangular Pulse in Rectangular Room (Case 1)

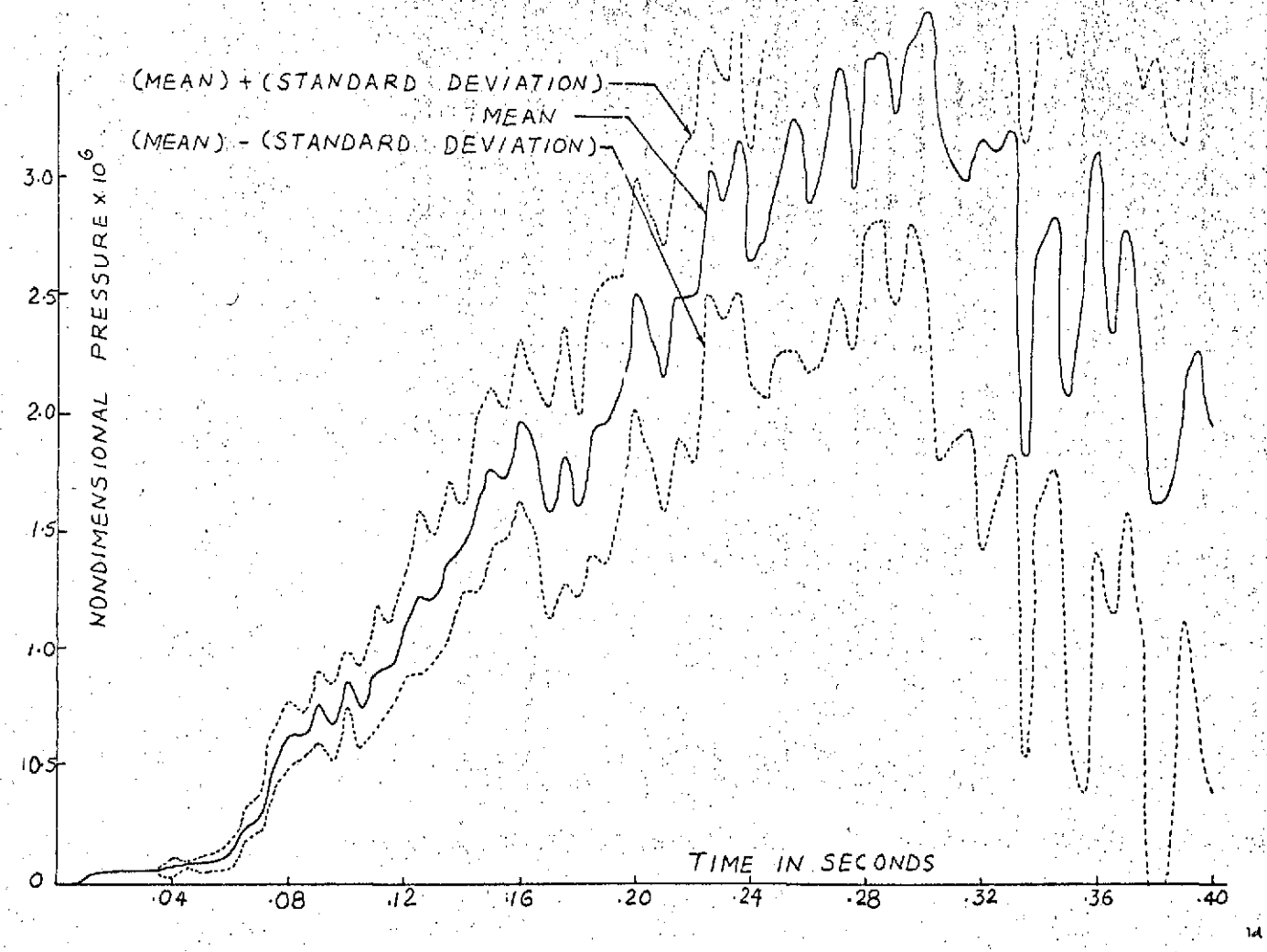

Fig. 13.1 Pressure Time History at Receiving Point D for Single Cycle Double Rectangular Pulse in Rectangular Room (Case 1)

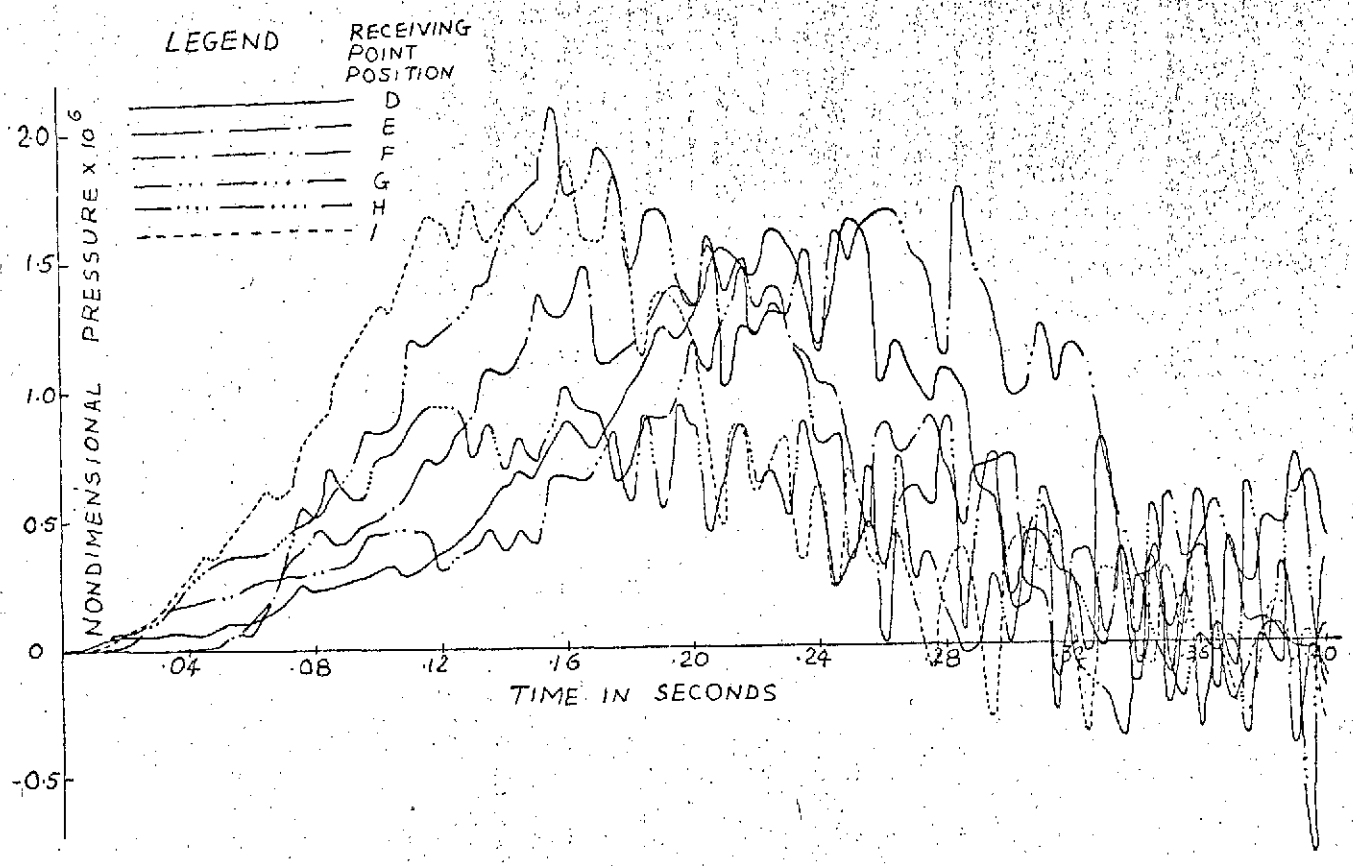

Fig. 14 Pressure Time History at Six Different Receiving Points for Single Cycle Double Rectangular Pulse in Rectangular Room (Case 2)

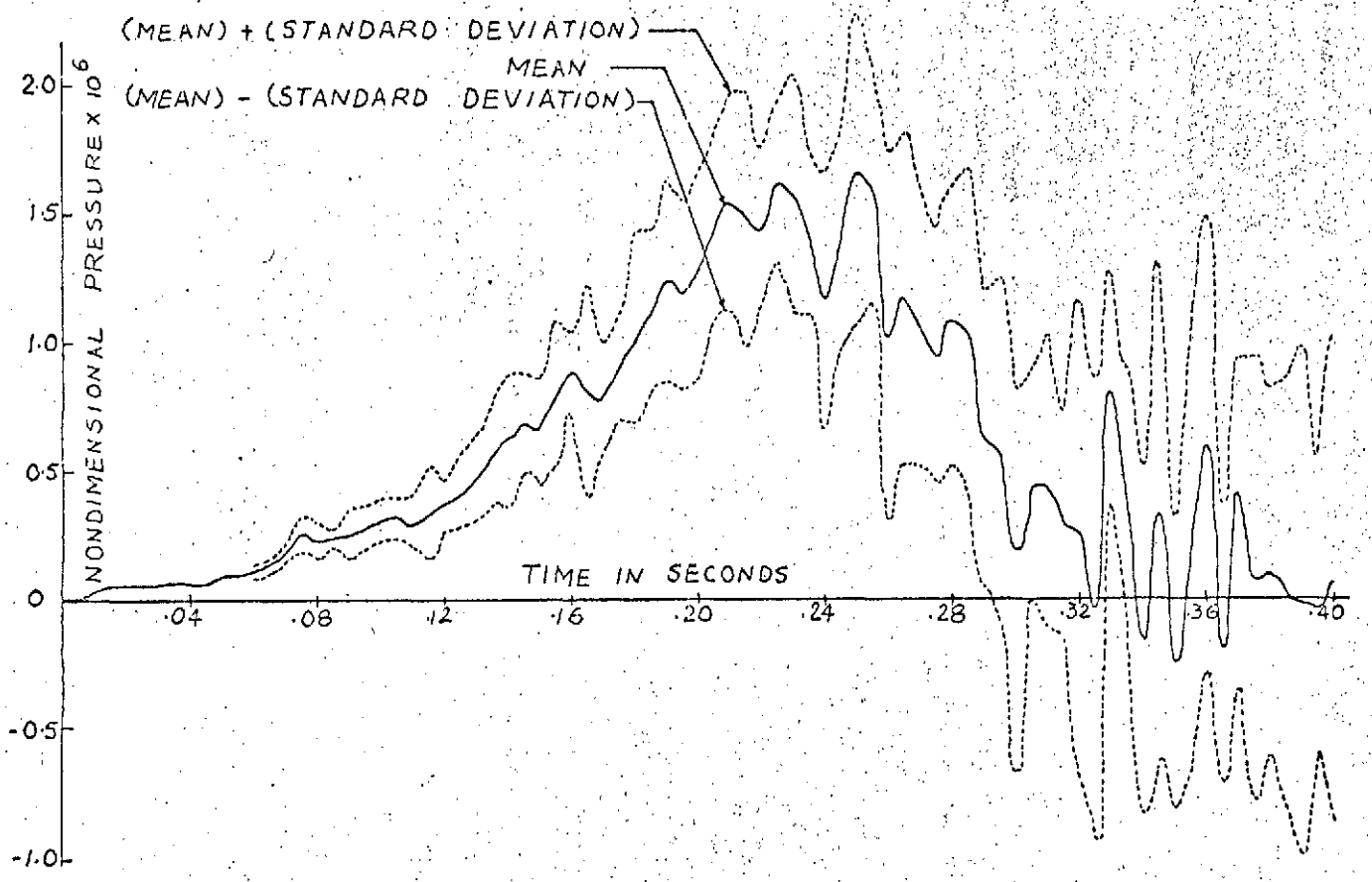

Fig. 14.1 Pressure Time History at Receiving Point D for Single [2d] Cycle Double Rectangular Pulse in Rectangular Room (Case 2)

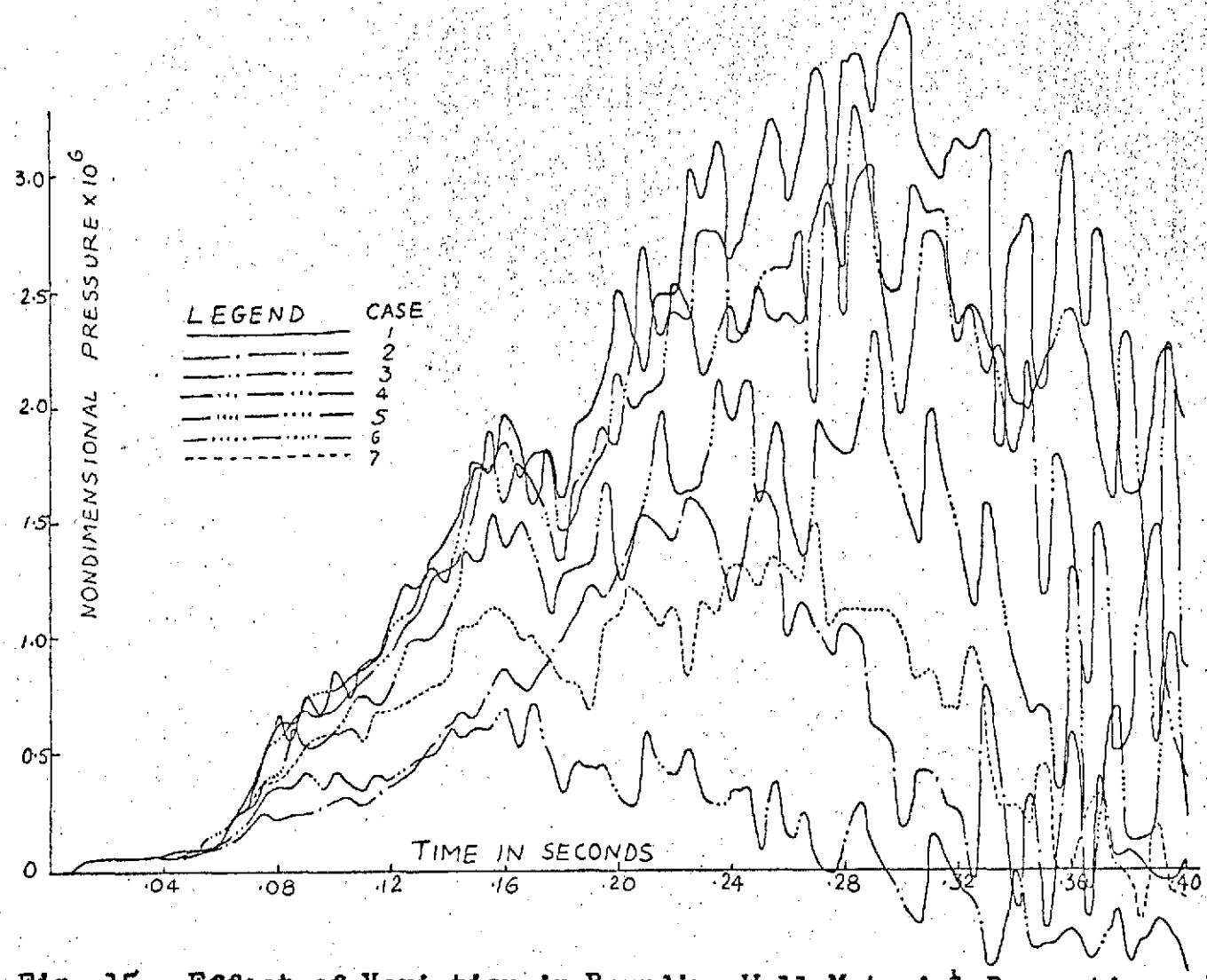

Fig. 15 Effect of Variation in Bounding Wall Material Properties on the Pressure Time History at Receiving Point D for Single Cycle Double Rectangular Pulse in Rectangular Room

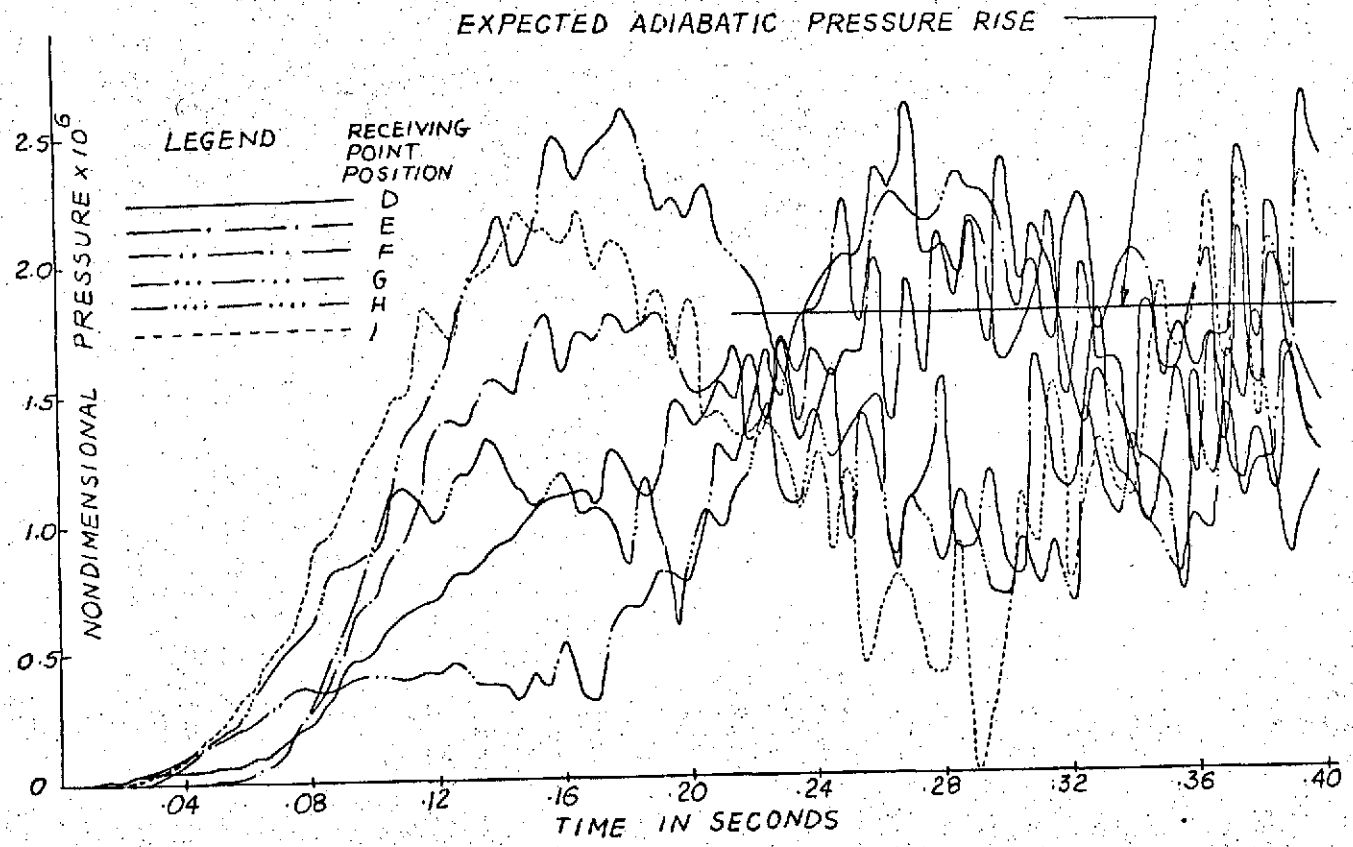

Fig. 16 Pressure Time History at Six Different Receivinng Points for Single Cycle Sinusoidal Pulse in Rectangular Room (Case 1)

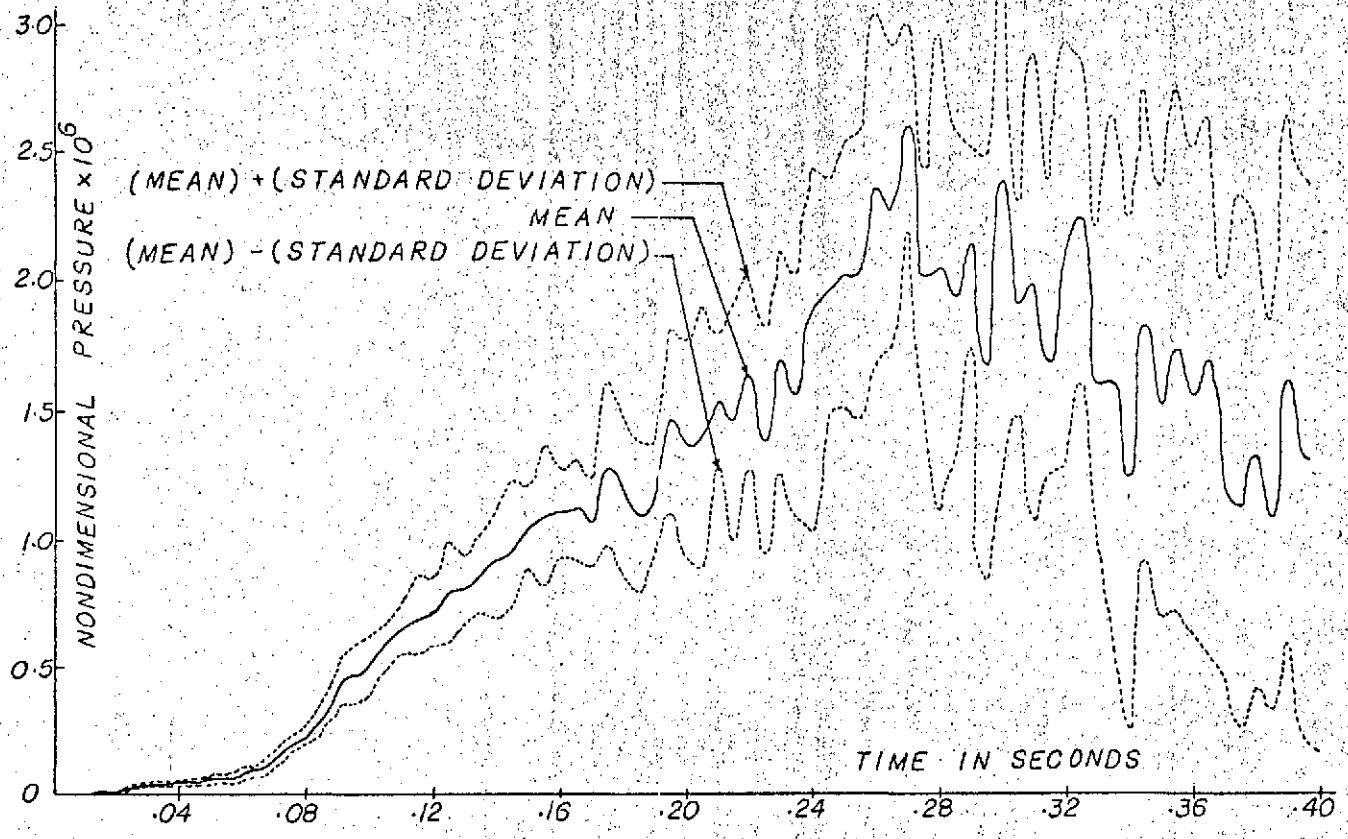

Fig. 16.1 Pressure Time History at Receiving Point D for Single Cycle Sinusoidal Pulse in Rectangular Room (Case 1)

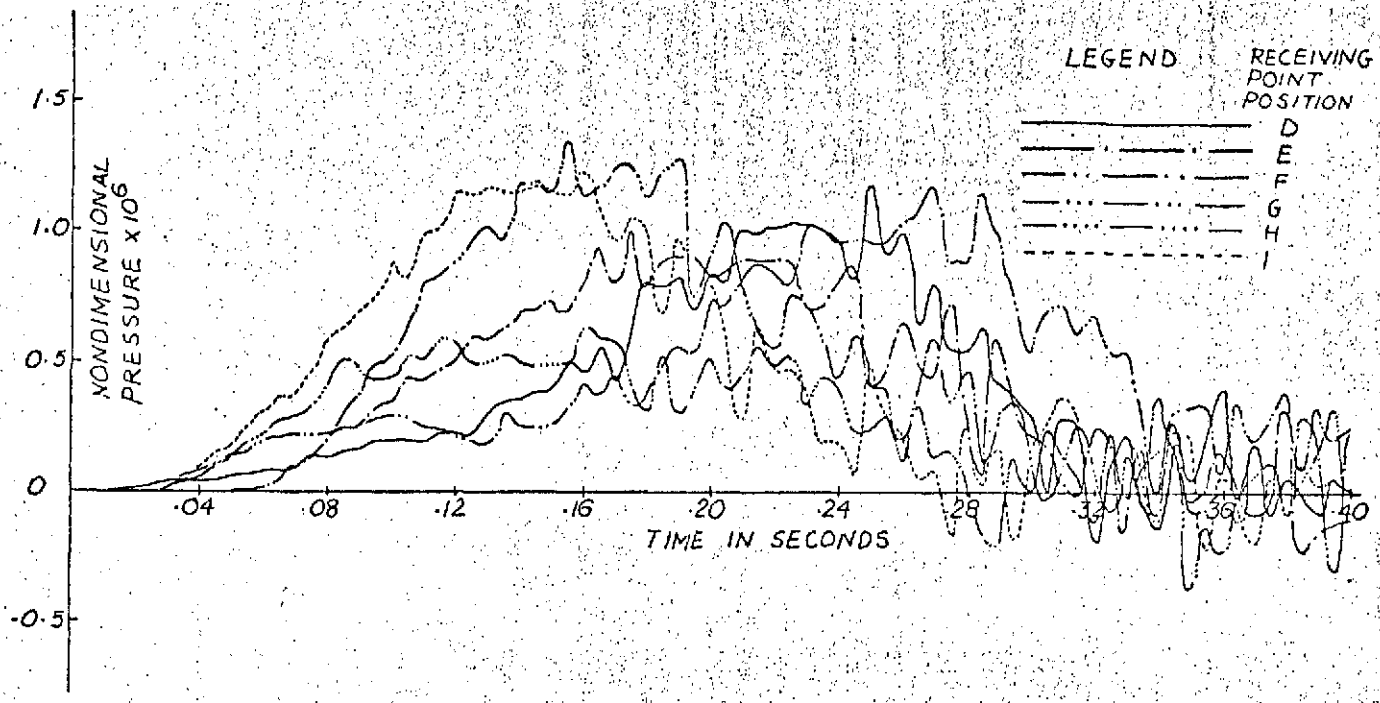

Fig. 17 Pressure Time History at Six Different Receiving Points for Single Cycle Sinusoidal Pulse in Rectangular Room (Case 2)

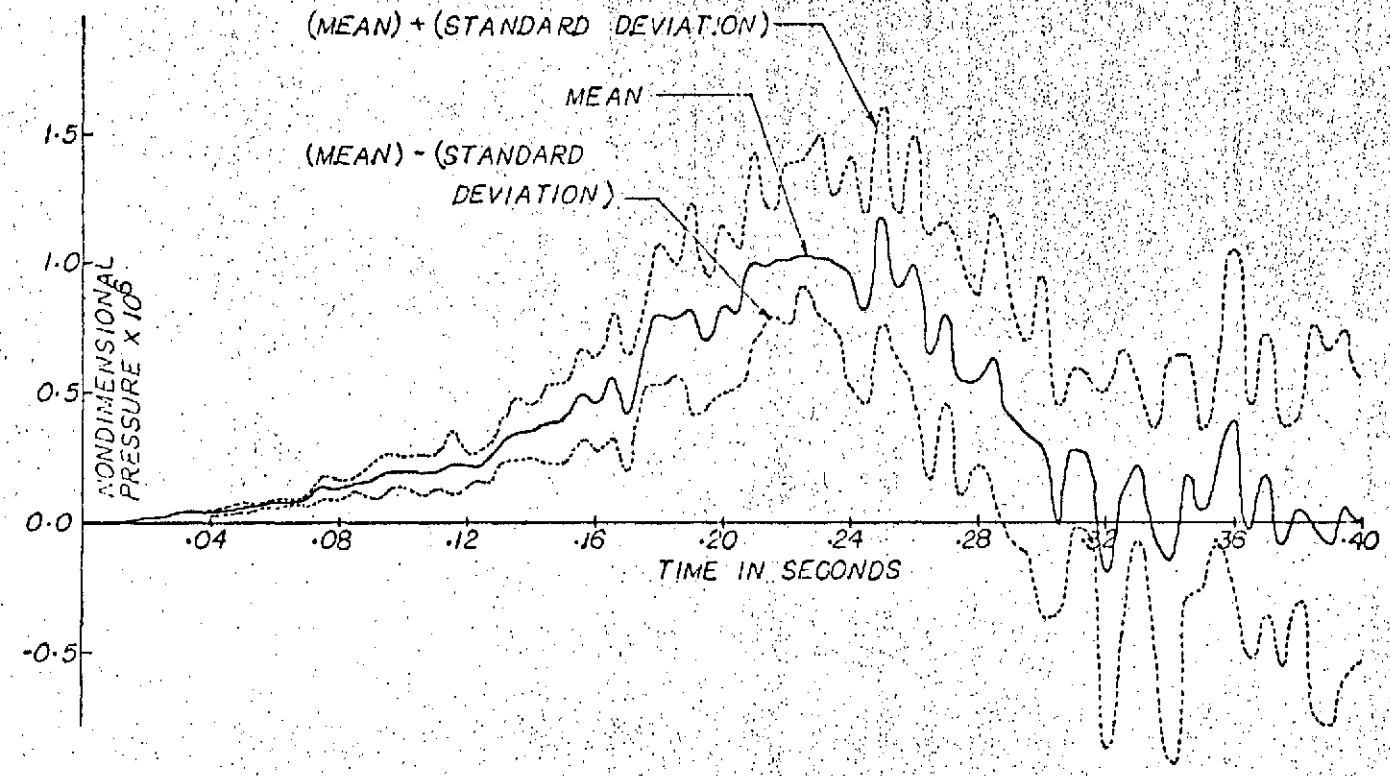

Fig. 17.1 Pressure Time History at Receiving Point D for Single Cycle Sinusoidal Pulse in Rectangular Room (Case 2)

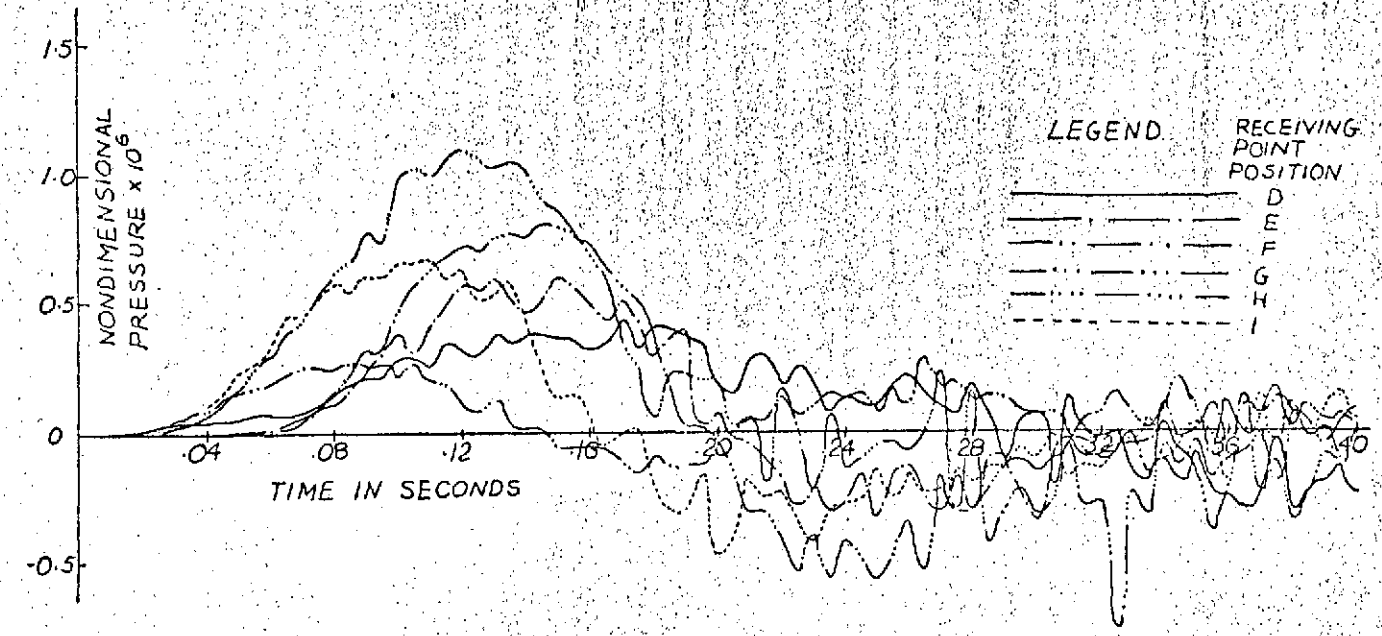

Fig. 18 Pressure Time History at Six Different Receivinng Points for Single Cycle Sinusoidal Pulse in Rectangular Room (Case 3)

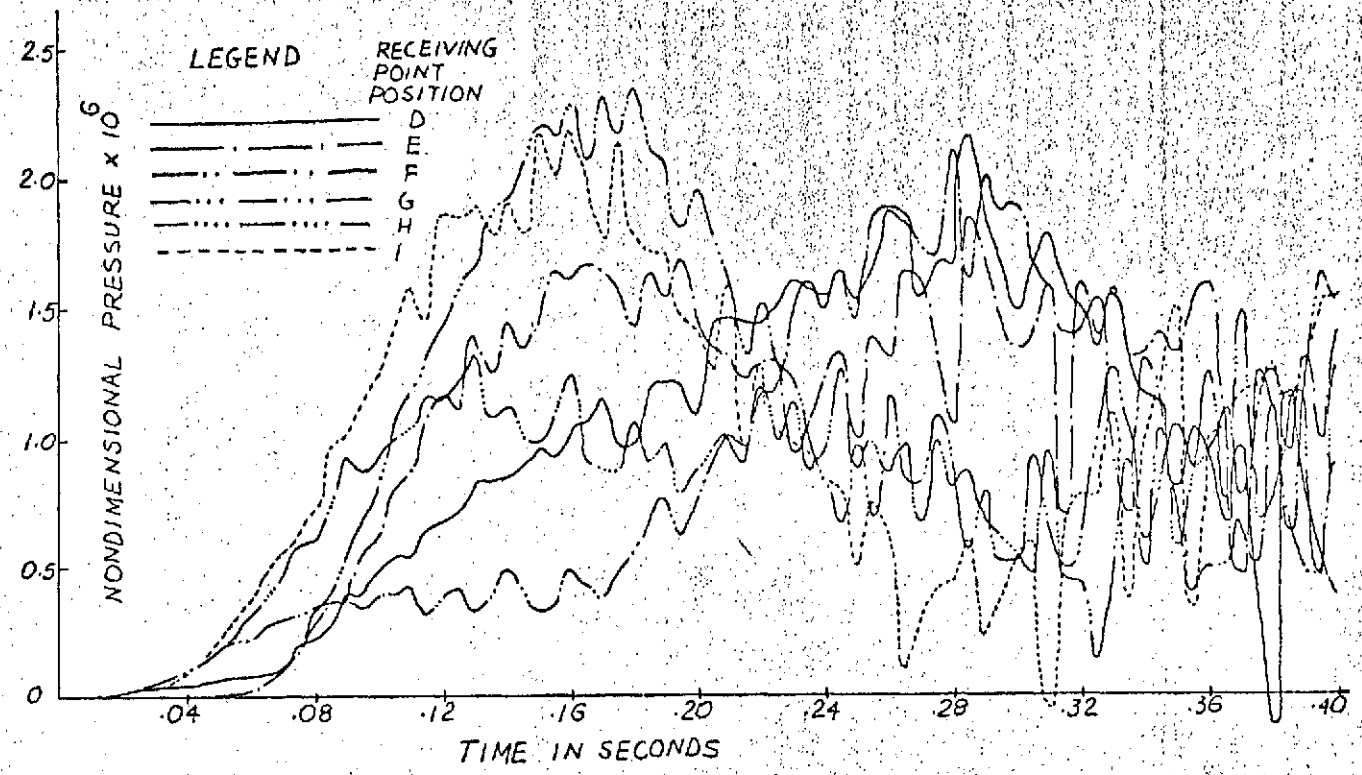

Fig. 19 Pressure Time History at Six Different Receiving Points for Single Cycle Sinusoidal Pulse in Rectangular Room (Case 4)

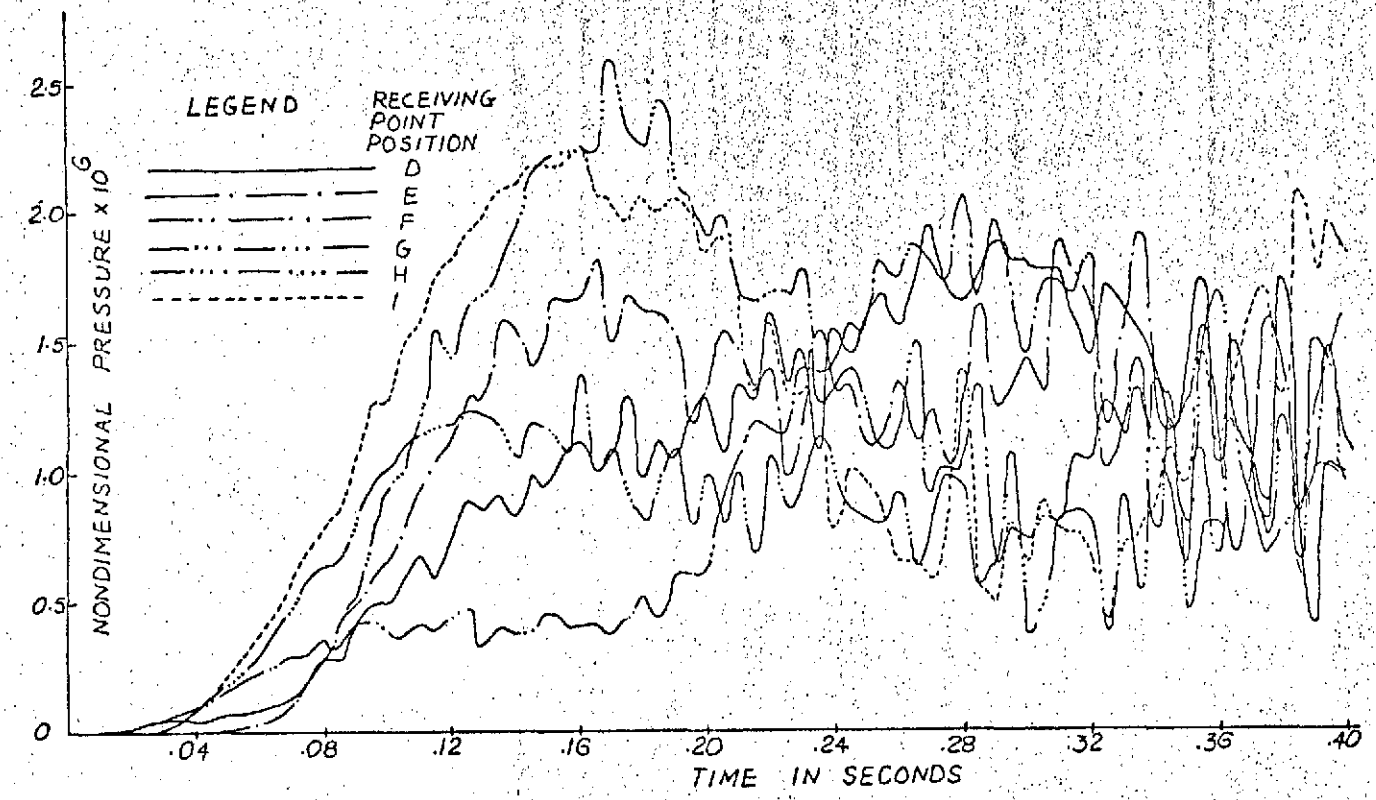

Fig. 20 Pressure Time History at Six Different Receiving Points for Single Cycle Sinusoidal Pulse in Rectangular Room (Case 5)

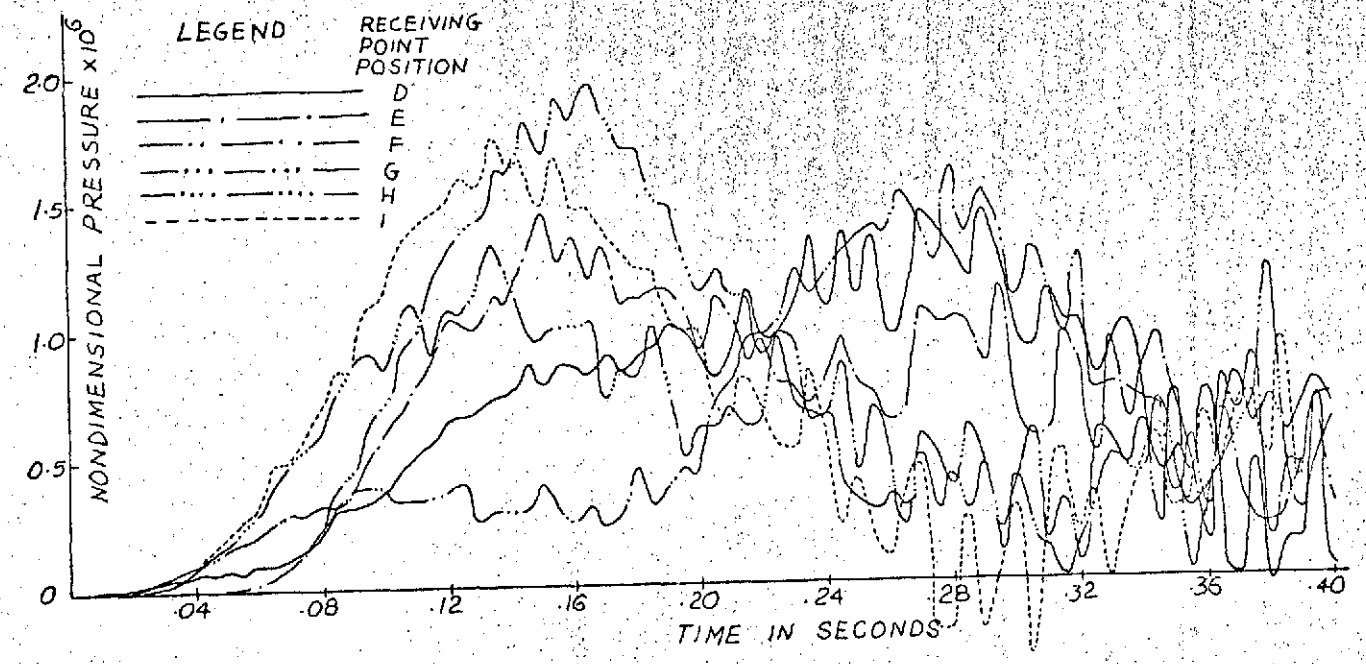

Fig. 21 Pressure Time History at Six Different Receiving Points for Single Cycle Sinusoidal Pulse in Rectangular Room (Case 6)

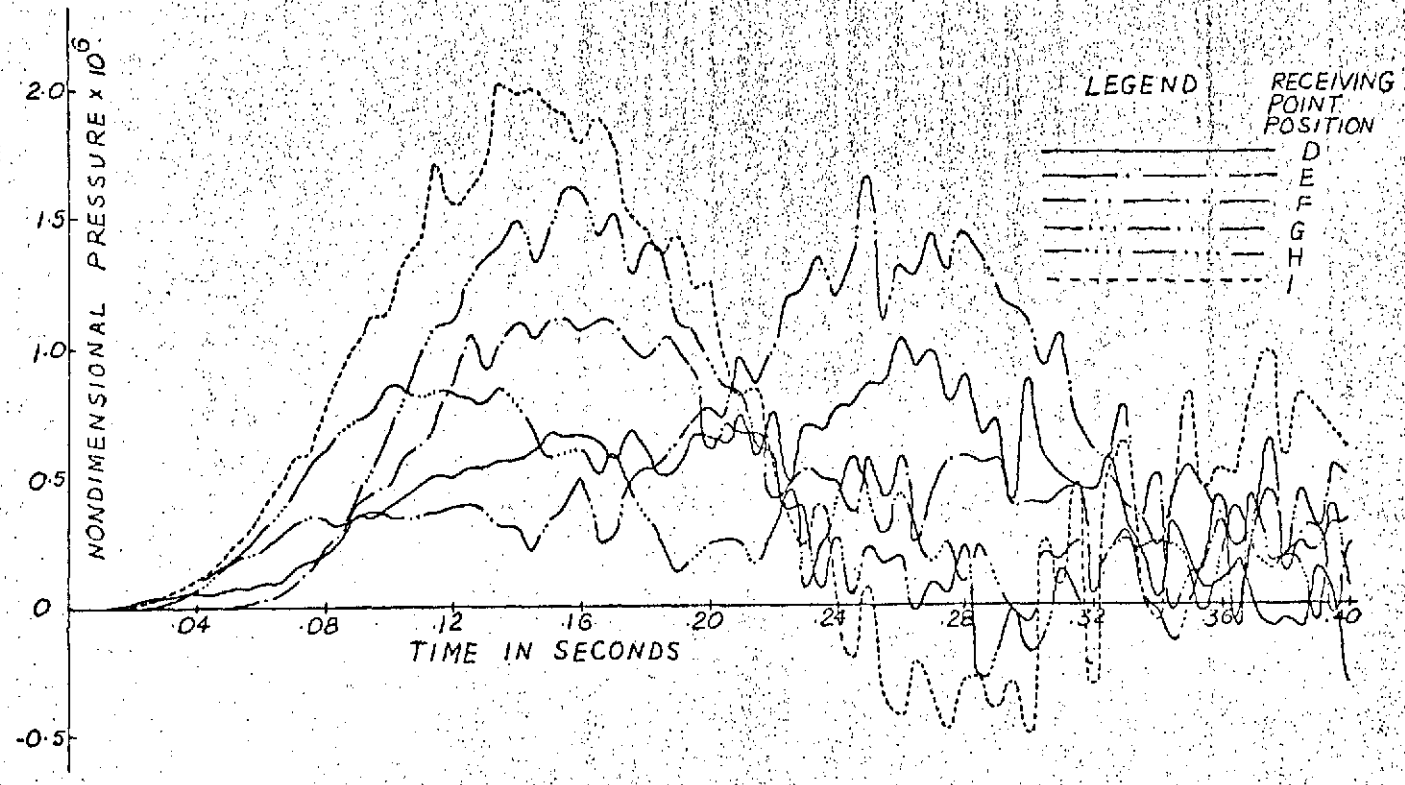

Fig. 22 Pressure Time History at Six Different Receiving Points for Single Cycle Sinusoidal Pulse in Rectangular Room (Case 7)

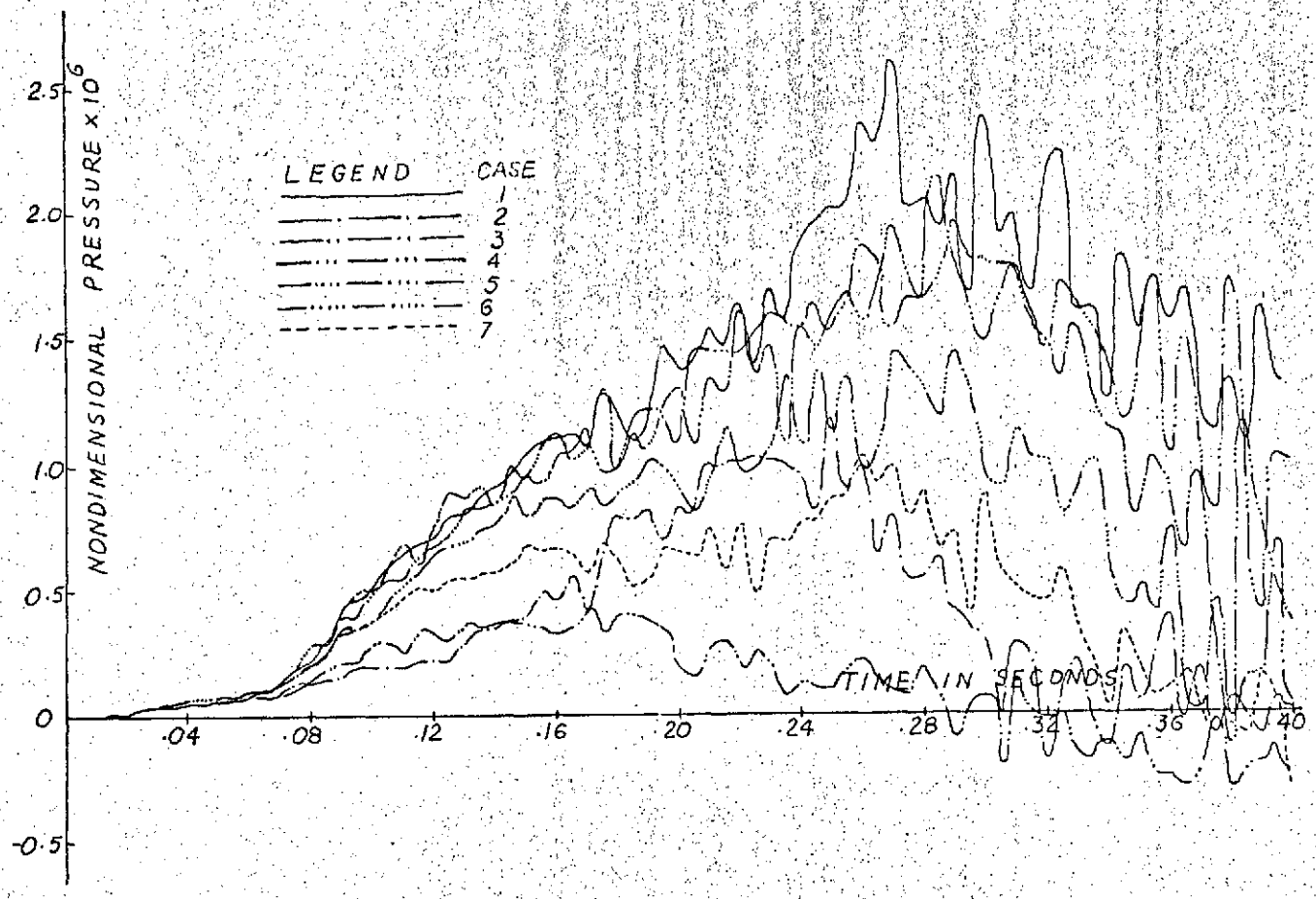

Fig. 23 Effect of Variations in Bounding Wall Material Properties on the Pressure Time History at Receiving Point D for Single Cycle Sinusoidal Pulse in Rectangular Room

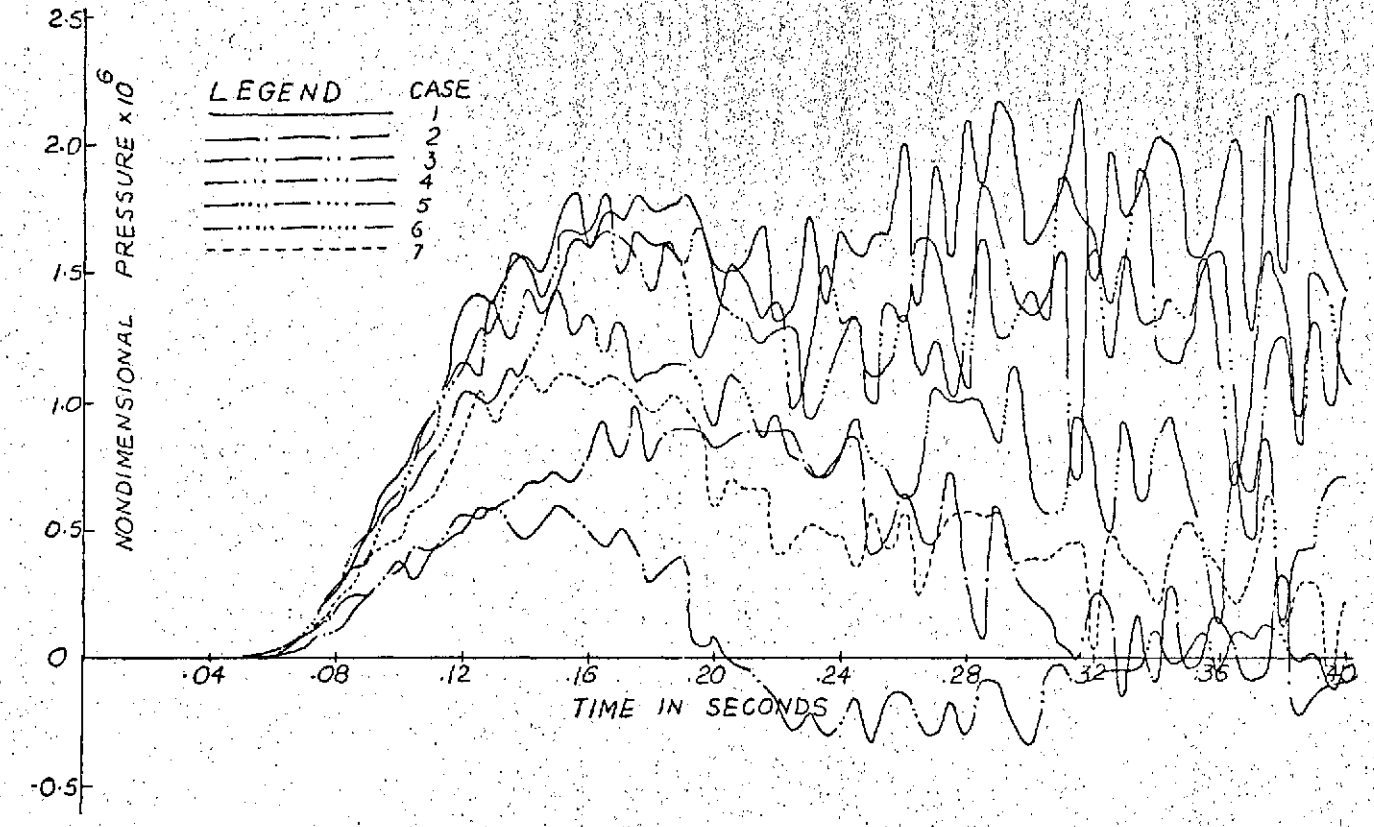

Fig. 24 Effect of Variations in Bounding Wall Material Properties on the Pressure Time History at Receiving Point E for Single Cycle Sinusoidal Pulse in Rectangular Room

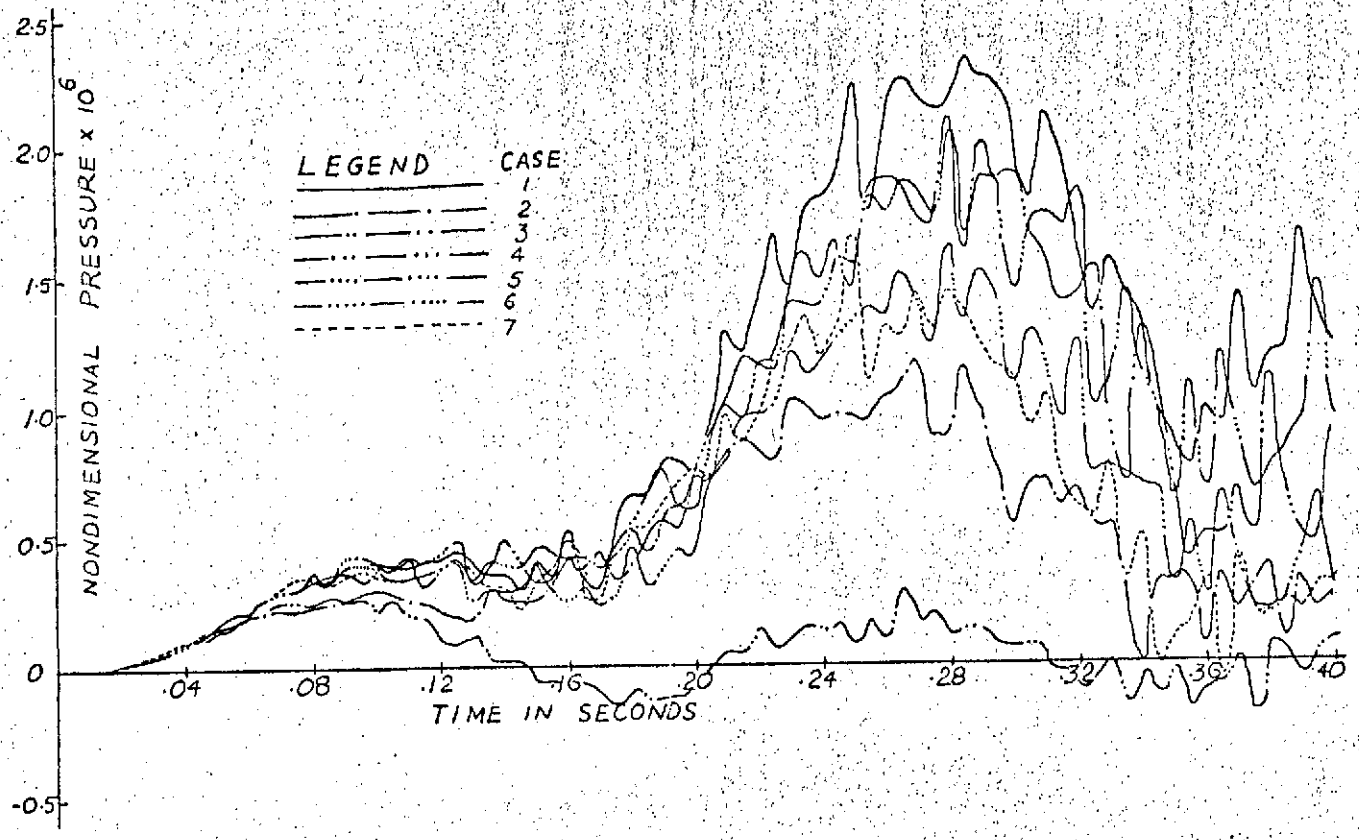

Fig. 25 Effect of Variations in Bounding Wall Material Properties on the Pressure Time History at Receiving Point F for Single Cycle Sinusoidal Pulse in Rectangular Room

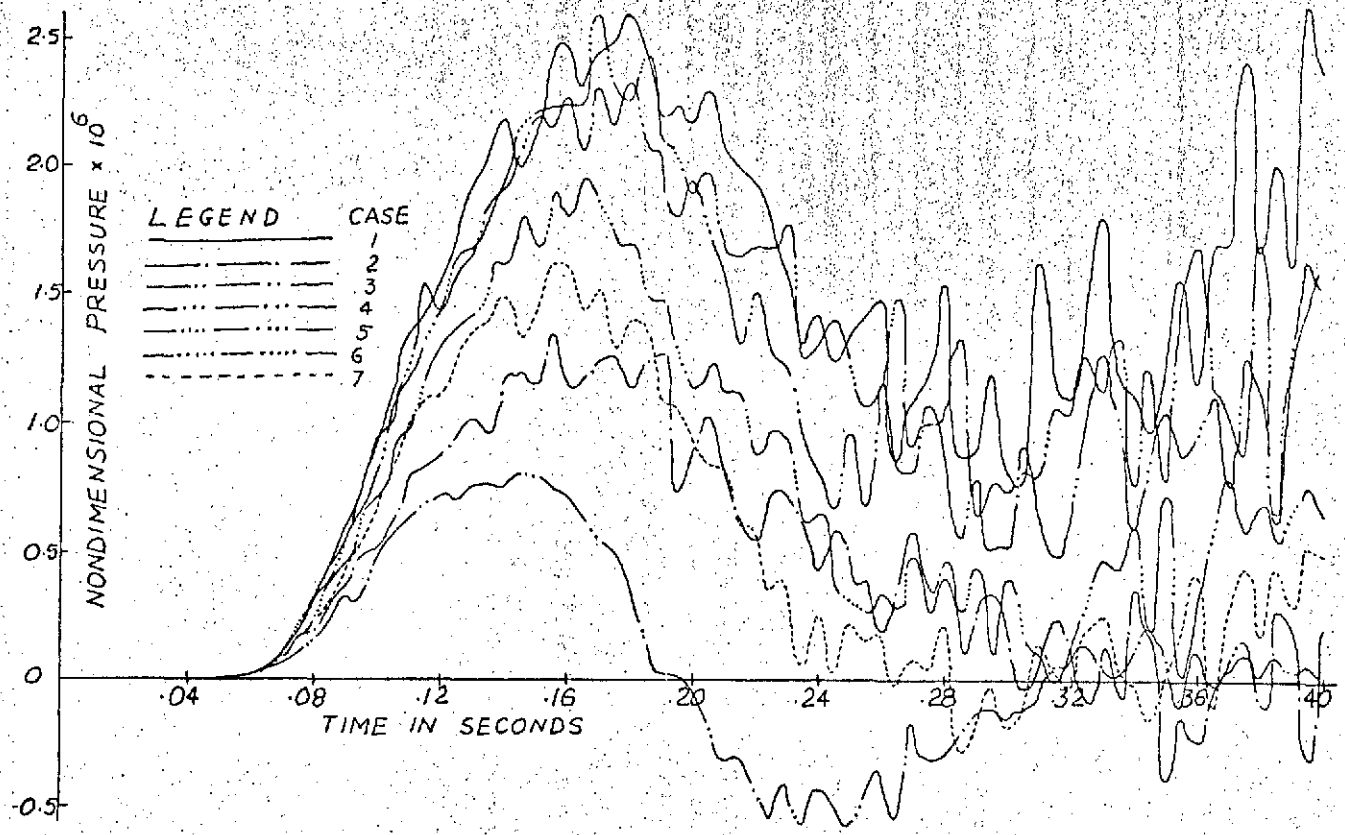

Fig. 26 Effect of Variations in Bounding Wall Material Properties on the Pressure Time History at Receiving Point G for Single Cycle Sinusoidal Pulse in Rectangular Room

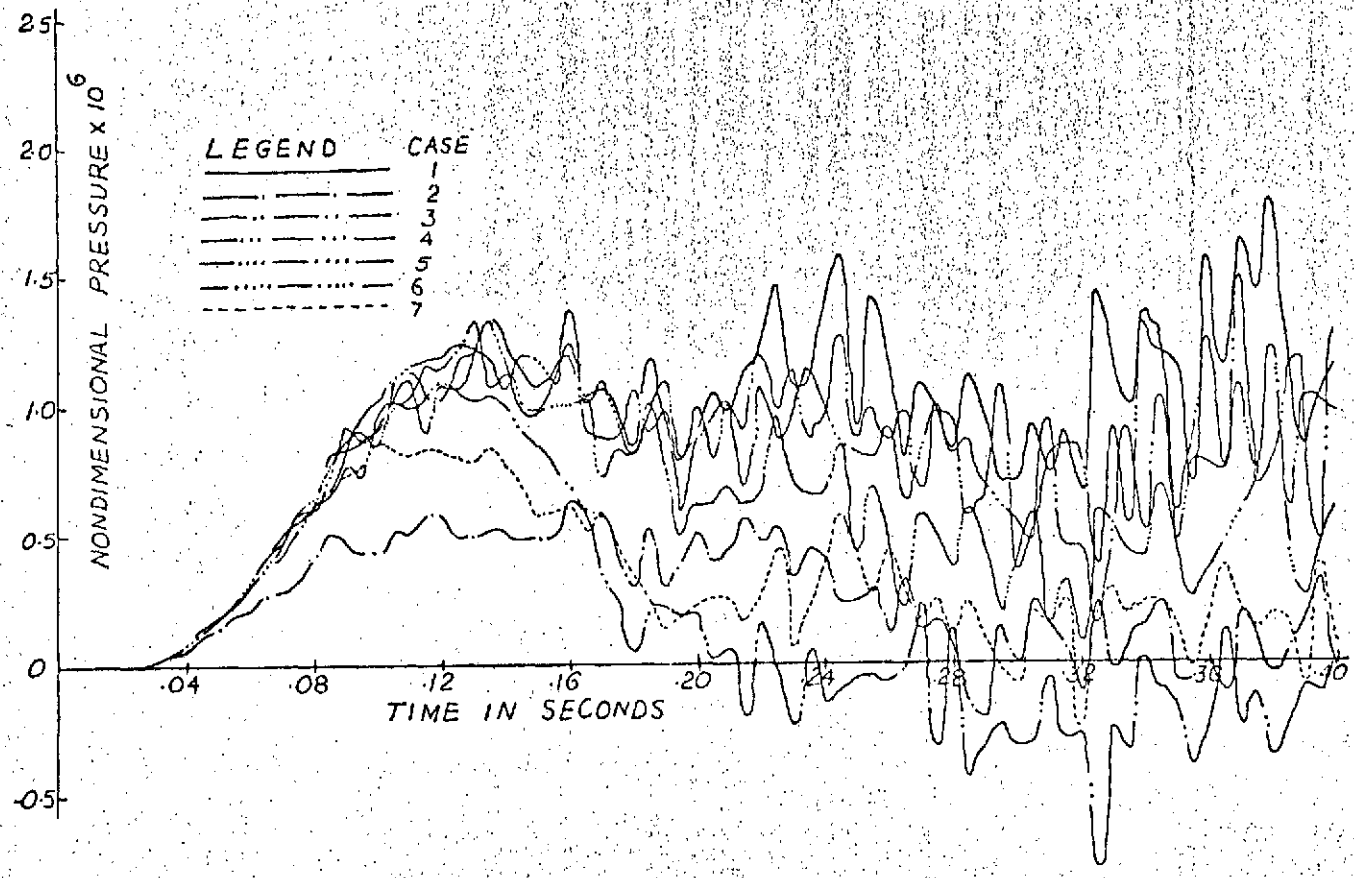

Fig. 27 Effect of Variations in Bounding Wall Material Properties on the Pressure Time History at Receiving Point H for Single Cycle Sinusoidal Pulse in Rectangular Room

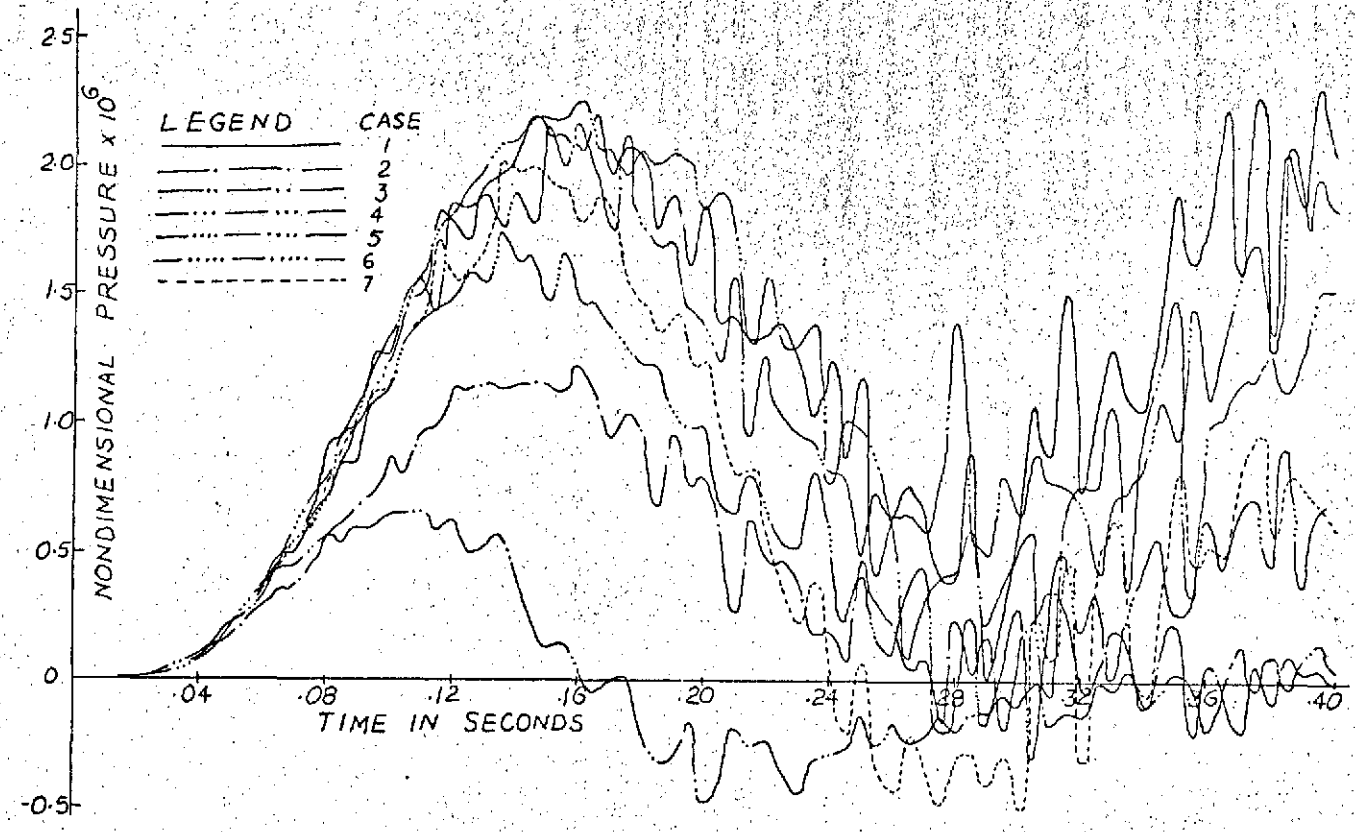

Fig. 28 Effect of Variations in Bounding Wall Material Properties on the Pressure Time History at Receiving Point I for Single Cycle Sinusoidal Pulse in Rectangular Room

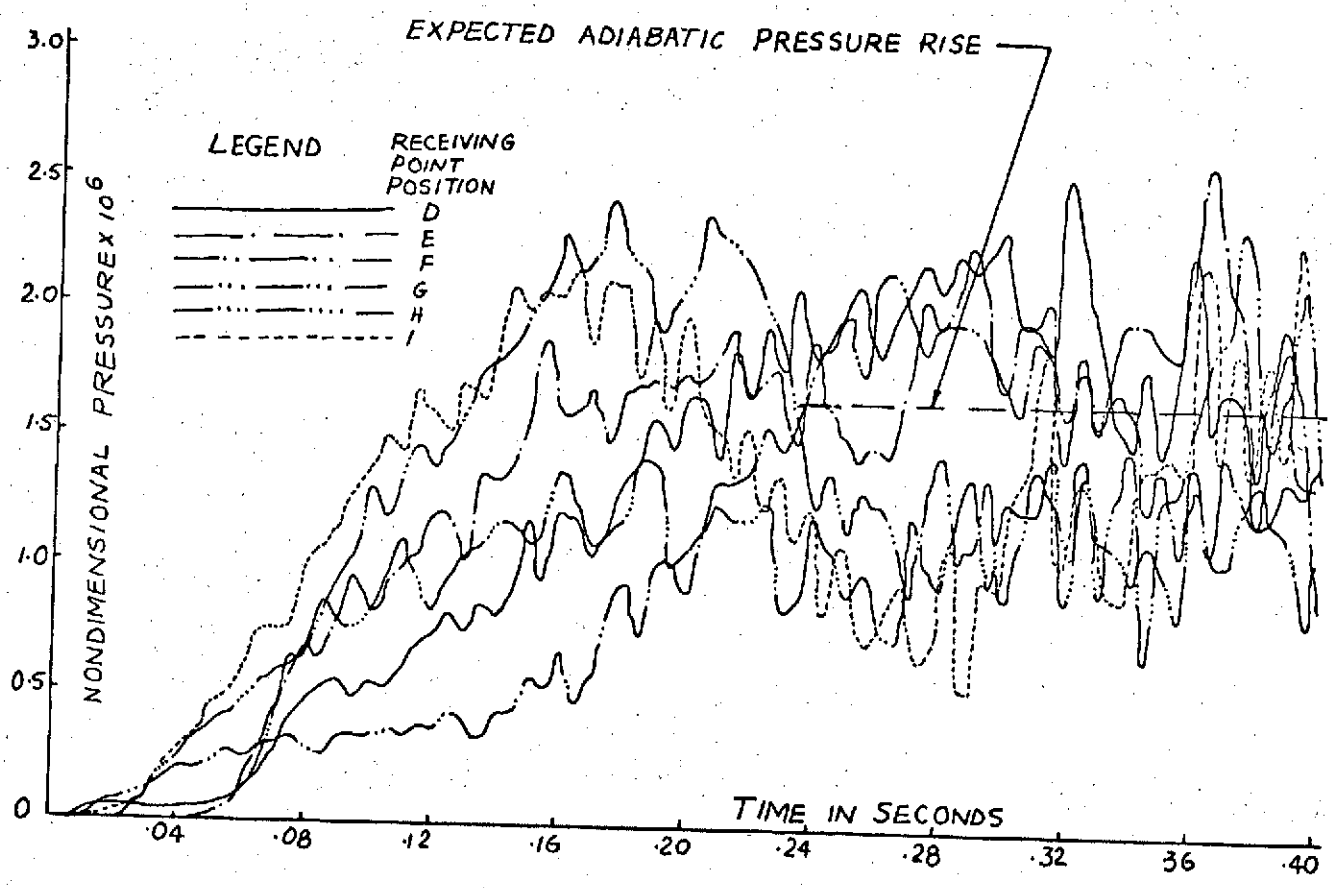

Fig. 29 Pressure Time History at Six Different Receiving Points for Single Cycle N-shape Pulse in Rectangular Room (Case 1)

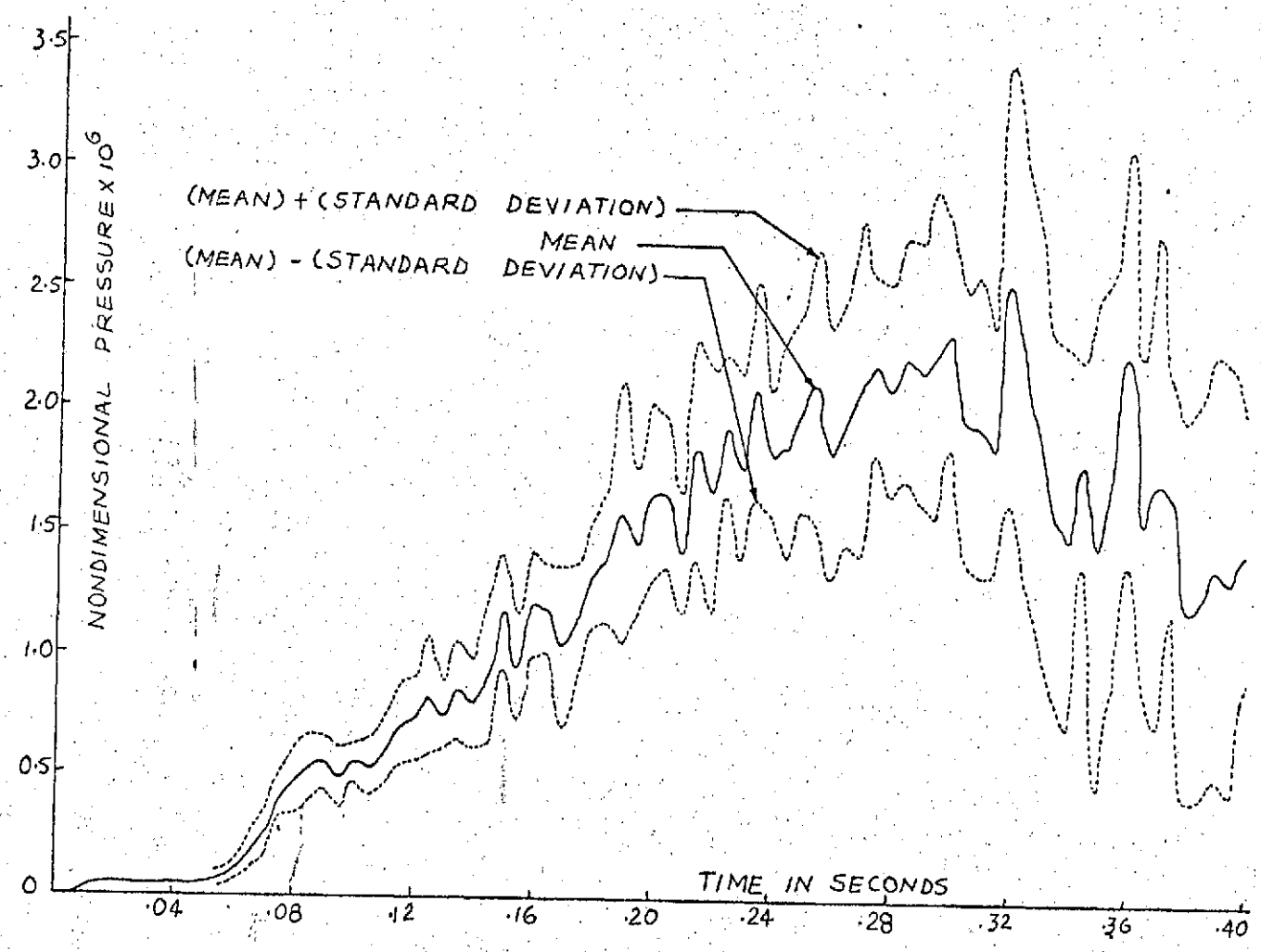

Fig. 29.1 Pressure Time History at Receiving Point D for Single Cycle N-shape Pulse in Rectangular Room (Case 1)

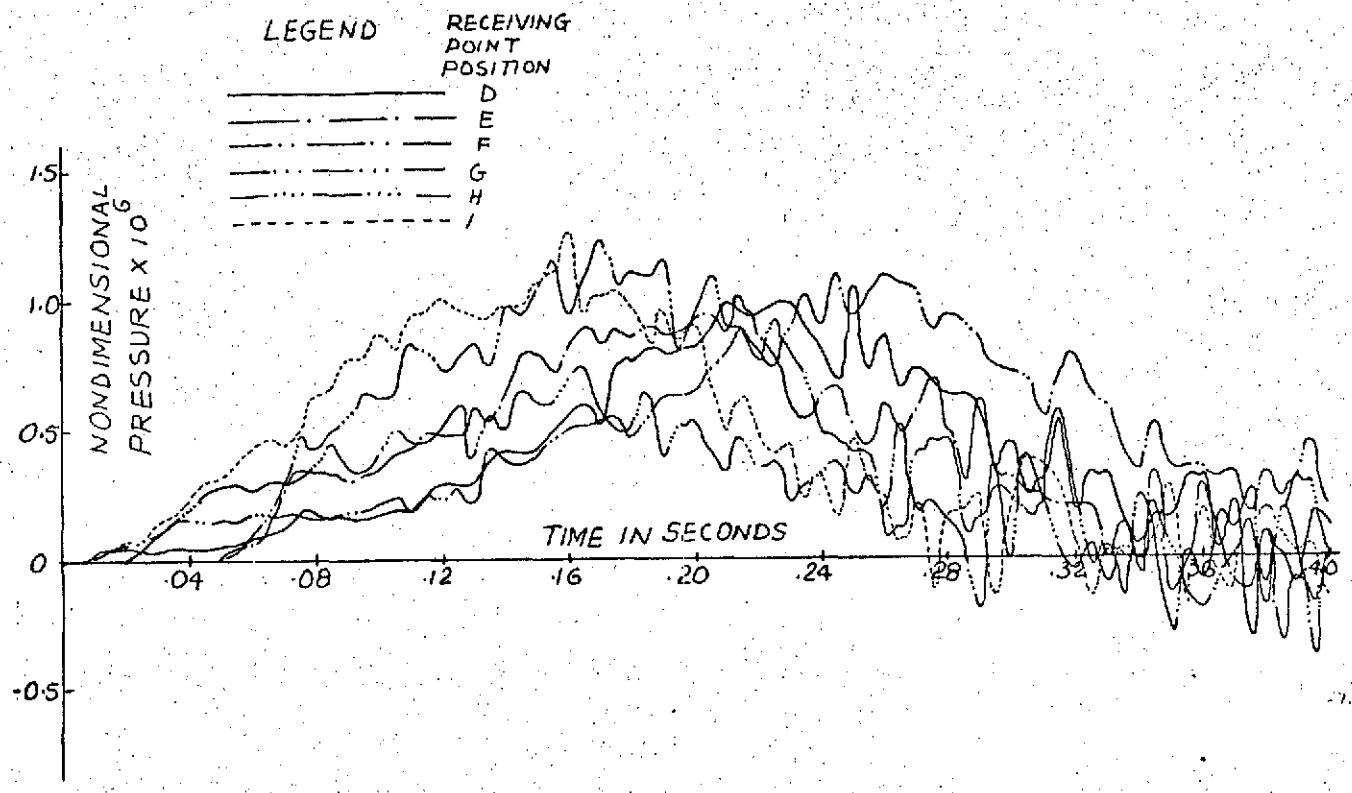

Fig. 30 Pressure Time History at Six Different Receiving Points for Single Cycle N-shape Pulse in Rectangular Room (Case 2)

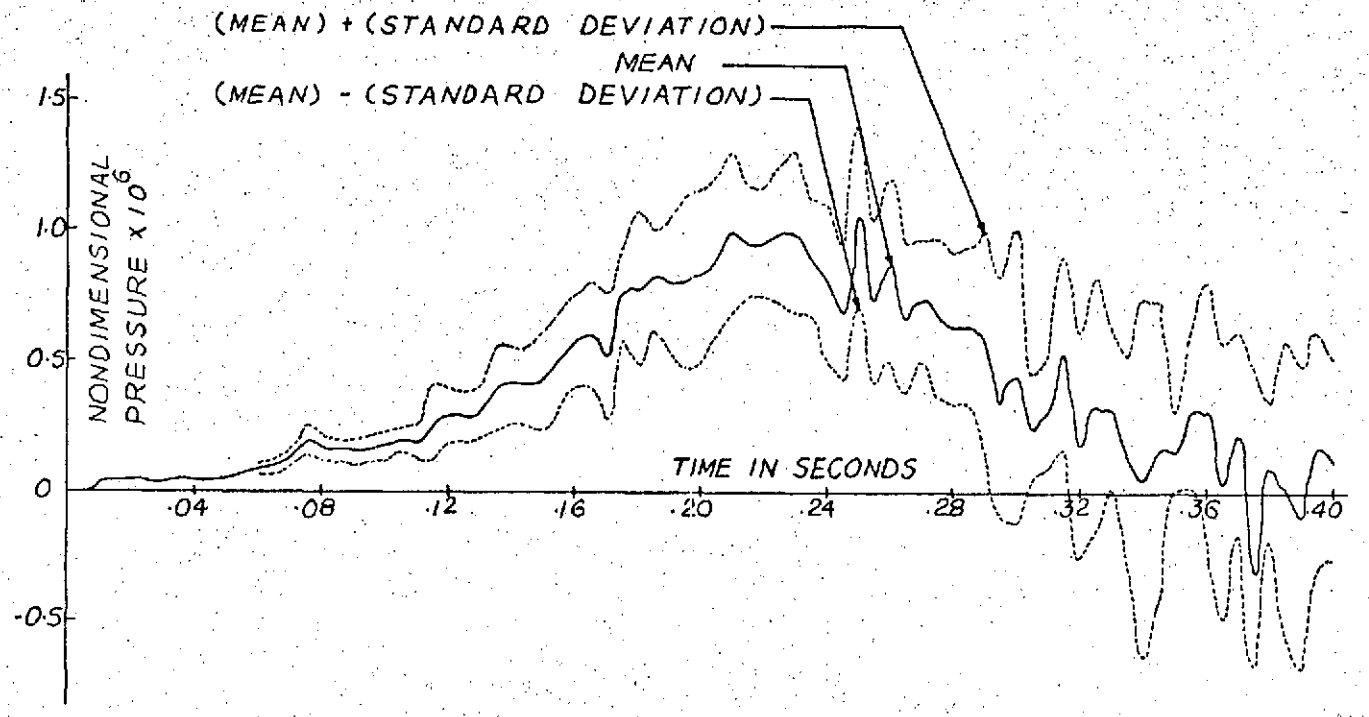

Fig. 30.1 Pressure Time History at Receiving Point D for Single Cycle N-shape Pulse in Rectangular Room (Case 2)

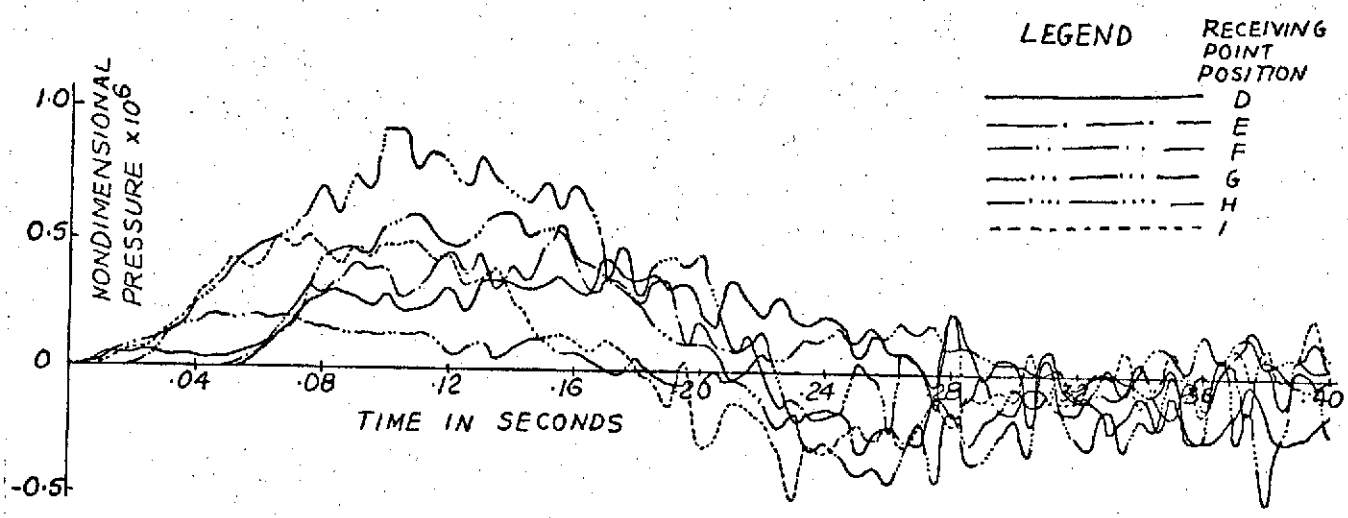

Fig. 31 Pressure Time History at Six Different Receiving Points for Single Cycle N-shape Pulse in Rectangular Room (Case 3)

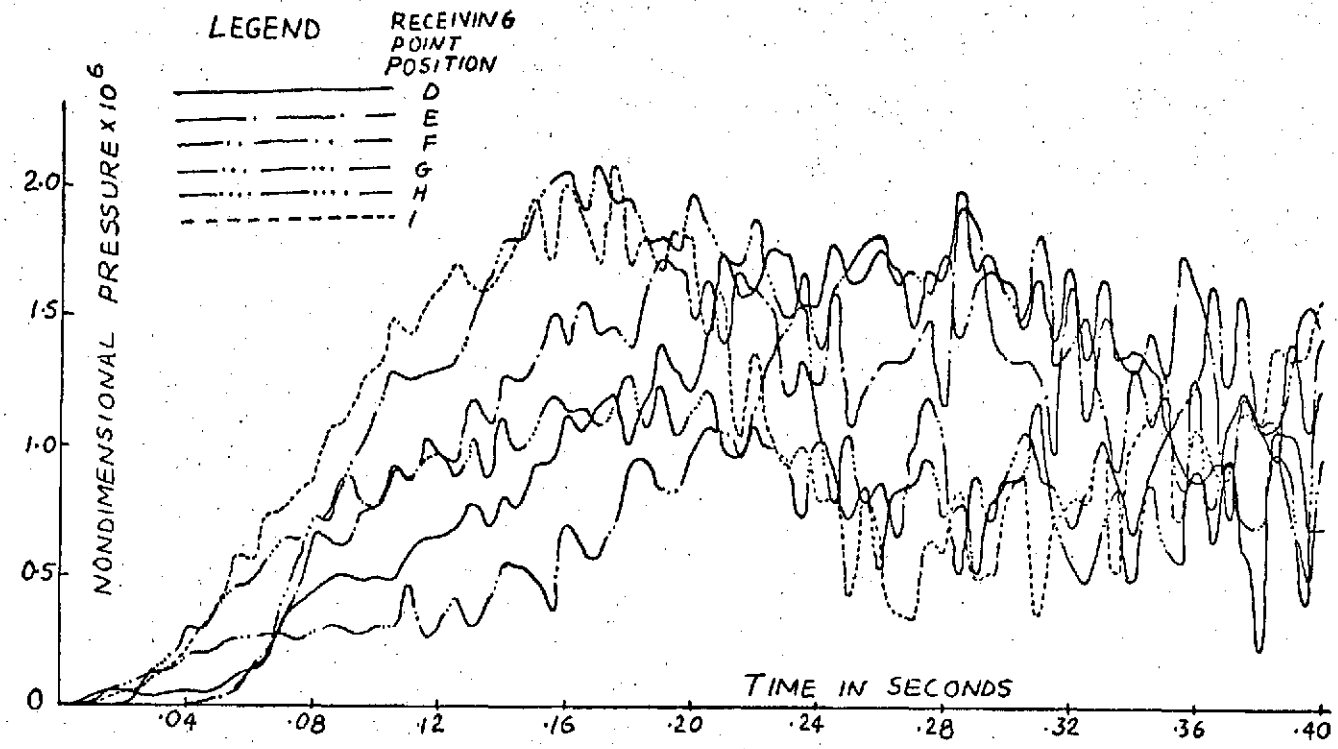

Fig. 32 Pressure Time History at Six Different Receiving Points for Single Cycle N-shape Pulse in Rectangular Room (Case 4)

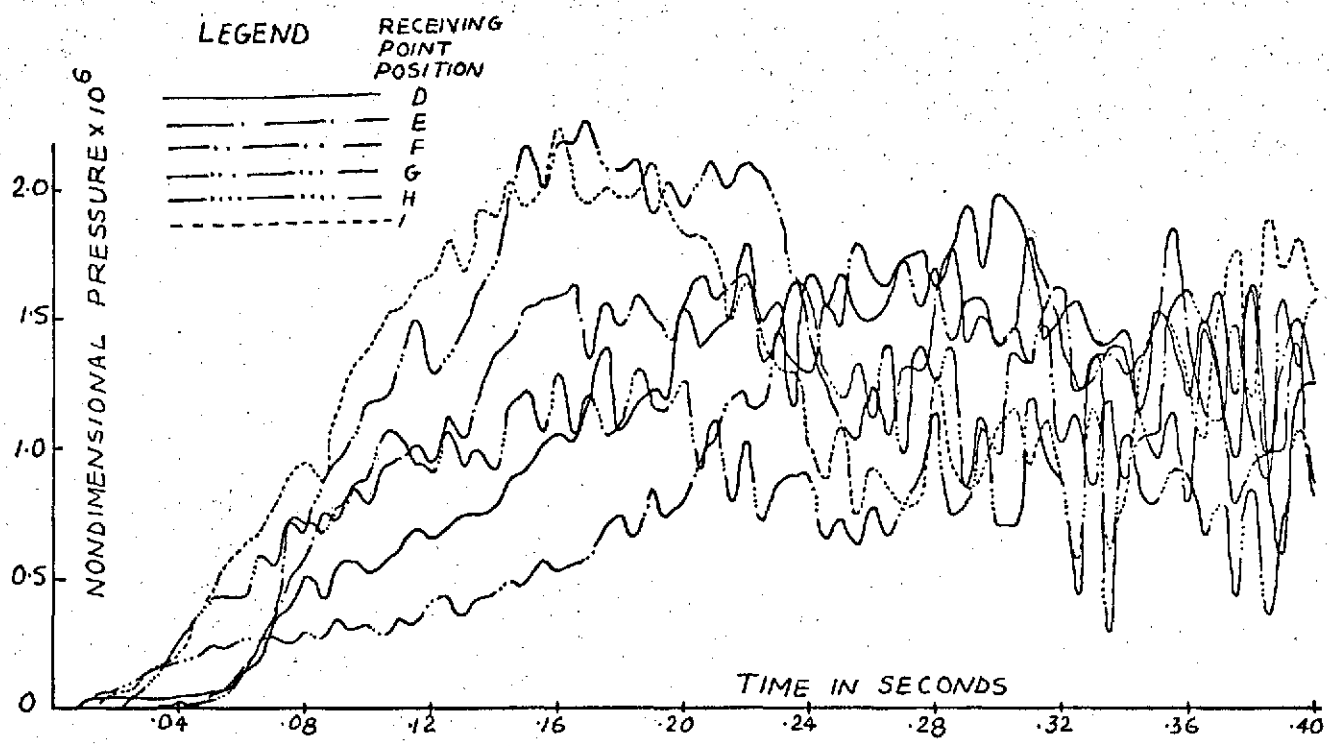

Fig. 33 Pressure Time History at Six Different Receiving Points for Single Cycle N-shape Pulse in Rectangular Room (Case 5)

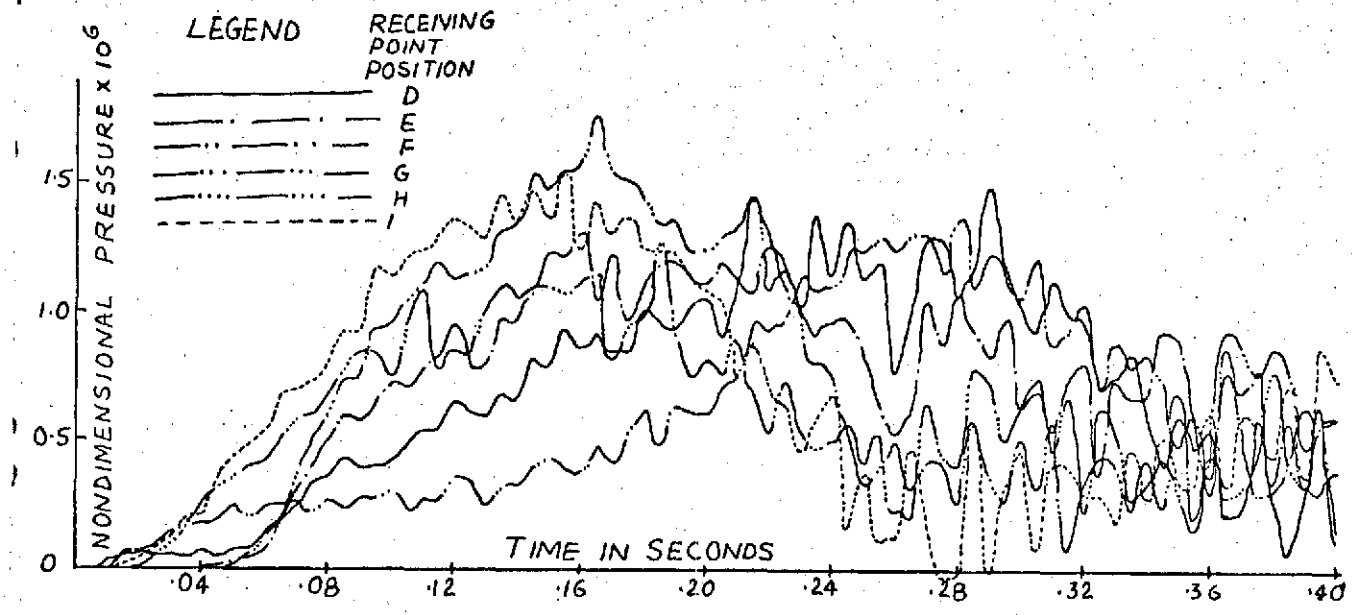

Fig. 34 Pressure Time History at Six Different Receiving Points for Single Cycle N-shape Pulse in Rectangular Room (Case 6)

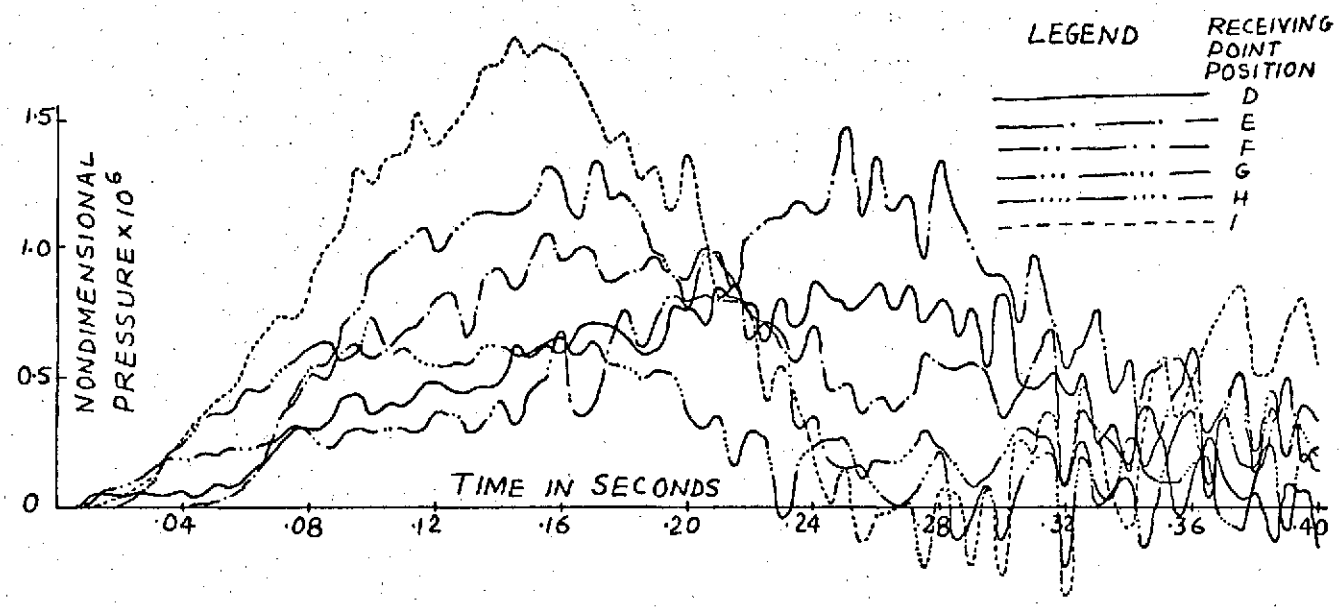

Fig. 35 Pressure Time History at Six Different Receiving Points for Single Cycle N-shape Pulse in Rectangular Room (Case 7)

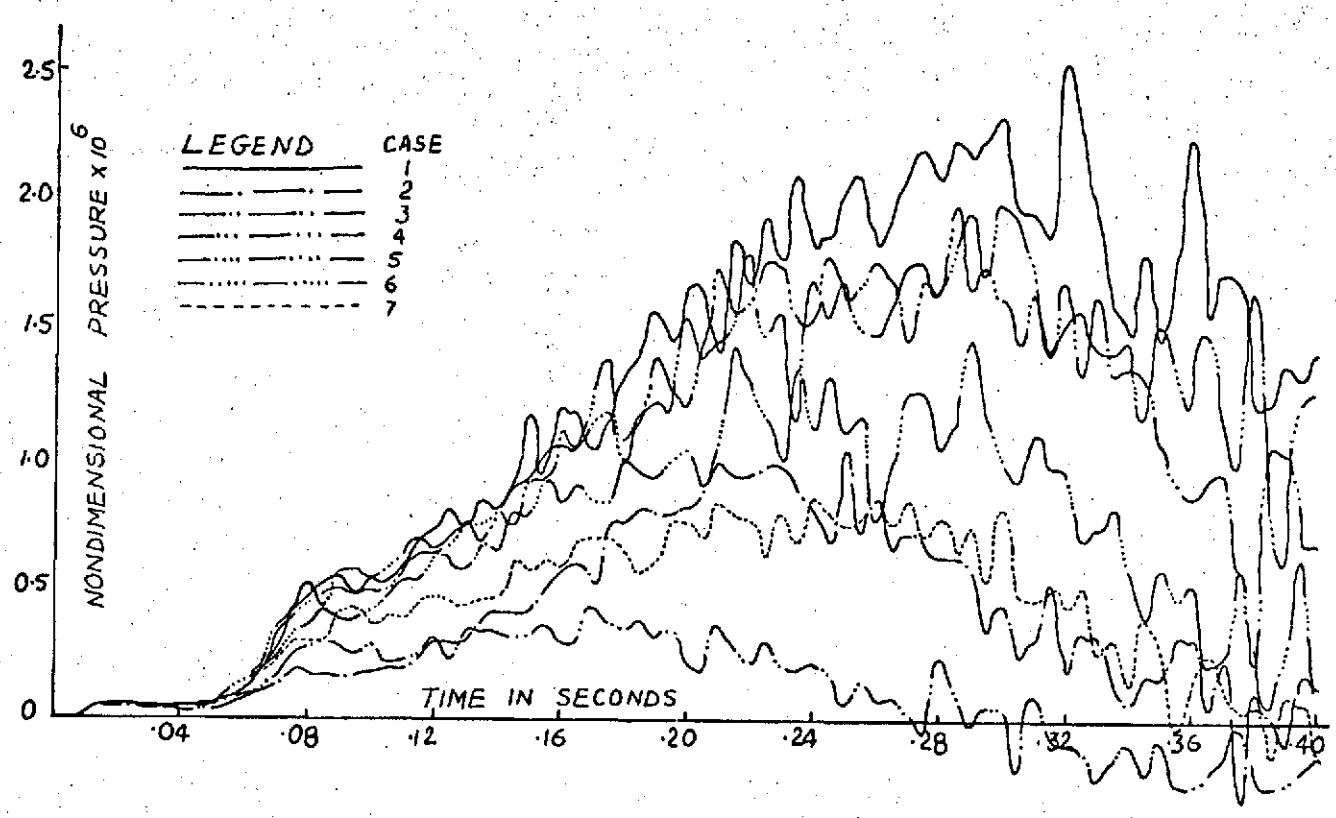

Fig. 36 Effect of Variations in Bounding Wall Material Properties on the Pressure Time History at Receiving Point D for Single Cycle N-shape Pulse in Rectangular Room

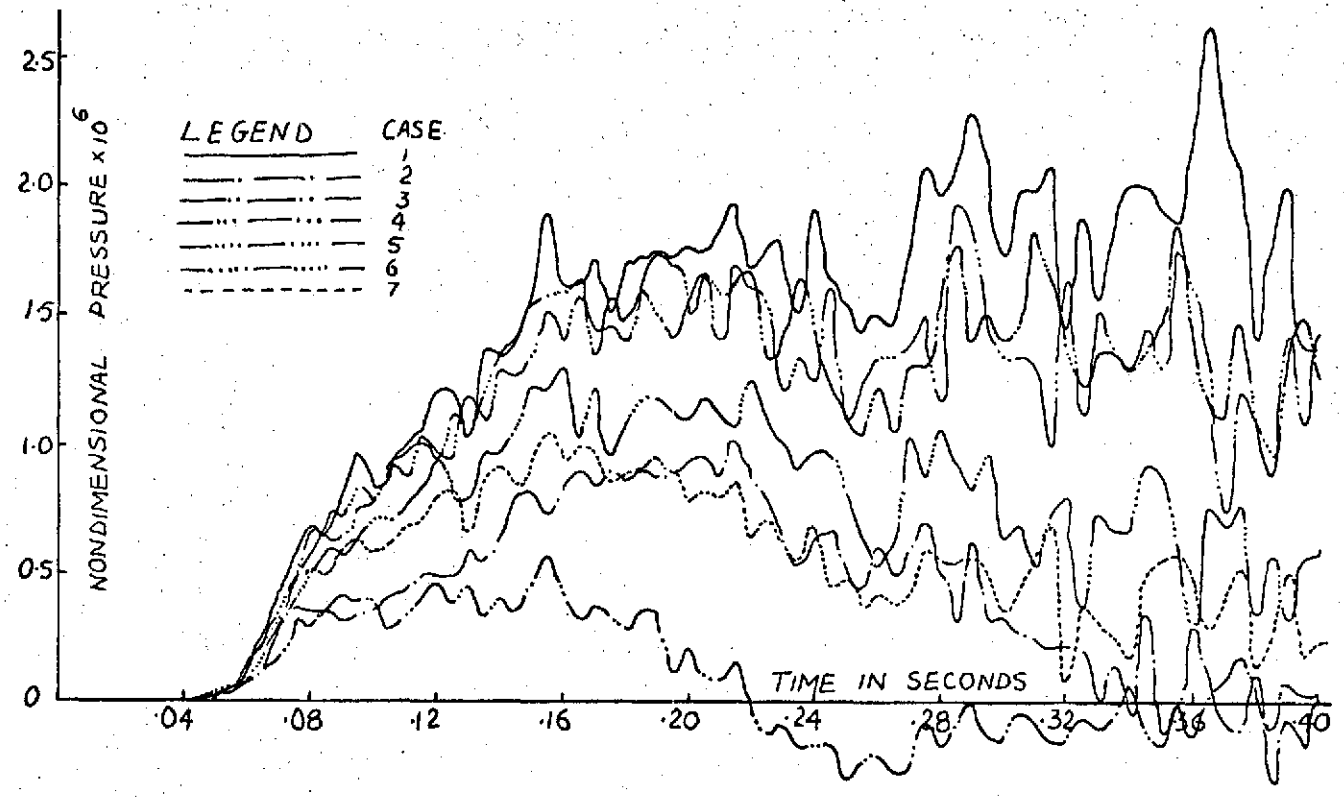

Fig. 37 Effect of Variations in Bounding Wall Material Properties on the Pressure Time History at Receiving Point E for Single Cycle N-shape Pulse in Rectangular Room

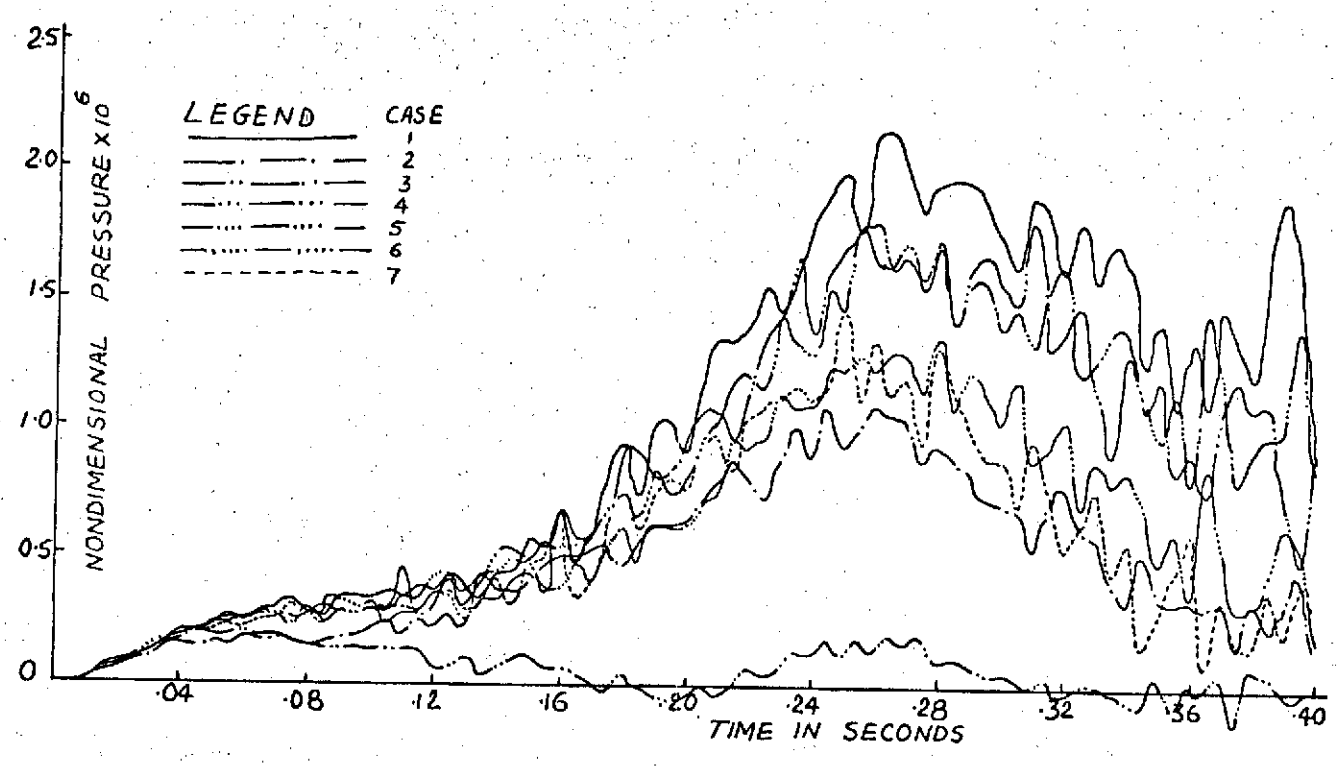

Fig. 38 Effect of Variations in Bounding Wall Material Properties on the Pressure Time History at Receiving Point F for Single Cycle N-shape Pulse in Rectangular Room

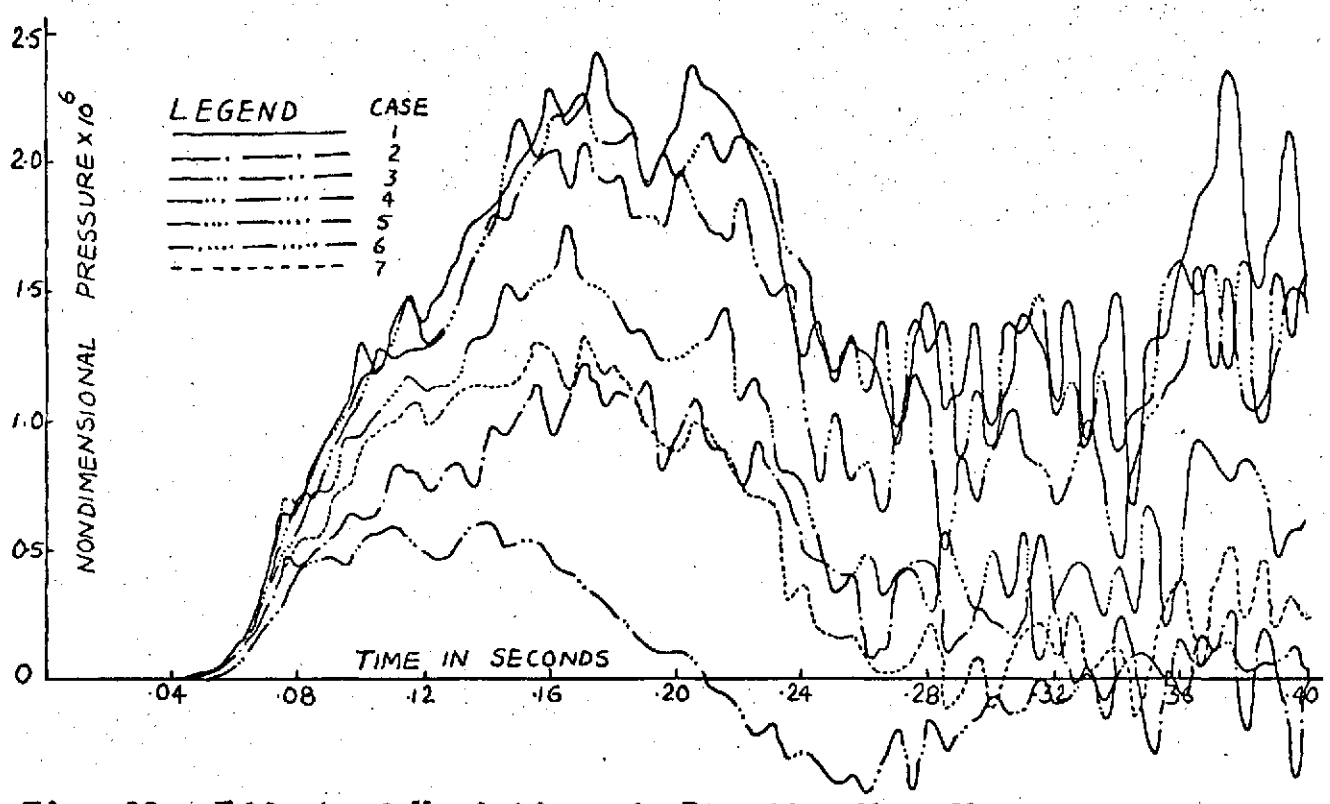

Fig. 39 Effect of Variations in Bounding Wall Material Properties on the Pressure Time History at Receiving Point G for Single Cycle N-shape Pulse in Rectangular Room

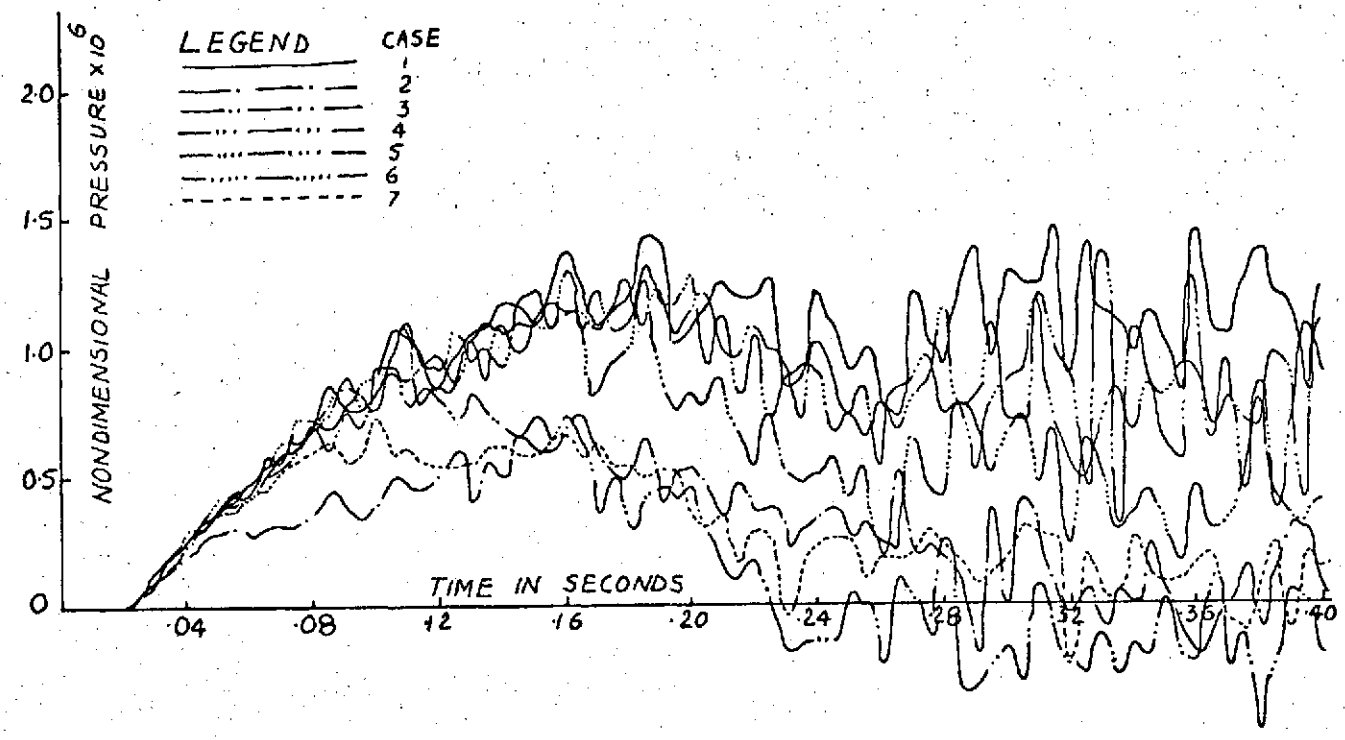

Fig. 40 Effect of Variations in Bounding Wall Material Properties on the Pressure Time History at Receiving Point H for Single Cycle N-shape Pulse in Rectangular Room

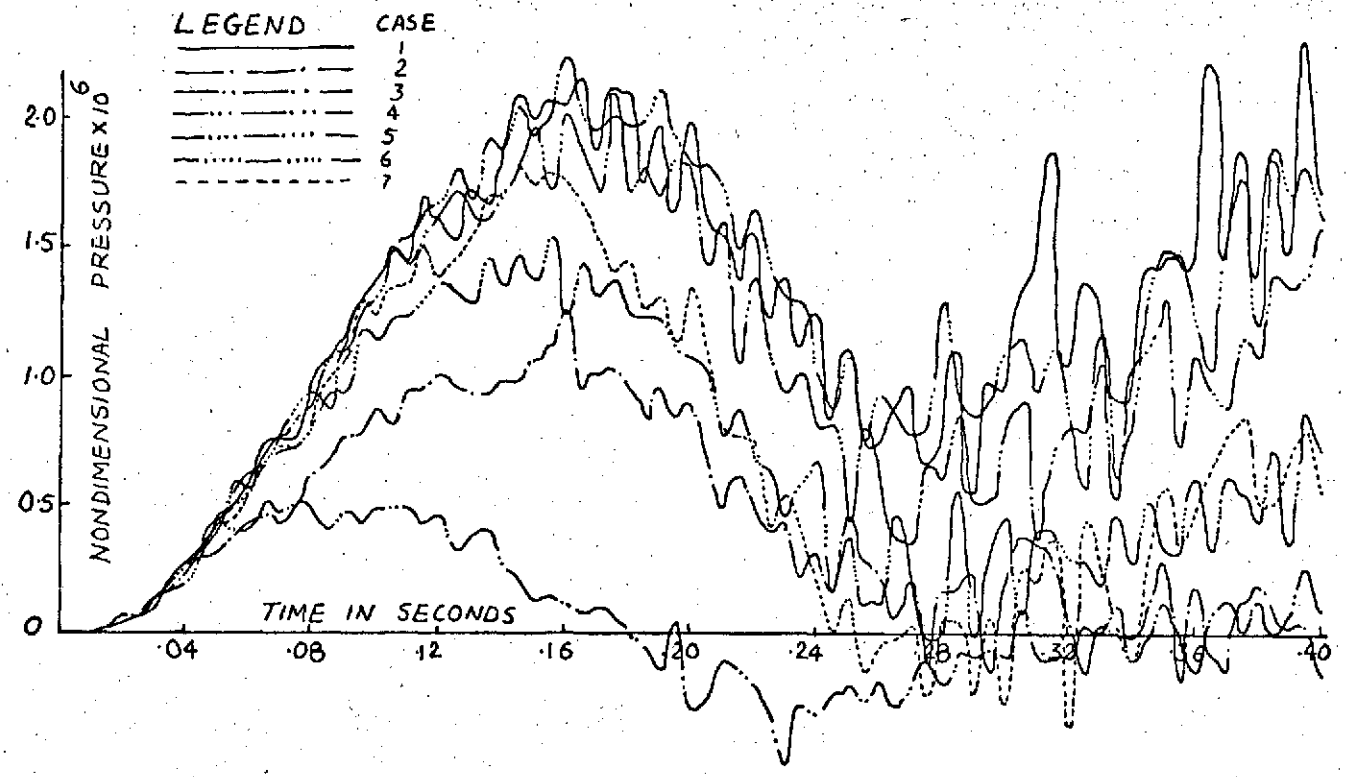

Fig. 41 Effect of Variations in Bounding Wall Material Properties on the Pressure Time History at Receiving Point I for Single Cycle N-shape Pulse in Rectangular Room

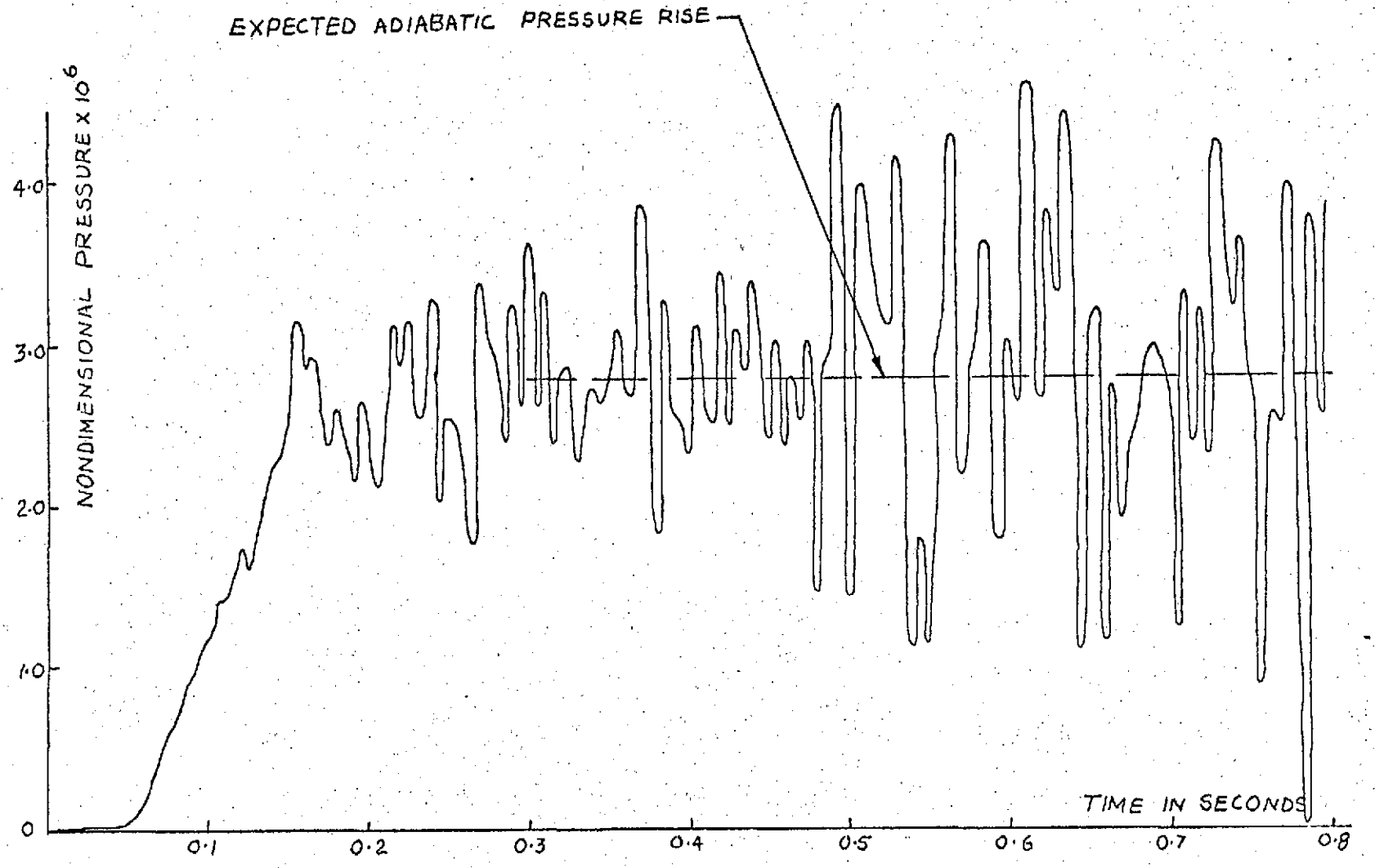

Fig. 42 Pressure Time History for Extended Time at Receiving Point E for Single Cycle Double Rectangular Pulse in Rectangular Room (Case 1)

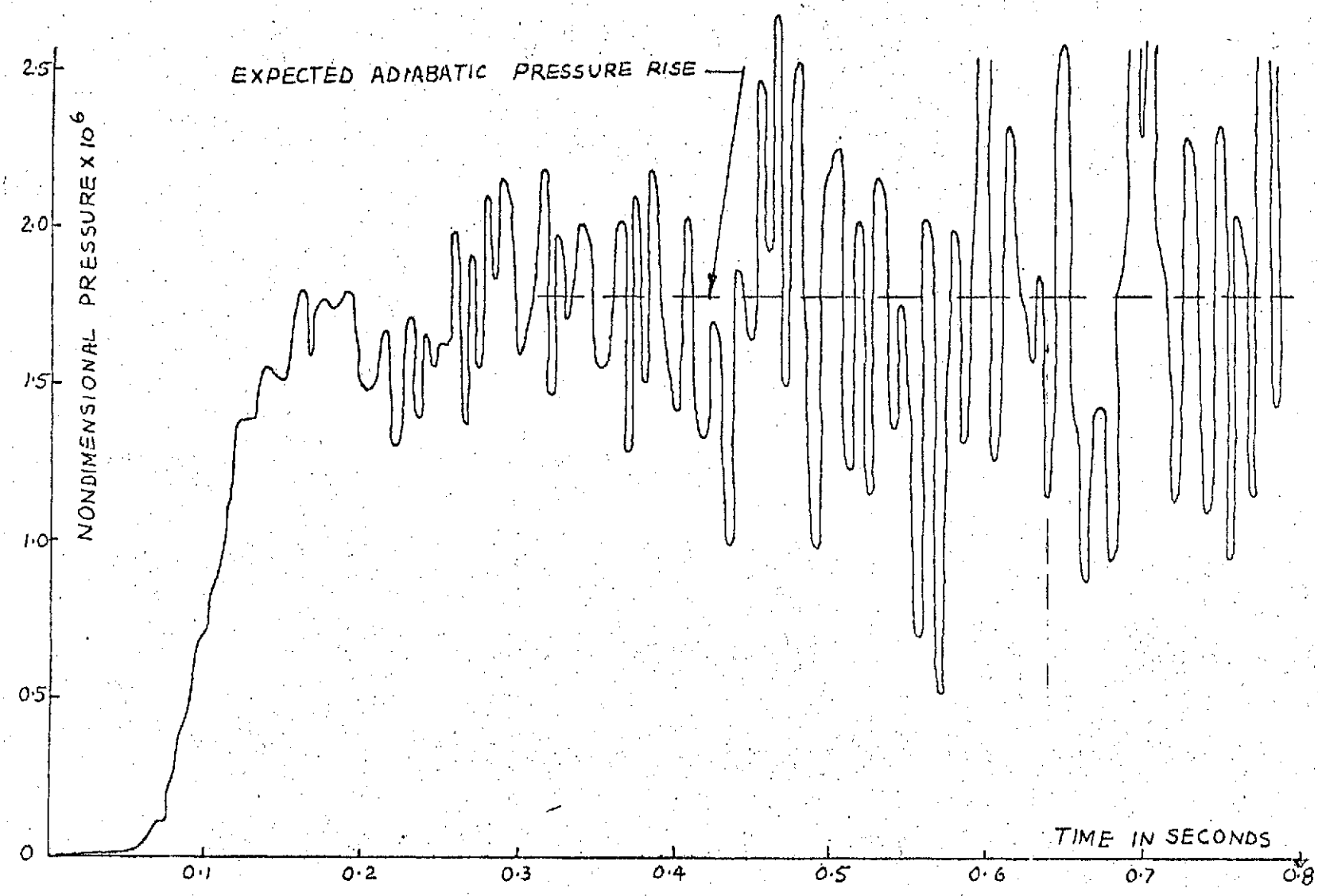

Fig. 43 Pressure Time History for Extended Time at Receiving Point E for Single Cycle Sinusoidal Pulse in Rectangular Room (Case 1)

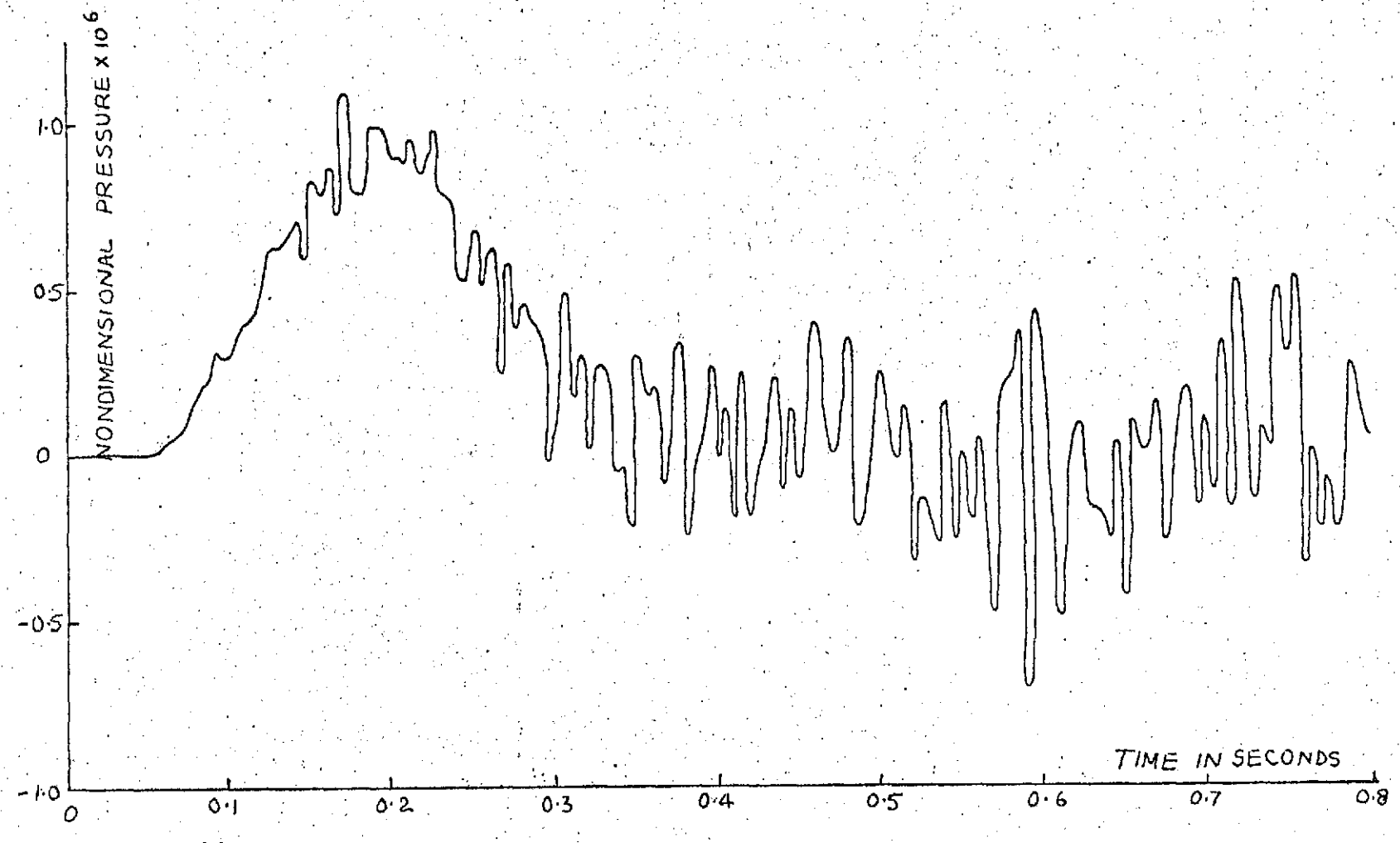

Fig. 44 Pressure Time History for Extended Time at Receiving Point E for Single Cycle Sinusoidal Pulse in Rectangular Room (Case 2)

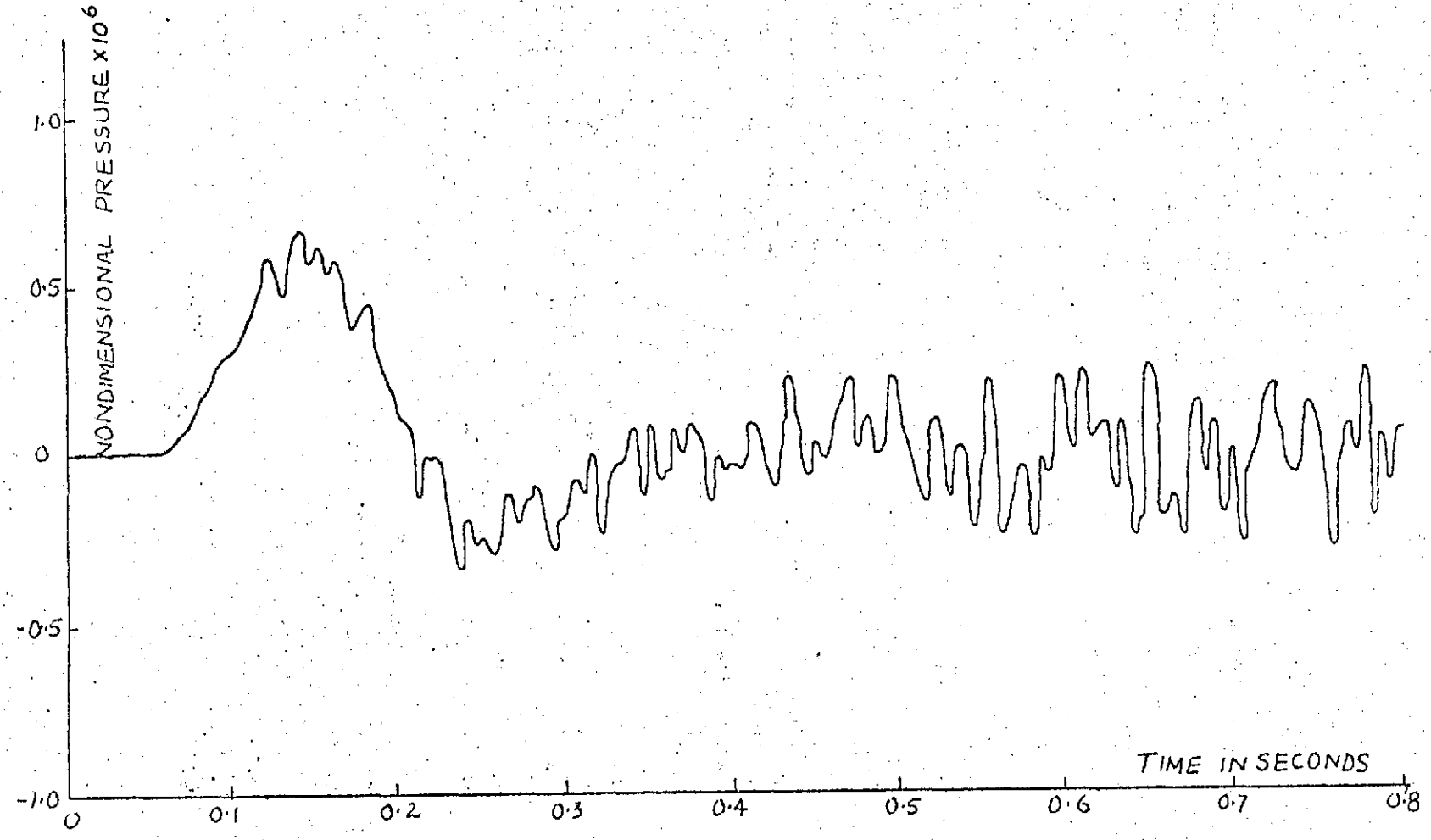

Fig. 45 Pressure Time History for Extended Time at Receiving Point E for Single Cycle Sinusoidal Pulse in Rectangular Room (Case 3)

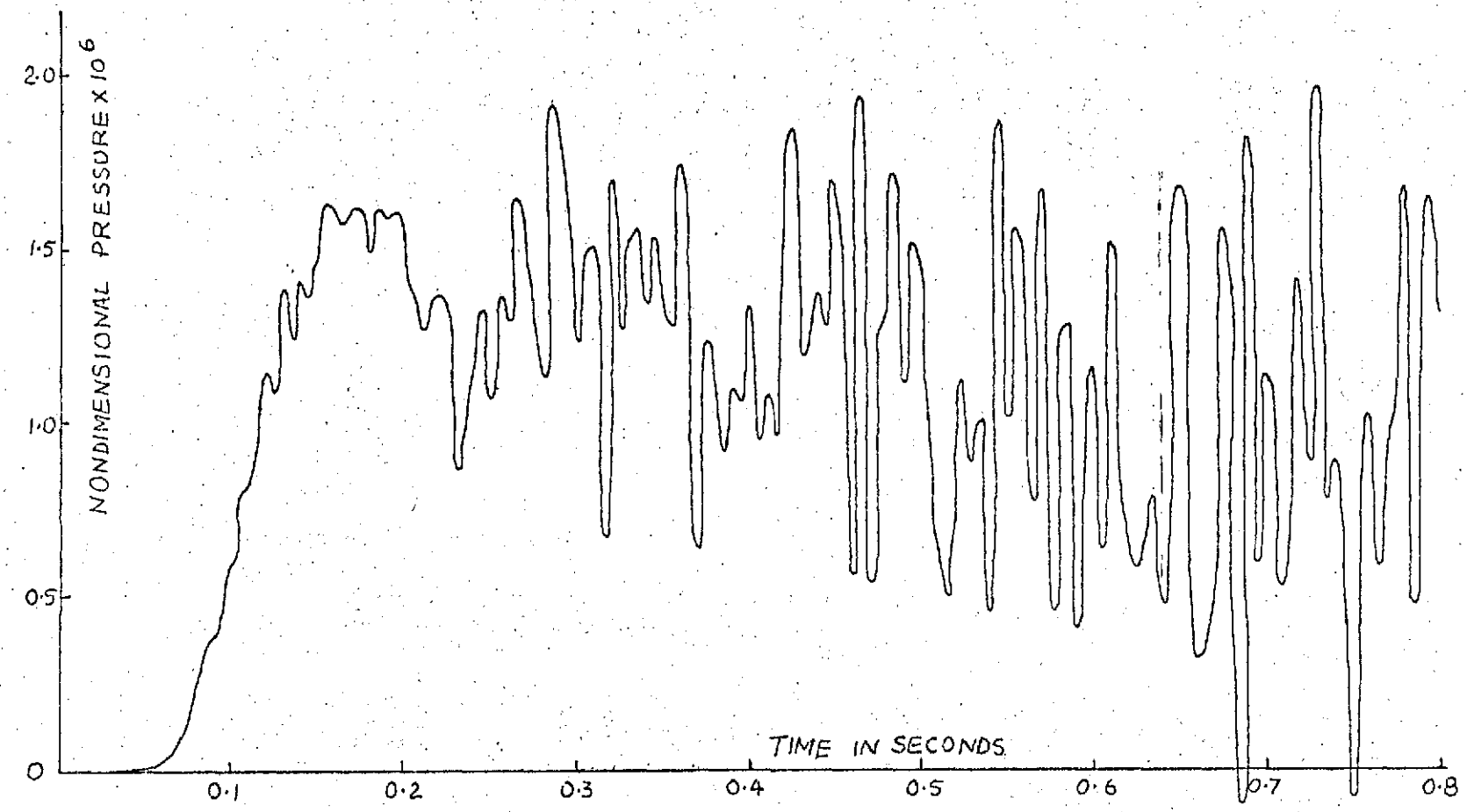

Fig. 46 Pressure Time History for Extended Time at Receiving Point E for Single Cycle Sinusoidal Pulse in Rectangular Room (Case 4)

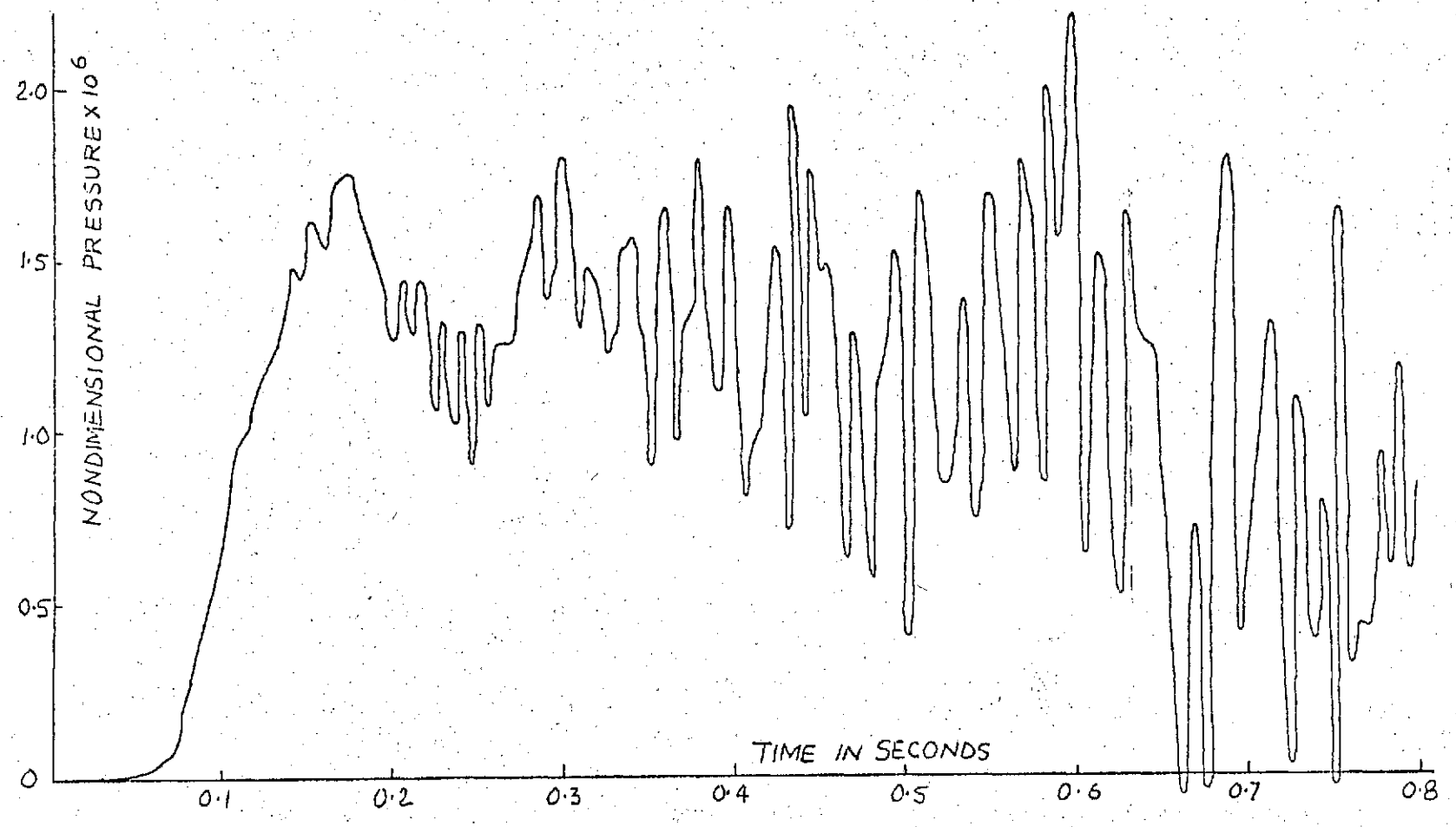

Fig. 47 Pressure Time History for Extended Time at Receiving Point E for Single Cycle Sinusoidal Pulse in Rectangular Room (Case 5)

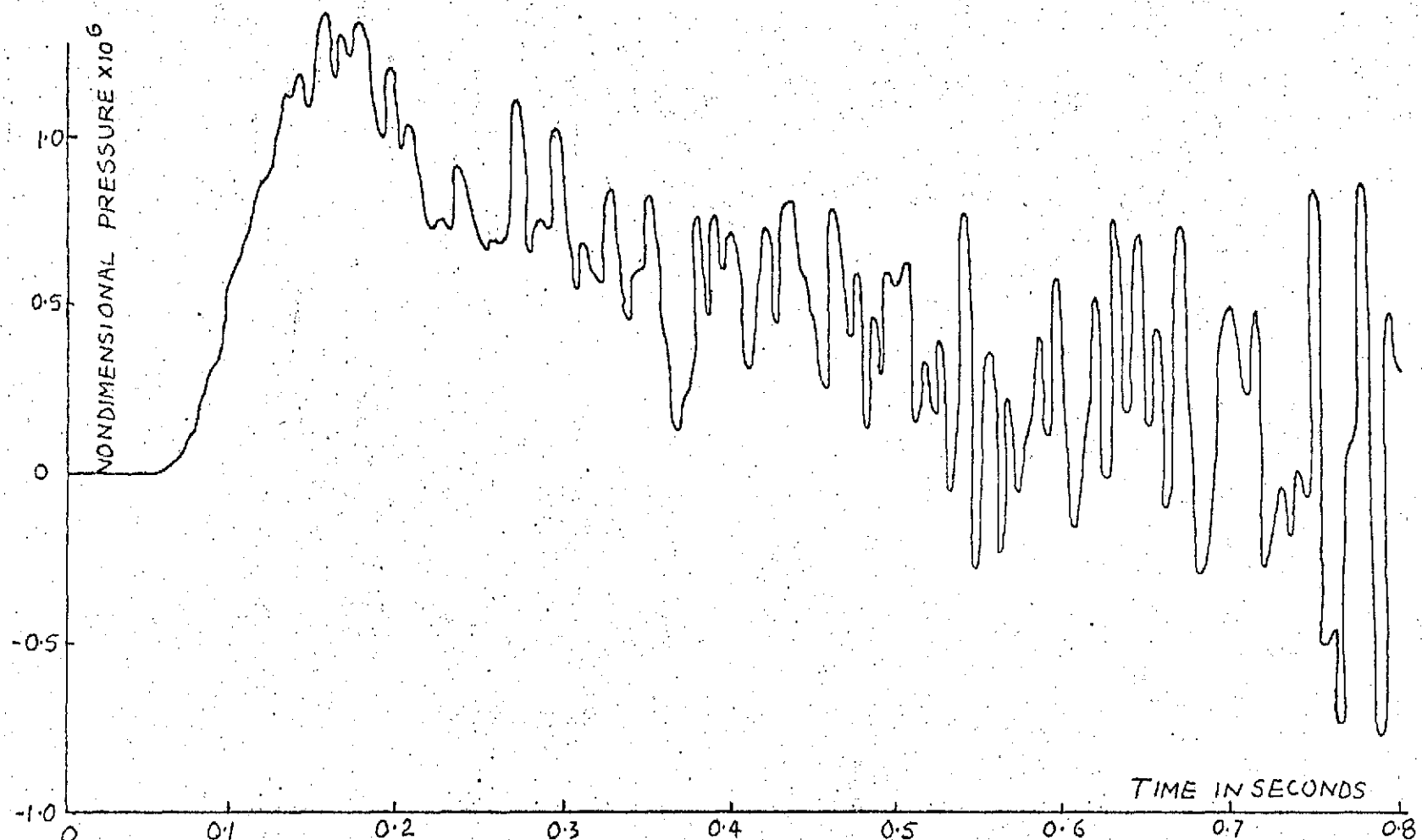

Fig. 48 Pressure Time History for Extended Time at Receiving Point E for Single Cycle Sinusoidal Pulse in Rectangular Room (Case 6)

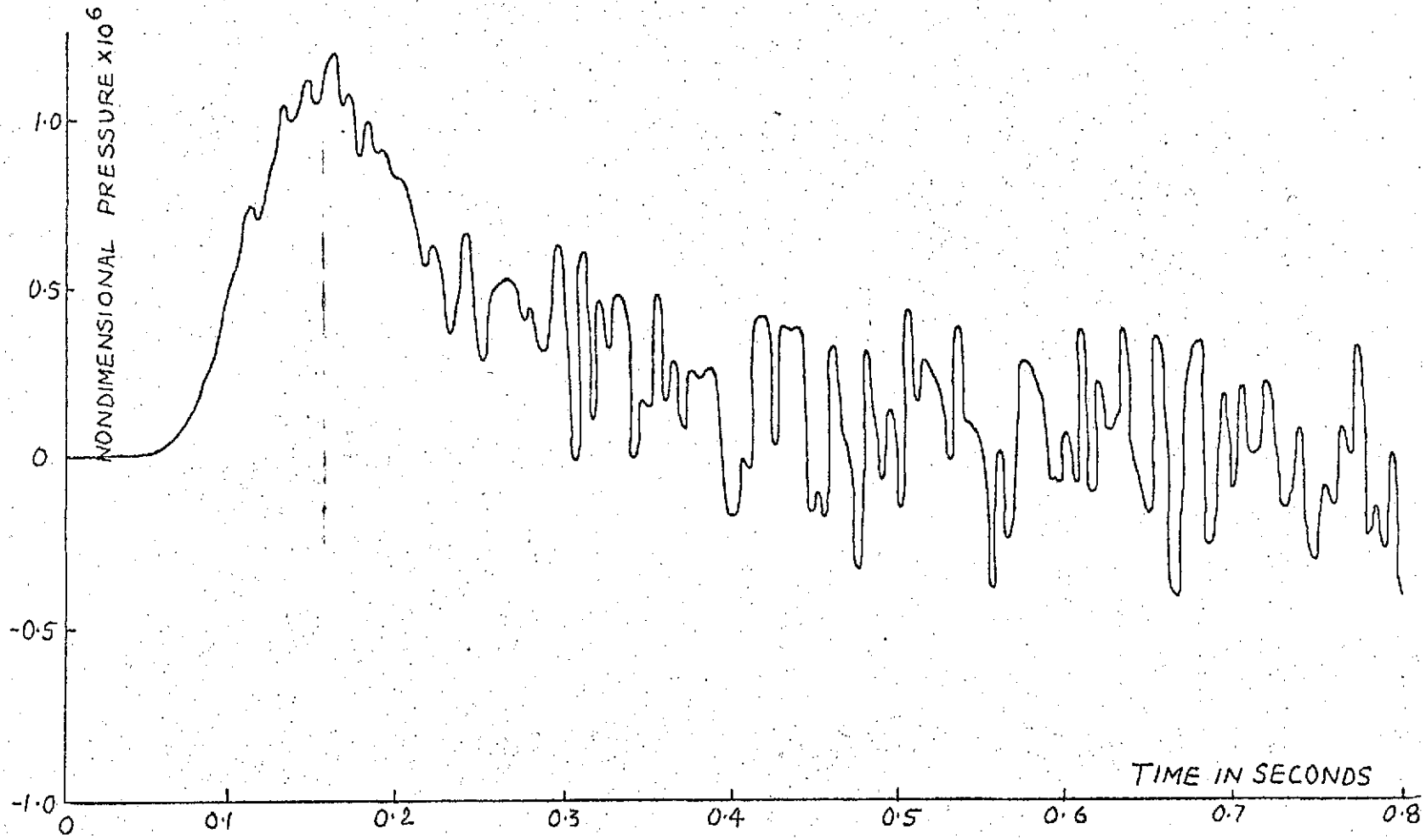

Fig. 49 Pressure Time History for Extended Time at Receiving Point E for Single Cycle Sinusoidal Pulse in Rectangular Room (Case 7)

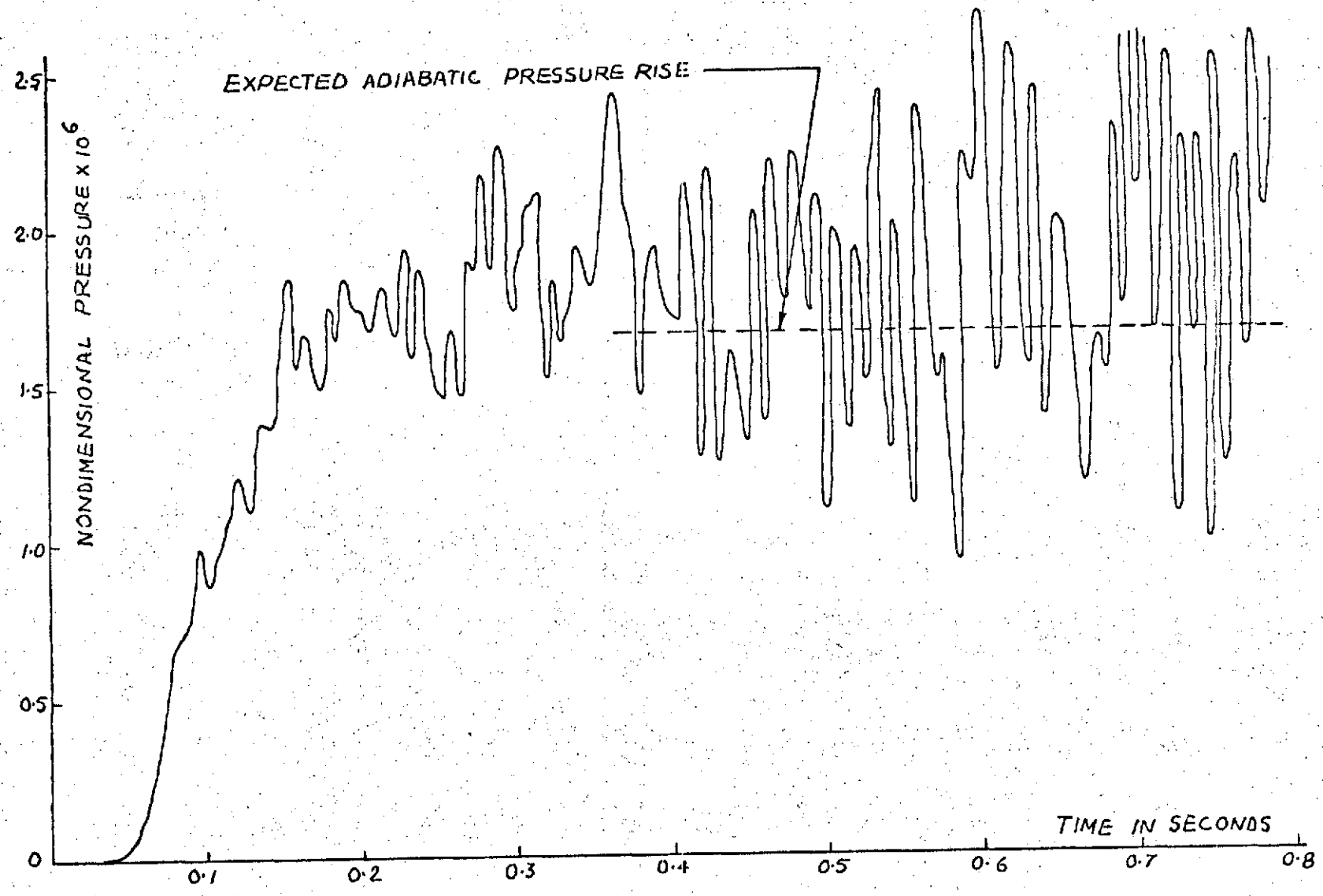

Fig. 50 Pressure Time History for Extended Time at Receiving Point E for Single Cycle N-shape Pulse in Rectangular Room (Case 1)

Some noticeable aspects of these pressure time histories are discussed in the following sections with a note on the problems that are encountered in specifying the proper boundary conditions for the problem.

PROBLEMS ENCOUNTERED IN BOUNDARY CONDITION SPECIFICATION

A survey of the existing room acoustic theory indicates that a customary procedure is to describe the pressure field in an enclosure in terms of normal modes (Morse, 1944), and to consider the pressure at a receiving point to be the summation of the contributions from each excited normal mode of vibration. In such an analysis, based on the concept of 'frequency space', the large number of the excited modes are subdivided into a number of subgroups having common properties. As shown by Hunt (1939) the complete decay equation, when assembled, contains one decay term for each subgroup and each term contains the number of modes of vibration, weighting factor, and an exponential decay factor. The expressions in the frequency domain are, by themselves, fairly useful, for example, in the case when the data about the incoming wave is available, and the spectrum of the system response is to be calculated. However, recently there is an increasing interest in obtaining the solution in the time domain; one common example that can be

cited is the study of the loudness of an acoustical signal from a dual point of view, both subjective and structural. From the subjective point of view it is the earlier part of the time history of the response signal, inclusive of the details of the rise time, that receives the highly favourable weighting; whilst it is the overall response that is of importance from the structural point of view.

Transitional Characteristics

The hitherto common technique of obtaining the transitional characteristics of an enclosure is the application of the methods of operational calculus, as explained by Morse (1944). It assumes the knowledge of the steady state response of the system to an input of, say, unit amplitude. In brief, it consists of evaluating the response of the system to either a delta excitation or a unit step excitation using the Fourier and the Laplace transforms.

Let $X(\omega)\, e^{-i\omega t}$ be the steady state response of the system to an input of unit amplitude $e^{-i\omega t}$; then its response $X_\delta(t)$ to a delta excitation

$$\delta(t) = \int_{-\infty}^{\infty} (1/2\pi)\, e^{-i\omega t}\, d\omega \qquad (4)$$

is given by

$$X_{\delta}(t) = \int_{-\infty}^{\infty} (1/2\pi)\, X(\omega)\, e^{-i\omega t}\, d\omega \qquad (5)$$

and to a unit impulse excitation

$$H(t) = \int_{-\infty}^{\infty} (-1/2\pi i\omega)\, e^{-i\omega t}\, d\omega \qquad (6)$$

is given by

$$X_H(t) = \int_{-\infty}^{\infty} (-1/2\pi i\omega)\; X(\omega)\, e^{-i\omega t}\, d\omega \qquad (7)$$

Substitution of

$$s = -i\omega$$

$$\& \quad \bar{X}(s) = X(is) = X(\omega) \qquad (8)$$

in Eqs. 5, and 7 above gives

$$X(t) = \mathcal{L}^{-1}\{\bar{X}(s)\}$$

$$X_H(t) = \mathcal{L}^{-1}\{\bar{X}(s)/s\} \qquad (9)$$

Thus the method essentially reduces to the following three steps :

I. Formulating $\bar{X}(s)$ from $X(\omega)$, using Eq. 8

II. Finding either $\mathcal{L}^{-1}\{\bar{X}(s)\}$ or $\mathcal{L}^{-1}\{\bar{X}(s)/s\}$

III. Using appropriate convolution relationship to find the response to a given function f(t).

Even with availability of an extensive collection of formulae to obtain $\mathcal{L}^{-1}\{\bar{X}(s)\}$ from $\bar{X}(s)$, such as that edited by Erdelyi (1954), the applicability of this method is limited to a class of problems where the forcing function f(t) is expressible in a suitable analytical form. In this regard the proposed Monte Carlo technique is more general, being able to handle any arbitrary forcing function, since in this method no transforms are involved, the complete evaluation is in the time domain itself.

Absorption Coefficient & Acoustic Impedence

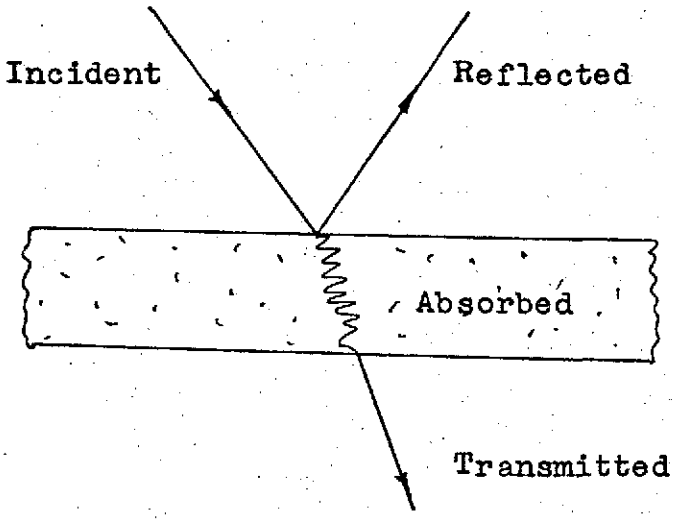

Fig. 51. Sound Incident on a Layer of Material

When sound impinges on a layer of material, part of its incident energy is reflected while the remainder penetrates the material and is either absorbed or transmitted. The amount reflected from the porous material is usually small, there the absorption may be large depending on the thickness. On the other hand from a solid surface such as a plastered tile, 95 % or more of the sound is reflected and very little is absorbed; any transmitted sound for this case would be entirely due to the vibrations of the surface

generated by the incident wave. Taking the intensity of the transmitted sound to be negligibly small it can be shown that the absorption coefficient a can be expressed as

$$a = 1 - |r|^2 \qquad (10)$$

where r is the complex reflection coefficient defined as

$$r = p_r/p_i = (z \cos\theta - \rho c)/(z \cos\theta + \rho c) \qquad (11)$$

z is the specific acoustic impedence at the point, and is expressed as

$$z = p/u = (p_i + p_r)/(u_i + u_r) \qquad (12)$$

u_i & u_r are the particle velocities in the direction of the reflecting surface due to the incoming & reflected waves resp.

θ is the angle of incidence.

In general, the specific acoustic impedance z, given by Eq. 12, is a complex quantity, its real part giving the component of the normal particle velocity at the surface which is in phase with pressure. In the results reported in this work the reflection coefficient was considered to be real. In the Monte Carlo technique account can be taken of both the resistive and reactive components of r, by tracing the ray that is being followed inside the solid surface, at

the incident point, before it gets reflected off the solid surface. This does not present any major difficulty, and the procedure outlined in the preceding chapter can be modified suitably.

When working in the time domain instead of the frequency domain the main difficulty would be in correctly specifing the boundary conditions. As stated earlier since the room acoustic theory based on the Normal Mode approach is in the frequency domain, the material specification is available as a function of frequency. For example, a fair approximation to the impedance of rigidly backed commercial sound absorbents is given by

$$z = g - i \cot (\omega d/c) \qquad (13)$$

where g is a constant independent of frequency

d is the lining thickness.

A deeper study aided by experimental verifications would be essential in transforming such a boundary condition to the time domain for its eventual use in the Monte Carlo technique.

DISCUSSION OF THE RESULTS

Every room, except those enclosed by totally absorptive boundaries, is a resonant chamber capable of being excited into resonant vibration of one or many of triply-infinite series of frequencies, these frequencies being determined by the dimensions of the room and the velocity of sound. For a rectangular room these are given by the well-known Rayleigh formula

$$\nu_M = (c/2) \left\{ \sum_{j=1}^{3} (m_j / L_j)^2 \right\}^{\frac{1}{2}}$$

where m_j's are any non-negative integers (Chapter 6)

L_j's are the dimensions of the room (Fig. 12)

($j = 1, 2, 3$)

In a rectangular room shown in Fig. 12, for which the calculations are presented, the resonant or normal modes of vibration have frequency values shown in column 5 of Table I, calculated based on the value of c as 1100 ft/sec. Columns 2, 3, and 4 of Table I give the X1, X2, and X3 order numbers of the normal modes. It is seen that there are 63 such normal modes with frequencies lower than 50 cycles, and several hundred modes with higher frequencies. Whenever sound is produced in such a room, at least one, and usually many, of

Table I. Normal Mode Frequencies

Sl. No.	m_1	m_2	m_3	Resonance Freq. cps	Impressed Freq. cps		
					Double Rect.	Sinusoidal	N-shape
1	1	0	0	5.000	5.000	5.000	5.000
2	0	1	0	8.333			
3	1	1	0	9.718			
4	2	0	0	10.000			10.000
5	0	0	1	12.500			
6	2	1	0	13.017			
7	1	0	1	13.463			
8	3	0	0	15.000	15.000		15.000
9	0	1	1	15.023			
10	1	1	1	15.833			
11	2	0	1	16.008			
12	0	2	0	16.667			
13	3	1	0	17.159			
14	1	2	0	17.400			
15	2	1	1	18.047			
16	2	2	0	19.437			
17	3	0	1	19.521			
18	0	2	1	20.833			20.000
19	3	1	1	21.230			
20	1	2	1	21.425			
21	3	2	0	22.423			
22	2	2	1	23.108			
23	0	0	2	25.000	25.000		25.000
24	0	3	0	25.000			
25	1	0	2	25.495			
26	1	3	0	25.495			

Table I (continued)

Sl. No.	m_1	m_2	m_3	Resonance Freq. cps	Impressed Freq. cps		
					Double Rect.	Sinusoidal	N-shape
27	3	2	1	25.672			
28	0	1	2	26.353			
29	1	1	2	26.823			
30	2	0	2	26.926			
31	2	3	0	26.926			
32	0	3	1	27.951			
33	2	1	2	28.186			
34	1	3	1	28.395			
35	3	0	2	29.155			
36	3	3	0	29.686			
37	2	3	1	29.686			
38	0	2	2	30.047			30.000
39	3	1	2	30.323			
40	1	2	2	30.460			
41	2	2	2	31.667			
42	3	3	1	31.722			
43	3	2	2	33.583			
44	0	3	2	35.356	35.000		35.000
45	1	3	2	35.708			
46	2	3	2	36.743			
47	0	0	3	37.501			
48	1	0	3	37.832			
49	3	3	2	38.406			
50	0	1	3	38.415			

Table I (continued)

Sl. No.	m_1	m_2	m_3	Resonance Freq. cps	Impressed Freq. cps		
					Double Rect.	Sinusoidal	N-shape
51	1	1	3	38.739			
52	2	0	3	38.811			
53	2	1	3	39.696			
54	3	0	3	40.389			40.000
55	0	2	3	41.038			
56	3	1	3	41.240			
57	1	2	3	41.341			
58	2	2	3	42.238			
59	3	2	3	43.693			
60	0	3	3	45.070	45.000		45.000
61	1	3	3	45.347			
62	2	3	3	46.166			
63	3	3	3	47.501			

these resonant vibrations are excited. The resulting sound pattern in the room is a composite of the sound radiated directly by the source and the resonant vibrations excited by the source of sound.

Reference to Fig. 11 and Eqs. 1 to 3 above indicates that the source configurations that are under consideration are characterized by specific frequency values shown in Columns 6 to 8 of Table I. Since the sinusoidal pulse is a 'pure tone' one it has a single frequency, although this frequency is the fundamental frequency, the double rectangular as well as the N-shape pulse have additional higher harmonic 'over tones'. In a specific case chosen(Fig. 11) the fundamental frequency of the source coincides with the normal mode of Sl. No. 1, and as a result this particular normal mode is strongly excited making the room to 'sing' or resonate at this frequency. This is true for all the three configurations of the source (Fig. 11). In case of the double rectangular shape pulse Sl. No. 8, 23, 44, 60, etc. and in the case of the N-shape pulse Sl. No. 4, 8, 18, 23, 38, 44, 54, 60, etc. are the additional normal modes that would be excited strongly in this room.

Depending upon the type of the standing waves they represent the modes are classified as the axial, tangential and oblique. It could be expected from the existing room acoustic theory that the earlier part of the

pressure time history would be dominated by the axial modes. With the passage of time, the tangential and axial modes would be generated to a substantial extent, and the field could be more & more diffused. The transitional period representing the pressure build-up extends from the instant the source is initiated to the commencement of the steady state. During the build-up stage the motion is quite complicated by the continuous shift that takes place from the natural frequencies of the standing waves to the forcing frequency of the source. In the investigation of the responce of a rectangular room to a sonic boom signal in the time domain, Vaidya (1969) has found that the earlier part of the time history resulting from the build-up of the modes is typically of the form as shown in Fig. 52, where the ordinate is proportional to the pressure value. The Monte Carlo results (Fig. 13 to 50) are seen to be in confirmity with this.

When the sound from a source in an enclosed space is suddenly stopped, it is wellknown that the sound appears to die away slowly rather than immediately. When the driving ceases, due to the energy stored up in the system, oscillations persist and again there is a transitional period, known as the decay period, in which the motion is complicated by the shift from the forced frequency, the frequency at which the system was vibrating during the steady state, to

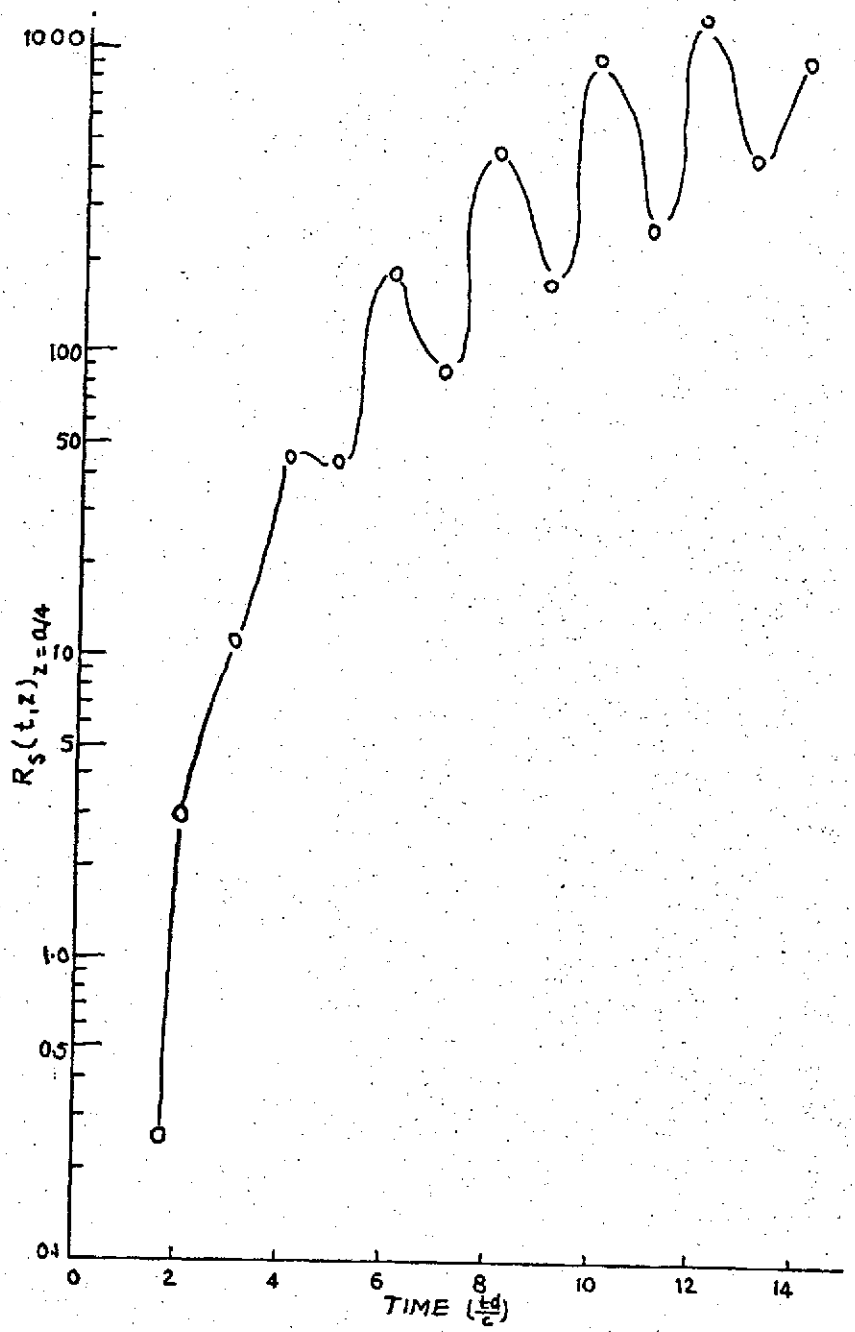

Fig. 52 Typical Build up of the Pressure Modes (Vaidya, 1969, Fig. 11.3, p. 163)

the natural frequencies of the standing waves.

In cases where the two or more eigentones have their natural frequencies closer than the average spacing the corresponding standing waves may be excited strongly. The interference and the beating effects between the nearest modes of vibration explain the peaks or irregularities exhibited in the pressure time histories of Figs. 13 to 50 and Fig. 52. After the source cut-off the total sound energy in the room will not fluctuate, but at any given point in the room, the pressure will fluctuate because of the interference between the normal vibrations; particularly in the case of excitation by only a few frequencies the fluctuations produced by such interference may be important. To describe the observed irregularities in sound decay curves Watson (1946) uses the term 'modulation' defined as the deviations of the sound decay curves from a simple exponential decay irrespective of the cause or the nature of the deviations. The theory and experiment (Beranek 1971, Knudsen 1967, Watson 1946, Jones 1940) indicate the following three primary reasons in the modulation of the sound decay curves

1. The presence of beats produced by the interference among the resonance frequencies of the room
2. The occurence of multiple decay rates resulting from the shape of the room or the nonuniform

distribution of absorption on the walls

3. The abrupt changes in the pressure due to the passage of the terminations of the wavetrains from the source.

An alternative approach to visualize the situation that prevails during the transitional period is to attempt to 'follow' the sound waves around the room as they are reflected back and forth from the walls (Bolt 1950). In essence this method consists of replacing the effect of the boundaries of the room by an infinite array of image sources (Fig. 6), each image corresponding to one of the multiple reflections of the original wave emitted by the source. Using this approach of multiple reflections in conjunction with the Laplace Transform technique Mintzer (1950) has presented a method for the description of a transient pressure field in a rectangular room. Figure 53 presents his results showing the variation of the pressure at the receiving point (33',33',22') in a room (Fig. 12) due to a point source of double rectangular pulse shape(Fig. 11b) when all the walls are perfectly reflecting. The corresponding pressure curves obtained by the application of the Monte Carlo technique are seen in Fig. 13. Monte Carlo results are seen to be in qualitative agreement with the Mintzer's results but their quantitative comparison cannot be offered because the

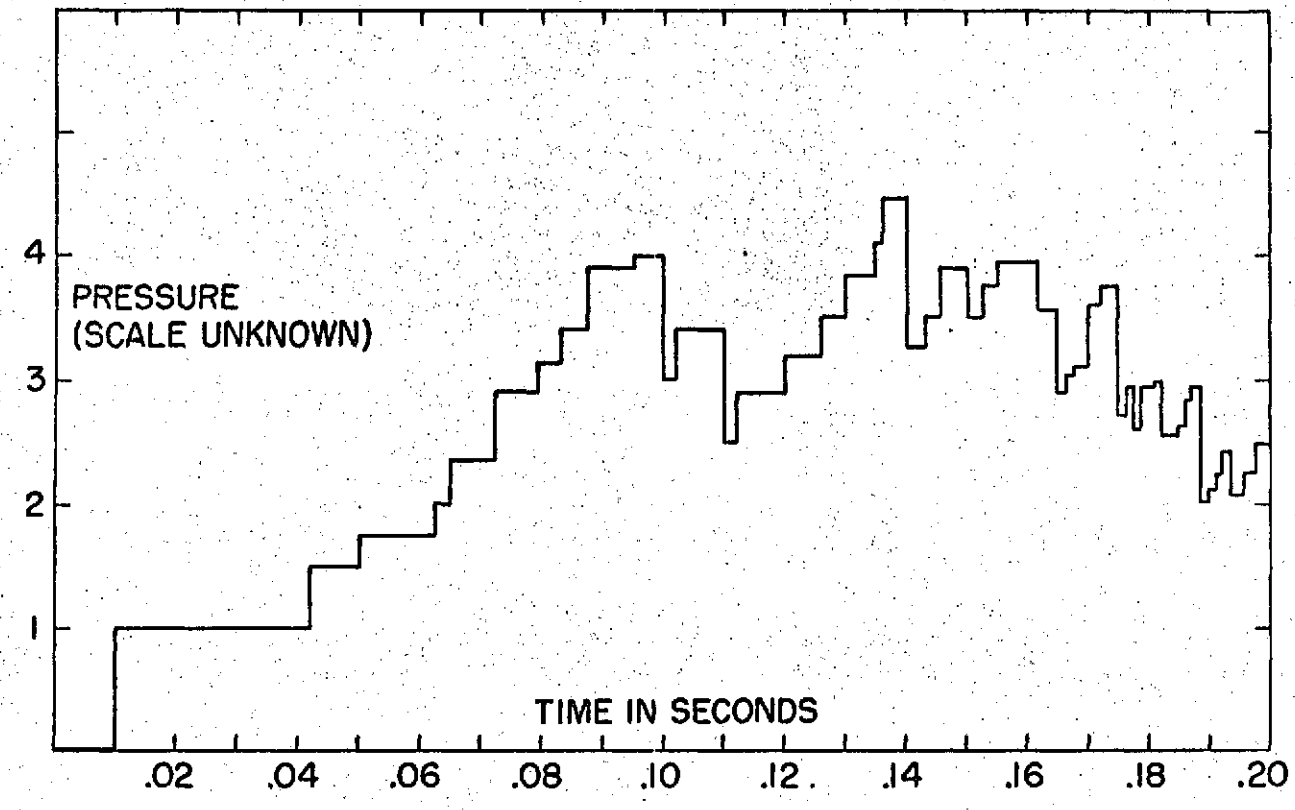

Fig. 53 Pressure Time History at Receiving Point (33',33',22') for Single Cycle Double Rectangular Pulse in Rectangular Room (Case 1) Mintzer's (1950, Fig. 9, p. 350) Results

normalization factor used in the Mintzer's results is not available.

Consider, for example, Fig. 13.1. It shows the mean pressure values, with plus and minus one standard deviation, obtained from the Monte Carlo application, at the receiving point D, for Case 1, when the source is of the double rectangular shape (Fig. 11a). The mean pressure curve of Fig. 13.1 is one of the constituent curves shown in Figs. 13 and 15. The initial build-up of the pressure that is observed (Fig. 13.1) is the result of the multiple reflections of the pressure waves that appear in the lossless medium. It is also noticed that in the latter portion of the observation period the rate of the pressure build-up is not that high as it was in the first half; this is because the effect of the pressure wave reflections from the negative half of the source cycle, now, partly balances the continued build-up from the positive half. After the source cut-off at 0.2 secs. the pressure is seen to fluctuate at a frequency that is not very much different from the forced frequency, coincident with the strongly excited normal mode of Sl. No. 1 (Table I), but around the mean pressure value of 2.8 E -6, which is the level of the expected adiabatic pressure rise referred to earlier and marked in Fig. 13.

In the Mintzer's method each reflection at the boundary wall is described by means of a unit function with a suitable retarded time argument and results in a series of integrals in a transformed space. The terms of the series are in the form of plane wave expansions around the image source points. At a given time the series is seen to possess a finite number of nonzero terms. It is obvious that the Mintzer's method can be applied to cases where the images can be found analytically. It is in very few special cases will the images be the 'mirror images'. Even in these special cases the calculations are quite involved requiring to be able to obtain the transforms; subsequently the integrals are approximated by the method of the steepest descent. In contrast the calculations in the Monte Carlo method are very simple.

Consider Fig. 13 again. Until the source cut-off, which occurs at 0.2 secs., the pressure values at all the six receiving points D, E, F, G, H, & I are on increase, although at different rates, but later, more specifically during the interval 0.20 to 0.32 secs., the pressure values are seen to be above the expected adiabatic pressure line for the receiving points D, E, & F whilst below that line for the receiving points G, H, & I. This behaviour can be explained on the basis of the following

physical reasoning. The decay at a point that results after the source cut-off consists of a series of discrete changes in the pressure level resulting from the passage of the termination of the wavetrains from the source and its first few reflections. The drop due to the passage of the wavetrain termination from the source is probably the most important, since the wavetrains from the images have various phases and amplitudes and hence do not necessarily recombine to give the same abrupt change at the receiving point. For the case shown in Fig. 13, viz. Case 1, there is no absorption at the walls. In such a case since the various wave trains set up a well-defined standing wave system it is possible that the passage of the termination of the wavetrain from the source may change the pressure at the receiving point from a node in the standing wave system to a loop. Thus the pressure at the receiving point may rise by a discrete amount at the beginning of the decay; or in a similar manner, may fall by a discrete amount if a loop is changed into a node at the receiving point.

Another point that can be noticed from Fig. 13 is that the first local peak on the pressure curve occurs at the receiving point F at 0.04 secs. and not at the receiving point D which is nearer to the source (Fig. 12). This is to be expected because the receiving point F is in the vicinity of one of the corners of the enclosure and as a

consequence it receives the contribution from the reflected pressure wave much earlier than any other receiving point. This statement is substantiated by another observation that the first pressure peak, seen on the curve for the receiving point F in Fig. 13 is absent from the corresponding curve in Fig. 14. It is recalled that Fig. 14 is for the Case 2 where the side wall WL1 (Fig. 12) of the enclosure is 100 % absorptive and as such there can be no reflected wave from this wall.

In Fig. 14, at any receiving point, the pressure does not build up to as high a value as it does in the perfectly reflecting case (Fig. 13). In Fig. 14 the pressure soon drops to zero. The pressure value in Fig. 14 is seen to be very nearly same at all the six receiving points D, E, F, G, H & I around 0.36 secs. Such a phenomenon is noticeable in Fig. 13 also.

Figure 15 shows the effect of variations in the bounding wall material properties on the pressure time history at the receiving point D when the source is of the double rectangular pulse shape. At any given time the highest pressure level is marked, as to be expected, by the pressure curve corresponding to Case 1, all walls perfectly reflecting; this particular curve is seen to be an enveloping curve

of the pressure values as a function of time that can possibly be attained in this chamber at the receiving point D for the particular source configuration (Fig. 11a) that is under investigation.

Consider, now, from Fig. 15 the individual pressure curves corresponding to Case 1, Case 2 and Case 3. In Case 1 all walls are perfectly reflecting, here the reverberant field generated from the initial portion of the positive half of the source cycle builds up to mask completely the wave field generated from the remaining portion of the positive half of the source cycle, the negative half of the source cycle and the source termination. In Case 2 the side wall WL1 is considered 100 % absorptive, and in Case 3 the ceiling i. e. wall WL6 is 100 % absorptive, while the other walls are perfectly reflecting. Some of the effects of sound absorbent materials is shown by these three curves. In Case 2 the pressure does not build up, as pointed out earlier, to as high a value as it does in the perfectly reflecting case (Case 1), while in Case 3, where the area of the absorbent material is still larger, the maximum value of the pressure is even less. In the curve corresponding to this Case 3 the pressure soon drops to zero point and then goes to negative, thereby showing that the wall reflections due to the first half of the source cycle are not sufficient enough to mask totally the latter part of the wave that comes from the

negative half of the source cycle. A look at Figs. 16, 23, 29 and 36 reveals that this is true, as to be expected, when the source configuration is of single cycle sinusoidal or N-shape pulse.

Figures 16 to 22 show, for Case 1 to Case 7 respectively, the composite pictures of the pressure variations at the six receiving points D, E, F, G, H & I when the source is a point source with single cycle sinusoidal pulse configuration. The value of the expected adiabatic pressure rise shown in Fig. 16 for the sinusoidal pulse is $2/\pi$ times that was found (Fig. 13) for the double rectangular pulse. A very striking indication from the Monte Carlo results of Figs. 16 to 22, common to all of these, is that after the source cut-off at 0.20 secs. the time interval between, say, 0.22 to 0.34 secs. roughly corresponds to half cycle length of the pressure vibrations that prevail in the region under investigation. This is in confirmity with the earlier observation that when the source is of sinusoidal configuration as shown in Fig. 11b, the pure tone source, in principle although a large number of vibrational modes are excited, it is the mode with Sl. No. 1 of Table I that becomes predominant, its frequency being coincident with the source frequency of 5 cycles.

A comparison of any particular curve from Fig. 16 or 17 with the corresponding curve from Fig. 13 or 14 indicates tht the number of local pressure peaks, referred to above as 'modulations', is larger and at the same time much more pronounced for the double rectangular case than for the sinusoidal case, the reason being the rectangular pulse has, in addition to its fundamental frequency of 5 cycles, higher harmonics of frequencies (Table I) 15, 25, 35, 45, etc. and the normal modes that are in the vicinity of these overtones are also excited strongly. This can be seen more clearly from Figs. 13.1, 14.1, 16.1 & 17.1 which indicate separately the constituent curves for the receiving point D of Figs 13, 14, 16 & 17 respectively. The more absorbent area in Case 3 makes the pressure values more negative in Fig. 18 than in Fig. 17.

Figures 23 to 28 indicate, for the receiving points D, E, F, G, H & I respectively, the effect of variations in the bounding wall material properties when the source is a point source with a single cycle sinusoidal pulse configuration. The curve corresponding to Case 1, all walls perfectly reflecting, forms the enveloping curve representing the limit pressure values. The lowermost curve is for the Case 3 where the absorbent surface is large.

A comparison of Figures 29.1 & 30.1, which show the constituent curves of Figs. 29 & 30 separately for the receiving point D, with Figs. 13.1 & 14.1 indicates that the number of modulations referred to earlier is larger when the source configuration is of N-shape than when it is of the double rectangular shape; this being due to the fact that, as shown in Table I, the N-shape configuration has additional number of higher harmonics with the frequencies in the neighbourhood of some additional groups of normal modes.

Expressing the transient pressure response curves, obtained from these Monte Carlo calculations, as the Fourier series with the same fundamental frequency as that of the input and utilizing the approach presented by Walters (1950) that makes use of the matrix method for numerical evaluation of the coefficients it is possible to find the transfer functions for the system. This approach of Walters is specifically aimed at the expansion of a finite part of the nonperiodic function into Fourier series. In the present study such an evaluation of the transfer functions for the system was not undertaken but the experimental results, reproduced in Fig. 54, that were reported originally by Bhatt (1939) seem to have a bearing on this subject.

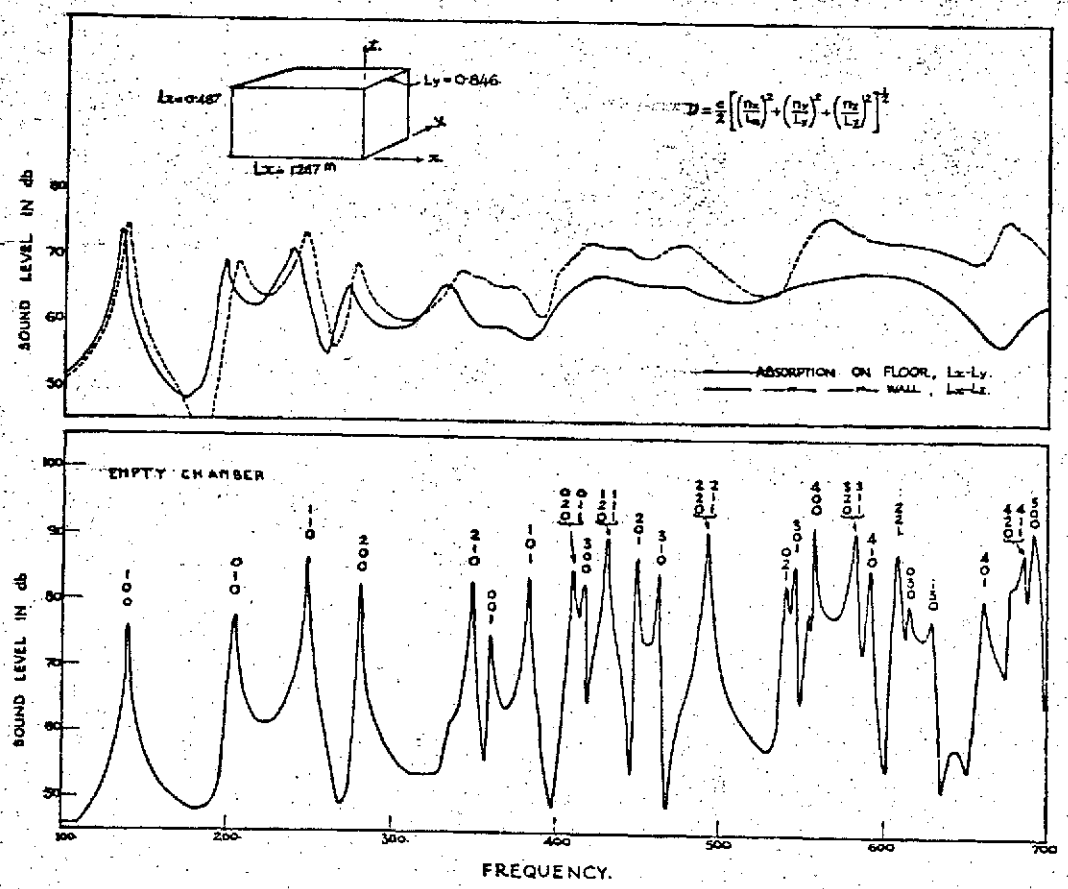

Resonance response curve of a rectangular chamber 49″×33½″×19″ with (a) bare walls, and (b) one wall covered completely with Acousti Celotex C4. Microphone is placed in a corner diagonally opposite to the source.

Fig. 54 Typical Resonance Response Curve

(Bhatt, 1939, Fig. 1, p. 68)

The linear dimensions of the room shown in Fig. 12 and that for the results of Fig. 54 are in the ratio 2.5 : 1.5 : 1 and 2.56 : 1.7 : 1 respectively; whilst their maximum dimensions are in the ratio 26.9 : 1. A comparison of the mode designation integers on the resonance peaks of Fig. 54 with those in Table I shows that the order of occurrence of the normal modes is very nearly the same in both these cases, but for the use with the room shown in Fig. 12 the frequency scale in Fig. 54 needs to be multiplied by a factor 1/26.9. Thus for example, the first mode 1,0,0 then occurs at the frequency 130/26.9 = 5.018 which is in agreement with the value shown in Table I.

Figure 54 shows that the effect of placing the absorption material on the floor, corresponding to Case 3 in the present study, is the drop in intensity of the first five peaks, all these with $m_3 = 0$, and the merger of the higher frequency peaks in a uniform response. The effect of placing the absorption material on the side wall, corresponding to Case 2 in the present study, is to merge the higher modes as before, but the loss of intensity is not as much as in the previous case due to a smaller absorption area. The wave corresponding to the normal mode 0,0,1 is normally incident on the floor and grazes the side wall. Thus when the material is on the side wall its absorption is small but is quite high when the material is on the floor, this is the

reason pointed out by Bhatt for the absence of the peak corresponding to the 0,0,1 mode from the solid line curve of Fig. 54.

According to Strutt (1929) in acoustics the room can be classified as a 'large room' only when the condition existing in a given room is such that the first free frequency of oscillation is very small with respect to the forced frequency. This clearly shows that even with the large dimensions (Fig. 12), the room that is considered here cannot be labelled as a 'large room'. The Monte Carlo calculations are not restricted to any particular class of room, large or small.

The four walls WL1, WL2, WL3 & WL4 (Fig. 12) forming the two corners with the receiving points F & I are perfectly reflecting in Case 1 & Case 6; thus in these cases at the points on these walls, or in particular roughly in the vicinity of the receiving points F & I there are the velocity nodes which are equivalent to the pressure extremals. This is the reason why for the most part of the observational period in Figs. 13, 16, 21, 29 and 34 the pressure curves corresponding to the receiving points F & I form the enveloping curves indicating either the maximum or the minimum pressure values.

The effect of varying the wall material properties for the N-shape source configuration is seen in Figs. 36 to 41 at the receiving points D, E, F, G, H & I resp.

As is expected, for most part of the observation period, the uppermost curve is that corresponding to Case 1 where all the walls are perfectly reflecting; whilst the lowermost curve is the one that corresponds to Case 3 where the area of absorption is maximum.

The modulations of the decay curve and the beat notes that result after the source cut-off are seen more clearly in Figs. 42 to 50; these are the pressure curves for an extended time period of 0.8 secs., four times the source time period T_p, at the receiving point E which is in the vicinity of the geometrical centre of the rectangular room. All of the odd modes of vibrations have the pressure nodes at the centre of the room and hence will not contribute to the pressure value there. Figures 42, 43 & 50 are for the Case 1 where all the walls are perfectly reflecting and there is no loss in the medium. As time advances more and more reflections arrive at the receiving point making the sound field directionally and spatially diffuse. Piling up of energy takes place at a set of frequency values close to which there are number of normal modes. Indicated in these figures are the expected adiabatic pressure values in each case of the source configuration. Considerable absorption that is present in Case 2, Case 3 and Case 7, for example, is the cause for the drop in the pressure intensity that is seen in Figs. 44, 45 & 49. The nature of these figures can be

explained on the basis of the interaction of two adjacent modes with the help of the experimental observations first reported by Knudsen (1967) and reproduced in Fig. 55.

In a rectangular room of dimensions 30' x 19' x 24' by making oscillograms of two separate modes 0,2,0 (37.439 cps) and 1,0,1 (37.662 cps), and then taking account of the changing phase differences and the different rates of decay Knudsen has verified that the intermediate curves in the top set of seven curves in Fig. 55 are some typical decays resulting from the interaction of these two adjacent modes.

In the bottom three curves of Fig. 55 the upper and lower records show the decay curves obtained by Knudsen for the two modes 0,4,0 (75.16 cps) and 2,0,2 (75.70 cps) whilst the middle record is the interaction of these two modes obtained by exciting the room at the intermediate frequency of 75.54 cps.; here the beat frequency corresponds precisely to the difference between 75.16 & 75.70 cps. A reference to Table I and the decay curves, for example Figs. 42, 43, 50, etc., shows that the Monte Carlo calculations are in general agreement with these observations of Knudsen.

The above discussion establishes the qualitative agreement of the Monte Carlo results with the other known results; in the following chapter is presented a

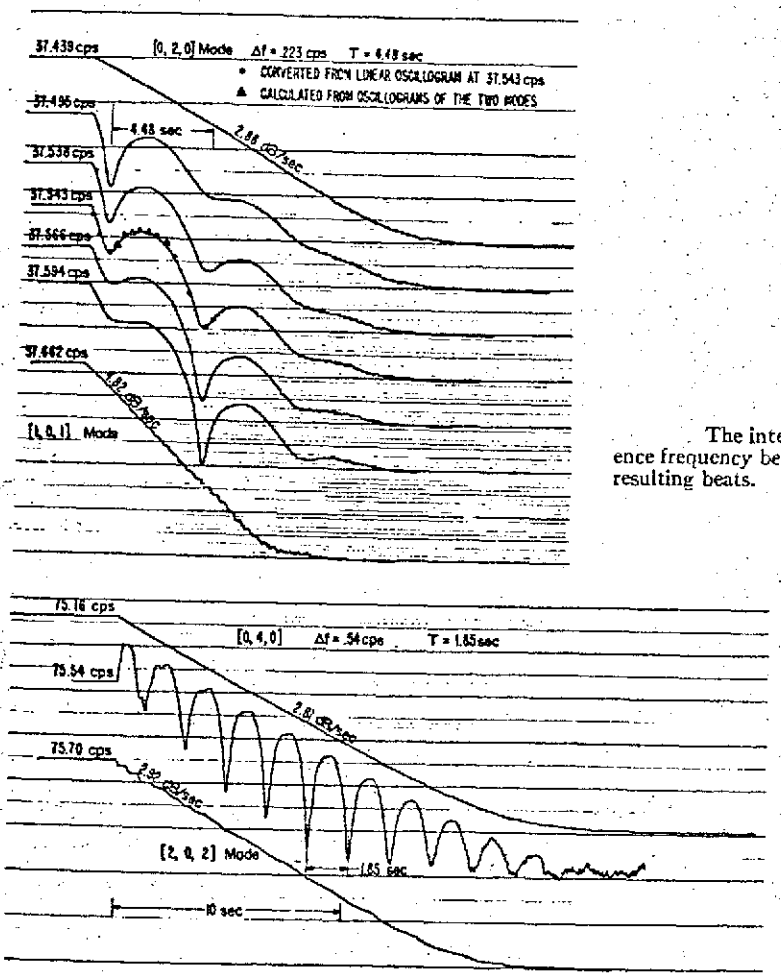

The interaction of two adjacent modes. ΔF is the difference frequency between the two modes, and T is the period of the resulting beats.

Fig. 55 The Interaction of Two Adjacent Modes

(Knudsen, 1967, Fig. 6, p. 958)

quantitative comparison using an analytical solution based on the Normal Mode method.

Chapter 6

PRESSURE FIELD INSIDE A RECTANGULAR ROOM

NORMAL MODE SOLUTION

The problem that is considered here is the investigation of the sound field inside a region bounded by rectangular walls using the normal mode point of view. In practical applications the walls of any enclosure possess certain amount of elasticity and heat conductivity. Inclusion of the finite elasticity and heat conductivity considerably complicates the solution of the problem. In order to visualize the situation more clearly, the side walls of the room are considered to be absolutely rigid, and non-heat conducting. The supporting medium inside the room is assumed to be homogeneous, and at rest initially.

It is customary to describe the pressure field inside the rooms in terms of the normal modes, considering the medium enclosed to be a three dimensional elastic body having its own natural modes of vibration, governed by

the mechanical constant of the mass of the medium, and the boundary conditions on the enclosing surface. In other words, this is to consider the enclosed medium as an assemblage of resonators, standing waves that can be set into motion by the source, and that will die exponentially when the source is stopped.

In this method the sound field inside a rectangular room is expressed as a sum of triply infinite set of eigenfunctions; depending upon the type of the standing waves they represent, the modes are classified as the axial, tangential, and oblique. It could be expected from the existing room acoustic theory that the earlier part of the response field, characterized by the pressure time history, would be dominated by the axial modes; with the passage of time, the tangential and the axial modes would be generated to a substantial extent, and as a result the field would be more and more diffused.

GOVERNING EQUATION

Consider a pressure field caused by a simple point source, radiating from a given source position $\underset{\sim}{x}_s$ in the region under investigation. It is governed by a nonhomogeneous wave equation of the type

$$\left\{ (1/c^2).(\partial^2/\partial t^2) - \nabla^2 \right\} p(x_r,t) = \rho\, \dot{Q}(t).\delta(\underset{\sim}{x}_r - \underset{\sim}{x}_s) \quad (1)$$

where c is the characteristic wave speed

$p(\underset{\sim}{x}_r,t)$ is the fluctuating acoustical pressure at a given receiving point $\underset{\sim}{x}_r$ at time t

ρ is the mass density of the medium

$Q(t)$ is the strength of the source, measured as the volume of fluid introduced by the source per unit time.

Consider, now, the point source characterized by a single cycle sinusoidal pulse(Fig. 11). Its mathematical representation is rewritten, using Eq. 2 of Chapter 5, as

$$\dot{Q}(t).\delta(\underset{\sim}{x}_r - \underset{\sim}{x}_s) = \left\{ \sin(2\pi t / T_p).\delta(\underset{\sim}{x}_r - \underset{\sim}{x}_s) \right\} [1 - H(t)]$$

$$= \mathcal{R}e \left\{ Q_0(\underset{\sim}{x}_s).\, e^{-i\omega t} \right\} [1 - H(t)] \quad (2)$$

where $\mathcal{R}e$ represents the real part of the quantity involved

$$Q_0(\underset{\sim}{x}_s) = -i \quad (3)$$

ω is the circular frequency of the source, given by

$$\omega = 2\pi / T_p \quad (4)$$

T_p is the source time period

$H(t)$ is the unit step function defined as

$$H(t) = \begin{cases} 0 & , \quad t < T_p \\ 1 & , \quad t > T_p \end{cases} \qquad (5)$$

Since the walls are considered to be rigid, the pressure field satisfies the boundary condition

$$(\partial / \partial n)\ p(\underset{\sim}{x}_r, t) = 0 \qquad \text{on the boundary} \qquad (6)$$

where $\underset{\sim}{n}$ is a direction normal to the boundary surface. The source is started at $t = 0$, and prior to that the quiescent condition exists; hence the initial conditions that need to be satisfied by the pressure field are the following two

$$\begin{aligned} p(\underset{\sim}{x}_r, 0) &= 0 \\ (\partial/\partial t)p(\underset{\sim}{x}_r, 0) &= 0 \end{aligned} \qquad (7)$$

NORMAL MODE REPRESENTATION

The pressure field inside the region is, now, assumed to be expressible in terms of the normal modes of vibration of the system as

$$p(\underset{\sim}{x}_r, t) = \sum_M \alpha_M(t) \cdot \Psi_M(\underset{\sim}{x}_r) \qquad (8)$$

where α_M is the coefficient to be determined

Ψ_M is the orthonormal eigenfunction that satisfies the homogeneous Helmholtz equation

$$\nabla^2 \Psi_M + \mu_M^2 \Psi_M = 0 \qquad (9)$$

μ_M^2 is the corresponding eigenvalue for the M^{th} mode of vibration; since no energy is absorbed either in the medium, or at the walls, all μ's are real

$M = (m_1, m_2, m_3)$ is an Integer Triad.

It is seen that Eq. 6 is satisfied only when

$$(\partial / \partial n)\, \Psi_M = 0 \quad \text{on the boundary} \qquad (10)$$

Selecting the Cartesian coordinate system as shown in Fig. 12, and denoting the length, width, and height of the room by L1, L2, and L3 resp., the eigenfunctions satisfying Eqs. 8 and 9 are expressed as

$$\Psi_M(\underset{\sim}{x}) = \cos(D1.X1) \cdot \cos(D2.X2) \cdot \cos(D3.X3)$$

with $\mu_M = \{ D1^2 + D2^2 + D3^2 \}^{\frac{1}{2}}$

where $Dj = \pi m_j / Lj$

$$\underset{\sim}{x} = (X1, X2, X3) \qquad (11)$$

GREEN'S FUNCTION EXPRESSION

For the region bounded by the rectangular walls use can be made of the Green's function expression given by Morse (1961), which when expressed in the present

notation takes the following form

$$G(k \mid \underset{\sim}{x}_r \mid \underset{\sim}{x}_s) = \sum_M A_M / k_M^2 \qquad (12)$$

where $k = \omega / c$, $k_M = \{ k^2 - \mu_M^2 \}^{\frac{1}{2}}$ (13)

$$A_M = \Psi_M(\underset{\sim}{x}_r) \; \Psi_M(\underset{\sim}{x}_s) / N_M \qquad (14)$$

N_M is the normalizing factor, defined as

$$N_M = \iiint_V \Psi_M(\underset{\sim}{x}) \; \Psi_N(\underset{\sim}{x}) \; dX1 \; dX2 \; dX3 \; . \delta_{MN}$$

$$= (L1 \; L2 \; L3) \; . \; (\varepsilon_{m_1} \varepsilon_{m_2} \varepsilon_{m_3})$$

$$= V \; . \; \varepsilon_M \qquad (15)$$

$$\varepsilon_j = \begin{cases} 1 & , \text{for } j \; 0 \\ \frac{1}{2} & , \text{for } j \; 0 \end{cases}$$

V is the volume of the enclosure.

Let $B_M = (1/2 k_M) \; . \; \left\{ e^{-i k_M ct} / (k_M - \omega / c) \right.$

$$\left. + \; e^{i k_M ct} / (k_M + \omega / c) \right\}$$

$$= - \{ \cos (k_M ct) - i \, (\omega / c \, k_M) \sin (k_M ct) \} / \mu_M^2$$

(16)

Then the pressure field in the nondimensional form, for the interval $0 \leq t \leq T_p$, can be expressed as

$$p^*(\underset{\sim}{x}_r, t) = \{Q_0(\underset{\sim}{x}_s)/c^2\} \mathcal{R}e\{-G(k|\underset{\sim}{x}_r|\underset{\sim}{x}_s)\, e^{-i\omega t} + \sum_M A_M B_M\}$$

$$= (1/c^2) \sum_M \left\{ A_M \sin(\omega t)/(k^2 - \mu_M^2) \right.$$

$$\left. + (k/k_M) \sin(\mu_M c t)/\mu_M^2 \right\} \quad (17)$$

Differentiation of this expression partially with respect to t gives

$$(\partial/\partial t)\, p^*(\underset{\sim}{x}_r, 0) = (\omega/c^2) \sum_M A_M / \mu_M^2 \{1 - (\mu_M/k)^2\} \quad (18)$$

Since $M = (m_1, m_2, m_3)$ is an Integer Triad, the summation over M is in fact a triple summation

$$\sum_M = \sum_{m_1=0}^{\infty} \sum_{m_2=0}^{\infty} \sum_{m_3=0}^{\infty} \quad (19)$$

For a given source frequency, the wave number k is a constant but the eigenvalue μ_M (Eq. 11) increases as the integer components m_1, m_2, m_3 take higher and higher values, and as a consequence, with the increase in the number of terms in the summation over M

$$1 / \mu_M^2 \{1 - (\mu_M / R)^2\} \rightarrow 0$$

This shows that the Eq. 18 satisfies the requisite initial conditions specified in Eq. 7. It is also noticed that the pressure amplitude increases considerably as

$$\mu_M \rightarrow R \quad .$$

This case is investigated separately by the application of l'Hospital's Rule; the resulting expression is

$$p^*(\underset{\sim}{x}_r, t) = (1/c^2)\left[\sum_M A_M \{ \sin(\omega t)/(R^2 - \mu_M^2) \right.$$

$$(\mu_M \neq R) \qquad + (R/R_M) \sin(R_M ct)/\mu_M^2 \}$$

$$\left. + (A_M/R^2) \{ \omega t/2 - \sin(\omega t) \} \right]$$

$$(\mu_M = R)$$

$$(\ 0 \leq t \leq T_p\ ) \qquad (\ 20\ )$$

At $t = T_p$ the source is cut-off (Fig. 11), the subsequent pressure field is expressed as

$$p^*(\underset{\sim}{x}_r,t) = (1/c^2) \sum_M A_M \left\{ a_M \cos(\kappa_M ct) + b_M \sin(\kappa_M ct) \right\} \qquad (21)$$

where the coefficients a_M and b_M are determined from the following two conditions at $t = T_p$

$$p^*(\underset{\sim}{x}_r,T_{p_+}) = p^*(\underset{\sim}{x}_r,T_{p_-})$$

$$(\partial/\partial t)\, p^*(\underset{\sim}{x}_r,T_{p_+}) = (\partial/\partial t)\, p^*(\underset{\sim}{x}_r,T_{p_-}) \qquad (22)$$

It is readily shown that this leads to

$$p^*(\underset{\sim}{x}_r,t) = (1/c^2) \sum_M A_M \Big[\left\{ \sin(\omega T_p).\ \cos[\kappa_M c(t-T_p)] \right\} / (\kappa^2 - \mu_M^2) \Big\}$$
$$+ (\kappa/\kappa_M) \left\{ \sin(\kappa_M ct)/\mu_M^2 \right.$$
$$\left. + \cos(\omega T_p).\ \sin[\kappa_M c(t-T_p)] / (\kappa^2 - \mu_M^2) \right\} \Big] \qquad (t > T_p)$$

$$(23)$$

Appendix 5 provides the computer programme for these relations, with a printout of the computed results for the pressure field at the receiving point D (Fig. 12) (Case 1). The Normal Mode Solution results thus obtained are shown compared with the corresponding Monte Carlo solution results(Appendix 4 programme and the result printout) in Fig. 56.

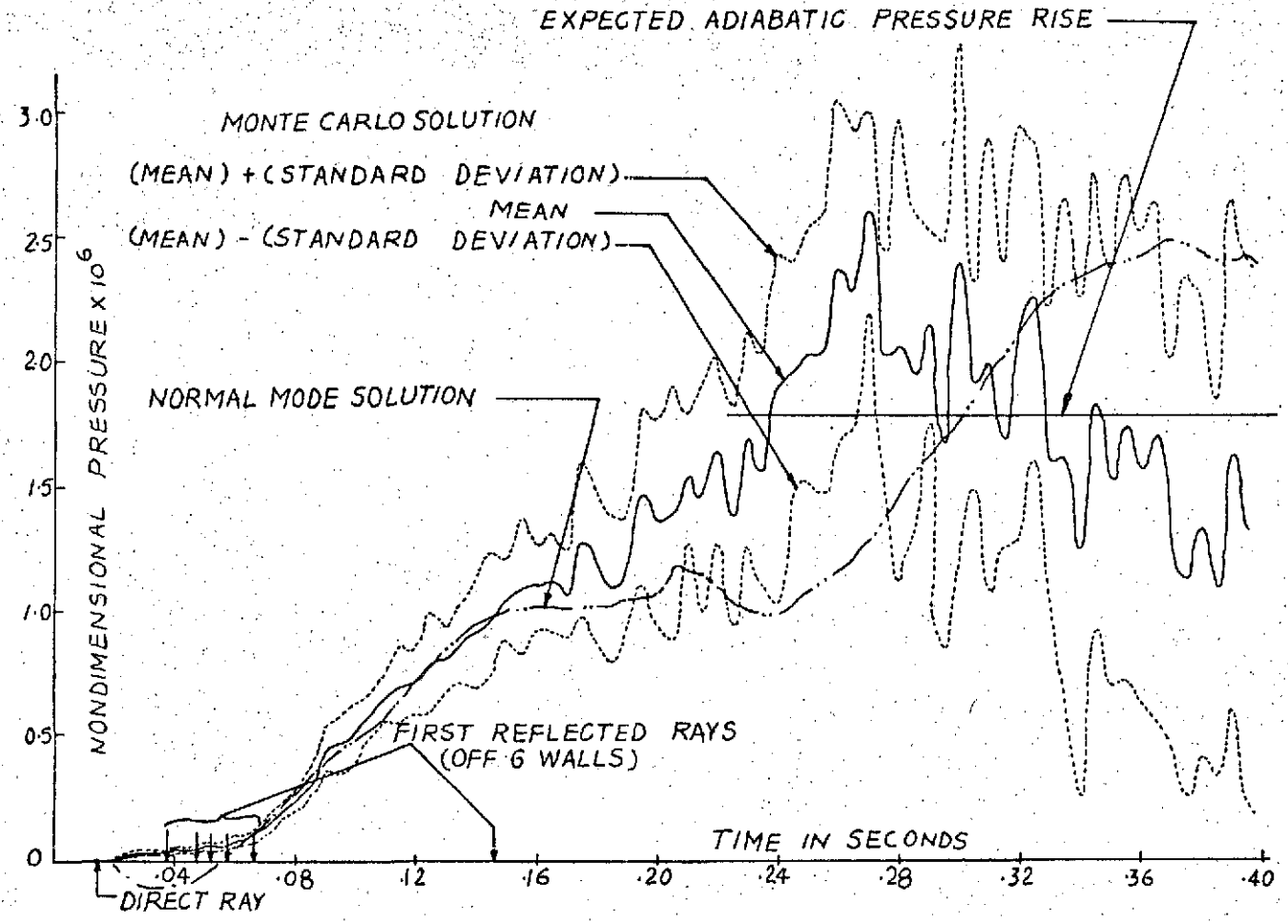

Fig. 56 Pressure Time History at Receiving Point D for Single Cycle Sinusoidal Pulse in Rectangular Room (Case 1) Comparison of the Monte Carlo and the Normal Mode Solutions

OBSERVATIONS

The Monte Carlo calculations of Fig. 56 consisted of ten blocks totalling 50000 selected ray pulses, and took 211 seconds of core time (Appendix 4) on the CDC 6400 computer at the University of Virginia's Computation Center. The normal mode solution included from (1,0,0) upto (15,15,15) and required 118 seconds (Appendix 5). Therefore, computation times were comparable, although results of equivalent accuracy would have been obtained by the normal mode method with less modes and consequently less time.

It will be seen from Fig. 56 that the results of the two methods are in general agreement, when it is considered that the normal mode solution should only be expected to be within the limits of plus and minus one standard deviation about 68% of the time (Appendix 2). Using Eq. 15 of Appendix 2, the probable relative error in these calculations is expressed as

$$\delta_{prob} = (0.68 \,/\, E\{p_j^*\}) \cdot (D^2\{p_j^*\} \,/\, N)^{\frac{1}{2}}$$

where $E\{p_j^*\}$ is the expected pressure value at the time index j

$D^2\{p_j^*\}$ is its variance

N is the sample size

For each block the sample size N was 5000. Choosing $j = 64$, for example, it is seen from the printout results of Appendix 4 that

$$E\{p_{64}^*\} = 2.10562361\ E\ -06 \qquad \text{and}$$

$$D^2\{p_{64}^*\} = 6.80646248\ E\ -13\ .$$

Then the corresponding value of the probable relative error is

$$\delta_{prob} = 0.0038\ .$$

It is noticed that whenever the variance is large, the value of the probable relative error gets large.

Chapter 7

MONTE CARLO APPLICATIONS TO ACOUSTICAL FIELD SOLUTIONS INSIDE A CURVED BOUNDARY

INTRODUCTION

In order to adapt the Monte Carlo technique that is developed in Chapter 3 to the cases of practical importance where the boundaries are not at right angles, certain modifications become essential especially to cover such eventualities as the occurrence of possible focussing effects, the associated singularities, etc. in the region under investigation. Such modifications and the extension of the proposed Monte Carlo technique to cover the cases of curved boundaries, not necessarily of simple geometric shape, are considered in the present chapter.

The problem of quantitative description of an acoustical field in a given region of curved boundaries, in the presence of acoustical sources, is basically similar to that identified earlier in Chapter 3. By specifying the

physical and thermodynamical characteristics of the supporting medium as well as the boundaries involved, and by utilizing the notion of the multipole sound sources for the generation of sound, a conceptual model is created to represent the given acoustical system.

MONOPOLE FIELD NONDIMENSIONAL FORM

Consider a representative monopole situated at a position, say, $\underset{\sim}{x}_s$ (Fig. 2) in an unbounded medium. Its pressure contribution at a receiving point $\underset{\sim}{x}_r$ is given by Eq. 8 of Chapter 3. When considering the effects of curved boundaries it is more convenient to express this equation in a nondimensional form. This is achieved by introducing a set of new nondimensional variables defined as

$$R^* = R/a, \quad V'^* = V'/a^3, \quad \underset{\sim}{x}_r^* = \underset{\sim}{x}_r/a, \quad \underset{\sim}{x}_s^* = \underset{\sim}{x}_s/a$$

$$t^* = ct/a, \quad \tau^* = c\tau/a, \quad m^* = m/\rho, \quad p^* = p/\rho c^2 \qquad (1)$$

where a is some characteristic length of the problem that is under investigation; for example, when considering the field inside a cylindrical duct, a can be conveniently chosen to be the maximum radius of the duct. Substitution of these variables in Eq. 8 of Chapter 3 results in an expression for the nondimensional pressure distribution caused by the source under investigation, and it is given by

$$p^*(\underset{\sim}{x}_r^*, t^*) = (V'^*/4\pi R^*).(\partial^2/\partial t^{*2})\, m^*(\underset{\sim}{x}_s^*, \tau^*)$$

$$= \dot{Q}^*(\tau^*) / R^* \qquad (2)$$

where $Q^*(t^*) = V'^*\, \dot{m}^*(x_s^*, t^*) / 4\pi$

is the quantity that represents the strength time history of the energy source.

ENERGY SOURCE FINITE INTERVAL TIME REPRESENTATION

A typical strength time history of an acoustical point source is shown in Fig. 57a. Its total period of activation

$$T_p^* = c\, T_p / a \qquad (3)$$

where T_p is the source time period in seconds, is divided into a finite number of intervals

$$2\, n_p = T_p^* / \Delta\tau^* \qquad (4)$$

where $\Delta\tau^*$ is a width of any individual interval. In each of these intervals the strength of the source is approximated as constant. The use of finite number of elementary pulses thus defined, as shown in Fig. 57b, then represents the required approximate finite time interval representation that is necessary for the Monte Carlo simulation.

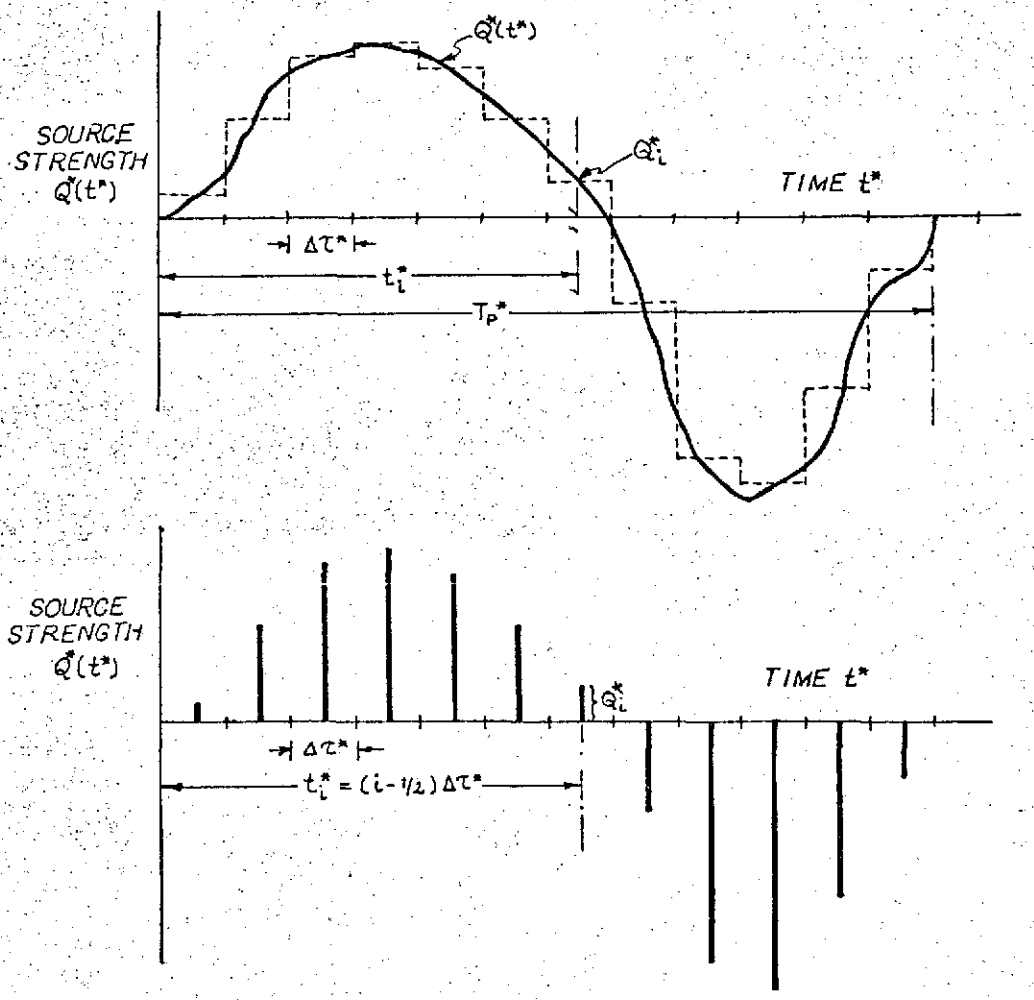

Fig. 57 Typical Source Strength Time History in Nondimensional Variables

Now considering i as an integral index such that

$$1 \leq i \leq 2 n_p \qquad (5)$$

it is seen that a pulse corresponding to it can be defined to be the one with

$$\text{strength} \quad Q_i^*$$

$$\text{and time of origin} \quad t_i^* = (i - \tfrac{1}{2}) \Delta\tau^* \qquad (6)$$

Then with the use of Eq. 2 it can be shown that its pressure contribution at the observation point $\underset{\sim}{x}_r^*$ is given by

$$p_i^*(\underset{\sim}{x}_r^*, t^*) = \dot{Q}^*(t_i^*) / R^* \qquad (7)$$

where the relation between the three variables t^*, t_i^* and R^* can be very easily shown to be

$$t^* = t_i^* + R^* \qquad (8)$$

or in other words

$$t_i^* = t^* - R^* \qquad (9)$$

where $R^* = |\underset{\sim}{x}_r^* - \underset{\sim}{x}_s^*|$

Recalling the definition given in Eq. 1 it is seen that an equivalent dimensional form of Eq. 9 is given by

$$t_i = t - R / c \qquad (10)$$

From this relation and the relation given by Eq. 5 of Chapter 3 it can be inferred that when t^* is considered to be an instant at which the wave of pressure disturbance that was originated at the source position $\underset{\sim}{x}_s^*$, and at time t_i^* arrives at the receiving point $\underset{\sim}{x}_r^*$, the time of origin t_i^* given by Eq. 6 and the retarded time τ^* defined by Eq. 1 above and Eq. 5 of Chapter 3 are synonymous.

Since the pulse of index i produces, in the immediate neighbourhood of the source position $\underset{\sim}{x}_s^*$, a pressure disturbance in a short interval, say, t_i^* to $(t_i^* + \epsilon)$, its effect at any subsequent instant $t^* (> t_i^*)$ is localized within a very thin spherical shell with centre $\underset{\sim}{x}_s^*$ and radius $R^* (= t^* - t_i^*)$. To be more specific, let a new variable t_m^* be introduced to represent the instant at which the disturbance wavefront that was originated at time t_i^* and at the source position $\underset{\sim}{x}_s^*$ arrives at the receiving point $\underset{\sim}{x}_r^*$; then using a δ-function, the pressure contribution from the i^{th} pulse given by Eq. 7 can be written as

$$p_i^*(\underset{\sim}{x}_r^*, t^*) = (\dot{Q}_i^* / R_m^*) \cdot \delta(t^* - t_m^* - t_i^*) \qquad (11)$$

where $R_m^* = R^* = |\underset{\sim}{x}_r^* - \underset{\sim}{x}_s^*|$

is the distance traversed by the disturbance wave during the interval t_i^* to t_m^*.

Now suppose that a given length of the transitional period, the period for which the solution is to be studied, is divided into J time cells, each of duration Δt^*. Let $p_{ij}{}^*(\underset{\sim}{x}_r{}^*)$ be the mean value of the pressure $p_i{}^*(\underset{\sim}{x}_r{}^*, t^*)$ given by Eq. 11 taken over the j^{th} time interval; then

$$p_{ij}{}^*(x_r{}^*) = (1/\Delta t^*) \int_{j\,\Delta t^* - 1}^{j\,\Delta t^*} p_i{}^*(\underset{\sim}{x}_r{}^*, t^*)\, dt^*$$

$$= \Delta\tau^*\, \dot{Q}_i{}^* \,/\, R_m{}^*\, \Delta t^*$$

if the disturbance wavefront of the i^{th} pulse passes through the receiving point during the j^{th} time interval

$$= \quad 0 \quad \text{otherwise} \qquad (12)$$

When the length of the time cell Δt^* of the transitional period is considered to be the same as $\Delta\tau^*$, the length of any individual subinterval used in the finite time interval representation of the energy source (Fig. 57); i.e. when

$$\Delta t^* = \Delta\tau^* \qquad (13)$$

Eq. 12 reduces to

$$p_{ij}^{*}(\underline{x}_r^{*}) = \dot{Q}_i^{*} / R_m^{*}$$

if the disturbance wavefront of the i^{th} pulse passes through the receiving point during the j^{th} time interval

$$= 0 \quad \text{otherwise} \qquad (14)$$

RAY PROPAGATION IN A BOUNDED MEDIUM

At every point in a medium the signal that describes the pressure disturbance propagates along a direction normal to the wavefront surface. The locus of this wavefront normal is the requisite trajectory along which the acoustical ray propagates. In general this is a function of

I. Initial direction of any particular ray, emanating from the energy source

II. Spatial variations of the physical and thermodynamical characteristics of the fluid medium

III. Spatial variations of the geometric shape and the thermodynamical characteristics of the boundaries that enclose the region under investigation.

Mathematical specification of these, as pointed out earlier, is essential in order to make the problem of the determination

of the ray trajectory a determinate one; thereby enabling a formulation of a set of equations that defines the ray direction successively.

When the medium under investigation does not extend to infinity but is bounded at finite distances from the energy source, it becomes essential to redefine the variable R^*, or R_m^*, appearing in the above formulation, as the arcual distance, measured along the ray trajectory, starting from the source position $\underset{\sim}{x}_s^*$ to the receiving point position $\underset{\sim}{x}_r^*$; this takes into account any reflections from the solid boundary that might have taken place during the progress of that particular ray.

RAY TUBE

In the region under investigation, in general, the physical and thermodynamical variations are present; in the course of the ray trajectory, any possible eventualities resulting from such variations can be taken care of more conveniently by following not only a single ray but instead a small ray tube, consisting of a bundle of rays, that originates from the energy source, within a given elemental solid angle $\Delta\Omega$, centred around a randomly selected ray (α, β, γ). Such a ray tube and its trajectory are shown in Fig. 58. At any point along its trajectory the variables that define such a ray tube are its spatial and directional

coordinates along with its weight; a ray tube weight is its intensity. Q_i^* is the initial weight of the ray tube that is used to characterize the randomly selected pulse with an integral index i, given by Eq. 5.

In the present analysis it is assumed that the influence of the selected pulse is confined within the ray tube that is traced. Then this pulse can contribute towards the construction of a pressure field at a given receiving point in the region, only when such a point is intercepted by the propagating ray tube. The pressure amplitude determined by the ray tube there would represent the extent of the pressure contribution from the ray at the time of such an occurrence.

Ray Tube Divergence Factor

Figure 58 shows two receiving points $\underset{\sim}{x}_{r1}^*$ and $\underset{\sim}{x}_{r2}^*$ that come under the influence of the propagating ray tube, in the course of its trajectory, after suffering a few collisions with the solid surface on its way.

Let s_1^* and s_2^* represent the ray tube cross-sectional areas in the nondimensional form, normal to the central ray (α, β, γ); and let, in general, n_1 and n_2 be the indices of refraction of the supporting medium at these two points $\underset{\sim}{x}_{r1}^*$ and $\underset{\sim}{x}_{r2}^*$ respectively. Initially for the application of the proposed Monte Carlo technique, in

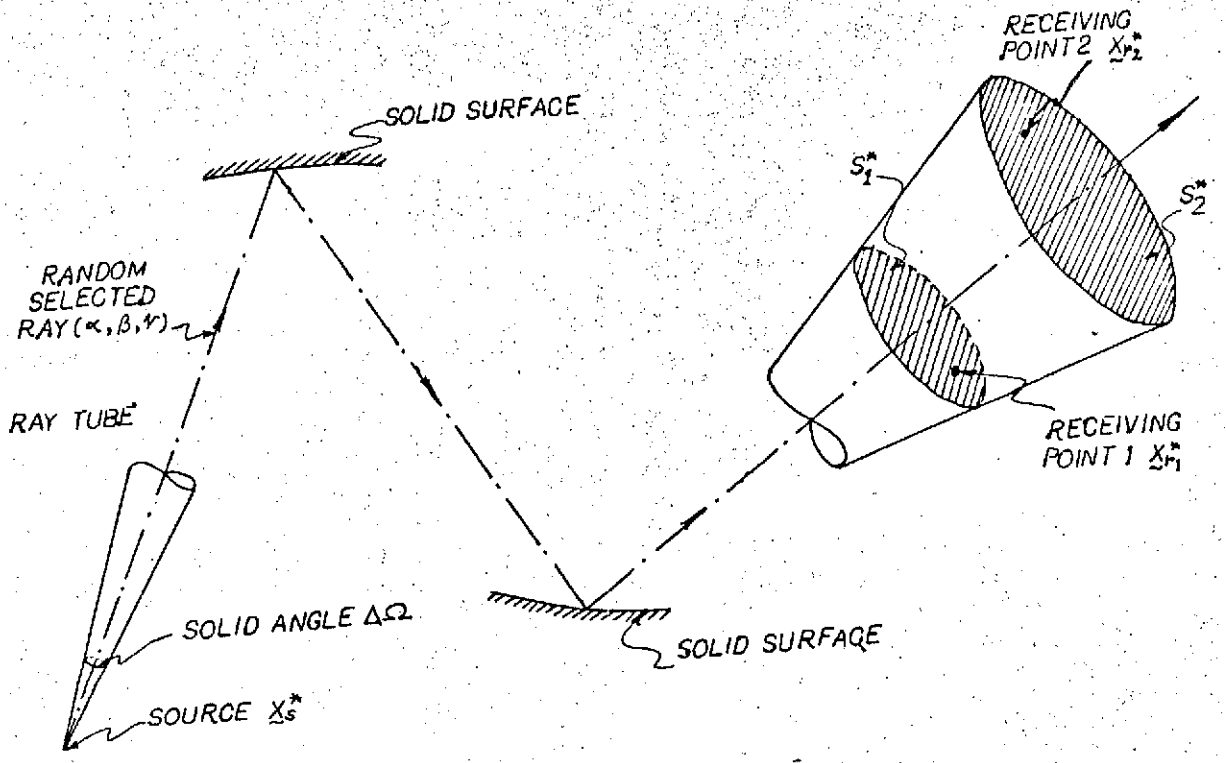

Fig. 58 Trajectory of the Ray Tube

the present work, a particular case of homogeneous medium is considered; then

$$n_1 = n_2 = \text{constant} \qquad (15)$$

throughout the region. In a more general case, depending on the extent of the variations in the refractive indices from one point to another, it would be essential to take the proper account of the resulting scattering effects.

If p_{i1}^* is considered to be the pressure contribution from this ray (α, β, γ) at the position $\underset{\sim}{x}_{r1}^*$, then that at $\underset{\sim}{x}_{r2}^*$ can be expressed as

$$p_{i2}^*(\underset{\sim}{x}_{r2}^*, t_2^*) = p_{i1}^*(\underset{\sim}{x}_{r1}^*, t_1^*) \cdot DF12 \qquad (16)$$

where DF12 is the ray tube divergence (or convergence) factor defined, in general, as

$$DF12 = \left\{ (n_1 / n_2).(s_1^* / s_2^*) \right\}^{\frac{1}{2}} \qquad (17)$$

and

$$t_2^* = t_1^* + | \underset{\sim}{x}_{r2}^* - \underset{\sim}{x}_{r1}^* |$$

$$= (t_i^* + R_1^*) + R_1^* / DF12 \qquad (18)$$

R_1^* being the arcual distance, measured along the ray(α, β, γ) trajectory from the source position $\underset{\sim}{x}_s^*$ to the receiving point $\underset{\sim}{x}_{r1}^*$.

Variation in Ray Tube Cross-sectional Area

It is seen from above that in order to estimate the pressure contribution at any point in the region it is essential to be able to follow the variations in the ray tube cross-sectional area during its lifetime. A number of alternate methods were investigated, the one that requires the minimal computational efforts is outlined below.

This method consists of simultaneous following of three rays originating from the same source. Out of these three, one is the random selected ray (α, β, γ); whilst the other two are simply adjacent to it with very small elemental differences in their directional coordinates initially. At any point along the trajectory the area formed by the triangle with vertices corresponding to points on these three rays there now represents, when normalized, the required variation in the ray tube area. This variation, in general, is a function of the local geometry and the material characteristics of the region that is under investigation, and so at the latter stage of the trajectory there is a likelihood of these three rays being reflected from the surface positions with differing characteristics. This eventuality is reduced to a minium by holding the initial differences in the components of the directional coordinates

of these three rays to an absolute minimum, which in other words amounts to having the distances between these three rays, initially, as small as possible. As defined earlier, when the linear dimension is normalized by the maximum boundary radius, at a distance of the order of 0.5 from the source position, the initial ray tube area of the order of 1.0 E -25 magnitude has been tried. The technique that is developed for such a processing is dealt with in considerable detail in the following chapter.

Chapter 8

CURVED BOUNDARY PROBLEM

RAY TUBE PROCESSING

INTRODUCTION

The estimation of the pressure at a given receiving point in the region under investigation is based on the study of the propagation of the ray tube, starting from a given source, in a material medium of known geometry and physical properties. The Monte Carlo technique that is developed for this purpose is quite general. It is explained here with the help of a specific problem of prediction of the transient acoustic field caused by a sound source inside a cylindrical duct. The procedure for a more general case is outlined in Appendix 6.

MODEL SPECIFICATION

The proposed Monte Carlo method, as pointed out earlier, is not restricted to cases where the bounding

surface is of simple geometrical shape; however, for clarity and definiteness in the presentation of the technique that is developed, the region that is selected for the first application is the one that is bounded by a cylindrical duct surface of circular cross-section, rigidly closed on the left and terminating on the right in a perfectly absorptive medium (Fig. 59).

A small acoustic driver, mounted at the centre of the duct on the left bounding surface, is assumed to give an emission corresponding to a 'point source' of sound.

With a view of presenting a tractable analytical solution for the same problem, thereby providing a quantitative evaluation of the results obtained from the application of the Monte Carlo technique, the cylindrical surface is considered to be perfectly reflecting, and the supporting medium is assumed to be homogeneous, being at rest initially. The main feature of such a medium is that, here, originating from the source, the ray tube propagation is essentially in paths composed of straight lines from one collision to another one with the bounding surface.

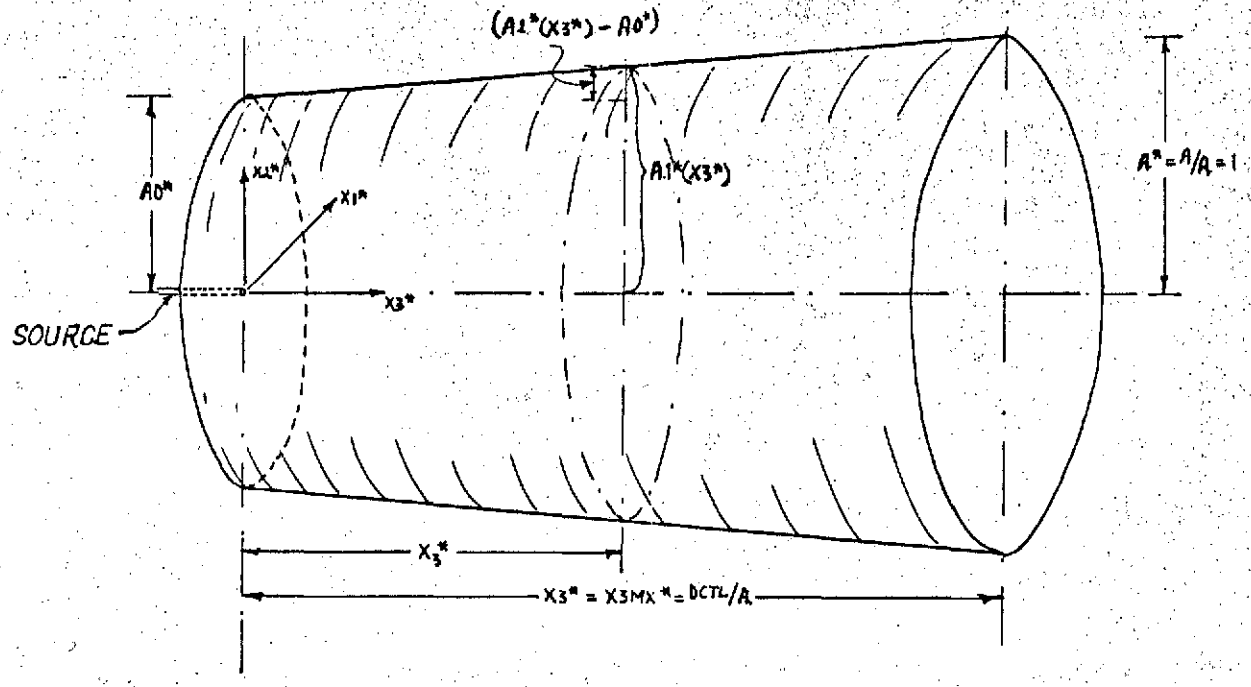

Fig. 59 Cylindrical Duct

RAY TUBE VARIABLES

For any ray the starting point is the position of the source, which is denoted in the following formulation, for brevity, by

$$\underline{XS}^*(1,2,3) = (XS1^*, XS2^*, XS3^*) \qquad (1)$$

In the particular case that is under investigation here, and shown in Fig. 59, the source position is coincident with the origin of the coordinate system.

As explained in Appendix 6 the directional law that is applicable in this case is the Cosine Distribution Law DL(2). Let the unit vector in the direction of the randomly selected ray (α, β, γ) be denoted by

$$\underline{DCI}(1,2,3) = (DCI1, DCI2, DCI3) \qquad (2)$$

then the equation of this ray in parametric form, with U as a parameter, can be expressed, when the supporting fluid medium is homogeneous and is at rest initially, by the following set of equations

$$\begin{aligned} XI1^* &= DCI1 \cdot U \\ XI2^* &= DCI2 \cdot U \\ XI3^* &= DCI3 \cdot U \end{aligned} \qquad (3)$$

where $\underline{XI}^*(1,2,3) = (XI1^*, XI2^*, XI3^*)$

is a point on the selected ray. The parameter U which is still undetermined is chosen such that this point $\underline{XI}^*(1,2,3)$ is a point that is common to the ray and a cylindrical surface of arbitrarily chosen radius

$$AREF^* = 0.5 \qquad (4)$$

This results in a relation

$$XI1^{*2} + XI2^{*2} = 0.25$$

which with Eq. 3 yields

$$U^2 \cdot (DCI1^2 + DCI2^2) = 0.25 \qquad (5)$$

Since the components of Eq. 2 are the direction cosines, they obey the relation

$$DCI1^2 + DCI2^2 + DCI3^2 = 1$$

which with Eq. 5 gives

$$U = 0.5 / (1 - DCI3^2)^{\frac{1}{2}} \qquad (6)$$

Let DCTL be the length of the duct, and A be its maximum crosssectional radius; then the geometrical variations in the radial direction (Fig. 59), when present, can be expressed mathematically by a definition of the local cross-sectional radius $A1^*(X3^*)$ as

$$A1^*(X3^*) = A0^* + A2^* \cdot X3^* \qquad (7)$$

where $A2^* = (1 - A0^*) / X3MX^*$

$$= (1 - A0^*) \cdot A / DCTL \qquad (8)$$

The point $\underline{XI}^*(1,2,3)$ defined by Eqs. 23 and 20 is considered to be a reference point for the initial definition of the ray tube area, if the relation

$$A1^*(XI3^*) > AREF^* \qquad (9)$$

is satisfied.

It is noticed that when the relation of Eq. 9 is not satisfied, the point $\underline{XI}^*(1,2,3)$ lies outside the region, in which case it becomes essential to redefine the value of $AREF^*$ in Eq. 4 and repeat the process until Eq. 9 is satisfied; when this is achieved, two additional points are defined such that

$$\underline{XI}^*(4,5,6) = (XI4^*, XI5^*, XI6^*) = (XI1^*, XI2^*, XI3^* + DPHI)$$

$$\underline{XI}^*(7,8,9) = (XI7^*, XI8^*, XI9^*) = (XI1^* + DPSI, XI2^*, XI3^*) \qquad (10)$$

where DPHI and DPSI are nondimensional elemental lengths of absolutely small magnitudes; for example, the results presented in Chapter 10, later, use

$$DPHI = DPSI = 1.0\,E\,-12 \qquad (11)$$

Originating from the source (Eq. 1) two additional rays are made to pass through these points (Eq. 10), and defined the unit vectors in these directions as

$$\underline{DCI}(4,5,6) = (DCI4,\ DCI5,\ DCI6)$$

$$= \left\{ \underline{XI}^*(4,5,6) - \underline{XS}^*(1,2,3) \right\} / \left| \underline{XI}^*(4,5,6) - \underline{XS}^*(1,2,3) \right|$$

$$\underline{DCI}(7,8,9) = (DCI7,\ DCI8,\ DCI9)$$

$$= \left\{ \underline{XI}^*(7,8,9) - \underline{XS}^*(1,2,3) \right\} / \left| \underline{XI}^*(7,8,9) - \underline{XS}^*(1,2,3) \right| \qquad (12)$$

This completes the identification of the three rays that are to be followed in the study of the variations in the ray tube cross-sectional area during its lifetime.

Consider a triangle shown in Fig. 60. Let B0, B1, B2, and B3 be its three sides, and the semiperimeter respectively; then using Heron's formula its area is given by the expression

$$\text{Area}\left[\underline{X}(1,2,3),\ \underline{X}(4,5,6),\ \underline{X}(7,8,9)\right]$$

$$= \left\{ B3 \cdot (B3 - B0) \cdot (B3 - B1) \cdot (B3 - B2) \right\}^{\frac{1}{2}} \qquad (13)$$

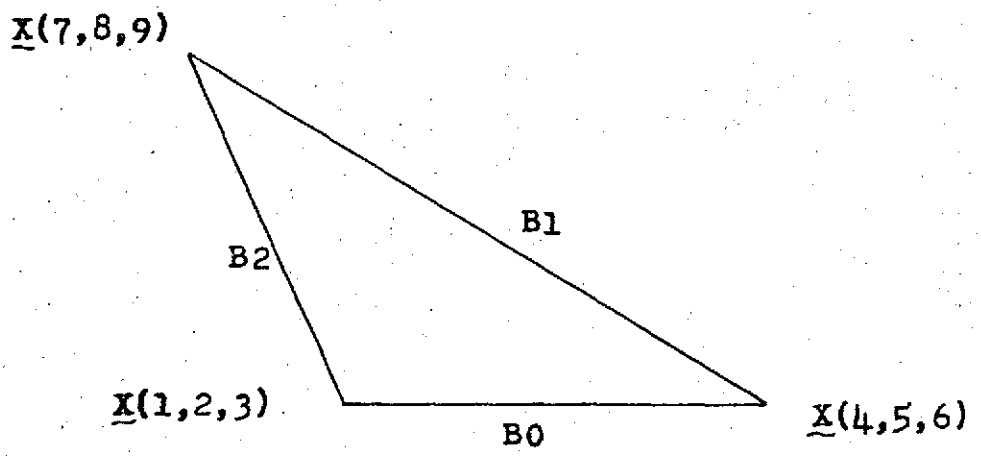

Fig. 60. Area of a Triangle by Heron's Formula

where $B0 = |\underset{\sim}{X}(1,2,3) - \underset{\sim}{X}(4,5,6)|$

$B1 = |\underset{\sim}{X}(4,5,6) - \underset{\sim}{X}(7,8,9)|$

$B2 = |\underset{\sim}{X}(7,8,9) - \underset{\sim}{X}(1,2,3)|$

$B3 = \frac{1}{2}(B0 + B1 + B2)$

For the purpose of normalization of the ray tube, consider

$$ARTO^* = \text{Area}\left[\underset{\sim}{XI}^*(1,2,3),\ \underset{\sim}{XI}^*(4,5,6),\ \underset{\sim}{XI}^*(7,8,9)\right] \qquad (14)$$

to be the reference ray tube area. It is situated on a reference plane, which is at a distance

$$RREF^* = |\underset{\sim}{XI}^*(1,2,3) - \underset{\sim}{XS}^*(1,2,3)| \qquad (15)$$

from the source position; hence the pressure intensity there is expressible as (see Eqs. 7, and 8, Chapter 7)

$$PREF^* = p_i^*(\underline{XI}^*(1,2,3), TREF^*)$$
$$= \dot{Q}^*(TI^*) \; / \; RREF^* \qquad (16)$$

where $TREF^* = TI^* + RREF^*$ (17)

It is recalled that the nondimensional time parameter TI^* is defined as

$$TI^* = c \; . \; TI \; / \; A \qquad (18)$$

where TI is the time of origin of the selected pulse in seconds.

After having these quantities as the initial specifications for the ray tube at the reference plane, the next logical step is to investigate what changes they undergo on meeting the solid surface of the enclosing boundary.

COLLISION WITH THE BOUNDARY SURFACE

For brevity, the three vertex points of the ray tube in the reference plane, and the direction coordinates of the three rays are designated, respectively, by

$$\underset{\sim}{XI}^*(j,\ j+1,\ j+2) = (XI^*_j,\ XI^*_{j+1},\ XI^*_{j+2})$$

$$\underset{\sim}{DCI}(j,\ j+1,\ j+2) = (DCI_j,\ DCI_{j+1},\ DCI_{j+2})$$

(where $j = 1, 4,$ and 7) (19)

Let the points of collision of these three rays with the boundary surface be denoted by

$$\underset{\sim}{XC}^*(j,\ j+1,\ j+2) = (XC^*_j,\ XC^*_{j+1},\ XC^*_{j+2}) \quad (20)$$

The equation for the cylindrical duct surface (Fig. 59) is given by

$$F(X1^*, X2^*, X3^*) = X1^{*2} + X2^{*2} - A1^{*2}(X3^*) = 0 \quad (21)$$

where the local duct radius $A1^*(X3^*)$ at the axial position $X3^*$ is given by Eq. 7.

The point of collision, given by Eq. 20, is common both to the ray and to the boundary surface; hence it satisfies the relations

$$\frac{XC^*_j - XI^*_j}{DCI_j} = \frac{XC^*_{j+1} - XI^*_{j+1}}{DCI_{j+1}} = \frac{XC^*_{j+2} - XI^*_{j+2}}{DCI_{j+2}}$$

$$XC^{*2}_j + XC^{*2}_{j+1} - (A0^* + A2^* \cdot XC^*_{j+2})^2 = 0 \quad (22)$$

From the first of these relations, the following set of equations follows

$$XC^*_j = A12 \cdot (XC^*_{j+1} - XI^*_{j+1}) + XI^*_j$$
$$XC^*_{j+2} = A32 \cdot (XC^*_{j+1} - XI^*_{j+1}) + XI^*_{j+2} \qquad (23)$$

where $A12 = DCI_j / DCI_{j+1}$, $A32 = DCI_{j+2} / DCI_{j+1}$

Substitution of these in the latter relation of Eq. 22 yields a quadratic equation for the determination of XC^*_{j+1}

$$AA \cdot XC^{*2}_{j+1} + 2\,BB \cdot XC^*_{j+1} - CC = 0 \qquad (24)$$

where $AA = 1 + A12^2 + (A2^* \cdot A32)^2$

$$BB = A12 \cdot (XI^*_j - A12 \cdot XI^*_{j+1}) - A2^* \cdot \left\{ A0^* + A2^* \cdot (XI^*_{j+2} - A32 \cdot XI^*_{j+1}) \right\}$$

$$CC = \left\{ A0^* + A2^* \cdot (XI^*_{j+2} - A32 \cdot XI^*_{j+1}) \right\}^2 - (XI^*_j - A12 \cdot XI^*_{j\,1})^2$$

The two roots of this equation are expressed as

$$XC^*_{j+1} = UMX, \text{ or } UMN \qquad (25)$$

where $UMX = \max (UA, UB)$

$UMN = \min (UA, UB)$

$$UA = (- BB + D) / AA$$

$$UB = (- BB - D) / AA$$

$$D = (BB^2 + AA \cdot CC)^{\frac{1}{2}}$$

Noticing that the vector drawn from the point $\underset{\sim}{XI}^*(j, j+1, j+2)$ towards the collision point $\underset{\sim}{XC}^*(j, j+1, j+2)$ must necessarily point in the positive direction of the propagating ray, depending upon the value of the direction coordinate DCI_{j+1}, there result the following two cases :

$$\begin{aligned} &\text{Case 1} : DCI_{j+1} > 0; \text{ then } XC^*_{j+1} = UMX \\ &\text{Case 2} : DCI_{j+1} < 0; \text{ then } XC^*_{j+1} = UMN \end{aligned} \qquad (26)$$

Substitution of thus selected value of XC^*_{j+1} in Eq. 23 completes the determination of the collision point $\underset{\sim}{XC}^*(j, j+1, j+2)$.

REFLECTED RAY

Since Eq. 21 describes the cylindrical surface, the equation satisfied by the inward normal to the tangent plane (Fig. 61) at the point $\underset{\sim}{XC}^*(j, j+1, j+2)$ can be written as

$$(X1^* - XC^*_j)/a1 = (X2^* - XC^*_{j+1})/a2 = (X3^* - XC^*_{j+2})/a3 \qquad (27)$$

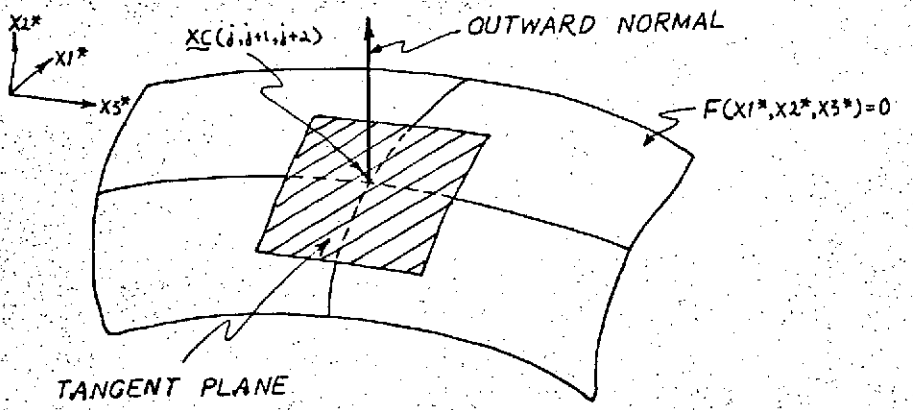

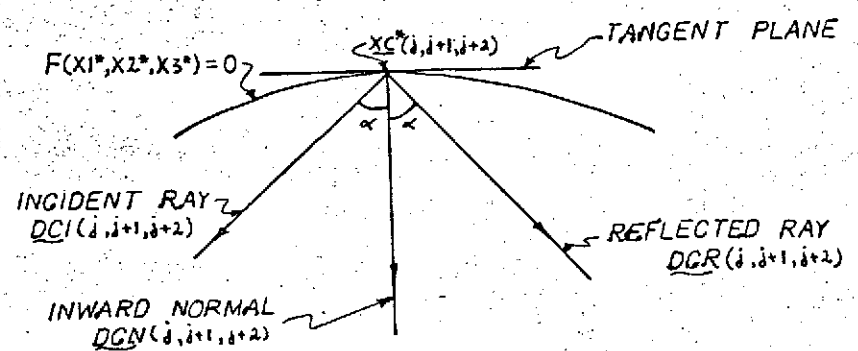

Fig. 61 Tangent Plane and the Reflected Ray

where a1, a2, and a3 are the direction ratios given by

$$a1 = -F_{X^*_j}\Big|_{\underline{XC}^*(j,j+1,j+2)} = -2\,XC^*_j$$

$$a2 = -F_{X^*_{j+1}}\Big|_{\underline{XC}^*(j,j+1,j+2)} = -2\,XC^*_{j\,1}$$

$$a3 = -F_{X^*_{j+2}}\Big|_{\underline{XC}^*(j,j+1,j+2)} = 2\,(A0^* + A2^* \cdot XC^*_{j\,2}) \cdot A2^*$$

Let $a0 = (a1^2 + a2^2 + a3^2)^{\frac{1}{2}}$ (28)

then the direction cosines of the inward normal are given by

$$\underline{DCN}(j,j+1,j+2) = (DCN_j, DCN_{j+1}, DCN_{j+2})$$

$$= (a1/a0,\ a2/a0,\ a3/a0) \quad (29)$$

The angle of incidence α is given by

$$\cos\alpha = -(DCI_j \cdot DCN_j + DCI_{j+1} \cdot DCN_{j+1} + DCI_{j+2} \cdot DCN_{j+2}) \quad (30)$$

Since the angle of reflection is equal to the angle of incidence, the direction coordinates for the reflected ray can now be expressed as

$$\underline{DCR}(j,j+1,j+2) = (DCR_j, DCR_{j+1}, DCR_{j+2}) \quad (31)$$

where $DCR_k = DCI_k + (2 \cos \alpha) \cdot DCN_k$

for $k = j, j+1,$ and $j+2$

The knowledge of these now enables the location of any required point on the reflected ray. Let

$$\underline{XR}^*(j, j+1, j+2) = (XR^*_j, XR^*_{j+1}, XR^*_{j+2})$$

be a point that is common both to the reflected ray, and, say, an imaginary cylindrical surface of radius RAD^* (Fig. 62); then the equations determining this point are

$$\frac{XR^*_j - XC^*_j}{DCR_j} = \frac{XR^*_{j+1} - XC^*_{j+1}}{DCR_{j+1}} = \frac{XR^*_{j+2} - XC^*_{j+2}}{DCR_{j+2}} \qquad (32)$$

$$XR^{*2}_j + XR^{*2}_{j+1} - RAD^{*2} = 0 \qquad (33)$$

Let $A12 = DCR_j / DCR_{j+1}$

$A32 = DCR_{j+2} / DCR_{j+1}$

then Eq. 32 can be rewritten as

$$XR^*_j = A12 \cdot (XR^*_{j+1} - XC^*_{j+1}) + XC^*_j$$
$$XR^*_{j+2} = A32 \cdot (XR^*_{j+1} - XC^*_{j+1}) + XC^*_{j+2} \qquad (34)$$

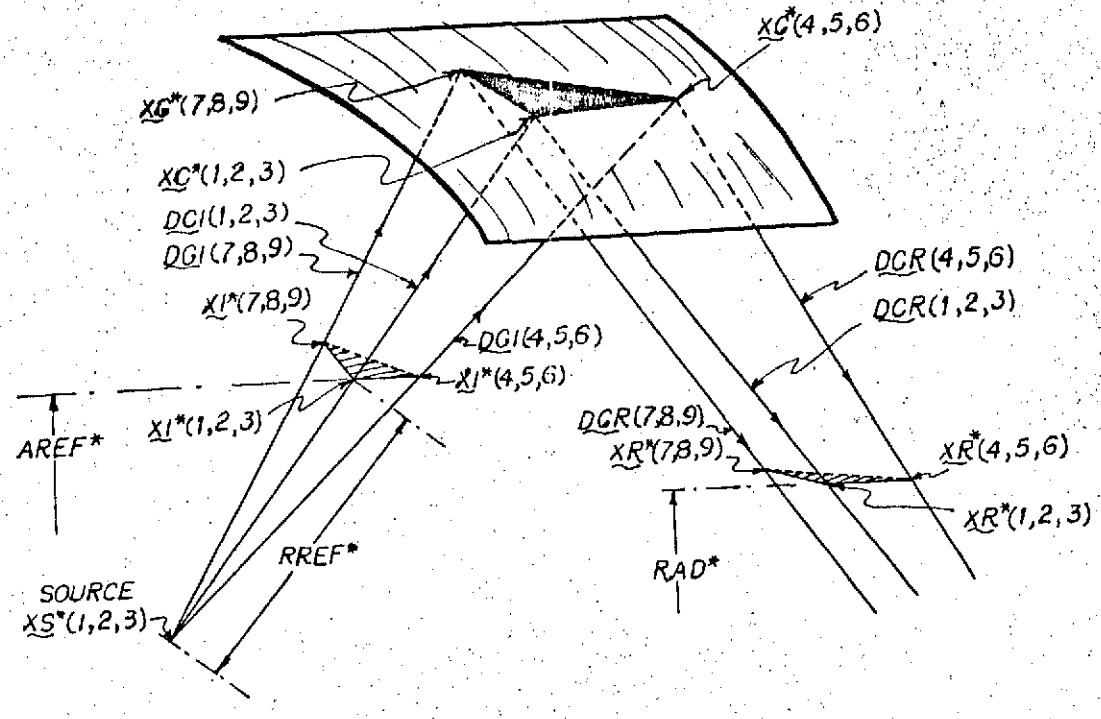

Fig. 62 Incident and Reflected Ray Tube

Substitution of these in Eq. 33 gives a quadratic equation for XR^*_{j+1} as

$$AA \cdot XR^{*2}_{j+1} + 2\,BB \cdot XR^*_{j+1} - CC = 0 \qquad (35)$$

where $AA = 1 + A12^2$

$BB = (XC^*_j - A12 \cdot XC^*_{j+1}) \cdot A12$

$CC = RAD^{*2} - (BB / A12)^2$

Hence $$XR^*_{j+1} = UMX \text{ , or } UMN \qquad (36)$$

where $UMX = \max (UA, UB)$

$UMN = \min (UA, UB)$

$UA = (- BB + D) / AA$

$UB = (- BB - D) / AA$

$D = (BB^2 + AA \cdot CC)^{\frac{1}{2}}$

There are two possible points, each one lying on either side of the duct axis, of intersection of the reflected ray with the cylindrical surface of radius RAD^*, let these be denoted by $\underline{XRA}^*(j, j+1, j+2)$, and $\underline{XRB}^*(j, j+1, j+2)$, the former being nearer to the position $\underline{XC}^*(j, j+1, j+2)$ (Fig. 63); then depending upon the value of the coordinate XC^*_{j+1} there result the following two cases :

Case 1 : $XC^*_{j+1} > 0$; then $XRA^*_{j+1} = UMX$

and $XRB^*_{j+1} = UMN$

Case 2 : $XC^*_{j+1} < 0$; then $XRA^*_{j+1} = UMN$

and $XRB^*_{j+1} = UMX$ (37)

Substitution of these values in Eq. 34 completely determines the two points $\underline{XRA}^*(j, j+1, j+2)$, and $\underline{XRB}^*(j, j+1, j+2)$ on the reflected ray. An additional point on the reflected ray that can be obtained comparatively easily is its intersection point with the duct axis. The coordinates of this point are given by

$$XRF^*_j = XRF^*_{j+1} = 0$$

$$XRF^*_{j+2} = XC^*_{j+2} - (DCR_{j+2} / DCR_{j+1}) \cdot XC^*_{j+1} \qquad (38)$$

The above analysis provides a technique for the successive determination of the points that are traversed by the ray tube during its propagation through the medium. If any of these points happens to be coincident with the given receiving point, then there it is necessary to evaluate the contribution to the pressure field from this ray. A procedure for this is developed in the following section.

PRESSURE CONTRIBUTION AT THE RECEIVING POINT

The receiving points are the preselected, or the given, positions in the region at which the pressure field is to be determined. This pressure field is the radiation effect of the emission from the given acoustical source. It is recalled that in the Monte Carlo technique use is made of a finite number of elementary pulses, and the corresponding ray tubes with randomly selected ray directions, for the representation of the radiation effect of the source in question; the effect of any particular ray, characterizing the propagating disturbance signal, being considered to be confined within the ray tube. This clearly points out that, for a ray (α, β, γ) to have a pressure contribution at a given receiving point, denoted by,

$$\underline{XR}^*(1,2,3) = (XR1^*, XR2^*, XR3^*) \qquad (39)$$

the corresponding ray tube must necessarily encounter this point during its propagation through the region.

The occurrence of such an encounter is tested by localizing the receiving point with respect to the variable point on the ray trajectory. It is easily shown that for the ray tube to be in the vicinity of the given receiving point (Eq. 39), it is essential to have satisfied

one of the following two relations :

$$XC3^* < XR3^* < XRF3^*$$
$$XRF3^* < XR3^* < XC3^* \qquad (40)$$

where $\underline{XRF}^*(1,2,3) = (XRF1^*, XRF2^*, XRF3^*)$

$\underline{XC}^*(1,2,3) = (XC1^*, XC2^*, XC3^*)$

are the latest points of intersection of the ray (α, β, γ) with the duct axis, and the duct boundary surface, respectively.

The relation of Eq. 40 ensures the localization of the ray tube and the receiving point in question within two cross-sectional planes (Fig. 63)

$$X3^* = XRF3^*$$
$$X3^* = XC3^* \qquad (41)$$

Test Sphere

Consider a small elemental sphere, surrounding the receiving point (Eq. 39), with a nondimensional radius ε , a preassigned small value, and the receiving point itself as the center. Along its trajectory, if the ray (α, β, γ) intersects the surface of this test sphere, the receiving

point is considered to be under the influence of this ray; and the pressure contribution is estimated. In addition to the value of the normalized ray tube area, the other variable on which the pressure contribution depends is the extent of this ray penetration into the test sphere. It is seen to be maximum when the receiving point lies exactly on the ray trajectory, in which case the ray penetration is twice the radius of the test sphere; on the other hand, the ray penetration, and hence the pressure contribution from this ray, is zero when the ray is either just tangential to the test sphere, or does not touch it at all.

Penetration Distance

Let (x1,x2,x3), and (y1,y2,y3) be the two points (Fig. 63) that are common to the penetrating ray, and the test sphere; then since this ray also passes through the axial point $\underline{XRF}^*(1,2,3)$ given by Eq. 38, the set of equations that is available here can be expressed as

$$x1 \,/\, DCR1 = x2 \,/\, DCR2 = (x3 - XRF3^*) \,/\, DCR3 \qquad (42)$$

$$(x1 - XR1^*)^2 + (x2 - XR2^*)^2 + (x3 - XR3^*)^2 - \varepsilon^2 = 0 \qquad (43)$$

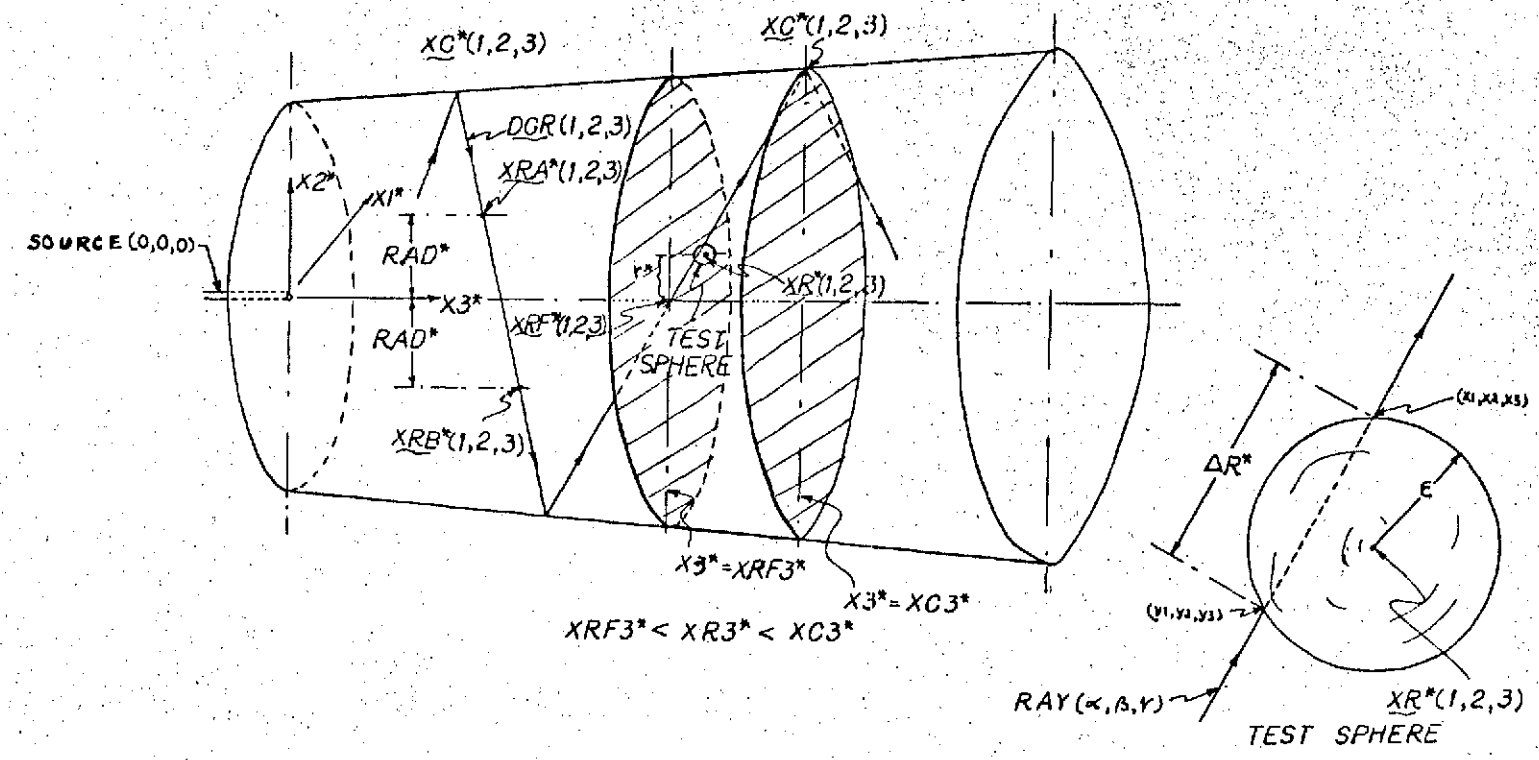

Fig. 63 Test Sphere and the Ray Penetration

Equation 42 gives

$$x1 = (DCR1 / DCR2) \cdot x2$$

$$x2 = (DCR3 / DCR2) \cdot x2 + XRF3^{*} \qquad (44)$$

Substitution of these in Eq. 43 results in a quadratic of the form

$$(DCR1 / DCR2)^2 + 1 + (DCR3 / DCR2)^2 \cdot x2^2$$

$$2 \cdot \{ - (DCR1 / DCR2) \cdot XR1^{*} - XR2^{*} + (DCR3 / DCR2) \cdot (XRF3^{*} - XR3^{*}) \} \cdot x2$$

$$- \{ \varepsilon^2 - (XR1^{*2} + XR2^{*2}) - (XRF3^{*} - XR3^{*})^2 \} = 0 \qquad (45)$$

Utilizing the relationship that is satisfied by the direction cosines, viz.

$$DCR1^2 + DCR2^2 + DCR3^2 = 1$$

and defining

$$AA = 1 / DCR2^2$$

$$BB = - (DCR1 / DCR2) \cdot XR1^{*} - XR2^{*} (DCR3 / DCR2) \cdot (XRF3^{*} - XR3^{*})$$

$$CC = \varepsilon^2 - (XR1^{*2} + XR2^{*2}) - (XRF3^{*} - XR3^{*})^2 \qquad (46)$$

Eq. 45 is rewritten as

$$AA \cdot x2^2 + 2\,BB \cdot x2 - CC = 0 \qquad (47)$$

of which one root corresponds to x2 (Fig. 63), whilst the other corresponds to y2; then it indicates that

$$(x2 - y2)^2 = 2\,(BB^2 + AA \cdot CC) / AA^2 \qquad (48)$$

Using Eqs. 44, 46, and 47 it can be shown that the penetration distance ΔR^* of the ray (α, β, γ) into the test sphere is given by

$$\Delta R^{*2} = (x1 - y1)^2 + (x2 - y2)^2 + (x3 - y3)^2$$

$$= AA \cdot (x2 - y2)^2$$

$$= 2\,(BB^2 / AA + CC) \qquad (49)$$

It can be easily seen from this expression that ΔR^* is real, i.e. the ray penetration takes place into the sphere, only when the relation

$$BB^2 / AA + CC > 0 \qquad (50)$$

is satisfied.

Equivalent Distance

Reference to Eqs. 16 and 17 above shows that at the instant TREF* the ray (α, β, γ), that is presently under progress, contributes a pressure PREF* at a distance RREF* from the source position $\underset{\sim}{XS}^*(1,2,3)$; it is also recalled that the ray tube cross-sectional area was denoted there by ART0* ; the reference ray tube area for the normalization.

Consider now the divergence factor DF12 defined as (see Eq. 17, Chapter 7)

$$DF12 = (ART0^* / ARTR^*)^{\frac{1}{2}} \qquad (51)$$

where ARTR* is the cross-sectional area of the same ray tube, but in the proximity of the receiving point $\underset{\sim}{XR}^*(1,2,3)$.

It is now argued that since the ray tube was at a distance RREF* from the source when it had its area as ART0* , the receiving point $\underset{\sim}{XR}^*(1,2,3)$ where the ray tube area is ARTR* can be thought to be at an 'equivalent distance' REQ* from the source; this equivalent distance REQ* being defined mathematically to be

$$REQ^* = RREF^* / DF12$$

$$\approx RREF^* / DF12 + \Delta R^* / 2 \qquad (52)$$

Introducing the 'penetration factor' defined as

$$PNF = (RREF^* / DF12) \cdot (\Delta R^* / DF12)$$

$$= REQ^* \cdot \Delta R^* / DF12 \qquad (53)$$

it is possible to express the pressure contribution from this ray (α, β, γ) at the receiving point $\underset{\sim}{XR}^*(1,2,3)$, using Eq. 16, Chapter 7, in the form

$$p_i^*(XR^*, T^*) = PREF^* \cdot DF12 \cdot PNF$$

$$= PREF^* \cdot REQ^* \cdot \Delta R^* \qquad (54)$$

where $T^* = TREF^* + REQ^*$

$$= (TI^* + RREF^*) + REQ^*$$

using Eq. 17 above .

As was explained in Chapter 7, the given length of the total transitional period, the period for which the solution is to be studied, is divided into J time cells, each of duration $\Delta\tau^*$, and $p_{ij}^*(\underset{\sim}{XR}^*)$ is considered to be the mean value of the pressure $p_i^*(\underset{\sim}{XR}^*, T^*)$, given by Eq. 54, taken over the j^{th} time interval, i.e.

$$p_{ij}^*(\underset{\sim}{XR}^*) = (1 / \Delta\tau^*) \int_{j\Delta\tau^* - 1}^{j\Delta\tau^*} p_i^*(\underset{\sim}{XR}^*, T^*)\, dT^*$$

$$= (PREF^* \cdot REQ^* \cdot \Delta R^*)_i \qquad (55)$$

where $j = T^* / \Delta\tau^* + 1$

$$= (TI^* + RREF^* + REQ^*) / \Delta\tau^* + 1 \qquad (56)$$

The index i that is introduced as a suffix to the right hand side expression of Eq. 55 is just to recall the fact that the quantities included in the bracket there are those of the ray tube that has originated from the randomly selected pulse with the integral index i.

It is emphasized here that the pressure value given by Eq. 55 above is an <u>averaged</u> pressure value that is obtained by the process of averaging over an elemental, but finite, space-time volume

$$\Delta V^* \cdot \Delta\tau^* = (4/3)\pi\varepsilon^3 \cdot \Delta\tau^* \qquad (57)$$

of the test sphere, that replaces the actual receiving point in the Monte Carlo technique.

The process leading to the relation of Eq. 55 is repeated for the totality of NR ray tubes in a particular sample, and the pressure is accumulated over the time cells for a given receiving point. This completes the ray tube processing.

VARIANCE ANALYSIS

The data accumulated while the ray tubes were being followed are now analyzed. At the end of the processing of, say, NR ray tubes, the accumulated pressure values in the different time cells are averaged over the number NR , and the space-time volume of the test sphere (Eq. 57) used therein to represent the actual receiving point. The pressure field thus accumulated is then expressed as

$$p_j^*(\underline{XR}^*) = (T_p^* / NR \,.\, \Delta V^* \,.\, \Delta \tau^*) \,. \cdot \sum_{i=1}^{NR} (PREF^* \,.\, REQ^* \,.\, \Delta R^*)_i \qquad (58)$$

This expression is seen to have a striking resemblance to the algorithm of the former part of the dissertation (see, for example, Eq. 26, Chapter 3).

Equation 58 represents a single statistical sample, as a result of the Monte Carlo calculations; and further requires the knowledge of the standard deviation. This is obtained by repeating the calculations leading to Eq. 58 in, say K different blocks. The results of these are conveniently expressed as

$$p_j^*(XR^*)_k = (T_p^* / NR_k \cdot \Delta V^* \cdot \Delta \tau^*) \cdot \sum_{i=1}^{NR_k} (PREF^* \cdot REQ^* \cdot \Delta R^*)_i \qquad (59)$$

where NR_k is the number of the ray tubes followed in the k^{th} block

$$(1 \leq k \leq K) .$$

By assigning equal statistical weight to each selection, the required pressure field, which is the statistical mean of all the samples, is given by

$$p_j^*(\underset{\sim}{XR}^*) = \sum_{k=1}^{K} W_k \cdot [p_j^*(\underset{\sim}{XR}^*)]_k \qquad (60)$$

where W_k is the statistical weight defined as

$$W_k = NR_k / \sum_{i=1}^{K} NR_i \qquad (61)$$

The variance of such a pressure field is then given by

$$D^2\, p_j^*(XR^*) = \sum_{k=1}^{K} W_k^2 \cdot \left\{ \left[p_j^*(XR^*) \right]_k - p_j^*(XR^*) \right\}^2$$

$$= \sigma_{p_j^*}^2 \qquad (62)$$

where $\sigma_{p_j^*}$ is the required deviation of the predicted acoustical pressure in the j^{th} time interval at the receiving point $\underset{\sim}{XR}^*(1,2,3)$.

The results of the application of the Monte Carlo technique thus developed are presented in Chapter 10; before that, in the following chapter, the problem of the pressure field inside a duct of constant radius is studied from the normal mode point of view.

Chapter 9

PRESSURE FIELD INSIDE A CYLINDRICAL DUCT

NORMAL MODE SOLUTION

The problem that is considered here is the investigation of the acoustic field inside a region bounded by a cylindrical duct surface, using the normal mode point of view. In practical applications the walls of a sound conducting duct possesss certain amount of elasticity, and heat conductivity. Inclusion of the finite elasticity and heat conductivity considerably complicates the solution of the problem. In order to visualize the situation more clearly, the side walls of the duct are considered to be absolutely rigid, and non-heat conducting. The supporting medium inside the duct is assumed to be homogeneous, and at rest initially. The duct is considered to be rigidly closed on the left, and terminating on the right in a perfectly absorptive medium.

Consider a pressure field caused by a simple point source, radiating from a given source position $\underset{\sim}{x}_s$ in the field. It is governed by a nonhomogeneous wave equation of the type

$$\left\{(1/c^2).(\partial^2/\partial t^2) - \nabla^2\right\} p(\underset{\sim}{x}_r,t) = (\partial/\partial t)\, \dot{m} \,.\, \delta\,(\underset{\sim}{x}_r - \underset{\sim}{x}_s) \qquad (1)$$

where c is the characteristic wave speed

$p(\underset{\sim}{x}_r,t)$ is the fluctuating acoustical pressure at a given receiving point $\underset{\sim}{x}_r$, at time t

$\dot{m}$ is the rate of mass injection, per unit volume, from the source centre.

When considering the field analytically inside a cylindrical region, as is done here, it becomes more convenient to use the cylindrical coordinate system (r, θ, z) (Fig. 64) instead of the usual Cartesian coordinate system. In this case Eq. 1 takes the form

$$\left\{ \partial^2/\partial r^2 + (1/r).(\partial/\partial r) + (1/r^2).(\partial^2/\partial \theta^2) + (\partial^2/\partial z^2) - (1/c^2).(\partial^2/\partial t^2) \right\} p(r,\theta,z) = (\partial^2/\partial t^2)\, m \,.\, \delta\,(\underset{\sim}{x}_r - \underset{\sim}{x}_s) \qquad (2)$$

where $\underset{\sim}{x}_r = x_r(r, \theta, z)$.

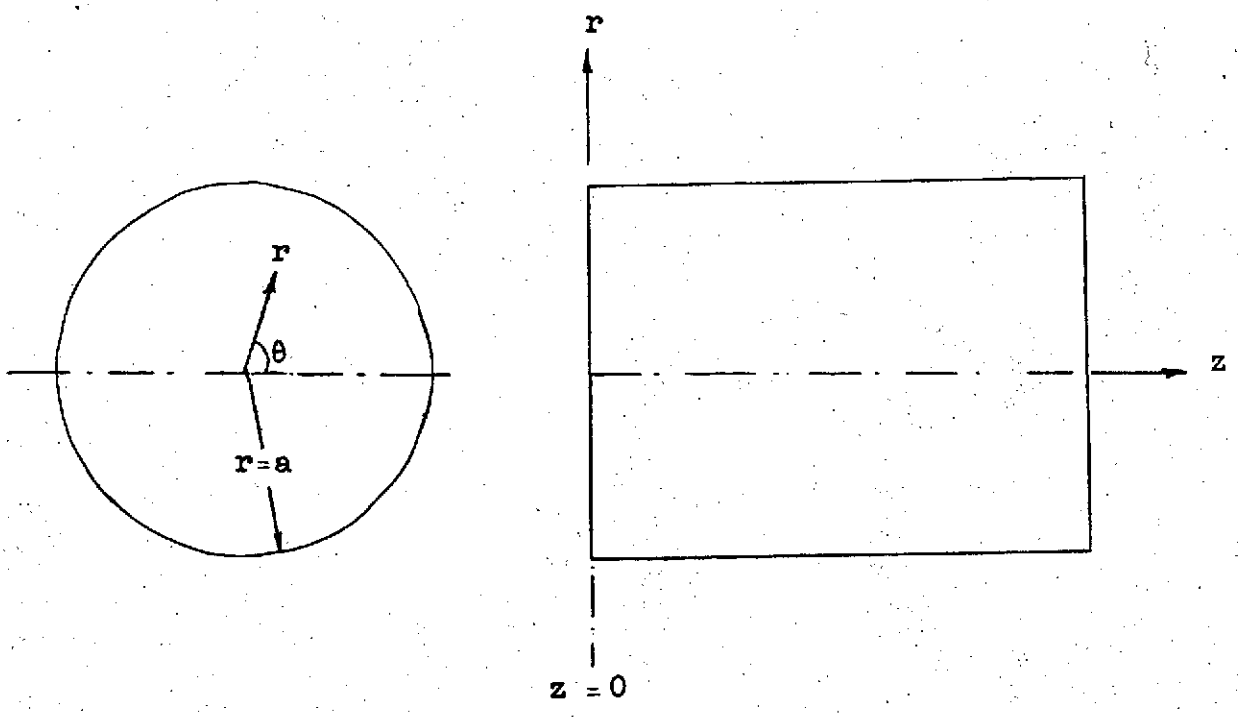

Fig. 64. Cylindrical Duct Coordinate System

The pressure field $p(r, \theta, z)$ satisfies the boundary conditions

i. p is a continuous function

ii. the radial component of the pressure gradient vanishes at the boundary walls, i.e.

$$(\partial p / \partial r) = 0 \quad \text{at} \quad r = a \qquad (3)$$

iii. at a reference plane, $z = 0$, normal to the duct axis, the perturbation due to the source is specified as an arbitrary function of r satisfying (i), and (ii), and a periodic function of time t.

In linear acoustics, for the inviscid medium, in the absence of the convective velocity, the relation between the particle velocity $\underset{\sim}{v}$, and the acoustic pressure p, at any point in the medium, is provided by the momentum equation

$$\rho\,(\partial \underset{\sim}{v}/\partial t) + \nabla p = 0 \qquad (4)$$

At this point it is convenient to define the following new variables, similar to those used in Eq.1 of Chapter 7,

$$r^* = r/a, \quad z^* = z/a, \quad t^* = ct/a, \quad p^* = p/\rho c^2$$
$$m^* = m/\rho, \quad \underset{\sim}{v}^* = \underset{\sim}{v}/c, \quad \underset{\sim}{x}_r^* = \underset{\sim}{x}_r/a, \quad \underset{\sim}{x}_s^* \quad \underset{\sim}{x}_s/a \qquad (5)$$

and rewrite Eq. 2 in the nondimensional form as

$$\left\{ (\partial^2/\partial r^{*2}) + (1/r^*).(\partial/\partial r^*) + (1/r^{*2}).(\partial^2/\partial \Theta^2) \right.$$
$$\left. (\partial^2/\partial z^{*2}) - (\partial^2/\partial t^{*2}) \right\} p^*$$
$$= (\partial^2/\partial t^{*2})\, m^* \,.\, \delta(\underset{\sim}{x}_r^* - \underset{\sim}{x}_s^*) \qquad (6)$$

where $p^* = p^*(\underset{\sim}{x}_r^*, t^*) = p^*(r^*, \Theta, z^*, t^*)$.

The pressure field inside the duct is now assumed to be expressible in the terms of the natural modes of vibration as

$$p^*(\underset{\sim}{x}_r^*, t^*) = \sum_{i=0}^{\infty} \sum_{j=0}^{\infty} p_j^*(z^*, t^*) \cdot R_j(r^*).(a_i \cos i\theta + b_i \sin i\theta) \qquad (7)$$

where i is a characteristic number restricted to the integral values by the continuity requirement

$$p^*(\Theta) = p^*(\theta + 2\pi)$$
$$p^{*\prime}(\Theta) = p^{*\prime}(\theta + 2\pi) \qquad (8)$$

(prime (') denotes the differentiation with respect to the argument)

a_i, b_i are the coefficients to be determined from the given boundary conditions in the reference plane $z^* = 0$.

Substitution of Eq. 7 into Eq. 5 results in the separation of equations

$$\left\{ (\partial^2/\partial r^{*2}) + (1/r^*).(\partial/\partial r^*) + (K_{ij}^2 - i^2/r^{*2}) \right\} R_j(r^*) = 0 \qquad (9)$$

$$\left\{ (\partial^2/\partial t^{*2}) - (\partial^2/\partial z^{*2}) + K_{ij}^* \right\} p_j^*(z^*, t^*) = (\partial^2/\partial t^{*2})\, m^*.\delta(\underset{\sim}{x}_r^* - \underset{\sim}{x}_s^*) \qquad (10)$$

where $-K_{ij}^2$ is the separation constant .

The characteristic value K_{ij}, which in turn fixes the value of the separation constant $-K_{ij}^2$, is determined from the appropriate boundary conditions at the duct walls, such as that presented by Eq. 3 for the particular case that is under investigation here.

Equation 9 is recognized to be a Bessel equation of order i, and as such its solution is expressible as

$$R_j(r^*) = J_i(K_{ij}\, r^*) \qquad (11)$$

where J_i is the i^{th} order Bessel function of the First Kind.

It is observed that the boundary condition at the duct walls, given by Eq. 3, is satisfied if and only if the characteristic values K_{ij} are the roots of the transcendental equation

$$J_i'(K_{ij}) = 0 \qquad (12)$$

In other words, the characteristic values K_{ij} are the successive zeros of the Eq. 12, where the index j takes on the values 0, 1, 2, ... successively.

A similar expression to that of Eq. 7 can be written for the particle velocity $\underset{\sim}{v}^*(\underset{\sim}{x}_r^*, t^*)$. Then using Eq. 4, it can be shown that the relation satisfied by the axial component of the particle velocity, denoted by $v_{zj}^*(z^*, t^*)$,

and the corresponding pressure $p_j^*(z^*,t^*)$ during the j^{th} mode of vibration is

$$\partial p_j^* / \partial z^* = -\partial v_{zj}^* / \partial t^* \qquad (13)$$

The medium is considered to be quiescent initially, and hence the initial conditions for the problem can be expressed as

$$p_j^*(z^*, 0_+) = 0 \qquad (14)$$

$$v_j^*(z^*, 0_+) = 0 \qquad (15)$$

$$\partial p_j^*(z^*, 0_+)/\partial t^* = 0 \qquad (16)$$

where the source is initiated at time $t^* = 0$

Now the pressure $p_j^*(z^*,t^*)$ is expressed as the sum of two components

$$p_j^*(z^*,t^*) = q_j(z^*,t^*) + g_j(t^*) \qquad (17)$$

On substitution, this allows the separation of Eq. 10 into the following two equations

$$\left\{(\partial^2/\partial t^{*2}) + K_{ij}^2\right\} g(t^*) = (d/dt^*)\, \dot{m}^* \cdot \delta(\underset{\sim}{x}_r^* - \underset{\sim}{x}_s^*) \qquad (18)$$

$$\left\{(\partial^2/\partial t^{*2}) - (\partial^2/\partial z^{*2}) + K_{ij}^2\right\} q_j(z^*,t^*) = 0 \qquad (19)$$

with the corresponding initial conditions as

$$g_j(0_+) = 0 \qquad (20)$$

$$\partial g_j(0_+) / \partial t^* = 0$$

$$q_j(z^*, 0_+) = 0 \qquad (21)$$

$$\partial q_j(z^*, 0_+) / \partial t^* = 0$$

The solutions of Eqs. 18, and 19 can be obtained most conveniently by the use of the Laplace Transforms. Defining

$$\mathcal{L}\left\{g_j(t^*)\right\} = G_j(s^*) = \int_0^\infty e^{-s^* t^*} g_j(t^*)\, dt^* \qquad (22)$$

$$\mathcal{L}\left\{\dot{m}^*(t^*)\right\} = \dot{M}^*(s^*) = \int_0^\infty e^{-s^* t^*} \dot{m}^*(t^*)\, dt^*$$

where $s^* = s\, a / c$

and taking the transform of Eq. 18 results in, on making use of the initial condition given by Eq. 20 above,

$$G(s^*) = \left\{ s^* . \dot{M}^*(s^*) - \dot{m}^*(0_+) \right\} / (s^{*2} + K_{ij}^2) \qquad (23)$$

Using the convolution theorem, the inverse transform of Eq. 23 is expressible as

$$g_j(t^*) = \left\{ \int_0^{t^*} \dot{m}\,(t^* - \xi)\cos K_{ij}\xi \; d\xi \right.$$

$$\left. - (\sin K_{ij}t^* \cdot \dot{m}^*(0_+)) / K_{ij} \right\} \cdot \delta(\underset{\sim}{x}_r^* - \underset{\sim}{x}_s^*) \qquad (24)$$

Similarly defining

$$\mathcal{L}\left\{q_j(z^*,t^*)\right\} = Q_j(z^*,s^*) = \int_0^{\infty} e^{-s^*t^*}\, q_j(z^*,t^*)\, dt^*$$

$$\mathcal{L}\left\{v_{zj}^*(z^*,t^*)\right\} = V_{zj}^*(z^*,s^*) = \int_0^{\infty} e^{-s^*t^*}\, v_{zj}^*(z^*,t^*)\, dt^* \qquad (25)$$

and taking the transform of Eq. 19 results in, on making use of the initial conditions given in Eq. 21, a differential equation

$$\left\{(\partial^2/\partial z^{*2}) - (s^{*2} + K_{ij}^2)\right\} Q_j(z^*,s^*) = 0 \qquad (26)$$

This has two solutions given by

$$Q(z^*,s^*) = S(s^*) \begin{cases} \exp\left[+(s^{*2} + K_{ij}^2)^{\frac{1}{2}} \cdot z^*\right] \\ \exp\left[-(s^{*2} + K_{ij}^2)^{\frac{1}{2}} \cdot z^*\right] \end{cases} \qquad (27)$$

where $S(s^*)$ is an arbitrary function, to be determined from the specified distribution of the source function in the reference plane $z^* = 0$

From these two solutions only the one is selected that vanishes at $z^* = +\infty$; and it is given by

$$Q_j(z^*,s^*) = S(s^*) \cdot \exp\left[-(s^{*2} + K_{ij}^2)^{\frac{1}{2}} \cdot z^*\right] \quad (27)$$

On partial differentiation with respect to z^*, this gives

$$\partial Q_j(0,s^*) / \partial z^* = - S(s^*) \cdot (s^{*2} + K_{ij}^2)^{\frac{1}{2}} \quad (28)$$

Using the initial condition given in Eq. 15, the transform of Eq. 13 can be written as

$$\partial Q_j(z^*,s^*) / \partial z^* = -s^* \cdot V_{zj}^*(z^*,s^*)$$

This together with Eq. 28 gives

$$S(s^*) = s^* \cdot V_{zj}^*(0,s^*) / (s^{*2} + K_{ij}^2)^{\frac{1}{2}}$$

substitution of which in Eq, 27 results in

$$Q_j(z^*,s^*) = s^* \cdot V_{zj}^*(0,s^*) \cdot D(s^*,z^*)$$

where

$$D(z^*,s^*) = \exp\left[- (s^{*2} + K_{ij}^2) \cdot z^*\right] / (s^{*2} + K_{ij}^2) \quad (29)$$

From Tables of Laplace Transforms (for example, Abromwitz, 1964, p. 1027, and p. 1021) the following relations are obtainable

$$\mathcal{L}^{-1}\left\{D(z^*,s^*)\right\} = \begin{cases} 0 & , \ t^* < z^* \\ J_0\left[K_{ij} \cdot (t^{*2} - z^{*2})^{\frac{1}{2}}\right] & , \ t^* > z^* \end{cases}$$

$$\mathcal{L}^{-1}\left\{(1/s^*) \cdot Q_j(z^*,s^*)\right\} = \int_0^{t^*} q_j(z^*, \xi)\, d\xi$$

$$\mathcal{L}^{-1}\left\{F_1(s^*) \cdot F_2(s^*)\right\} = \int_0^{t^*} f_1(t^* - \xi) \cdot f_2(\xi)\, d\xi$$

Using these results the inverse transform of Eq. 29 is expressed as

$$\int_0^{t^*} q_j(z^*,t^*) = \begin{cases} 0 & , \quad t^* < z^* \\ \displaystyle\int_{z^*}^{t^*} v_{zj}^*(0,t^*-\xi) \cdot J_0\left[K_{ij} \cdot (\xi^2 - z^{*2})^{\frac{1}{2}}\right] d\xi & , \quad t^* > z^* \end{cases}$$

Differentiation of this relation with respect to t^* gives

$$q_j(z^*,t^*) = \begin{cases} 0 & , \quad t^* < z^* \\ I & , \quad t^* > z^* \end{cases} \qquad (30)$$

where $I = (\partial/\partial t^*) \displaystyle\int_{z^*}^{t^*} v_{zj}^*(0,t^*-\xi) \cdot J_0\left[K_{ij} \cdot (\xi^2 - z^{*2})^{\frac{1}{2}}\right] d\xi$

For the evaluation of this expression use is made of the

Leibniz's rule which states that

$$(\partial/\partial t^*) = \int_{g_0(t^*)}^{g_1(t^*)} f(t^*, \xi)\, d\xi$$

$$= \int_{g_0(t^*)}^{g_1(t^*)} \partial f(t^*, \xi) / \partial t^* .\, d\xi$$

$$- f\left[t^*, g_0(t^*)\right] \cdot dg_0(t^*) / dt^*$$

$$+ f\left[t^*, g_1(t^*)\right] \cdot dg_1(t^*) / dt^* \qquad (31)$$

Here $f(t^*, \xi) = v_{zj}^*(0, t^* - \xi) \cdot J_0\left[K_{ij} \cdot (\xi^2 - z^{*2})^{\frac{1}{2}}\right]$

$g_0(t^*) = z^* \quad ; \quad g_1(t^*) = t^*$

$$\partial f(t^*, \xi)/\partial t^* = \left[(\partial/\partial t^*) \cdot v_{zj}^*(0, t^* - \xi)\right] \cdot \cdot J_0\left[K_{ij} \cdot (\xi^2 - z^{*2})^{\frac{1}{2}}\right]$$

$$= -J_0\left[K_{ij} \cdot (\xi^2 - z^{*2})^{\frac{1}{2}}\right] \cdot (\partial/\partial\xi)\, v_{zj}^*(0, t^* - \xi)$$

$dg_0(t^*)/dt^* = 0 \quad ; \quad dg_1(t^*)/dt^* = 1$

$f\left[t^*, g_1(t^*)\right] = 0$ since $v_{zj}^*(0,0) = 0$

Substitution of these values in Eq. 31 results in the

the following expression for I

$$I = -\int_{z^*}^{t^*} J_0[K_{ij}\,.(\xi^2 - z^{*2})^{\frac{1}{2}}].(\partial/\partial\xi)\, v_{zj}{}^*(0,t^* - \xi)\; d\xi$$

Let $u = J_0[K_{ij}.(\xi^2 - z^{*2})^{\frac{1}{2}}]$

$$dw = (\partial/\partial\xi)\, v_{zj}{}^*(0,t^* - \xi)\; .\; d\xi$$

$$du = J_0'\,[K_{ij}\,.(\xi^2 - z^{*2})^{\frac{1}{2}}].\{d[K_{ij}\,.(\xi^2 - z^{*2})^{\frac{1}{2}}]/d\xi\}\; d\xi$$

$$= -\,J_1[K_{ij}\,.(\xi^2 - z^{*2})^{\frac{1}{2}}].\{K_{ij}\,\xi/(\xi^2 - z^{*2})^{\frac{1}{2}}\}\; d\xi$$

since $J_0' = J_1$

then making use of the rule of integration by parts

$$I = v_{zj}{}^*(0,t^* - z^*) - \int_{z^*}^{t^*} v_{zj}{}^*(0,t^* - \xi)\; .\; J_1[K_{ij}\,.(\xi^2 - z^{*2})^{\frac{1}{2}}] \cdot\{K_{ij}\,.\,\xi/(\xi^2 - z^{*2})^{\frac{1}{2}}\}\; d\xi \qquad (32)$$

Then using Eqs. 7, 11, 17, and 30 the pressure field inside the duct is expressed as

$$p^*(\underset{\sim}{x}_r^*, t^*) = \sum_{i=0}^{\infty} \sum_{j=0}^{\infty} J_i(K_{ij} r^*).(a_i \cos i\theta + b_i \sin i\theta). \left[g_j(t^*) + \begin{cases} 0 & , t^* < z^* \\ I & , t^* > z^* \end{cases} \right] \quad (33)$$

It is noticed that the expression for $g_j(t^*)$ as given by Eq. 24 contains a Kronecker delta function, and as a result it does not contribute to a pressure field at any other point different than the point coincident with the source position.

Eventhough from the knowledge of $v_{zj}^*(0,t^*)$ it is possible to evaluate I in Eq. 33 (see Eq. 32), yet the pressure field cannot be determined, since the values of the coefficients a_i, and b_i are still undetermined; these are determined from the matching conditions in the reference plane $z^* = 0$ as shown below.

From Eqs. 13, and 33, following a similar procedure as above in the use of the Lebinitz rule, and carrying out a few mathematical steps, it can be readily shown that the expression for the axial component of the particle velocity inside the duct reduces to

$$v_z^*(\underset{\sim}{x}_r^*, t^*) = v_z^*(r^*, \theta, z^*, t^*)$$

$$= \sum_{i=0}^{\infty} \sum_{j=0}^{\infty} J_i(K_{ij} r^*).(a_i \cos i\theta + b_i \sin i\theta).\begin{cases} 0 , & t^* < z^* \\ I_1, & t^* > z^* \end{cases}$$

where $I_1 = v_{zj}^*(0, t^* - z^*) - z^* \cdot \int_0^{t^*-z^*} v_{zj}^*(o, t^* - z^* - \xi).$

$$\cdot J_1\left[K_{ij}.\left\{\xi(\xi + 2z^*)\right\}^{\frac{1}{2}}\right] \cdot K_{ij} / \left\{\xi(\xi + z^*)^{\frac{1}{2}}\right\} . d\xi$$

(34)

Thus in the reference plane ($z^* = 0$) the axial component of the particle velocity is given by

$$v_z^*(r^*, \theta, 0, t^*) = \sum_{i=0}^{} \sum_{j=0}^{} J_i(K_{ij} r^*).(a_i \cos i\theta + b_i \sin i\theta).v_{zj}^*(0, t^*)$$

(35)

In order to determine the numerical coefficients a_i, and b_i in the above expressions it is necessary to specify, for example, certain distributions of the velocities in the initial section $z^* = 0$, as an effect of the actuating source. In general it has the form

$$v^*(r^*, \theta, 0, t^*) = F(r^*, \theta).T(t^*) \qquad (36)$$

where the function $F(r^*, \theta)$ can be expanded into a double series involving the characteristic functions of the problem that is under investigation

$$F(r^*, \theta) = \sum_{i=0}^{\infty} \sum_{j=0}^{\infty} (\alpha_{ij} \cos i\theta + \beta_{ij} \sin i\theta).J_i(K_{ij}r^*) \qquad (37)$$

Using the orthogonality property of the trignometric functions, and the Bessel functions, the coefficients α_{ij} and β_{ij} are evaluated; the resulting expressions (Rschevkin,1963,p.193) are

$$\alpha_{0j} = \left\{1/\pi J_0^2(K_{0j}r^*)\right\} \cdot \int_0^1 \int_0^{2\pi} F(r^*, \theta).J_0(K_{0j}r^*).r^* \, dr^* \, d\theta$$

$$\beta_{0j} = 0$$

$$\alpha_{ij} = (1/\pi M_{ij}) \int_0^1 \int_0^{2\pi} F(r^*, \theta).J_i(K_{ij}r^*).\cos i\theta .r^* \, dr^* \, d\theta$$

$$\beta_{ij} = (1/\pi M_{ij}) \int_0^1 \int_0^{2\pi} F(r^*, \theta).J_i(K_{ij}r^*).\sin i\theta .r^* \, dr^* \, d\theta$$

where $M_{ij} = \frac{1}{2}\left\{(K_{ij}/i)^2 - 1\right\} . J_{i-1}^2(K_{ij})$

(38)

When the source is a simple point source, in the proximity of the source plane ($z^* = 0$), the disturbance propagates as the plane wave motion; then the velocity distribution resulting from the source in the plane $z^* = 0$ can be expressed, for example, by the functions

$$F(r^*, \theta) = 1$$

$$T(t^*) = \begin{cases} 0 & , \ t^* \leq 0 \\ \sin(2\pi t^* / T_p^*) & , \ 0 < t^* < T_p^* \\ 0 & , \ t^* \geq T_p^* \end{cases} \qquad (39)$$

where $T_p^* = c\, T_p / a$, T_p being the period of the source pulse in seconds.

Then in this case Eq. 38 gives

$$\alpha_{0j} = \left\{ 2/J_0^2(K_{0j}) \right\} \cdot \int_0^1 J_0(K_{0j} r^*) . r^* \, dr^*$$

$$\beta_{0j} = 0$$

$$\alpha_{ij} = \beta_{ij} = 0 \quad , \text{ for } \quad i \neq 0 \qquad (40)$$

These relations together with Eqs. 36, and 37 give

$$v^*(r^*, \Theta, 0, t^*) = \sum_{j=0}^{\infty} \alpha_{0j} \cdot J_0(K_{0j} r^*) . T(t^*) \qquad (41)$$

Comparison of Eqs. 35, and 41 shows the matching condition, viz.

$$v_z^*(r^*, \Theta, 0, t^*) = v^*(r^*, \Theta, 0, t^*) \qquad (42)$$

requires that for the particular source, having the source functions defined as in Eqs. 37, and 39

$$i = 0$$

$$a_i . v_{zj}^*(0, t^*) = \alpha_{0j} . T(t^*) \qquad (43)$$

In the light of these relations Eq. 33 can now be rewritten as

$$p^*(x_r^*, t^*) = \sum_{j=0}^{\infty} \alpha_{0j} . J_0(K_{0j} r^*) \cdot \left[g_j(t^*) + \begin{cases} 0 , & t^* < z^* \\ I , & t^* > z^* \end{cases} \right] \qquad (44)$$

where $I = T(t^* - z^*) - \int_{z^*}^{t^*} T(t^* - \xi) . J_1 \left[K_{0j} . (\xi^2 - z^{*2})^{\frac{1}{2}} \right] . \left\{ K_{0j} . \xi \; / \; (\xi^2 - z^{*2})^{\frac{1}{2}} \right\} . d\xi$

$$= T(t^*-z^*) + \int_{z^*}^{t^*} T(t^*-\xi).J_0'\left[K_{0j}.(\xi^2-z^{*2})^{\frac{1}{2}}\right] \cdot$$

$$\cdot\left\{d\left[K_{0j}.(\xi^2-z^{*2})^{\frac{1}{2}}\right]/d\xi\right\}. \; d\xi$$

Let $dw = J_0'\left[K_{0j}.(\xi^2-z^{*2})^{\frac{1}{2}}\right].\left\{d\left[K_{0j}.(\xi^2-z^{*2})^{\frac{1}{2}}\right]/d\xi\right\}. \; d\xi$

$$u = T(t^*-\xi)$$

then $$w = J_0\left[K_{0j}.(\xi^2-z^{*2})^{\frac{1}{2}}\right]$$

$$du = -T'(t^*-\xi)\, d\xi$$

Use of these in conjunction with the rule of integration by parts reduces the above expression to the following form

$$I = T(t^*-z^*) + T(t^*-\xi).J_0\left[K_{0j}.(\xi^2-z^{*2})^{\frac{1}{2}}\right]_{z^*}^{t^*}$$

$$+ \int_{z^*}^{t^*} T'(t^*-\xi).J_0\left[K_{0j}.(\xi^2-z^{*2})^{\frac{1}{2}}\right]. \; d\xi$$

$$\int_{z^*}^{t^*} T'(t^*-\xi).J_0\left[K_{0j}.(\xi^2-z^{*2})^{\frac{1}{2}}\right]. \; d\xi$$

since $T(0) = 0$, and $J_0(0) = 1$

(45)

In order to evaluate the coefficients α_{0j} in the above relations, use can be made of the following property of the Bessel functions

$$(d/dx)\left\{x^n J_n(x)\right\} = x^n J_{n-1}(x) \qquad (46)$$

which, for the particular case with $n=1$, on integration between the limits 0 and 1, gives

$$x \cdot J_1(x) = \int_0^x t \cdot J_0(t)\, dt \qquad (47)$$

Let $t = K_{0j} \cdot r^*$; then

$$\int_0^1 J(K_{0j} r^*)\, r^*\, dr^* = (1/K_{0j}^2) \cdot \int_0^{K_{0j}} t \cdot J_0(t)\, dt$$

$$= J_1(K_{0j}) / K_{0j}$$

Substitution of this result in Eq. 40 simplifies the expression for the coefficients in the following form

$$\alpha_{0j} = (2/K_{0j}) \cdot J_1(K_{0j}) / J_0^2(K_{0j}) \qquad (48)$$

The numerical results from this analysis are presented in the following chapter, as a comparison with those obtained from the application of the Monte Carlo technique presented in the preceding chapter.

Chapter 10

CALCULATIONS FOR CYLINDRICAL DUCT

PREASSIGNED CONSTANTS

For the demonstration of the applicability of the proposed Monte Carlo technique to a problem involving a curved boundary, the acoustic source is considered to be of sinusoidal shape, characterizing its strength-time history. The following is a list of the preassigned constants, used in this problem, expressed in dimensional form (FPS system) :

Source Strength Factor $\dot{Q}_0 = 1$

Source Period T_p = 2.0 E -03

Duct Radius A = 7.5

Wave Speed C = 1.10 E 03

Elemental Time Interval ΔT = 5.0 E -05

Characteristic Mass Density of the Medium ρ = 2.3780 E-03

Source Cartesian Coordinates XS(1,2,3) = (0,0,0)

Receiver Cartesian Coordinates XR(1,2,3) = (1,3,10)

Duct Minimum Radius A0 = 7.5

Duct Length DCTL = 1.2 E 02

Radius of the Test Sphere ξ = 1.0 E -01

DPHI = DPSI = 1.0 E -12

No. of Rays followed in one Sample NR = 5000

MONTE CARLO SOLUTION

The Monte Carlo results are shown compared with the Normal Mode calculations in Fig. 65. These Monte Carlo calculations consisted of five blocks, totalling 2500 selected ray tubes; and took 189 seconds of core time, each block requiring about 39 seconds of core time, on the CDC 6400 computer at the Computational Centre of the University of Virginia (Appendix 7).

NORMAL MODE SOLUTION

The Normal Mode solution included the summation of the series for the first 26 modes. In order to save the computational time, extensive use was made of the tabulated results for the requisite zeroth order Bessel functions, first order Bessel functions (McClain, 1962), and the successive zeros of the Bessel function of the first order (Watson, 1962, p. 748).

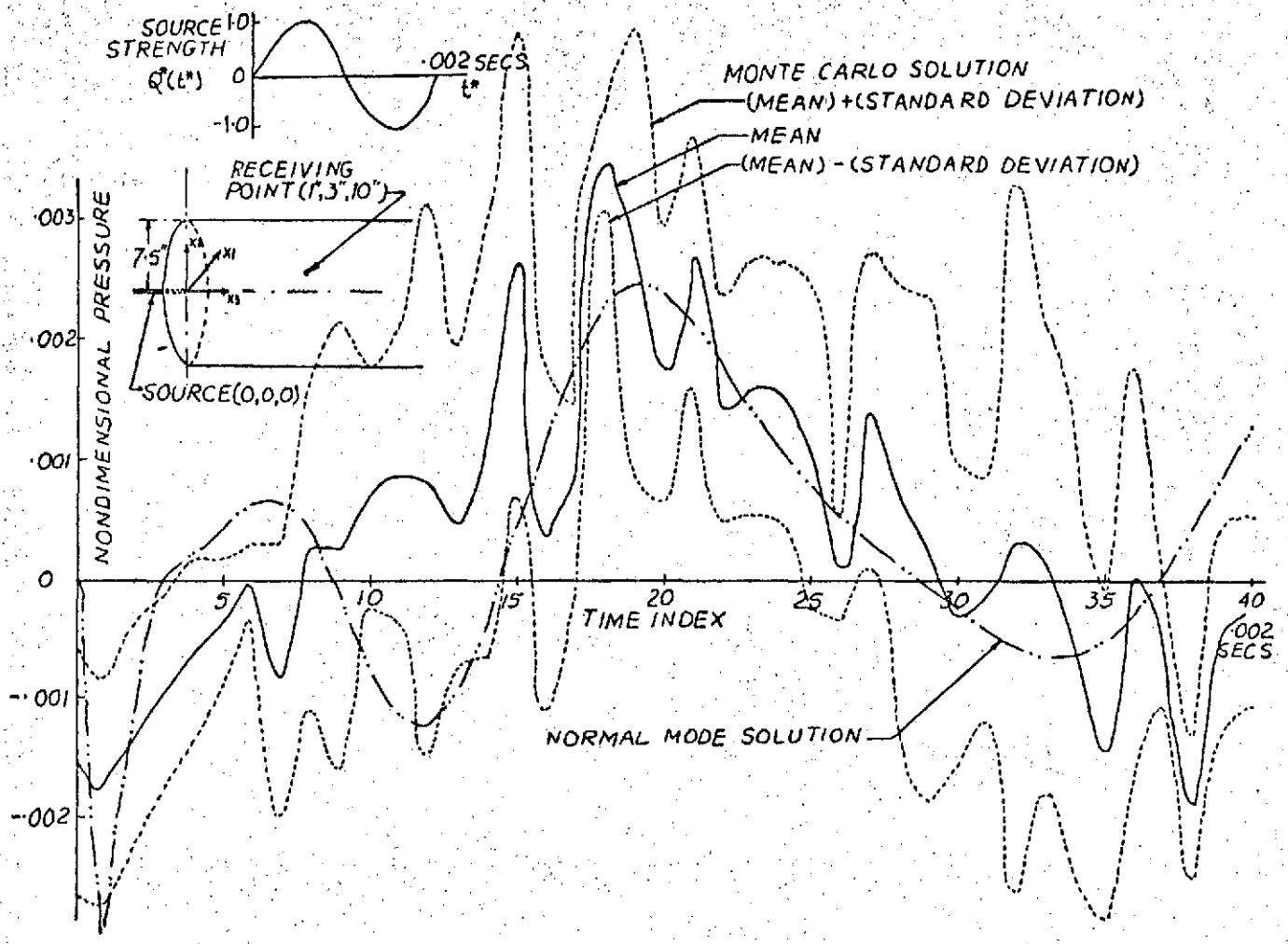

Fig. 65 Pressure Time History at a Receiving Point for Single Cycle Sinusoidal Pulse in Cylindrical Duct Comparison of the Monte Carlo and the Normal Mode Solutions

The approximate evaluation of the definite integral (Eq. 32, Chapter 9) appearing in the expression for the pressure field by the Normal Mode method was carried out separately by making use of two different methods, the first was based on the composite trapezoidal rule, repeated interval halving, together with the Romberg's extrapolation technique; whilst the second one was based on the Chebyshev's formula (Rekotrys, 1969, p. 594) for six terms. The normal mode results from these two methods were found to be in close agreement (Appendix 8).

OBSERVATIONS

It is evident from Fig. 65 that the results of the Monte Carlo technique are in close general agreement with those from the Normal Mode method, when it is considered that the Normal Mode solution should only be expected to be within the limits of plus and minus one standard deviation about 68 % of the time.

Another point that is noticeable is the certain amount of shift along the time axis. In the Normal Mode solution the time interval between the commencement and the termination of the pressure contribution at the receiving point is sharply defined, thecommencement being coincident with the instant at which the initial portion of the direct

disturbance wave reaches the receiving point. Obviously this is a minimum time that a disturbance wavefront takes to reach the given point. In contrast, in the Monte Carlo solution since the directions of the ray tubes that are followed are selected at random, the probability of selecting the exact values of the direction components coincident with those of the direct ray is negligibly small; and as a consequence the randomly selected signal path, in general, takes a certain amount of additional time before reaching the receiving point. This results in a certain amount of shift along the time axis.

Using Eq. 15 of Appendix 2, the probable relative error in the calculated pressure values can be expressed as

$$\delta_{prob} = (0.68/E\{p_j^*\}) \cdot (D^2\{p_j^*\}/N)^{\frac{1}{2}}$$

where $E\{p_j^*\}$ is the expected pressure value at the time index j

$D^2\{p_j^*\}$ is its variance

N is the sample size

Choosing j = 30, for example, it is seen from the printout results of Appendix 7 that

$$E\{p_{30}^*\} = 1.16754349 \text{ E } -04$$

$$D^2\{p_{30}^*\} = 1.89393499 \text{ E } -07$$

$$N = 5000 .$$

The corresponding value of the probable relative error is

$$\delta_{prob} = 0.035$$

In general, the values of the standard deviations for the Monte Carlo results of Fig. 65 are relatively high, indicating a wide scope of further refinements in the basic sampling technique, directed towards the reduction of the variances.

In Fig. 66 are shown the results of two additional blocks of the Monte Carlo calculations; the curve corresponding to Block 3 is the same as that seen in Fig. 65. From Fig. 66 it can be concluded that, for most part of the observational period, the Monte Carlo solution is in general agreement with the Normal Mode solution.

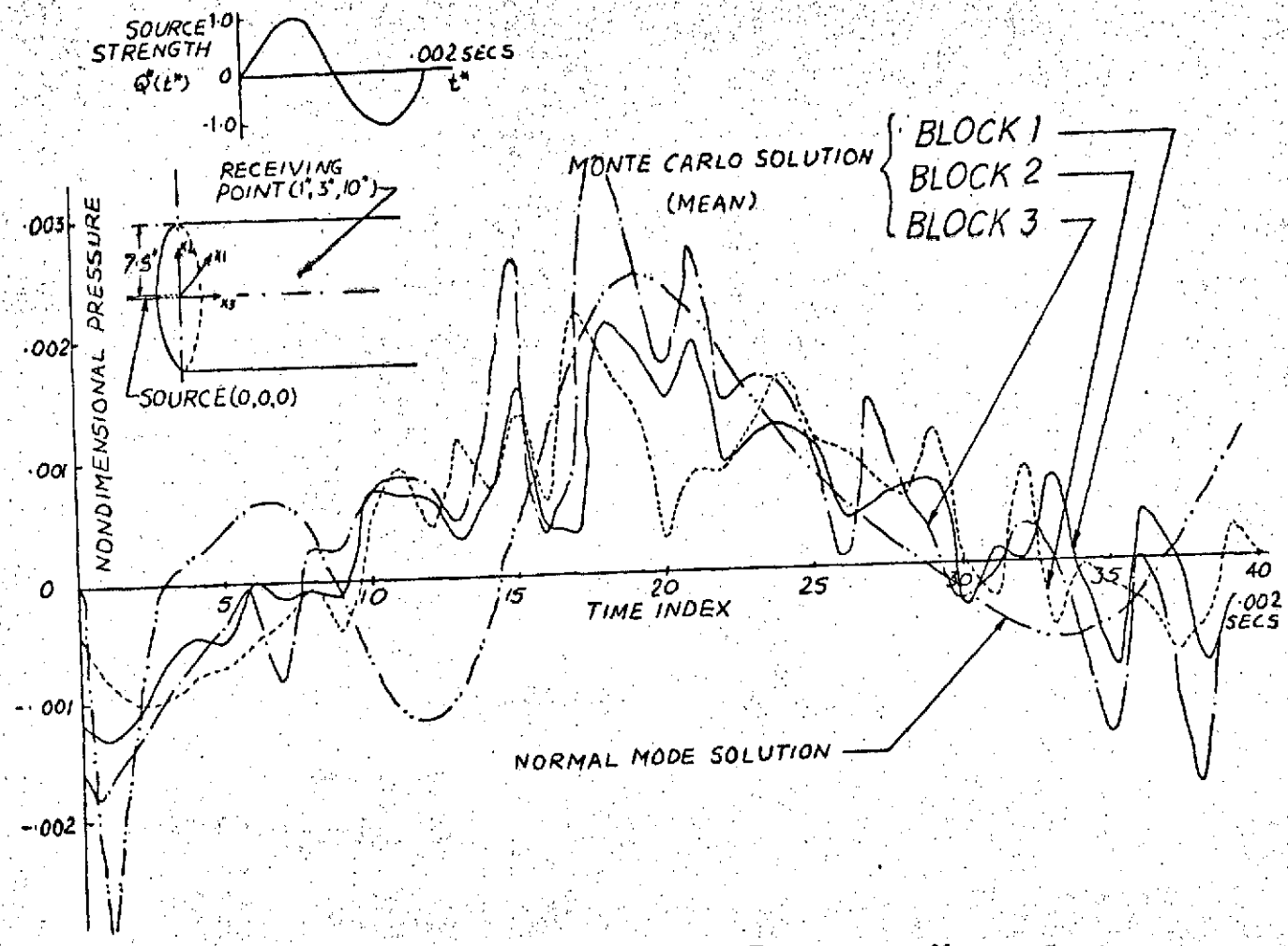

Fig. 66 Results from Two Additional Blocks of Monte Carlo Calculations Cylindrical Duct Problem

Chapter 11

CONCLUSIONS

The Monte Carlo technique is developed and proposed for the determination of the pressure-time history at a chosen point in a partial enclosure. At present, its applicability is demonstrated when the medium is homogeneous and is enclosed by either rectangular or curved boundaries. Although the present study considers the behaviour due to simple point sources, it is possible to study the effect of any sort of source by building up a distribution of point sources of various intensities.

When all of the acoustical material is on one surface of a room, the room is never satisfactory acoustically as there are prolonged reflections between the opposite surfaces which do not have acoustical material. The Monte Carlo analysis of the transient acoustic field, presented in Chapter 5, is restricted to rooms containing no 'sound scattering' obstacles, having each wall uniform absorption. The removal of each of these restrictions is essential in

making the proposed Monte Carlo technique more generally applicable and requires further study. In order to make the Monte Carlo application economically competitive it is highly desirable to explore the possibility of implimenting one or more of the variance reducing techniques, such as, Stratification, Control Variates, Antithetic Variates, etc.

As emphasized by Knudsen (1940), it is the detailed nature of the sound decay, especially during the early stages of decay, and not merely the average rate of decay, that affects the acoustical excellence of the music rooms or the auditoria; thus it appears that a fairly detailed experimental and theoretical investigations of the short term transient response of rooms having various shapes and absorptive treatments should prove highly instructive. The proper control of the distribution of sound energy throught a room and of the growth and decay of sounds are the prime objectives of good acoustical design. One attains scientifically rigorous and predeterminable control of these objectives by a comprehensive study. The proposed Monte Carlo technique, when developed further, is foreseen to provide valuable computational tool in such a study.

For complex problems, it is anticipated that, the proposed Monte Carlo approach may prove to be exacting and even indispensible; but before long one needs

to make developments, in brief, on the following lines:

a. Adapt the method to inhomogeneous and moving media. This means that a method of tracing the signal paths through variable media, in the presence of flow is required

b. Adapt the method to problems involving scattering, which is present in many problems of practical interest. Analytical solutions can be obtained in simple geometries, such as scattering of plane waves by cylinders. On the other hand, scattering is ignored in classical optics. The problem here is to develop a 'game' under which the signal paths passing near an obstruction are deflected, so that the averaged result is correct.

It is seen from these subtasks that the research interest here encompasses such works as the development of the requisite probability theory as direct application to the many variable phenomena in acoustics, analysis associated with complicated boundary conditions in the acoustic radiation theory, and computations of acoustic interaction effects with due considerations to the problems in energy conversion mechanisms.

The subtask (b) above, relating to scattering, is judged to be the critical problem. A detailed study of known analytical solutions is called for, both to provide insight into the problem and to provide checks for future Monte Carlo calculations. The major difficulty here is that the equations governing the deflections of the signal paths have to be formulated when the results are given in terms of wave solutions. The ultimate measure of a mathematical model and the sampling techniques for its analysis is the degree to which their applications produce satisfaction to its user. This satisfaction can usually be produced when the computed values agree with the reliable experiments; and makes it essential to undertake certain experimental model studies for the final verification of the Monte Carlo results.

The research work, directed towards the further development of the proposed Monte Carlo technique into a valuable tool for applications to cases involving inhomogeneous medium and complex boundary conditions, presents a field of research which not only is fascinating but also holds promise of marked improvements in the understanding of the transient acoustic fields.

REFERENCES

Abromwitz, M. (1964), and I. A. Stegun (Eds.). Handbook of Mathematical Functions. U.S. Government Printing Office, Washigton,D.C.

Beranek, L. L. (Ed.) (1971). Noise and Vibration Control. McGraw Hill.

Bhatt, N. B. (1939). The Effect of an Absorbing Wall on the Decay of Normal Frequencies. J. Acoust. Soc. of Amer., vol. 11, pp. 67-73.

Bolt, R. H. (1950), P. E. Doak, and P. J. Westervelt. Pulse Statistics of Room Acoustics. J. Acoust. Soc. of Amer., vol. 22, pp. 328-340.

Bouquet, G. (1958), M. Feix, P. Nicourd, and C. Sajaloli. Emploi de la méthode de Monte Carlo pour la détermination du volume d'un cylinder. C. R. Acad. Sci., vol. 246, pp. 1382-1384.

Cashwell, E. D. (1957), and others. A Practical Manual on the Monte Carlo Method for Random Walk Problems. LA- 2120. Physics and Mathematics (TID-4500, 13th edition, Suppl.).

Los Almos Scientific Laboratory of the University of California.

Erdelyi, A. (Ed.) (1954). Tables of Integral Transforms. Bateman Manuscript Project, California Institute of Technology, McGraw Hill.

Hammersley, J. M. (1965), and D. C. Handscomb. Monte Carlo Methods. Methuen (London).

Haviland, J. K. (1965). The Solution of Two Molecular Flow Problems by the Monte Carlo Method in 'Methods of Computational Physics' (Ed. Berni Alder), vol. 4, pp. 164,165. Academic Press.

Hull, T. E. (1962), and A. R. Dobell. Random Number Generators. SIAM Review IV, pp. 230-254.

Hunt, F. V. (1939), L. L. Beranek, and D. Y. Maa. Analysis of Sound Decay in Rectangular Rooms. J. Acoust. Soc. of Amer., vol. 11, pp. 80-94.

Jones, R. C. (1940). Theory of Fluctuations in Decay of Sound. J. Acoust. Soc. of Amer., vol. 11, pp. 324-332.

Kahn, H. (1954). Application of Monte Carlo. Atomic Energy Commission, U.S.A., AECU - 3259 Physics.

Knudsen, V. O. (1940). Some Practical Aspects of Architectural Acoustics. J. Acoust. Soc. of Amer., vol. 11, pp. 383-395.

Knudsen, V. O. (1967), L. P. Delsasso, and R. W. Leonard. Reverberation-Room Acoustics-Effects of Various Boundary Conditions. J. Acoust. Soc. of Amer., vol. 42, pp. 953-965.

Krokstad, A. (1968), S. Strom, and S. Sorsdal. Calculating the Acoustical Room Response by the Use of a Ray Tracing Technique. J. Sound Vib., vol. 8, pp. 953-965.

McClain, J. W. (1962), F. C. Schoenig, Jr., and N. J. Palladino. Table of Bessel Functions to Arguments 85. Engineering Research Bulletin B-85. The Pensylvania State University.

Mintzer, D. (1950). Transient Sounds in Rooms. J. Acoust. Soc. of Amer., vol. 22, pp. 341-352.

Morse, P. M. (1944), and R. H. Bolt. Sound Waves in Rooms. Rev. of Mod. Phys., vol. 16, pp. 69-150.

Morse, P. M. (1961), and K. U. Ingard. Linear Acoustic Theory, vol. 11/1 of S. Flügge (Ed.), Handbuch der Physik , Springer-Verlag.

Morse, P. M. (1968), and K. U. Ingard. Theoretical Acoustics. pp. 554-599. McGraw Hill.

Mosteller, F. (1961), R. E. K. Rourke, and G. B. Thomas, Jr. Probability and Statistics. Chapter 5. Addision-Wesley.

Oden, J. T. (1969). A General Theory of Finite Elements- Part I & II. International Journal of Numerical Methods in Engineering, vol. 1.

Rektory, K. (Ed.) (1969). Survey of Applicable Mathematics. M. I. T. Press, Cambridge, Massachusetts.

Rschevkin, S. N. (1963). A Course of Lectures on The Theory of Sound. Pergamon Press.

Shreider, Yu. A. (Ed.) (1964). Method of Statistical Testing Monte Carlo Method. Elsevier Publishing Co.

Strutt, M. J. O. (1929). On the Acoustics of Large Rooms. Phil. Mag., vol. 8, pp. 236-250.

Tocher, K. D. (1963). The Art of Simulation. The English Universities Press (London).

Vaidya, P. G. (1969). Some Aspects of the Theory of Propagation of Periodic and Transient Sounds in Absorbent Ducts and in Rooms with open Window. Ph. D. Thesis, University of Southampton, England.

Walters, E. R. (1950), and J. B. Rea. Determination of Frequency Characteristics from Response to Arbitrary Input. J. Aero. Sci., vol. 17, pp. 446-452.

Watson, G. N. (1962). A Treaties on the Theory of Bessel Functions. Second Edition. Cambridge University Press.

Watson, R. B. (1946). The Modulation of Sound Decay Curves. J. Acoust. Soc. of Amer., vol. 18, pp. 119-129.

Zienkicwicz, O. C. (1967), and Y. K. Cheng. The Finite Element Methods in Structural and Continuum Mechanics. McGraw Hill.

Appendix 1

SIGNAL PATH FORMULATION

The Monte Carlo technique that is developed in Chapter 3 investigates what happens to the field in terms of the disturbance signal paths originating from the energy source, and based on the information so collected, reconstructs the field as a function of the space and time on a statistical basis. The formulation of the signal paths can be justified from the viewpoint of the Helmholtz Wave equation and the Eikonal equation; such a justification is presented in this Appendix.

Consider the effect of the radiating sound source in a medium which was at rest initially. When the attention is confined to a specific band of approximately constant frequency of the emitting source, the field can be expressed using the solution of the Helmholtz Wave equation

$$(\nabla^2 + k^2)\Psi = 0 \qquad (1)$$

where $\Psi(\underline{x})$ is the time-independent spatial part of the wave function

$K(\underline{x})$ is the wave number defined as

$$K(\underline{x}) = \omega / c(\underline{x}) = 2\pi / \lambda(\underline{x}) \qquad (2)$$

ω is the angular frequency of the source, considered approximately constant for a specific frequency band of the source

$\lambda(\underline{x})$ is the wavelength, characteristic length of the medium

$c(\underline{x})$ is the characteristic wave velocity of the medium.

Equation 2 clearly shows that for a given value of ω, the wavelength λ changes with the wave velocity c.

Equation 1 is a linear, elliptic, second order partial differential equation, which with proper boundary conditions represents the radiation problem in acoustics.. For a radiating surface with an arbitrary shape & distribution of , for example, a particle velocity on it, no standard method can be applied; a recourse has to be made to some numerical procedure. Assume a trial solution of the form

$$\Psi(\underline{x}) = A(\underline{x}) \cdot e^{iK_0 S(\underline{x})} \qquad (3)$$

where $A(\underline{x})$ is the amplitude function

K_0 is the standard wave number ($=\omega/c_0$), with c_0 as some standard wave velocity (constant)

$S(\underline{x})$ is the phase function(real)

When Eq. 3 is substituted in Eq. 1 and equated separately to zero the real and imaginary parts, the following two coupled differential equations result

$$\nabla^2 A + \left\{ k^2 - k_0^2 . (\nabla S)^2 \right\} A = 0 \qquad (4)$$

$$\nabla \left\{ \nabla S . A^2 \right\} = 0 \qquad (5)$$

No exact solutions are possible for these; however, an excellent approximate solution can be obtained by the Wentzel-Kramers-Brillouin (WKB) method. This is based on the fact that in a slowly varying medium the wave amplitude function $A(\underline{x})$ will also be a slowly varying function; and hence as a first approximation

$$\nabla^2 A \approx 0 \qquad (6)$$

Then Eq. 4 reduces to

$$(\nabla S)^2 = n^2 \qquad (7)$$

where $n(\underline{x}) = k(\underline{x}) / k_0 = c_0 / c(\underline{x})$ (8)

is the generalized refractive index of the medium. It is observed that Eq. 7 is a differential equation of the first order and second degree. In principle its solution can be found, given the spatial variation of the refractive index and the initial surface of constant S.

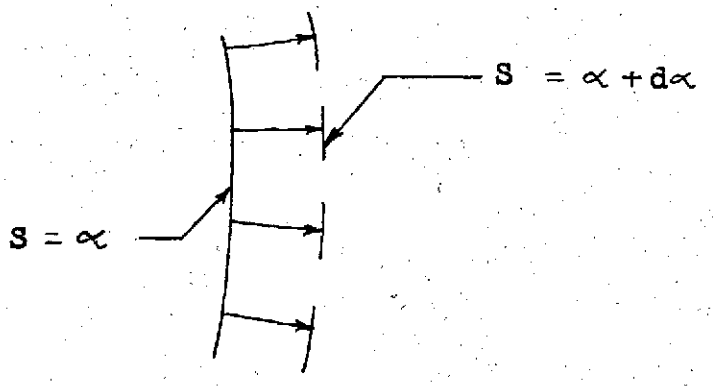

Fig. A1.1 Constuction of the Neighbouring Wavefront Surfaces

A surface of constant S forms an individual wavefront, and a set of wavefronts is a family of such surfaces having the values of the nondimensional quantity $R_0 S$ (Eq. 3) differing in increments of 2π. Let

$$S = \alpha$$

be a given initial wavefront. Its neighbouring surface

$$S = \alpha + d\alpha$$

is constructed by going out along each normal a distance

$$d\alpha \; / \; | \text{ grad } S |$$

and connecting the resulting terminal points (Fig. A1.1).

Continuation of this process sets up successive surfaces

$$S = \text{constant}$$

Now it is possible to integrate Eq. 7. The value of $S(\underset{\sim}{x})$ thus obtained is then substituted in Eq. 5, and solved for the amplitude function $A(\underset{\sim}{x})$. The solution of Eq. 7, in general, can be expressed as

$$\text{grad } S = n(\underset{\sim}{r}) \ \hat{\underset{\sim}{s}}(\underset{\sim}{r}) \qquad (9)$$

where $\hat{\underset{\sim}{s}}(\underset{\sim}{r})$ is a unit normal to the wavefront.
It is observed that in Eq. 9 $\underset{\sim}{r}$ signifies the spatial dependence on the three coordinates of the point, but does not imply a particular choice of the Cartesian coordinates only. The continuous curves that are everywhere parallel to the unit vector $\hat{\underset{\sim}{s}}(\underset{\sim}{r})$ are recognized to be the RAYS. These rays represent the required propagational paths of the disturbance signals.

Let s represent the arcual coordinate along the ray representing the ray distance; then the above relation can be expressed in a more suitable form as follows:

$$\begin{aligned}(d/ds)\,(n\,\hat{\underset{\sim}{s}}) &= (d/ds)\,(\text{grad } S) = \hat{\underset{\sim}{s}}\ \text{div}(\text{grad } S) \\ &= (1/n)(\text{grad } S)\{\text{div}(\text{grad } S)\}\ , \quad \text{from Eq. 9} \\ &= (1/2n)\nabla(\text{grad } S)^2 = (1/2n)\nabla(n^2)\ , \quad \text{from Eq. 7} \\ &= \nabla n \qquad (10)\end{aligned}$$

Given the spatial variation of the refractive index n at the local point, and the initial direction $\hat{s}_0$ of the desired ray, using Eq. 10 it is possible to make the successive evaluation of the ray trajectory. The effects caused by fluctuations in such physical veriables, for example, as density, temperature, convective velocity, etc. can be added to this basic form as and when required.

It is recalled that the basic form represented by Eq. 10 is based on the WKB approximation. Before its use it is worthwhile to examine its validity and the conditions imposed thereof. Taking for simplicity the one dimensional case, the <u>exact</u> Eqs. 4 & 5 now take the form

$$\left\{(d^2/dx^2) + \left[n^2 - (dS/dx)^2\right] k_0^2\right\} A = 0 \qquad (11)$$

$$(d/dx)\left\{(dS/dx)\, A^2\right\} = 0 \qquad (12)$$

In the WKB approximation the use is made of the relation

$$dS/dx \approx n \qquad (13)$$

then from Eq. 12

$$A(x) = B\left\{c(x)\right\}^{-\frac{1}{2}} \qquad (14)$$

where $B = A(x_0)\left\{c(x_0)\right\}^{\frac{1}{2}}$ is a constant.

The unknown exact derivative in Eq. 13 is now represented by

$$dS/dx = n\left\{1 + \varepsilon(x)\right\} \qquad (15)$$

Substitution of Eqs. 14 & 15 into Eq. 11 gives

$$\mathcal{E}(1 + \mathcal{E}/2) = (1/n^2)\left\{-(1/8c^2)(dc/dx)^2 - (1/4c)(d^2c/dx^2)\right\}(1/R_0^2) \quad (16)$$

In a slowly varying medium

i. the index of refraction deviates only slightly from its mean value equal to unity, i.e.

$$n(\underline{x}) = 1 + \mathcal{D}(\underline{x}), \text{ where } |\mathcal{D}| << 1$$

ii. $(d^2c/dx^2) << (dc/dx)^2$

Hence $$\mathcal{E} \simeq (1/8)\left\{(1/c)(dc/dx')^2\right\}, \text{ where } x' = x R_0 \quad (17)$$

It is noticed that $(1/c)(dc/dx')$ represents the relative change in the wave velocity in the distance of one local wavelength.

Generalizing the results of Eq. 17 it can be stated that the WKB approximation is good enough for a medium wherein the medium properties do not change appreciably in a distance of one local wavelength.

Appendix 2

ERROR ESTIMATION IN THE MONTE CARLO METHOD

The numerical answer to a given problem by the application of the Monte Carlo technique is obtained by averaging and analyzing the many results of repetations of an experiment on a high speed computer. Any single result is a function of a sequence of random numbers that are employed in that particular Monte Carlo run. It represents a random event, which is an event that has a chance of happening. A numerical measure of this chance is given by its probability; it is a number lying between 0 and 1, both inclusive, higher values indicate greater chances.

PROBABILITY ESTIMATE

Suppose that a random variable X has a finite mathematical expectation

$$E\{X\} = \mu \qquad (1)$$

Its variance and standard deviation are given by

$$D^2\{X\} = E\{X - E(X)\}^2 \qquad (2)$$

$$\sigma_X = \sqrt{D^2\{X\}} \qquad (3)$$

respectively. The probability of occurrence of an event connected with this variable can be examined in the light of Chebyshev's theorem which is stated as

"For any positive number h, there exists the probability relation

$$P\{|X - \mu| \geq h\sigma_X\} \leq 1/h^2 \qquad (4)$$

or equivalently

$$P\{|X - \mu| < h\sigma_X\} \geq 1 - 1/h^2 \qquad (5)$$

For example, it says that at least 3/4 of the total probability is within $\pm 2\sigma$ from the mean for any random variable. This theorem guarantees the lower bound; but when the sample size is large, which is the usual case with any Monte Carlo calculation, it has been found that the stronger results than those given by Chebyshev's theorem usually hold. A common empirical rule (Mosteller, 1961) indicates that about 68 %, 95 % and 99.7 % of the total probability values of a random variable lie within $\pm\sigma$, $\pm 2\sigma$ and $\pm 3\sigma$ from the mean. The numbers given for the emprical rule agree exactly with those for the normal probability distribution.

ERROR ANALYSIS

Suppose that $X_1, X_2, X_3, \ldots, X_n$ are the n independent outcomes resulting from n different runs of the Monte Carlo simulation of the above problem relating to the random variable X with finite mathematical expectation μ (Eq.1). It is reasonable to represent the Monte Carlo estimate of by

$$\mu_M = \frac{W_1X_1 + W_2X_2 + W_3X_3 + \ldots + W_nX_n}{W_1 + W_2 + W_3 + \ldots + W_n} \qquad (6)$$

where W_i is a 'weighting factor', a quantity that represents, in some sense, the length of the sequence of random numbers used and the sample size N_i which gives the number of independent trials in the i^{th} run. The error involved in the value μ_M given by the Monte Carlo method can then be expressed as

$$\delta = |\mu_M - \mu| \qquad (7)$$

The distribution of μ_M is obtained from the 'Limit Theorems' of the theory of probability. In the Monte Carlo method the values of the sample size N, which are commonly employed, are of the order of $10^3 - 10^6$ and as a result it is possible to consider μ_M to be distributed very nearly in accordance

with the Gaussian law. Then using the 'Three - Sigma Rule', where the error is known with the probability of 0.997, Shreider (1964) has shown that the exact estimate of the error δ of the Monte Carlo method is given by

$$\delta = |\mu_M - \mu| \leq 3\ D^2\{X\} / N^{\frac{1}{2}} = 3\sigma / N^{\frac{1}{2}} \quad (8)$$

It shows that the accuracy of the Monte Carlo method depends only on the sample size and the variance. Two ways of reducing this error are seen to be

1. Increase in the sample size N
2. Change in the sampling technique to make the variance $D^2\{X\}$ small; as stated earlier in Chapter 3, methods such as Stratification, Control Variates, Antithetic Variates, etc. can be employed for this purpose.

The extent to which each of these alternatives to be employed depends heavily on the relative cost of each for the particular problem that is under investigation. This is examined in what follows.

Efficiency of a Monte Carlo Technique

Suppose the Monte Carlo simulation of a given problem, on average, involves m_c number of computer operations per trial with a computer time t_c per operation;

then using Eq. 8, for the desired accuracy δ, the total computer time required for a Monte Carlo calculation of sample size N can be expressed as

$$T_c \approx N m_c t_c \approx 9 m_c \sigma^2 t_c / \delta^2 \qquad (9)$$

Equation 9 clearly shows that, with all other factors remaining same, to halve the error it is necessary to increase the total computer time four times; quite often this becomes impractical and the remedy lies in careful design of the way in which the samples are collected and analyzed.

As is evident from Eq. 9 the efficiency of a Monte Carlo technique is inversely proportional to the product of the sampling variance and the amount of labour expended in obtaining such an estimate; it is this product that is under control of an analyst for a preassigned desirable accuracy. A slight increase in the labour would be permissible if it results in overwhelming decrease in the sampling variance. The efficiency of method 2 relative to method 1 is given by

$$\eta_{21} = \eta_2 / \eta_1 = (m_{c1} / m_{c2}) \cdot (\sigma_1 / \sigma_2)^2$$

$$= l_{21} \cdot v_{21} \qquad (10)$$

where l_{21} is the labour ratio

v_{21} is the variance ratio

The labour ratio l_{21} depends partly on the computing machinery available and partly on the Monte Carlo method employed; whilst the variance ratio v_{21} depends mainly on the complexity of the particular problem that is under investigation and the details of the technique employed.

Economics

Consider a case where the requirement is to achieve a preassigned level of accuracy at a minimum cost. The total cost of a Monte Carlo method is made up of the following three parts

I. Cost of design of the experiment, this includes such costs as

the development cost of the basic sampling technique

an additional cost towards extra analysis performed, if any, in an attempt to reduce the sampling variance

II. Cost of programming

III. Computer machine cost.

The total cost s is given by

$$s = s_1 + s_2 = s_1 + \propto T_c \qquad (11)$$

where s_1 is the combined cost of I & II

s_2 is the cost of III

α is the factor of proportionality

T_c is the computer time for a sample of size N (Eq. 9).

As is seen from Eqs. 9, 10 and 11 any attempt towards the refinement of the technique is bound to alter both s_1 and s_2, the former through the cost of analysis whilst the latter through the efficiency factor $m_c \sigma^2$. This interdependency makes it impossible to predict in advance the form of the variations in the standard deviation σ.

Elimination of T_c from Eqs. 9 and 11 gives

$$s = s_1 + \beta \sigma^2 \qquad (12)$$

where $\beta = 9\, m_c \alpha / \delta^2$

The condition of minium cost requires

$$(ds / ds_1) = 1 + \sigma^2 (d\beta / ds_1) + 2\beta\sigma (d\sigma / ds_1) = 0 \qquad (13)$$

In fact the proportionality factor α in Eq. 11 is different for different sampling methods and thus is a function of s_1. The number of computer operations m_c is also different for different sampling methods. Under the assumption that these two variations more nearly balance each other, Eq. 13 reduces to a differential equation

$$(d\sigma / ds_1) = -1 / 2\beta\sigma \qquad (14)$$

the solution of which gives the sampling plan $\sigma(s_1)$. Substitution of this value in Eq. 8 gives the required sample size.

Probable Relative Error

Whenever a complicated problem is solved with the aid of a computer it is always necessary to consider the possibility of random error, this may result due to a fault or a rounding-off procedure. Under such circumstances, since the final result can only be regarded as reliable with certain probability approaching unity, the error can hardly be calculated from a theoretical formula.

Equation 6 above gives the Monte Carlo estimate μ_M of the variable X. The exact value μ (Eq. 1) is seldom known. This makes it impossible to evaluate the error δ (Eq. 7) in practice. Since the Monte Carlo results are the mathematical expectations of some random quantities, the following relation for the probable relative error, δ_{prob}, usually provides the order of the statistical error in the Monte Carlo calculations.

$$\delta_{prob} = (0.68 / E\{X\}) \cdot (D^2\{X\} / N)^{\frac{1}{2}} \qquad (15)$$

where $E\{X\}$ is the expectation value of X (Eq. 1)

$D^2\{X\}$ is the variance of X (Eq. 2)

N is the sample size.

A close observation of the variation in the results with increasing sample size N furnishes an additional information about the error. In the works of Bouquet (1958) it was assumed that the deviation from the exact value follows a normal distribution when $N \quad N_0$, where N_0 is the preassigned sample level; but Shreider (1964) has observed that this type of approach has not been adequately justified.

Appendix 3

A NOTE ON THE SELECTION OF RAY DIRECTION

The Monte Carlo method of random direction selection, outlined in Chapter 3, is examined here in more details first and is further compared with an alternative method conceivable on pure geometric considerations.

MONTE CARLO METHOD

Hemispherical section of a unit sphere is shown in Fig. A3.1. In the coordinate plane X1-X2, point A is selected at random such that it lies inside the circular cross-section. Let B be its projection on the spherical surface in X3 direction. Then the line joining the origin O to this point B provides the requisite direction for a ray. The method is based on the principle of Rejection Technique. In order to determine the efficiency of this method consider the shaded area of Fig. A3.1. It is defined by the curve

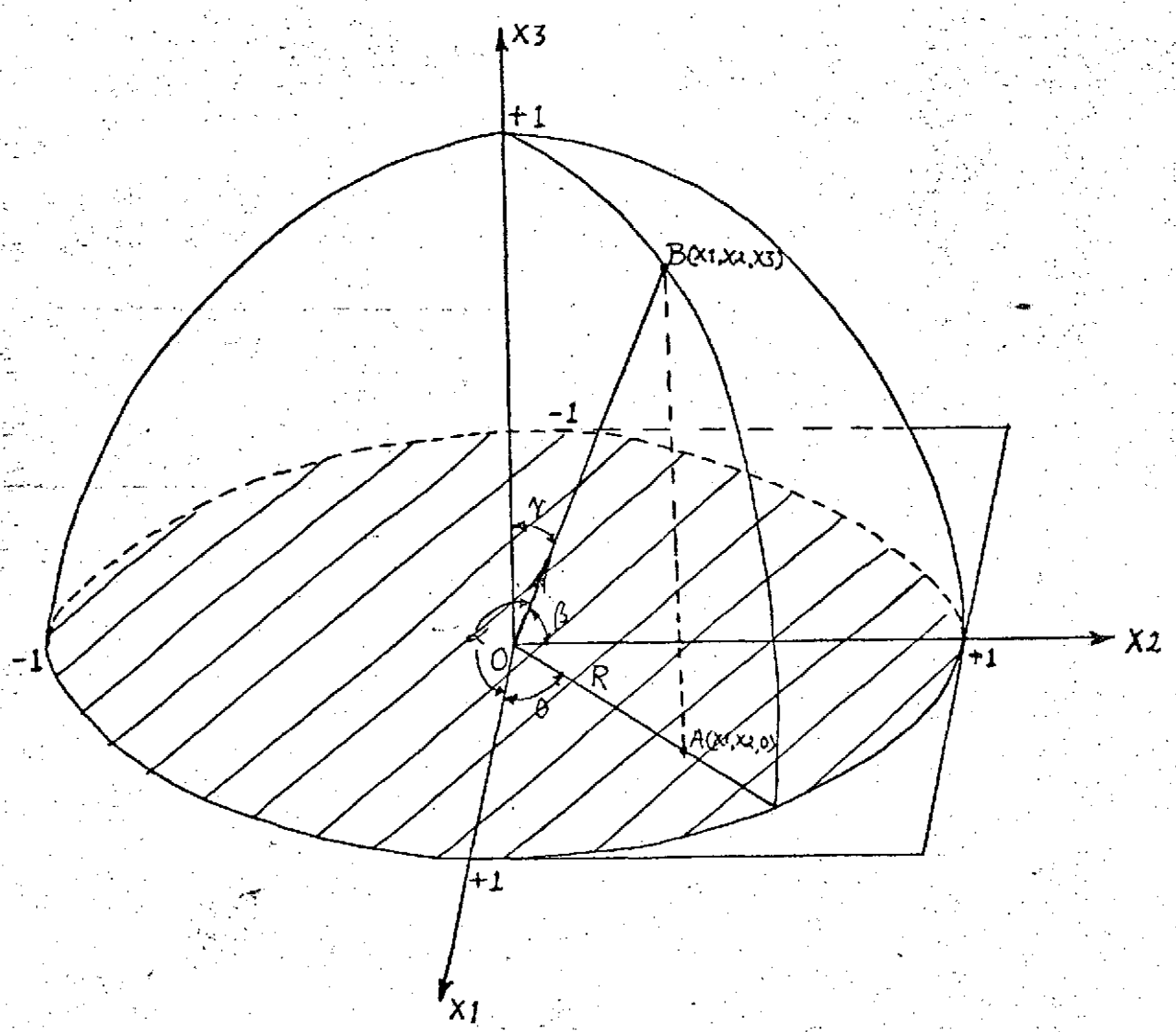

Fig. A3.1 Selection of Ray Direction Monte Carlo Method

$$X2 = f(X1) = \begin{cases} (1 - X1^2)^{\frac{1}{2}} , & -1 \leq X1 \leq 1 \\ 0 , & \text{elsewhere} \end{cases} \qquad (1)$$

Suppose that a point is chosen at random in the square

$$-1 \leq X1 \leq 1$$
$$-1 \leq X2 \leq 1$$

such that its coordinates are, independently, uniformly distributed in the interval (-1, 1). Such a point, defined by

$$X1 = 1 - 2\mathbb{R}1$$
$$X2 = 1 - 2\mathbb{R}2 \qquad (2)$$
$$X3 = 0$$

can be obtained by utilizing two random numbers $\mathbb{R}1$ and $\mathbb{R}2$ that are distributed uniformly in the interval $[0,1]$. The abscissa X1 of this point is acceptable as a sample value if this point falls inside the graph of f(X1), if not it is rejected and a new set of random numbers is tried.

In order to evaluate the probability of this point lying inside the shaded area of Fig. A3.1, consider its first quadrant. Under the assumption that $\mathbb{R}1$ and $\mathbb{R}2$ are independent the probability of selecting a value of X1 in the region X1 to X1 + ΔX1 is given by

$$\left\{ f(X1) \,/\, (X2)_{max} \right\} \cdot \left[\Delta X1 \,/\, (X1)_{max} \right\}$$

i. e. $\left\{ f(X1) \cdot \Delta X1 \right\}$

Then the probability of obtaining a satisfactory point at the first trial, which is called the efficiency η of the technique, is given by

$$\eta = \sum_i f(X1_i)\,\Delta X1_i = \lim_{\Delta X1_i \to 0} \sum_i f(X1_i)\,\Delta X1_i$$

$$= \int_0^1 f(X1)\,dX1 = \int_0^1 (1 - X1^2)^{\frac{1}{2}}\,dX1 = \pi / 4 \qquad (3)$$

The probability that the process will fail $(n - 1)$ times and then succeed on the n^{th} trial is given by

$$(1 - \eta)^{n-1}\,\eta$$

and the mathematical expectation of n is given by

$$E\{n\} = \sum_{n=1}^{\infty} n(1 - \eta)^{n-1} = 1/\eta = 4/\pi \qquad (4)$$

It is possible to prove that the distribution of the selected point B (Fig. A3.1) using this method is uniform. The line from O to B has as its direction vector

$$\underset{\sim}{DC}(1,2,3) = (DC1, DC2, DC3)$$

$$= (\cos\alpha, \cos\beta, \cos\gamma) \qquad (5)$$

Using Eq. 7 of Chapter 3 the component DC1 is rewritten as

$$DC1 = \cos\alpha = 1 - 2R^2$$

Then
$$R = \sin\alpha / 2$$
$$X1 = R\cos\theta \qquad (6)$$
$$X2 = R\sin\theta$$

In terms of the angles α and θ (Fig. A3.1), now, Eq. 5 is rewritten as

$$\underset{\sim}{DC}(1,2,3) = (\cos\alpha,\ \sin\alpha\cos\theta,\ \cos\alpha\sin\theta) \qquad (7)$$

Let P(x) be the probability of component x, then

$$P(\alpha,\theta)\,d\alpha\,d\theta = P(X1, X2)\,dX1\,dX2 = dX1\,dX2/\pi$$
$$= R\,dR\,d\theta/\pi = \sin\alpha\,d\alpha\,d\theta/4\pi$$
$$= d\Omega/4 \qquad (8)$$

Equation 8 shows that the above Monte Carlo method for selection of a ray direction provides an 'even distribution' of directions in the sense of 'equally probable' directions.

ALTERNATIVE METHOD

An alternative method, based on purely geometric considerations, is outlined by Krokstad (1968). This method consists of introducing n planes, parallel to the coordinate plane X1 - X2, between X3 = 0 to X3 = 1. Angle γ_i and the corresponding radius R_i of the circle shown in Fig. A3.2 are given by the following relations

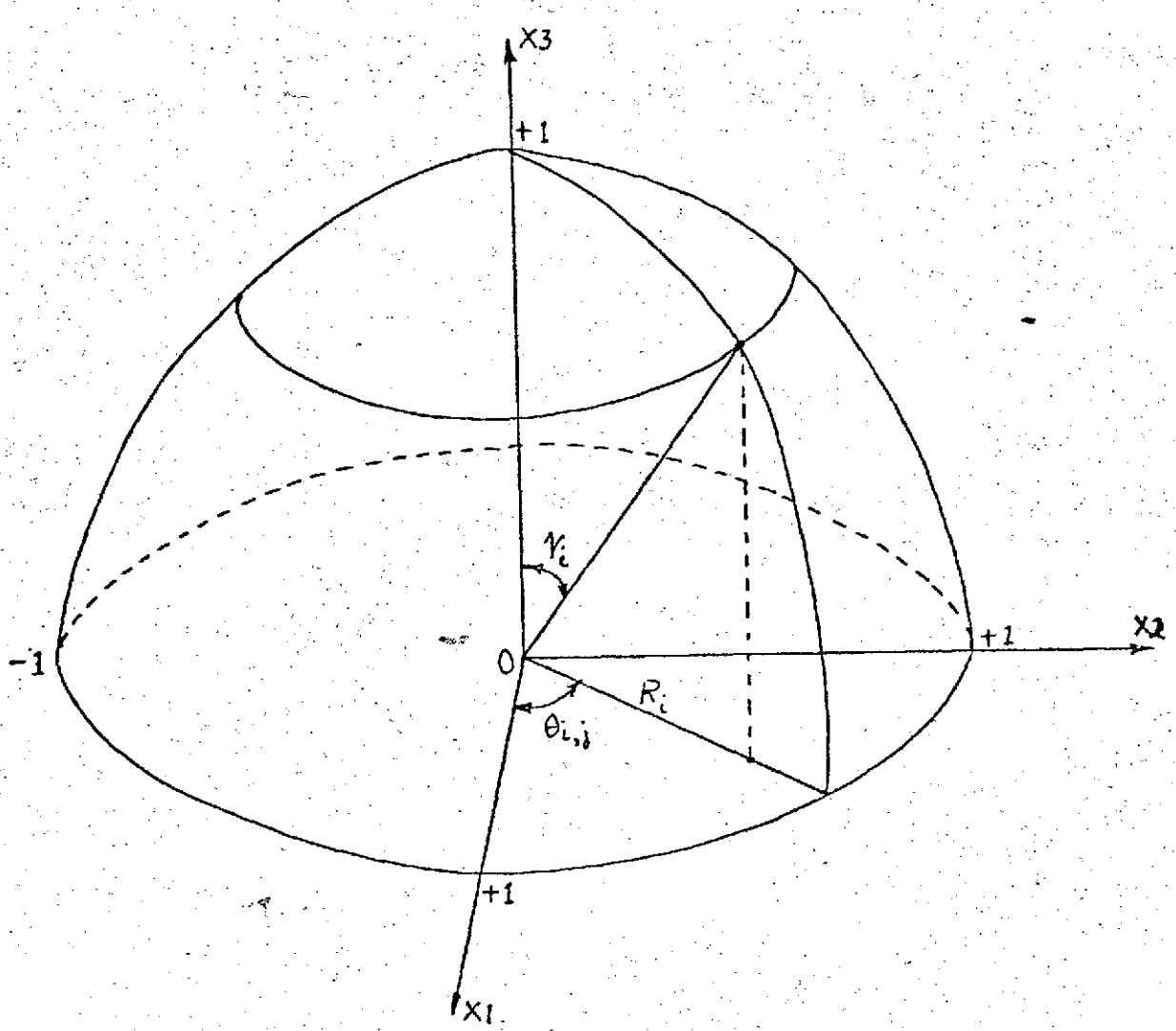

Fig. A3.2 Selection of Ray Direction Geometrical Method

$$\gamma_i = \frac{2i - 1}{2} \frac{90^\circ}{n}$$

$$R_i = \sin \gamma_i \qquad (i = 1,2,\ldots,n) \qquad (9)$$

On the spherical surface the distance between iwo adjacent circles is given by

$$b = \pi / 2n \qquad (10)$$

Let m_i be an integral number, representing the number of points that are considered on the i^{th} circle; it is defined by

$$m_i = \text{INT} [l_i / b] \qquad (11)$$

where $l_i = 2\pi R_i$

The angle $\theta_{i,j}$ shown in Fig. A3.2 is given by

$$\theta_{i,j} = \frac{2j - 1}{2} \frac{90^\circ}{m_i} \quad (j = 1,2,\ldots,m_i) \qquad (12)$$

The line from O to B has as its direction vector

$$\underset{\sim}{DC}(1,2,3) = (DC1, DC2, DC3)$$

$$(\sin \gamma_i \cos \theta_{i,j}, \sin \gamma_i \sin \theta_{i,j}, \cos \gamma_i)$$

(13)

In this method, the approximation of the quantity l_i/b by an integer m_i (Eq. 11) for different values of i, is seen to lead to a nonuniform distribution of the selected points; and as a consequence there appears an inherent degree of unevenness in the distribution of the selected directions obtained by this method.

Appendix 4

RECTANGULAR ROOM PROBLEM MONTE CARLO PROGRAMME

This appendix gives in full details the results of the application of the proposed Monte Carlo technique (Chapter 3) to a rectangular boundary problem that is under investigation (Chapter 5). Included herein is a complete listing of the programme that was used in these calculations on the CDC 6400 of the Computing Center of the University of Virginia. The printout results accompanying this listing correspond to the pressure values shown in Figs. 13.1 and 56.

```
      PROGRAM MONTEAC(INPUT, OUTPUT, TAPE10=INPUT, TAPE11=OUTPUT)
000003      DIMENSION MX(4),LCL(3),SORS(3),Q(50),UM(3),RT(3),DL(4),DC(4),
           1MAY(4),CL(6),RL(5),P(200),RA(4),CPA(4),CLMT(3),TR(3),CP8(4)
000033      COMMON/GGRAN/IRAN,RANNO
            C     SINGLE CYCLE SINUSOIDAL PULSE INPUT
000033      DIMENSION PRES(20,200)
            C     INPUT QUANTITIES
000033      READ(10,101)IMAX,NPULS,(MX(I),I=1,4),(LCL(I),I=1,3),IRAN,SONSP,
           1TPULS,UNST,(DL(I),I=1,4),(SORS(I),I=1,3)
000053      WRITE(11,201)IMAX,NPULS,(MX(I),I=1,4),(LCL(I),I=1,3),IRAN,SONSP,
           1TPULS,UNST,(DL(I),I=1,4),(SORS(I),I=1,3)
000123      FNORM=(UNST*TPULS*IMAX)/(DL(1)*DL(2)*DL(3)*DL(4)*NPULS) $ RLRG=0.0
000134      FNORM=FNORM/(UNST*(SONSP**2))
            C     NOW THIS PROVIDES NORMALIZED PRESSURE VALUES AT STATMENT NUMBER 35
            C     IN THE NONDIMENSIONAL FORM
000136      DO 2 I=1,3 $ DM(I)=DL(I)*MX(I) $ RLRG=RLRG+DM(I) $ NL(I)=0.0
000146      NL(I+3)=DM(I) $ CL(I)=DL(I)* LCL(I)    $ CL(I+3)=DL(I)*(LCL(I)+1)
000156    2 CONTINUE $ WRITE(11,201)(NL(I),I=1,6),(CL(I),I=1,6) $ JMAX=MX(4)
000241      WRITE(11,204) $ WRITE(11,206)IRAN $ DO 36 NRPT=1,10 $ NP=0
000215      DO 3 J=1,JMAX $ PRES(NRPT,J)=P(J)=0.0
000224    3 CONTINUE
            C     POSITION A ON FLOW DIAGRAM
000225   40 DO 4 I=1,3
000233    4 RAY(I)=SORS(I)
            C     GRAN SUBPORTION STARTS HERE
000243    5 CALL GRAN $ QTEMP=SIN(44.0*RANNO/7.0) $ NP=NP+1
000242      SORST=RAY(4)=RANNO*(TPULS*IMAX) $ RYDS=0.0
000253    6 CALL GRAN $ ETA=1-2*RANNO $ CALL GRAN $ PSI=1-2*RANNO $ RSQR=ETA**
           12+PSI**2 $ IF(RSQR.GT.1.0)GO TO 6  $ DC(1)=1-2*RSQR $ RSQT=SQRT(1-
           2RSQR) $ DC(2)=2*ETA*RSQT $ DC(3)=2*PSI*RSQT $ DC(4)=1/SONSP
            C     GRAN SUBPORTION ENDS HERE
            C     GRID SUBPORTION STARTS HERE
            C     POSITION B ON FLOW DIAGRAM
000313    7 RL=RLRG $ DO 12 I=1,3 $ IF(DC(I))8,12,9
000315    8 R=(NL(I)-RAY(I))/DC(I) $ GO TO 10
000321    9 R=(NL(I+3)-RAY(I))/DC(I)
000325   10 IF(R.LT.RL)11,12
000332   11 IC=I $ RL=R
000335   12 CONTINUE
            C     GRID SUBPORTION ENDS HERE
            C     FROM THIS SUBPORTION ONLY THIS IC VALUE IS USED FURTHER
000337      IF(DC(IC).GT.0.0)13,14
000344   13 IF(RAY(IC).LT.CL(IC))15,17
000352   14 IF(RAY(IC).GT.CL(IC+3))16,17
000360   15 R=(CL(IC)-RAY(IC))/DC(IC) $ GO TO 18
000364   16 R=(CL(IC+3)-RAY(IC))/DC(IC) $ GO TO 18
000373   17 R=0.0 $ GO TO 27
            C     END OF EVALUATION OF R UPTO MONITORED CELL WALL
            C     FURTHER FROM THIS SUBPORTION ONLY THIS R VALUE IS USED
            C     PATH SUBPORTION STARTS HERE
000372   18 RYDS=RYDS+R $ DO 22 I=1,3 $ RA(I)=R*DC(I)+RAY(I)
000401      IF(DC(I).GT.0.0)19,20
000406   19 IF(RA(I).GT.CL(I+3))27,21
000414   20 IF(RA(I).LT.CL(I))27,21
000422   21 CPA(I)=RA(I)
000424   22 CONTINUE $ CPA(4)= RYDS*DC(4)+SORST
000431      J=IFIX((CPA(4)/DL(4))+1 $ IF(J.GT.JMAX) GO TO 32
```

```
000437          DO 25 I=1,3 $ IF(DC(I).LT.0.0)23,24
000454    23    CLMT(I)=CL(I) $ GO TO 25
000447    24    CLMT(I)=CL(I+3)
000451    25    TR(I)=(CLMT(I)-CPA(I))/DC(I) $ RYPNT=AMIN1(TR(1),TR(2),TR(3))
000464          DO 26 I=1,4
000476    26    RAY(I)=CPA(I)+RYPNT*DC(I)+CPA(I)
000474          P(J)=P(J)+ATEMP*(RYOS+0.5*RYPNT)*RYPNT $ RYOS=RYOS+RYPNT
          C     PRINT SUBPORTION ENDS HERE
000534    27    IF(DC(IC).GT.0.0)28,29
000511    28    R=(WL(IC+3)-RAY(IC))/DC(IC) $ GO TO 30
000515    29    R=-RAY(IC)/DC(IC)
000521    30    DO 31 I=1,3 $ RAY(I)=RAY(I)+R*DC(I)
000527          IF(ABS(RAY(I)).LT.1.E-08) RAY(I)=0.0 $ IF(ABS(RAY(I)-WL(I+3)).LT.
                1E-06) RAY(I)=WL(I+3)
000541    31    CONTINUE $ RYOS=RYOS+R $ RAY(4)=RYOS*DC(4)+SORST
          C     TIME WALL TEST
000556          J=IFIX(RAY(4)/DL(4))+1 $ IF(J.GE.JMAX)32,33
000563    32    IF(NPULS-IPULS)34,40
000565    33    DC(IC)=-DC(IC) $ GO TO 7
          C     END OF SPATIAL WALL COLLISION
000573    34    DO 35 J=1,JMAX $ PRES(NRPT,J)=P(J)*PNORM*P(J)
000610    35    CONTINUE
000602          WRITE(11,202)(J,P(J),J=1,JMAX) $ WRITE(11,203) IRAN
000623    36    CONTINUE
          C      VRNSTD SUBPORTION STARTS HERE
000625          WRITE(11,207) $ DO 43 J=1,JMAX $ X1=X2=0.0 $ DO 41 I=1,NRPT
000635    41    X1=X1+PRES(I,J) $ X1=X1/NRPT $ DO 42 I=1, NRPT
000653    42    X2=X2+(PRES(I,J)-X1)**2 $ VRNS=X2/NRPT $ STDN=SQRT(VRNS)
000667          X1P=X1+STDN $ X1M=X1-STDN
000072    43    WRITE(11,208)J,X1,VRNS,STDN,X1P,X1M
          C      VRNSTD SUBPORTION ENDS HERE
          C     FORMATS
000715    101   FORMAT(9I5,I10,2E10.4/E10.4,9F5.2)
000715    200   FORMAT(1H1,30X*TRANSIENT ACOUSTIC FIELD IN RECTANGULAR CAVITY*3(/)
                15OX*PREASSIGNED CONSTANTS*//5X*IMAX =*I5,2X*NPULS =*I5,2X*MX(1,2,3
                2,4) =*4(I5,2X)*LCL(1,2,3) =*3(I5,2X)/5X*IRAN =*I10,2X*SONSP =*
                3E10.8,2X*TPULS =*E10.8,2X*UNST =*E10.8/5X*DL(1,2,3,4)=*4(E10.8,2X)
                4/5X*SORS(1,2,3) =*3(E10.8,2X)/15X*SINGLE CYCLE SINUSOIDAL PULSE SO
                URCE INPUT (PERIOD=IPULS.IMAX)*//)
000715    201   FORMAT(5X*SPATIAL BOUNDARY WALL(1,2,3,4,5,6)*/5X,6(E16.8,2X)//
                15X*MONITORED CELL WALL(1,2,3,4,5,6)*/5X,6(E16.8,2X))
000715    202   FORMAT(20X*NORMALIZED PRESSURE VALUES IN THE NONDIMENSIONAL FORM*/
                1(5(5X,I3,2X,E10.8)))
000715    203   FORMAT(5X*IRAN VALUE TO BE USED FOR FURTHER CALCULATIONS*I10)
000715    204   FORMAT(20X*CASE 1 : ALL WALLS PERFECTLY REFLECTING * //)
000715    206   FORMAT(10X*STARTING IRAN VALUE*2X,I8)
000715    207   FORMAT(30X*VARIANCE AND DEVIATION ANALYSIS*//10X*TIME INDEX*5X*MEA
                1N*14X*VARIANCE*11X*DEVIATION*7X*(MEAN)+(DEVIATION)*2X*(MEAN)-(DEVI
                2ATION)*//)
000715    208   FORMAT(12X,I3,5(4X,E16.8))
000715          STOP
000717          END
```

MONTE4U

PROGRAM LENGTH INCLUDING I/O BUFFERS
015574

FUNCTION ASSIGNMENTS

STATEMENT ASSIGNMENTS

4	-	000236	5	-	000233	6	-	000250	7	-	000310
8	-	000315	9	-	000321	10	-	000325	11	-	000332
12	-	000335	13	-	000344	14	-	000352	15	-	000360
16	-	000364	17	-	000370	18	-	000372	19	-	000406
24	-	000414	21	-	000422	23	-	000444	24	-	000447
25	-	000451	27	-	000504	28	-	000511	29	-	000515
30	-	000520	31	-	000541	32	-	000560	33	-	000565
34	-	000574	40	-	000226	41	-	000636	42	-	000650
101	-	000741	200	-	000745	201	-	001012	202	-	001027
203	-	001041	204	-	001050	206	-	001057	207	-	001064
208	-	001103									

BLOCK NAMES AND LENGTHS
CSTAT - 000002

VARIABLE ASSIGNMENTS

CL	-	001205	CLHT	-	001621	CPA	-	001615	CPB	-	001627
DC	-	001255	DL	-	001251	DM	-	001243	DNST	-	011500
ETA	-	011512	FNORM	-	011501	I	-	011475	IC	-	011520
IMAX	-	011473	IRAN	-	0000000001	J	-	011506	JMAX	-	011503
LGL	-	001163	MX	-	001147	NP	-	011505	NPULS	-	011474
NSPT	-	011504	P	-	001301	PRES	-	001633	PSI	-	011513
Q	-	001161	QTEMP	-	011507	R	-	011517	RA	-	001611
RANNJ	-	0000001001	RAY	-	001261	RL	-	011516	RLNG	-	011502
RSQR	-	011514	RSUM	-	011515	RT	-	001246	RYDS	-	011511
RYPNT	-	011521	SUMSP	-	011476	SORS	-	001156	SORST	-	011510
STJN	-	011525	TPULS	-	011477	TR	-	001624	VRMS	-	011524
WL	-	001273	X1	-	011522	X1M	-	011527	X1P	-	011526
X2	-	011523									

START OF CONSTANTS
000721

START OF TEMPORARIES
001110

START OF INDIRECTS
001132

UNUSED COMPILER SPACE
032203

```
      SUBROUTINE GRAN
      COMMON/CGRAN/IRAN,RANNO
      IRAN=SLZ>*IRAN $ I1=IRAN/67108864 $ IRAN=IRAN-I1*67108864
      RANNO=FLOAT(IRAN)/67108864
      RETURN $ END
```

```
GRAN

SUBPROGRAM LENGTH
000025

FUNCTION ASSIGNMENTS

STATEMENT ASSIGNMENTS

BLOCK NAMES AND LENGTHS
CGRAN  -  000002

VARIABLE ASSIGNMENTS
IRAN   -  000000001 II    -  000024    RANNO  -  000001C01

START OF CONSTANTS
000016

START OF TEMPORARIES
000020

START OF INDIRECTS
000024

UNUSED COMPILER SPACE
005500
```

```
CORE MAP  16.36.37.  NORMAL                    CONTROL                                          000100    023356    000000    000000
   ---TIME----JAN 10UE --L1--L2-----TYPE--------------USER-------CALL-------------FWA LOAD--LWA LOAD--BLNK COMN--LENGTH--
   FWA LOADER  035761  FWA TABLES  034106
   -PROGRAM----ADDRESS-                    --LABELED---COMMON--
   MONTEAC     000172                                  CGRAN       000100
   GRAN        015076                                  CGRAN       000100
   SINCOS      015723
   SQRT        016022
   SYSTEM      016060                                  SCOPE2      016065
   GETBA       017177
   INPUTC      017216
   KODER       017333
   KRAKEN      020005
   OUTPTC      021660
   SIOS        021723
   ----UNSATISFIED EXTERNALS-----                      REFERENCES
```

PREASSIGNED CONSTANTS

IMAX = 40 NPULS = 5000 MX(1,2,3,4) = 25 15 10 60 LCL(1,2,3) = 8 8 6
IRAN = 1001 SOUSP = 1.10000000E+03 TPULS = 5.00000000E-03 DNST = 2.37800000E-03
DL(1,2,3,4) = 4.40000000E+00 4.40000000E+00 4.40000000E+00 5.00000000E-03
SORS(1,2,3) = 2.20000000E+01 3.30000000E+01 2.20000000E+01
SINGLE CYCLE SINUSOIDAL PULSE SOURSE INPUT (PERIOD=TPULS.IMAX)

SPATIAL BOUNDARY WALL(1,2,3,4,5,6)
0. 0. 0. 1.10000000E+02 6.60000000E+01 4.40000000E+01

MONITORED CELL WALL(1,2,3,4,5,6)
3.52000000E+01 3.52000000E+01 2.64000000E+01 3.96000000E+01 3.96000000E+01 3.08000000E+01
CASE 1 : ALL WALLS PERFECTLY REFLECTING

STARTING IRAN VALUE 1001
NORMALIZED PRESSURE VALUES IN THE NONDIMENSIONAL FORM

1	0.	2	2.58257926E-09	3	1.44921085E-08	4	1.68704056E-08	5	3.17638353E-08
6	3.30479770E-08	7	4.81161590E-08	8	4.91252255E-08	9	5.14291209E-08	10	5.29584411E-08
11	9.61337033E-08	12	5.60373445E-08	13	6.97951486E-08	14	8.67054585E-08	15	1.35788912E-07
16	1.59[illegible]E-07	17	3.16428626E-07	18	4.42856609E-07	19	5.14498792E-07	20	5.44095797E-07
21	6.02[illegible]E-07	22	6.57986055E-07	23	4.40208649E-07	24	7.94206561E-07	25	5.33923897E-07
26	9.75[illegible]E-07	27	1.07098479E-06	28	8.40151350E-07	29	9.60112949E-07	30	1.24832107E-06
31	1.67[illegible]E-06	32	9.51740146E-07	33	1.02202095E-06	34	1.23185704E-06	35	7.96732031E-07
36	1.20[illegible]E-06	37	8.62622981E-07	38	1.19489469E-06	39	1.13759001E-06	40	1.89825261E-06
41	1.16[illegible]E-06	42	1.71170082E-06	43	1.50617846E-06	44	1.62020122E-06	45	1.40985104E-06
46	1.33[illegible]E-06	47	1.76159253E-06	48	2.31955523E-06	49	1.77835902E-06	50	1.77709622E-06
51	7.18[illegible]E-07	52	2.91379592E-06	53	2.19933321E-06	54	2.84545023E-06	55	2.71834272E-06
56	3.44[illegible]E-06	57	1.30202523E-06	58	2.38767447E-06	59	2.76174303E-06	60	2.88810551E-06
61	2.04[illegible]E-06	62	2.46369140E-06	63	2.24099039E-06	64	1.38984928E-06	65	1.03396793E-06
66	2.26[illegible]E-06	67	1.07824897E-06	68	2.07124703E-06	69	1.50210111E-06	70	2.07579253E-06
71	2.37[illegible]E-06	72	3.34929491E-06	73	-4.13044016E-07	74	2.59117168E-07	75	1.79751491E-06
76	2.01[illegible]E-06	77	1.46733220E-06	78	1.22691699E-06	79	5.76295973E-07	80	7.15894540E-07

IRAN VALUE TO BE USED FOR FURTHER CALCULATIONS 16361289
NORMALIZED PRESSURE VALUES IN THE NONDIMENSIONAL FORM

1	4.77[illegible]E-10	2	3.54695322E-09	3	1.42728632E-08	4	1.43840803E-08	5	4.24601194E-08
6	3.[illegible]E-08	7	3.98045286E-08	8	6.20429196E-08	9	3.74678648E-08	10	1.27208983E-07
11	3.24[illegible]E-08	12	7.52187166E-08	13	1.07492445E-07	14	2.02083729E-07	15	1.47074729E-07
16	2.16[illegible]E-07	17	4.[illegible]E-07	18	4.92787257E-07	19	5.42199014E-07	20	6.93667648E-07
21	5.56[illegible]E-07	22	7.33992594E-07	23	8.19342066E-07	24	8.68444078E-07	25	1.12909823E-06
26	8.63[illegible]E-07	27	7.51774771E-07	28	1.26946772E-06	29	7.52968654E-07	30	1.12604695E-06
31	1.10[illegible]E-06	32	8.78413715E-07	33	1.26495873E-06	34	9.00245177E-07	35	1.12350950E-06
36	1.13[illegible]E-06	37	1.40[illegible]E-06	38	9.53564918E-07	39	1.46105445E-06	40	1.68626152E-06
41	1.15[illegible]E-06	42	1.80814770E-06	43	1.86642417E-06	44	2.26374345E-06	45	8.51501198E-07
46	1.3[illegible]E-06	47	7.83371097E-07	48	1.94420523E-06	49	1.53499843E-06	50	3.00153202E-06
51	2.19[illegible]E-06	52	3.31396981E-06	53	1.[illegible]E-05	54	2.33756790E-06	55	2.37040324E-06
56	3.89[illegible]E-06	57	2.83369131E-06	58	2.75123446E-06	59	1.88795877E-06	60	2.32214147E-06
61	2.3[illegible]E-06	62	3.48259610E-06	63	1.81945028E-06	64	1.93361850E-06	65	1.73272003E-06
66	2.35[illegible]E-06	67	2.92045567E-06	68	9.09512566E-07	69	3.68169886E-06	70	2.95790352E-06
71	2.16[illegible]E-06	72	7.47047091E-07	73	1.43393780E-06	74	8.25213085E-07	75	1.41399174E-06
76	1.49[illegible]E-06	77	9.71183938E-07	78	2.74104350E-06	79	3.09744023E-06	80	1.25031765E-06

IRAN VALUE TO BE USED FOR FURTHER CALCULATIONS 21372889
NORMALIZED PRESSURE VALUES IN THE NONDIMENSIONAL FORM

1	7.20[illegible]E-12	2	2.65419861E-09	3	9.58393962E-09	4	2.00542533E-08	5	3.28775348E-08
6	4.91[illegible]E-08	7	4.43296070E-08	8	5.95319264E-08	9	4.85224501E-08	10	7.35035187E-08
11	7.01[illegible]E-08	12	1.25341120E-07	13	7.01659758E-08	14	1.27971646E-07	15	2.42149301E-07
16	2.46[illegible]E-07	17	3.28879744E-07	18	4.55374777E-07	19	3.79856395E-07	20	6.02985336E-07

21	6.36[illegible]E-07	22	6.07301446E-07	23	6.56928686E-07	24	5.76918633E-07	25	9.94780560E-07
26	8.42[illegible]E-07	27	9.92030562E-07	28	6.39080057E-07	29	7.15235288E-07	30	1.10771097E-06
31	1.50[illegible]E-06	32	1.15540360E-06	33	9.62543952E-07	34	9.59839076E-07	35	1.83631660E-06
36	1.40[illegible]E-06	37	9.83212421E-07	38	7.55496288E-07	39	2.22898794E-06	40	8.79724748E-07
41	1.81[illegible]E-06	42	1.78537767E-06	43	2.54298835E-06	44	1.60254652E-06	45	2.42231297E-06
46	1.33[illegible]E-06	47	9.95047031E-07	48	2.66851377E-06	49	1.55706873E-06	50	2.40237606E-06
51	2.26[illegible]E-06	52	1.33153718E-06	53	1.45983302E-06	54	2.62597434E-06	55	1.99434825E-06
56	1.57[illegible]E-06	57	2.75491365E-06	58	2.04974042E-06	59	1.90492261E-06	60	3.78616325E-06
61	1.37[illegible]E-06	62	2.53689514E-06	63	1.97363978E-06	64	2.77089150E-06	65	2.98309619E-06
66	1.64[illegible]E-06	67	-6.53916670E-06	68	1.31530520E-06	69	2.91635263E-06	70	1.09270221E-06
71	2.40[illegible]E-06	72	1.28469224E-06	73	1.14799409E-06	74	1.17614640E-06	75	2.53342950E-06
76	1.46[illegible]E-06	77	1.62518259E-06	78	3.15997324E-06	79	3.39667669E-06	80	-7.65215490E-07

IRAN VALUE TO BE USED FOR FURTHER CALCULATIONS 37308441

NORMALIZED PRESSURE VALUES IN THE NONDIMENSIONAL FORM

1	8.92[illegible]E-11	2	3.04495561E-09	3	1.47032993E-08	4	1.34911221E-08	5	2.04298943E-08
6	3.24[illegible]E-08	7	2.98113272E-08	8	5.33369886E-08	9	4.44631930E-08	10	7.96412726E-08
11	4.00[illegible]E-08	12	1.59257334E-07	13	8.29871682E-08	14	7.82840294E-08	15	2.02474142E-07
16	2.62[illegible]E-07	17	1.59714193E-07	18	4.49261447E-07	19	4.24507839E-07	20	2.74507358E-07
21	5.50[illegible]E-07	22	8.60035101E-07	23	7.87201969E-07	24	5.34669454E-07	25	5.99285761E-07
26	6.10[illegible]E-07	27	8.40863276E-07	28	6.28360597E-07	29	1.02800357E-06	30	1.26386899E-06
31	1.02[illegible]E-06	32	1.16307964E-06	33	7.74387575E-07	34	1.10018323E-06	35	1.39932635E-06
36	1.46[illegible]E-06	37	1.46116575E-06	38	1.19927423E-06	39	1.52677716E-06	40	1.07244391E-06
41	1.13[illegible]E-06	42	1.07392020E-06	43	9.40248539E-07	44	1.75642607E-06	45	1.10935431E-06
46	1.57[illegible]E-06	47	1.97379472E-06	48	1.26327214E-06	49	2.15000412E-06	50	2.27383535E-06
51	1.81[illegible]E-06	52	1.18259935E-06	53	3.35557861E-06	54	2.67230335E-06	55	1.18522344E-06
56	7.33[illegible]E-07	57	2.27670486E-06	58	2.40358088E-06	59	2.04173879E-06	60	2.78387248E-06
61	2.92[illegible]E-06	62	8.17086996E-07	63	2.16761496E-06	64	2.50481099E-06	65	2.39878114E-06
66	2.23[illegible]E-06	67	1.24415041E-06	68	2.15610565E-06	69	1.67761664E-06	70	5.78713320E-07
71	1.70[illegible]E-06	72	1.42365707E-06	73	1.14739729E-06	74	2.06990951E-06	75	1.36852699E-06
76	1.13[illegible]E-06	77	1.52980602E-06	78	2.17081068E-06	79	1.28835241E-06	80	8.34470341E-07

IRAN VALUE TO BE USED FOR FURTHER CALCULATIONS 42623145

NORMALIZED PRESSURE VALUES IN THE NONDIMENSIONAL FORM

1	3.32[illegible]E-10	2	3.45700739E-09	3	8.04567918E-09	4	2.14078492E-08	5	3.26185410E-08
6	3.27[illegible]E-08	7	5.03288373E-08	8	5.77498593E-08	9	2.68139721E-08	10	7.00262150E-08
11	6.87[illegible]E-08	12	7.72469420E-08	13	1.41975267E-07	14	1.49813432E-07	15	1.75791906E-07
16	2.36[illegible]E-07	17	2.20685258E-07	18	6.25785467E-07	19	6.38729015E-07	20	4.98151239E-07
21	5.79[illegible]E-07	22	5.87455717E-07	23	5.90989361E-07	24	9.67148151E-07	25	5.67602903E-07
26	6.46[illegible]E-07	27	9.14416683E-07	28	6.36836436E-07	29	1.50642951E-06	30	1.04921632E-06
31	1.17[illegible]E-06	32	1.34101701E-06	33	1.00884855E-06	34	9.16850741E-07	35	1.46709194E-06
36	9.18[illegible]E-07	37	1.04214703E-06	38	1.43680495E-06	39	1.18271405E-06	40	9.16884031E-07
41	2.12[illegible]E-06	42	1.42926122E-06	43	1.14730557E-06	44	1.75458634E-06	45	1.29261025E-06
46	1.14[illegible]E-06	47	1.11851262E-06	48	1.95720236E-06	49	2.32047696E-06	50	2.00603880E-06
51	2.64[illegible]E-06	52	2.38774631E-06	53	3.44678460E-06	54	2.50099780E-06	55	2.35790983E-06
56	1.80[illegible]E-06	57	1.93134606E-06	58	2.25470097E-06	59	2.25928797E-06	60	1.83092253E-06
61	1.70[illegible]E-06	62	5.42068417E-07	63	2.00492548E-06	64	3.52214915E-06	65	3.19713742E-06
66	9.04[illegible]E-07	67	2.46347630E-07	68	4.86268472E-07	69	2.08464124E-06	70	1.51871392E-06
71	1.69[illegible]E-06	72	-2.23860212E-07	73	2.24277574E-06	74	-3.71913370E-07	75	2.69257079E-06
76	1.60[illegible]E-06	77	1.34590342E-06	78	2.18050081E-06	79	1.59553658E-06	80	1.23782544E-07

IRAN VALUE TO BE USED FOR FURTHER CALCULATIONS 61929849

NORMALIZED PRESSURE VALUES IN THE NONDIMENSIONAL FORM

1	2.73[illegible]E-10	2	5.18726125E-09	3	7.35893576E-09	4	1.38959236E-08	5	2.80243272E-08
6	4.32[illegible]E-08	7	3.64300985E-08	8	4.83508269E-08	9	6.29392085E-08	10	7.91178935E-08
11	4.88[illegible]E-08	12	6.28673576E-08	13	8.35514430E-08	14	1.93679798E-07	15	2.58258895E-07
16	1.91[illegible]E-07	17	4.56434815E-07	18	4.62993327E-07	19	4.12667411E-07	20	6.55680299E-07
21	6.29[illegible]E-07	22	9.47919608E-07	23	7.34303568E-07	24	7.26168178E-07	25	1.04136208E-06
26	8.23[illegible]E-07	27	8.86339617E-07	28	9.18236005E-07	29	9.59202622E-07	30	9.62341395E-07
31	8.28[illegible]E-07	32	1.31826627E-06	33	1.51009277E-06	34	1.05035752E-06	35	1.53787265E-06
36	1.45[illegible]E-06	37	1.54492224E-06	38	1.38203786E-06	39	1.54786982E-06	40	1.76182617E-06
41	2.14[illegible]E-06	42	1.39811269E-06	43	1.27113716E-06	44	9.42681259E-07	45	9.66176964E-07
46	2.39[illegible]E-06	47	1.92231084E-06	48	2.09173606E-06	49	1.47620099E-06	50	2.40885316E-06
51	2.69[illegible]E-06	52	3.29266697E-06	53	1.75460338E-06	54	3.54406082E-06	55	1.55827696E-06
56	1.23[illegible]E-06	57	2.17212502E-06	58	1.49478530E-06	59	2.31163832E-06	60	4.20977893E-06
61	1.37[illegible]E-06	62	2.15579955E-06	63	2.62854235E-06	64	3.07425503E-06	65	2.67828818E-06
66	8.29[illegible]E-07	67	3.26255150E-06	68	1.21784162E-06	69	1.73271097E-06	70	1.67172895E-06
71	-1.57[illegible]E-07	72	1.19981686E-06	73	3.06263303E-06	74	1.28983853E-06	75	-1.25812135E-06
76	1.61[illegible]E-06	77	1.75595530E-06	78	6.47702997E-08	79	1.62661520E-06	80	6.73240078E-07

IRAN VALUE TO BE USED FOR FURTHER CALCULATIONS 34272433

NORMALIZED PRESSURE VALUES IN THE NONDIMENSIONAL FORM

1	1.2481[illegible]E-10	2	2.61237076E-09	3	8.25925861E-09	4	1.33294240E-08	5	3.44471622E-08
6	3.19472121E-08	7	6.41592467E-08	8	5.72070870E-08	9	5.40291008E-08	10	5.70395898E-08
11	2.5499873[illegible]E-08	12	8.91056884E-08	13	1.00062376E-07	14	1.72311378E-07	15	2.20650911E-07
16	1.9372327[illegible]E-07	17	3.49064470E-07	18	3.06219165E-07	19	6.19663946E-07	20	3.51865150E-07
21	6.42117[illegible]E-07	22	6.87489044E-07	23	6.92759677E-07	24	5.59731244E-07	25	8.22063254E-07
26	1.0417[illegible]E-06	27	9.52079021E-07	28	1.05564924E-06	29	9.61164647E-07	30	9.86433529E-07
31	1.0[illegible]E-06	32	1.29976250E-06	33	9.47438251E-07	34	1.11972543E-06	35	1.39391490E-06
36	3.60[illegible]E-07	37	1.04179237E-06	38	1.34552390E-06	39	8.73291260E-07	40	1.34382997E-06
41	9.91125[illegible]E-07	42	1.75481214E-06	43	9.21975457E-07	44	1.81354061E-06	45	1.73690690E-06
46	1.83[illegible]E-06	47	1.28658391E-06	48	2.70287089E-06	49	2.52148798E-06	50	2.01529907E-06
51	1.76[illegible]E-06	52	2.11397780E-06	53	2.62278350E-06	54	2.91465267E-06	55	1.59038324E-06
56	2.10[illegible]E-06	57	2.66036484E-06	58	1.65584377E-06	59	2.73663012E-07	60	2.65618099E-06
61	1.9157[illegible]E-06	62	1.88797302E-06	63	1.29118695E-06	64	1.70609269E-06	65	2.67222968E-06
66	8.2319[illegible]E-07	67	1.46286186E-06	68	7.87694596E-07	69	1.17188230E-06	70	1.50975525E-06
71	6.0507[illegible]E-07	72	2.36365431E-06	73	1.86531936E-06	74	2.01747252E-06	75	8.21702365E-07
76	1.612[illegible]E-06	77	6.03405802E-06	78	1.78138324E-06	79	7.67138827E-07	80	1.96610588E-06

IRAN VALUE TO BE USED FOR FURTHER CALCULATIONS 24626161

NORMALIZED PRESSURE VALUES IN THE NONDIMENSIONAL FORM

1	8.85131325E-11	2	5.47301196E-09	3	7.53893677E-09	4	1.13216288E-08	5	2.40986354E-08
6	2.06[illegible]E-08	7	3.29444690E-08	8	6.45090901E-08	9	7.30881749E-08	10	6.92512087E-08
11	7.96[illegible]E-08	12	7.11257865E-08	13	1.16426814E-07	14	1.21839545E-07	15	2.26477519E-07
16	2.23[illegible]E-07	17	2.72067979E-07	18	3.25037709E-07	19	5.28504994E-07	20	4.54059048E-07
21	7.16[illegible]E-07	22	6.47914591E-07	23	5.27834292E-07	24	7.80277585E-07	25	8.38249556E-07
26	7.70[illegible]E-07	27	6.65226759E-07	28	8.05519024E-07	29	1.32363697E-06	30	6.94156687E-07
31	1.03[illegible]E-06	32	9.92694546E-07	33	1.17271641E-06	34	9.99572266E-07	35	7.94979570E-07
36	1.16[illegible]E-06	37	7.33623611E-07	38	8.10240867E-07	39	1.75255313E-06	40	7.35546533E-07
41	9.58[illegible]E-07	42	1.58136386E-06	43	1.70155569E-06	44	1.73360827E-06	45	1.68145622E-06
46	2.23[illegible]E-06	47	1.63877090E-06	48	1.19744021E-06	49	1.33473090E-06	50	1.70610794E-06
51	1.93[illegible]E-06	52	2.51637756E-06	53	1.89752168E-06	54	2.06580163E-06	55	2.03995575E-06
56	1.42[illegible]E-06	57	6.72717589E-07	58	1.64414167E-06	59	1.66004500E-06	60	2.27043763E-06
61	2.29[illegible]E-06	62	8.80208102E-07	63	2.44157872E-07	64	2.19715225E-06	65	1.72206708E-06
66	1.65[illegible]E-06	67	2.65277460E-06	68	-1.00286437E-06	69	2.21248857E-06	70	2.74520558E-06
71	2.49[illegible]E-06	72	1.87718385E-06	73	4.02824133E-06	74	2.25106299E-06	75	-7.62238881E-07
76	1.35[illegible]E-06	77	-3.77117405E-07	78	5.01918923E-07	79	4.69474278E-07	80	6.73365161E-07

IRAN VALUE TO BE USED FOR FURTHER CALCULATIONS 3585993

NORMALIZED PRESSURE VALUES IN THE NONDIMENSIONAL FORM

1	4.22971337E-10	2	5.16398816E-09	3	9.02359866E-09	4	1.49017295E-08	5	3.83058205E-08
6	3.41237[illegible]E-08	7	6.76024497E-08	8	5.31925260E-08	9	2.99845816E-08	10	6.07829919E-08
11	7.56[illegible]E-08	12	1.14202414E-07	13	1.00878890E-07	14	1.46917863E-07	15	2.04112341E-07
16	2.89[illegible]E-07	17	2.05242543E-07	18	4.63951396E-07	19	2.99489247E-07	20	4.77462110E-07
21	5.41[illegible]E-07	22	7.74179165E-07	23	1.00672163E-06	24	6.57100004E-07	25	5.76798232E-07
26	7.40[illegible]E-07	27	1.03830357E-06	28	1.22946487E-06	29	1.00122906E-06	30	1.14766363E-06
31	1.49417476E-06	32	8.75697940E-07	33	1.09861525E-06	34	1.42593406E-06	35	1.51987123E-06
36	1.30[illegible]E-06	37	1.11999185E-06	38	1.23223372E-06	39	1.77703463E-06	40	1.88613247E-06
41	1.76[illegible]E-06	42	1.10783261E-06	43	1.41340607E-06	44	1.96142356E-06	45	1.28733677E-06
46	2.22[illegible]E-06	47	2.03851508E-06	48	1.55520232E-06	49	2.72490111E-06	50	1.58760788E-06
51	2.54[illegible]E-06	52	2.47740833E-06	53	1.92575146E-06	54	2.39859893E-06	55	2.12712766E-06
56	1.85[illegible]E-06	57	2.31541533E-06	58	2.36063727E-06	59	1.43727491E-06	60	1.69367568E-06
61	1.38[illegible]E-06	62	2.57914643E-06	63	7.62579915E-07	64	9.08203111E-07	65	2.26441984E-06
66	2.00[illegible]E-06	67	1.68212273E-06	68	2.73562990E-06	69	3.33003073E-07	70	6.18147289E-07
71	4.73[illegible]E-07	72	1.35562449E-06	73	9.60668323E-07	74	1.52095935E-06	75	9.46307079E-07
76	-1.64[illegible]E-06	77	3.67947255E-07	78	2.15032634E-06	79	-7.43005568E-08	80	-3.13552178E-07

IRAN VALUE TO BE USED FOR FURTHER CALCULATIONS 8312929

NORMALIZED PRESSURE VALUES IN THE NONDIMENSIONAL FORM

1	9.65[illegible]E-11	2	6.42955720E-09	3	4.64081257E-09	4	2.71577069E-08	5	2.76445437E-08
6	3.00[illegible]E-08	7	3.20640477E-08	8	2.86969895E-08	9	3.58537086E-08	10	5.25335059E-08
11	7.43[illegible]E-08	12	7.53758137E-08	13	7.08256473E-08	14	1.09304002E-07	15	1.38873211E-07
16	3.35[illegible]E-07	17	2.93028502E-07	18	4.80517505E-07	19	3.03947727E-07	20	4.91262505E-07
21	5.62[illegible]E-07	22	5.15112711E-07	23	8.32559037E-07	24	6.91452294E-07	25	9.10955386E-07
26	7.90[illegible]E-07	27	9.78596322E-07	28	1.10350187E-06	29	6.73627795E-07	30	1.03381992E-06
31	7.19[illegible]E-07	32	1.05952826E-06	33	1.46222081E-06	34	8.73549770E-07	35	1.11101275E-06
36	1.16[illegible]E-06	37	6.26247022E-07	38	1.23731246E-06	39	1.30801487E-06	40	1.34364861E-06
41	6.30[illegible]E-07	42	1.70308490E-06	43	1.21412327E-06	44	1.07084201E-06	45	1.05605548E-06
46	1.49[illegible]E-06	47	2.11807611E-06	48	1.31910692E-06	49	1.96802242E-06	50	1.88291327E-06

51	1.7349[illegible]E-06	52	2.09464316E-06	53	2.30144841E-06	54	2.09990538E-06	55	2.07942717E-06
56	2.3362[illegible]E-06	57	1.23075340E-06	58	2.36281098E-06	59	8.41727964E-08	60	1.17251153E-06
61	2.6022[illegible]E-06	62	2.46033516E-06	63	1.74802555E-06	64	1.04921357E-06	65	1.81731041E-06
66	1.0797[illegible]E-06	67	1.65012592E-06	68	1.72517478E-06	69	8.42610392E-07	70	4.41294421E-07
71	3.1234[illegible]E-06	72	2.34108289E-06	73	1.44009303E-06	74	1.15273349E-06	75	1.68579161E-06
76	2.7021[illegible]E-06	77	1.29776868E-07	78	2.22192841E-07	79	2.87188038E-07	80	-2.72736936E-07

IRAN VALUE TO BE USED FOR FURTHER CALCULATIONS 1433345

VARIANCE AND DEVIATION ANALYSIS

TIME INDEX	MEAN	VARIANCE	DEVIATION	(MEAN)+(DEVIATION)	(MEAN)-(DEVIATION)
1	1.91172391E-10	2.66050199E-20	1.63110453E-10	3.54282844E-10	2.80619375E-11
2	4.00327734E-09	1.78606336E-18	1.33643662E-09	5.34971416E-09	2.67284053E-09
3	9.73194322E-09	1.09853506E-17	3.31441558E-09	1.31063588E-08	6.47752765E-09
4	1.66314123E-08	2.09846739E-17	4.58092501E-09	2.12623373E-08	1.21004873E-08
5	3.12670514E-08	3.82074237E-17	6.18121539E-09	3.74482768E-08	2.50858460E-08
6	5.46178475E-08	5.98073295E-17	7.73534795E-09	4.19531955E-08	2.72824996E-08
7	4.49013711E-08	1.55786826E-16	1.24814594E-08	5.70425304E-08	3.20796117E-08
8	5.33713441E-08	9.22805994E-17	9.60627917E-09	6.23776232E-08	4.37650649E-08
9	4.64991333E-08	1.92160625E-16	1.38622013E-08	6.03213396E-08	3.25969370E-08
10	7.22136028E-08	4.26153210E-16	2.06434786E-08	9.28498406E-08	5.15628833E-08
11	6.19035128E-08	4.51137456E-16	2.12399966E-08	8.32235094E-08	4.07435162E-08
12	9.05776518E-08	9.46966249E-16	3.07728167E-08	1.21350669E-07	5.98050351E-08
13	9.44161172E-08	4.99041533E-16	2.23392375E-08	1.16755355E-07	7.20768797E-08
14	1.38099368E-07	1.59729674E-15	3.99601949E-08	1.78865283E-07	9.69328931E-08
15	1.99169137E-07	1.73341245E-15	4.16342701E-08	2.36799457E-07	1.53530916E-07
16	2.3078999[illegible]E-07	2.62186043E-15	5.12035978E-08	2.87973541E-07	1.85566345E-07
17	3.00230430E-07	7.39136218E-15	8.59730317E-08	3.86203521E-07	2.14257458E-07
18	4.55720308E-07	6.36619919E-15	7.99136984E-08	5.35642084E-07	3.75014668E-07
19	4.60400438E-07	1.31485021E-14	1.14663918E-07	5.81073356E-07	3.51739520E-07
20	5.04397649E-07	1.49659404E-14	1.22335360E-07	6.26733009E-07	3.82062289E-07
21	5.8c516123E-07	7.39756910E-15	8.60091222E-08	6.68525243E-07	4.96506998E-07
22	6.61435569E-07	1.00967798E-14	1.00492685E-07	7.62428275E-07	5.61442904E-07
23	7.[illegible]02894E-07	2.44802602E-14	1.56461689E-07	8.65344583E-07	5.52421204E-07
24	7.[illegible]24E-07	1.77379529E-14	1.33183906E-07	8.4879o325E-07	5.62428512E-07
25	8.61421967E-07	4.33615306E-14	2.08234316E-07	1.00965630E-06	5.93187670E-07
26	8.61019675E-07	1.59093609E-14	1.26449045E-07	9.27468720E-07	6.74570630E-07
27	8.69361537E-07	2.34254755E-14	1.53053832E-07	1.02211537E-06	7.16007705E-07
28	9.12527618E-07	5.33057248E-14	2.30880326E-07	1.14350794E-06	6.81747293E-07
29	9.98131106E-07	6.13867902E-14	2.47763577E-07	1.23594468E-06	7.40417528E-07
30	1.09[illegible]E-06	2.58747216E-14	1.60859214E-07	1.21481436E-06	8.93101933E-07
31	1.09o519[illegible]E-06	7.83763835E-14	2.79957824E-07	1.37647665E-06	8.16561197E-07
32	1.10358237E-06	2.87065845E-14	1.69430176E-07	1.27301255E-06	9.34152195E-07
33	1.12937402E-06	4.68061469E-14	2.16333416E-07	1.34570744E-06	9.13040608E-07
34	1.09781143E-06	2.63130201E-14	1.62212835E-07	1.22002432E-06	8.95598546E-07
35	1.24o6o275E-06	1.00791837E-13	3.17477301E-07	1.61354005E-06	9.78585452E-07
36	1.17660836E-06	1.03691933E-13	3.22012316E-07	1.49970066E-06	8.55676044E-07
37	1.08193419E-06	8.53111510E-14	2.92080693E-07	1.37401488E-06	7.89853496E-07
38	1.1o4943[illegible]E-06	5.83743457E-14	2.24442299E-07	1.37938561E-06	9.30501009E-07
39	1.47958873E-06	1.33394723E-13	3.65232431E-07	1.84482116E-06	1.11435630E-06
40	1.35245506E-06	1.73404839E-13	4.16419066E-07	1.76887412E-06	9.36035990E-07
41	1.39[illegible]E-06	2.57330345E-13	5.07277424E-07	1.90679204E-06	8.92237793E-07
42	1.5[illegible]E-06	6.72225427E-14	2.59273104E-07	1.79463448E-06	1.27608828E-06
43	1.49254027E-06	2.15363217E-13	4.64072426E-07	1.91661270E-06	9.88467847E-07
44	1.65[illegible]E-06	1.36849163E-13	3.69931295E-07	2.02189128E-06	1.28202870E-06
45	1.[illegible]E-06	1.95018944E-13	4.41809493E-07	1.82284590E-06	9.39626916E-07
46	1.6532590d[illegible]E-06	1.78126863E-13	4.22050783E-07	2.11530986E-06	1.27120830E-06
47	1.5[illegible]E-06	2.19193762E-13	4.68181335E-07	2.02289862E-06	1.08653595E-06
48	1.[illegible]E-06	2.80852880E-13	5.29955545E-07	2.43186605E-06	1.37195496E-06
49	1.94263397E-06	2.01695476E-13	4.49105195E-07	2.39173616E-06	1.49352577E-06
50	2.42[illegible]E-06	2.54771750E-13	5.04749196E-07	2.53091517E-06	1.52141678E-06
51	2.022[illegible]E-06	3.02286262E-13	5.49805658E-07	2.57187613E-06	1.47226482E-06
52	2.3[illegible]E-06	4.70799026E-13	6.86147962E-07	3.04941120E-06	1.67711528E-06
53	2.2[illegible]E-06	4.30495615E-13	6.56091316E-07	2.91364914E-06	1.60146651E-06
54	2.60[illegible]	[illegible]	[illegible]	3.01418569E-06	2.18687692E-06

55	2.[illegible]E-06	1.83152908E-13	4.27963676E-07	2.42970390E-06	1.57377615E-06
56	2.[illegible]E-06	8.51575800E-13	9.22808648E-07	2.97042048E-06	1.12480311E-06
57	1.93[illegible]E-06	4.01721927E-13	6.33815373E-07	2.56902102E-06	1.30139028E-06
58	2.13[illegible]E-06	1.52051704E-13	3.89938077E-07	2.52645310E-06	1.74657694E-06
59	1.00[illegible]E-06	6.71001077E-13	8.19146554E-07	2.48139107E-06	8.43097966E-07
60	2.34[illegible]E-06	1.25910165E-12	1.12209699E-06	3.51864296E-06	1.27449698E-06
61	1.5[illegible]E-06	1.61837083E-13	4.02289800E-07	2.33266152E-06	1.49808192E-06
62	1.56[illegible]E-06	8.06051011E-13	8.97803437E-07	2.87638347E-06	1.08277659E-06
63	1.68[illegible]E-06	4.72190578E-13	6.87161246E-07	2.37527260E-06	1.00095011E-06
64	2.40[illegible]E-06	6.80646248E-13	8.25012878E-07	2.93063649E-06	1.28061073E-06
65	2.24[illegible]E-06	3.91925585E-13	6.26039603E-07	2.80804219E-06	1.61596299E-06
66	1.59[illegible]E-06	3.66185534E-13	6.05132658E-07	2.19609749E-06	9.85832115E-07
67	1.61[illegible]E-06	1.06476769E-12	1.03187581E-06	2.64610051E-06	5.62346893E-07
68	1.24[illegible]E-06	9.92144001E-13	9.96044176E-07	2.23623572E-06	2.44147368E-07
69	1.61[illegible]E-06	8.61240481E-13	9.28030431E-07	2.74376101E-06	8.87700147E-07
70	1.52[illegible]E-06	6.94626700E-13	8.33442679E-07	2.35443838E-06	6.87553019E-07
71	1.73[illegible]E-06	1.03461489E-12	1.01716021E-06	2.75251899E-06	7.18198568E-07
72	1.5[illegible]E-06	8.66188473E-13	9.30692470E-07	2.50296982E-06	6.41584881E-07
73	1.63[illegible]E-06	1.33586946E-12	1.15579819E-06	2.84739976E-06	5.35803376E-07
74	1.21[illegible]E-06	6.13667440E-13	7.83369287E-07	2.00242526E-06	4.35686681E-07
75	1.12[illegible]E-06	1.47911929E-12	1.21619048E-06	2.33813616E-06	-9.42428087E-08
76	1.33[illegible]E-06	8.31407520E-13	9.11815508E-07	2.24842901E-06	4.24797997E-07
77	1.66[illegible]E-06	5.62454245E-13	7.49969496E-07	1.83457047E-06	3.34631476E-07
78	1.61[illegible]E-06	1.03307199E-12	1.01640149E-06	2.63633506E-06	6.03532075E-07
79	1.3[illegible]E-06	1.22117972E-12	1.10507001E-06	2.41011105E-06	1.99971041E-07
80	4.00[illegible]E-07	5.93098136E-13	7.70128649E-07	1.25869573E-06	-2.81561578E-07

```
  03/23/72   UNIV. OF VIRGINIA SCOPE  3.3 JAN 24,72 SUM 268
10.37.53.MONTE20
10.37.53.MONTE20,M2025M,T2000,CM42000. THANEDAR B
10.37.53. J ALGORITHM                              B
10.37.55.       RUN.
10.38.35.LOD
10.38.39. (REL - 0234301    CP   301.692 SEC.
10.39.08.                   PP   004.404 SEC.
10.38.08.                   IO   000.370 SEC.
10.41.24.STOP
10.41.25.CP     137.943 SEC.
10.41.25.PP     004.606 SEC.
10.41.25.IO     000.427 SEC.

                MONTE20  //// END OF LIST ////  0000595 LINES
```

Appendix 5

RECTANGULAR ROOM PROBLEM NORMAL MODE PROGRAMME

This appendix gives in full details the results of the application of the Normal Mode solution technique (Chapter 6) to a rectangular boundary problem that is under investigation (Chapter 5). Included herein is a complete listing of the programme that was used in these calculations on the CDC 6400 of the Computing Center of the University of Virginia. The printout results accompanying this listing correspond to the pressure values shown in Fig. 56.

```
      PROGRAM NORMAL(INPUT, OUTPUT, TAPE10=INPUT, TAPE11=OUTPUT)
000003      DIMENSION P(80),M(3),ENL(3),KS(3),XR(3)
000003      READ(10,30)SONSP,TPULS,T1,S0,(ENL(I),I=1,3),(XS(I),I=1,3),
           1(XR(I),I=1,3),EPSLN,PI,MEIGN $ AB=0.0 $ NEIGN=(MEIGN-1)*MEIGN**2
000054      WRITE(11,32)SONSP,TPULS,T1,S0,AB,AB,AB,(ENL(I),I=1,3),(XS(I),I=1,
           13),(XR(I),I=1,3),EPSLN,MEIGN,NEIGN $ OMEG=(2.0*PI)/T1
000130      JTPLS=T1/TPULS $ JT=JTPLS+1 $ JT2=2*JTPLS $ ANM= OMEG*S0/(ENL(1)*
           2ENL(2)*ENL(3)*SONSP**2) $ DO 2 J=1,JT2 $ P(J)=0.0
000147    2 CONTINUE $ OMSON=OMEG/SONSP $ OT1=OMEG*T1 $ SAO1=SIN(OT1) $ CAO1=
           1COS(OT1) $ OM2=OMSON**2 $ DO 24 INDX=1,MEIGN $ M(1)=INDX-1 $ DO 24
           2 JNDX=1,MEIGN $ M(2)=JNDX-1 $ DO 24 KNDX=1,MEIGN $ M(3)=KNDX-1
000173      UM2=0. $ ENM=01=1. $ DO 12 K=1,3 $ AM=PI*M(K)/ENL(K) $ SK=AM*XS(K)
000206      IF(M(K).NE.0)ENM=ENM/2 $ UM2=UM2+AM**2
000213      RK=AM*XR(K) $ D1=D1*(COS(SK))*(COS(RK))/ENM
000224   12 CONTINUE $ BM2=OM2-UM2 $ IF(UM2.EQ.0.0) GO TO 24
000232      EPS=ABS(BM2) $ IF(BM2.LT.EPSLN) GO TO 18
          C   NORMAL MODE FREQUENCY CLASSIFICATION
000235   14 BM=SQRT(BM2) $ BMC=BM*SONSP $ OM=OMSON/BM $ DO 15 J=1,JTPLS
000246      T=J*TPULS $ OT=OMEG*T $ SAO=SIN(OT) $ BT=BMC*T $ SAK=SIN(BT)
000260   15 P(J)=P(J)+D1*(SAO/BM2+OM*SAK/UM2) $ DO 16 J=JT,JT2 $ T=J*TPULS
000276      BT=BMC*T $ SAK=SIN(BT)
000302      BTA=BMC*(T-T1) $ SA1=SIN(BTA) $ CA1=COS(BTA)
000311   16 P(J)=P(J)+D1*(SAO1*CA1/BM2+OM*(SAK/UM2+CAO1*SA1/BM2)) $ GO TO 24
000331   18 D1=D1/OM2 $ DO 19 J=1,JTPLS $ T=J*TPULS $ OT=OMEG*T
000337   19 P(J)=P(J)+D1*(OT/2-SIN(OT)) $ D1=D1*1.2 $ DO 24 J=JT,JT2
000355      T=J*TPULS $ OT=OMEG*T $ P(J)=P(J)+D1*(OT/2-SIN(OT))
000371   24 CONTINUE $ DO 26 J=1,JT2 $ P(J)=ANM*P(J)
000406   26 CONTINUE $ WRITE(11,34)(J,P(J),J=1,JT2)
          C   FORMATS
000424   30 FORMAT(14F5.2,F8.5,I2)
000424   32 FORMAT(1H1,30X*TRANSIENT ACOUSTIC FIELD IN RECTANGULAR CAVITY*//
           145X*NORMAL MODE METHOD*//50X*PREASSIGNED CONSTANTS*//7X*SINGLE CYC
           2LE SINUSOIDAL PULSE  ALL WALLS PERFECTLY REFLECTING*//5X*SONSP =*
           3E16.8,2X*TPULS =*E16.8,2X*PULSE PERIOD =*E16.8,2X*PULSE STRENGTH =
           4*E16.8/5X*SPATIAL BOUNDARY WALLS(1,2,3,4,5,6)*/5X,6(E16.8,2X)/
           55X*SORS(1,2,3) =*3(E16.8,2X)/5X*RECR(1,2,3) =*3(E16.8,2X)/
           65X*EPSLN =*E16.8,2X*NEIGN =*I3,2X*NEIGN =*I6)
000424   34 FORMAT(20X*NORMALIZED PRESSURE VALUES IN THE NONDIMENSIONAL FORM*/
           1(5(5X,I2,2X,E16.8)))
000424      STOP
000426      END
```

```
NORMAL

PROGRAM LENGTH INCLUDING I/O BUFFERS
005040

FUNCTION ASSIGNMENTS

STATEMENT ASSIGNMENTS
14      =  000236    18      =  000330    24      =  000371    30      =  000445
32      =  000450    34      =  000525

BLOCK NAMES AND LENGTHS

VARIABLE ASSIGNMENTS
AB      =  000731    AM      =  000755    ANM     =  000737    BM      =  000761
BMG     =  000762    BM2     =  000760    BT      =  000767    BTA     =  000771
CA01    =  000744    CA1     =  000773    D1      =  000753    ENL     =  000718
ENM     =  000752    EPSLN   =  000726    I       =  000725    INDX    =  000746
J       =  000740    JNDX    =  000747    JT      =  000735    JTPLS   =  000734
JT2     =  000736    K       =  000754    KNDX    =  000750    M       =  000705
MEIGN   =  000730    MEIGN   =  000732    OM      =  000763    OMEG    =  000733
OMSQM   =  000741    OM2     =  000745    OT      =  000765    OT1     =  000742
P       =  000565    PI      =  000727    RK      =  000757    SAK     =  000770
SA0     =  000766    SA01    =  000743    SA1     =  000772    SK      =  000756
SQMSP   =  000721    SQ      =  000724    T       =  000764    TPULS   =  000722
T1      =  000723    UM2     =  000751    XR      =  000716    XS      =  000713

START OF CONSTANTS
000430

START OF TEMPORARIES
000540

START OF INDIRECTS
000563

UNUSED COMPILER SPACE
003503
```

```
CORE MAP  16.34.45.  NORMAL                CONTROL                                    000100    012572    000000    000000
   ---TIME---LOAD MODE --L1--L2-----TYPE----------USER---+---CALL----------FWA LOAD--LWA LOAD--BLNK COMM--LENGTH--
   FWA LOADER  035761  FWA TABLES  034141
   -PROGRAM----ADDRESS-                  --LABELED---COMMON--
   NORMAL      000100
   SINCOS      005140
   SORT        005237
   SYSTEM      005302                              SCOPE2     005302
   GETBA       006414
   INPUTC      006433
   KODER       006550
   KRAKER      010022
   OUTPTC      011073
   SIO$        011165
   ----UNSATISFIED EXTERNALS-----                  REFERENCES
```

TRANSIENT ACOUSTIC FIELD IN RECTANGULAR CAVITY

NORMAL MODE METHOD

PREASSIGNED CONSTANTS

SINGLE CYCLE SINUSOIDAL PULSE ALL WALLS PERFECTLY REFLECTING

SONSP = 1.10000000E+03 TPULS = 5.00000000E-03 PULSE PERIOD = 2.00000000E-01 PULSE STRENGTH = 1.00000000E+00

SPATIAL BOUNDARY WALLS(1,2,3,4,5,6)

0. 0. 0. 1.10000000E+02 6.60000000E+01 4.40000000E+01

SORS(1,2,3) = 2.20000000E+01 3.30000000E+01 2.20000000E+01

RESR(1,2,3) = 3.74000000E+01 3.74000000E+01 2.86000000E+01

EPSLN = 1.00000000E-03 MEIGN = 15 NEIGN = 3150

NORMALIZED PRESSURE VALUES IN THE NONDIMENSIONAL FORM

1	-1.10997455E-08	2	-4.83696176E-09	3	1.83493169E-08	4	-2.38841986E-08	5	-8.84355995E-08
6	-1.04664373E-07	7	-1.05871883E-07	8	-1.10455186E-07	9	-9.97832952E-08	10	-6.11416369E-08
11	-1.90697925E-08	12	3.51957281E-08	13	9.85431892E-08	14	1.55194229E-07	15	2.21929757E-07
16	2.73118475E-07	17	3.39505625E-07	18	4.04648067E-07	19	4.49586572E-07	20	4.85232143E-07
21	5.30552378E-07	22	5.85533246E-07	23	6.50086953E-07	24	7.14580052E-07	25	7.67371305E-07
26	8.49784436E-07	27	9.10933549E-07	28	9.59006162E-07	29	9.84345196E-07	30	9.98217465E-07
31	1.00610225E-06	32	1.01724901E-06	33	1.01769206E-06	34	1.00570291E-06	35	1.01113444E-06
36	1.01265343E-06	37	1.02405420E-06	38	1.04096973E-06	39	1.05802823E-06	40	1.05193683E-06
41	1.02295510E-06	42	1.16298058E-06	43	1.13923671E-06	44	1.08133034E-06	45	1.02395285E-06
46	9.85423856E-07	47	9.69764879E-07	48	9.72587089E-07	49	1.00947099E-06	50	1.07606940E-06
51	1.11997116E-06	52	1.16698689E-06	53	1.21545748E-06	54	1.27531121E-06	55	1.36967806E-06
56	1.45934393E-06	57	1.55024971E-06	58	1.62096622E-06	59	1.67708992E-06	60	1.74913746E-06
61	1.85163751E-06	62	1.94579308E-06	63	2.02321867E-06	64	2.10895319E-06	65	2.20087977E-06
66	2.26374297E-06	67	2.30303111E-06	68	2.33365170E-06	69	2.35157390E-06	70	2.37570545E-06
71	2.38416434E-06	72	2.41241506E-06	73	2.45657097E-06	74	2.47580488E-06	75	2.46894539E-06
76	2.41723682E-06	77	2.39592081E-06	78	2.40937144E-06	79	2.42509326E-06	80	2.41705846E-06

```
 03/23/72   UNIV. OF VIRGINIA SCOPE  3.3 JAN 24,72 SUN 288
16.34.30.NORMAA2
16.34.38.NORMAL,42025N,T500,CM42000. THANEDAR B D
16.34.39. AEROSPACE                          B
16.34.38.       RUN.
16.34.43.LGO
16.34.46. (PPL - 012600)    CP  001.048 SEC.
16.34.46.                   PP  005.210 SEC.
16.34.46.                   IO  000.340 SEC.
16.36.59.STOP
16.37.01.CP     116.505 SEC.
16.37.00.PP     005.699 SEC.
16.37.00.IO     000.347 SEC.

          NORMAA2  //// END OF LIST ////  0000221 LINES
```

Appendix 6

MONTE CARLO APPLICATIONS TO ACOUSTICAL FIELDS

A MORE GENERAL PROBLEM

The problem of investigation of the transient acoustical field, due to a monopole sound source, inside a cylindrical duct, considered in Chapter 8 represents a particular case of a more general problem in acoustics. In this appendix is presented an outline of a more general Monte Carlo flow diagram (Fig. A6.1) developed for investigation of an acoustical field inside a nonrectangular boundary, due to a distribution of sound sources. For convenience of discussion, the programme is subdivided under the following five major headings :

I. Input and Initiation

II. Source Routine

III. Ray Tube Initial Specification Routine

IV. Ray Tube Processing Routine

V. Analysis Routine

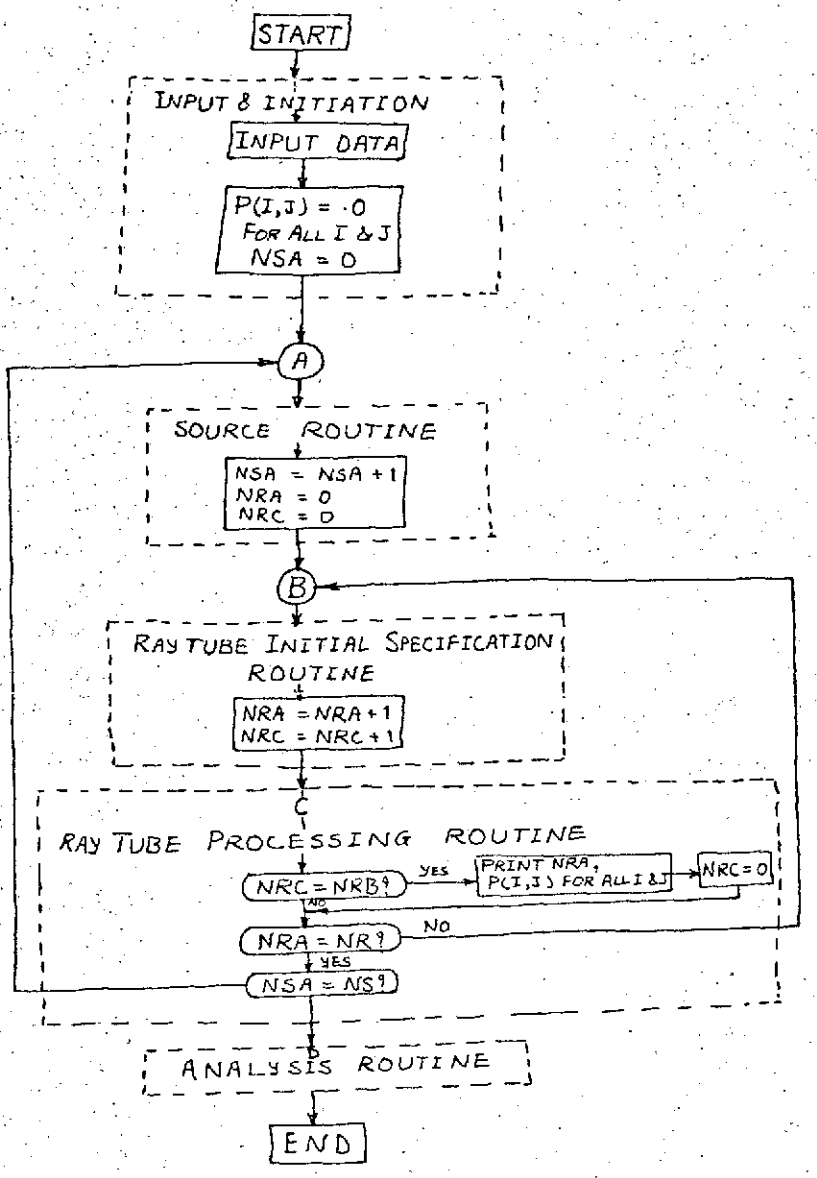

Fig. A6.1 Acoustical Field Inside a Curved Boundary General Monte Carlo Programme

The progressive, step by step, processing in the simulation is presented in the following sections.

INPUT AND INITIATION

The quantities NR, NS, and NRB that appear in Fig. A6.1 require the permanent storage; whilst NSA, NRA, and NRC require the dynamic storage.

In the conceptual, idealized, physical model of a given acoustical system for its appropriate description it becomes essential to consider a certain finite number of different acoustic sources; this number is designated by the quantity NS. As explained in Chapter 7, in the Monte Carlo application, the strength time history of each of these NS sources needs to be replaced by its equivalent finite interval time representation; from which is selected then a set of initial variables for the ray tube. The number of such ray tubes used to represent each of these NS sources, in any particular block of calculations, is given by the quantity NR. At any stage during the process (NSA - 1) is the number of sources already processed, and (NRA - 1) is the number of ray tubes that have been processed for the NSA^{th} source that is currently being processed. The ratio NRA/NR constitutes a sort of estimate of the probabilities, and in order to observe the convergence and the reasonableness, it is sometimes

desirable to initiate the results printout periodically, say after every NRB ray tubes. NRC denotes the number of ray tubes processed after the last printout, and is reset to zero after printout. During the entire problem, it is noticed that, NSA accumulates; whereas NRA accumulates only in a part of the problem corresponding to any particular source. For a particular source, if so desired, the computation may be terminated for that part for any ratio NRA/NR at which the statistical considerations indicate that the accuracy that has been obtained is sufficient enough.

All problems require the use of spatial and directional coordinates. In complicated geometries, for example in cylinders, even if there is a symmetry, as pointed out by Cashwell (1957), it is not worthwhile to use the coordinate system dictated by the symmetry, the reason being that when the ray tube proceeds from one position to another, the directional coordinates change; on the other hand, since the direction cosines remain unaltered under the linear displacements, the Cartesian rectangular coordinate system is preferable. In the analysis presented here the system that is used is the Cartesian rectangular coordinate system; this along with the directional coordinate system is defined as :

Spatial : $X1^*$, $X2^*$, $X3^*$

Directional : DC1, DC2, DC3

Temporal : T^*

Systems encountered in practice involve the variations in geometry and material properties of the enclosing bounding surface. A finite approximation for this would be to subdivide the region into appropriate zones with zonal index given by, say,

$$ZN = 1, 2, 3, \ldots, ZNMX$$

presuming that in each of these zones the properties are very nearly constant. This involves storing the material, and the geometrical properties as functions of spatial vector, say, RVEC, locating the position in the region, as well as the zonal index ZN. Permanent storage then contains the quantities such as

Material Properties : MTL(RVEC, ZN)

Geometrical Properties : GTL(RVEC, ZN) .

In such cases ZN is another parameter that must be added to the list of the ray tube parameters. Summarizing, the parameters for the ray tube are :

Space coordinates	$X1^*$, $X2^*$, $X3^*$
Direction coordinates	DC1, DC2, DC3
Time coordinate	T^*
Weight	Q^*
Zonal index	ZN .

In addition to the material and geometrical properties of the bounding surface, the quantities that require a permanent storage with specific memory location in

the machine are the positions of the receiving points, i.e. the points at which the acoustical field is to be determined, and the specification of the sources.

SOURCE ROUTINE

The machine is led from the start of the problem to the point A in Fig. A6.1; it is here that the proper assignment of the point source parameters takes place. After having finished the processing of a source, the machine returns to this position for assignment of a new source.

In the statistical model, representing the given acoustical system, the generation of sound is considered to be an effect of certain distributed point sources. This, in general would be a constitution of surface, as well as volume distributed sources, the locations of these being the points of singularities in the field.

It is possible to specify, in some practical applications, the exact number of the total point sources with their locations, origin times, strength time histories, and directional properties; then these are stored in the permanent storage of the machine as :

$$SORS(NSA) \equiv SORS(XS1, XS2, XS3, TS, DL(N))$$

$$\text{for } NSA = 1, 2, 3, \ldots, NS$$

where (XS1,XS2,XS3) are the three rectangular Cartesian coordinates, dimension length, of the source

position

TS is the time of origin, in seconds, of the source

N is the integral index calling a specific directional law DL(N) from the permanent storage .

In another important class of problems it is possible to specify the source distribution function. In the statistical model, the continuous variation is to be replaced by its equivalent finite approximation; in general, this will call for subdivision of the region containing the energy sources into source zones

SZN(I) = 1, 2, 3, ...

To each of these is associated an appropriate weighting function

SWF(N) , N = 1, 2, 3, ...

Now each source zone is a collection of the point sources, the number of these sources being directly proportional to the weighting function of that particular source zone, having identical strength time histories, and the directional properties characterized by a specific directional law DL(N). The selection is to be made at random, until from all of these source zones, the sources forming the totality NS are duly processed. A method to achieve this is to generate a random number, and to use the Rejection Technique. The source selection is exemplified by a few special cases of interest.

Volume Distributed Uniform Source

Let the interval of the three Cartesian rectangular coordinates representing a region in which the sources are distributed uniformly be given by

$$XA(I) \leq X(I) \leq XB(I) \quad \text{for} \quad I = 1,2,3 \qquad (1)$$

Let $f(x)$ be a probability density function (pdf), and $\mathbb{R}$ be a uniformly distributed random number over the interval $[0,1]$ (see Eq. 12, Chapter 3); then

$$\int_{XA}^{XB} f(x)\,dx = 1; \quad f(x)\,dx = dx / (XB - XA)$$

$$\mathbb{R} = F(X) = \int_{XA}^{X} f(x)\,dx = (X - XA) / (XB - XA)$$

Hence $$X = XA + \mathbb{R}(XB - XA) \qquad (2)$$

This relation determines the variable X as a function of the random number $\mathbb{R}$, and thus results in a selection routine as shown in Fig. A6.2.

Surface Distributed Uniform Source

For definiteness consider the surface

$$X3 = \text{constant}$$

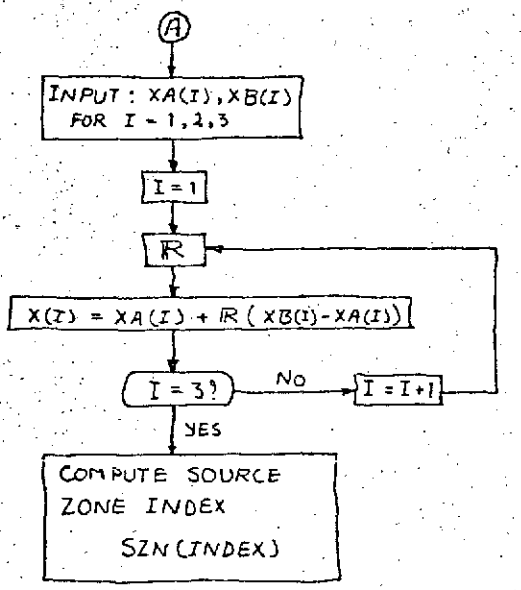

Fig. A6.2 Selection Routine for a Volume Distributed Uniform Source in an Interval $XA(I) \leq X(I) \leq XB(I)$, $(I = 1,2,3)$

to be the surface on which in an annulus of radii R0, and R1 (R0 < R1) the sources are distributed uniformly; here the object is to determine the source position inside this given annular region. In this case since the pdf can be expressed as

$$f(r)\,dr = 2\pi\, r\, dr / \pi(R1^2 - R0^2)$$

$$\mathbb{R} = F(R) = \int_{R0}^{R} f(r)\,dr = (R^2 - R0^2) / (R1^2 - R0^2)$$

Hence $$R = \{ R0^2 + \mathbb{R}\,(R1^2 - R0^2) \}^{\frac{1}{2}} \qquad (3)$$

This determines the radius R. In order to determine the polar angle ϕ use is made of another random number $\mathbb{R}$, the pdf here being

$$f(\phi)\,d\phi = d\phi / 2\pi$$

$$\mathbb{R} = \int_{-\pi}^{\phi} f(x)\,dx = (\phi + \pi) / 2\pi$$

Therefore $$\phi = \pi(2\,\mathbb{R} - 1) \qquad (4)$$

Equations 3 and 4 together form the required set of relations for the selection routine shown in Fig. A6.3.

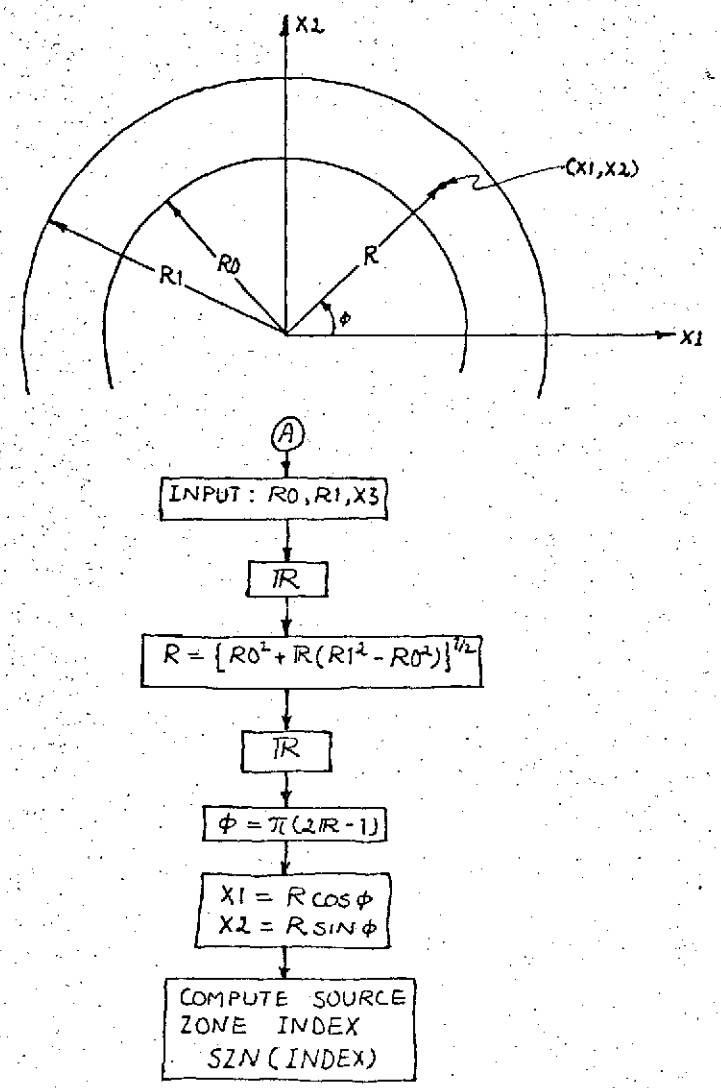

Fig. A6.3 Selection Routine for a Surface Distributed Uniform Source on an Annulus of Radii R0 and R1

RAY TUBE INITIAL SPECIFICATION ROUTINE

In the source routine the source position and its directional properties are specified for a particular value of the source index NSA by designating

$$SORS(NSA) \equiv SORS(XS1, XS2, XS3, TS, DL(N)) \qquad (5)$$

Now the machine is led from position A to position B in Fig. A6.1. It is here the proper assignment of the ray tube parameters takes place. After having finished the processing of a ray tube, the machine returns to this point B for assignment of a new ray tube.

From the permanent storage the quantities that need to be activated here are the directional law DL(N), and the set of elementary pulses

$$EP(NSA, I) \equiv EP(NSA, T(I), \dot{Q}(I)) \qquad (6)$$

where $T(I) = (I - \frac{1}{2})\,\Delta T$ for $I = 1$ to $2 n_p$

ΔT is the elemental time length such that the product of ΔT and $2 n_p$ gives the total activation period of the source given by Eq. 5 above.

From this set of elementary pulses, representing the strength time history of the source SORS(NSA), a random selection is

made of one, say EP(NSA, I), its strength being Q(I), and its time of origin being

$$TI = TS + T(I) \qquad (7)$$

At this time of origin this selected pulse emits disturbances in the medium in accordance with the directional law DL(N). These disturbances are to be represented by the ray tubes, and followed through along their trajectories. In order to accomplish thisit is essential to assign the initial direction coordinates DC1, DC2, DC3 to the ray tube at the position of the source, where it originates. A few of the directional laws of practical interest are considered below with the corresponding direction selection subroutines.

Isotropic Directional Law DL(1)

This is applicable to a point source which is not on or near to a solid boundary. Then the emission is isotropic in all directions. In such a case, the selection of the direction coordinates can be viewed as the selection of a random point on a unit sphere (Fig. A6.4) defined by

$$DC1^2 + DC2^2 + DC3^2 = 1 \qquad (8)$$

From Fig. A6.4 it is observed that

$$DC3 = \cos\theta$$

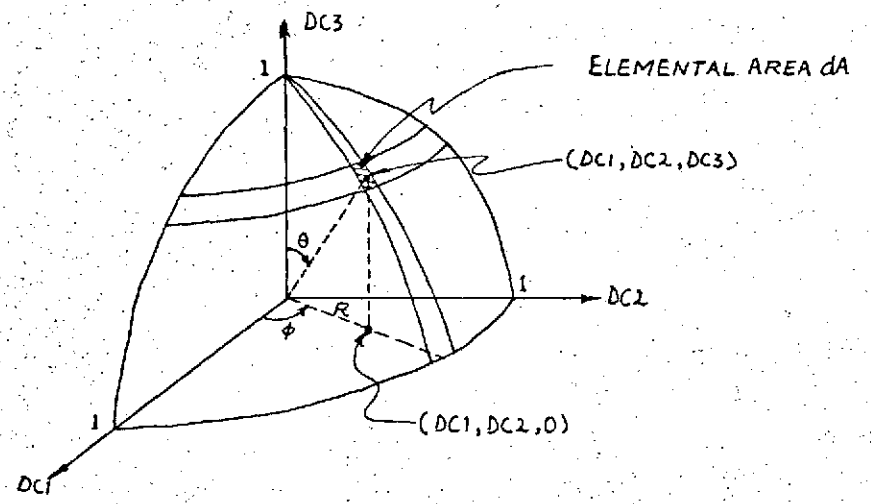

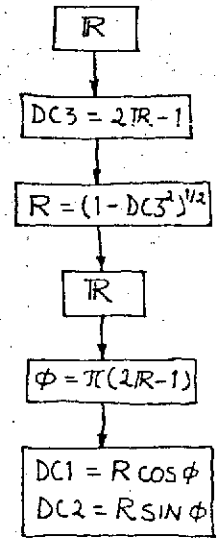

Fig. A6.4 Selection Routine for Isotropic Directional Law DL(1)

and the elemental area dA on the spherical surface is given by

$$dA = \sin\theta \; d\theta \; d\phi = dDC3 \; d\phi$$

Let f(DC3) be the pdf, and $\mathbb{R}$ be, as before, a uniformly distributed random number over the interval [0,1] ; then since

$$f(DC3)\, dDC3 = 2 \sin\theta \; d\theta \,/\, 4\pi = \tfrac{1}{2}\, dDC3$$

$$\mathbb{R} = F(DC3) = \int_{-1}^{DC3} f(x)\, dx = \tfrac{1}{2}\,(DC3 + 1)$$

Hence $$DC3 = 2\mathbb{R} - 1 \qquad (9)$$

The remaining two components DC1, and DC2 are then determined by using the equation for the circle (Fig. A6.4) in the DC1-DC2 plane to give

$$R = (DC1^2 + DC2^2)^{\frac{1}{2}} = (1 - DC3^2)^{\frac{1}{2}} \qquad (10)$$

and another random number $\mathbb{R}$ to provide the polar angle ϕ, just similar to that in the case of Fig. A6.3

$$\phi = \pi(2\mathbb{R} - 1) \qquad (11)$$

Then Eqs. 10 and 11 together define

$$DC1 = R \cos\phi , \quad DC2 = R \sin\phi \qquad (12)$$

resulting in a routine shown in Fig. A6.4.

Cosine Distribution Law DL(2)

This refers to a point source emanating from a surface; let the direction of the outer normal, pointing into the medium, to this surface be defined by the direction cosines

$$DC1 = 0, \quad DC2 = 0, \quad DC3 = 1$$

then by definition the cosine distribution has the pdf

$$f(DC3) = 2\,DC3 \qquad \text{with} \quad DC3 \geq 0$$

$$\mathbb{R} = F(DC3) = \int_0^{DC3} f(x)\,dx = DC3^2$$

Hence

$$DC3 = \mathbb{R}^{\frac{1}{2}} \qquad (13)$$

With this restriction, the other direction components DC1, DC2 are chosen by selecting a point on the unit sphere (Fig. A6.4); resulting in a routine shown in Fig. A6.5.

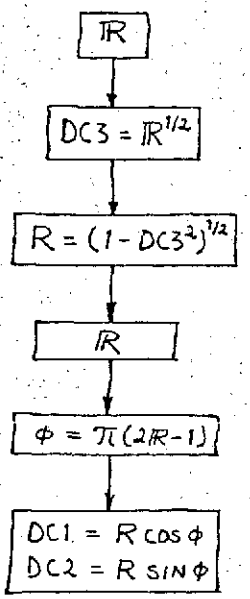

Fig. A6.5 Selection Routine for Cosine Distribution Law DL(2)

General Distribution in the Upper Half Directional Space DL(3)

Occasionally it is necessary to consider a point source with $DC3 \geq 0$ having some experimentally determined distribution of the direction component DC3, supplied in a tabular form. Let

$$DC3(0) = 1 > DC3(1) > \ldots. > DC3(I) = 0 \qquad (14)$$

then defining F(I) to be the probability of DC3 being greater than DC3(I), it can be tabulated as

$$F(0) = 0 < F(1) < \ldots. < F(I) = 1 \qquad (15)$$

With the use of these tables a routine as shown in Fig. A6.6 (Cashwell, 1957) can be constructed, where the method of interpolation is adopted for the determination of the exact value of DC3; the other components DC1, and DC2 are then obtained, as before, by locating a random point on the unit sphere (Figs. A6.5 & A6.4) with the above computed value of DC3.

Prejudiced Directional Law DL(4)

This corresponds to a prejudiced point source in which certain range of directions need to be sampled more thoroughly than the others. For example, consider a case in which DC3 is uniformly distributed on

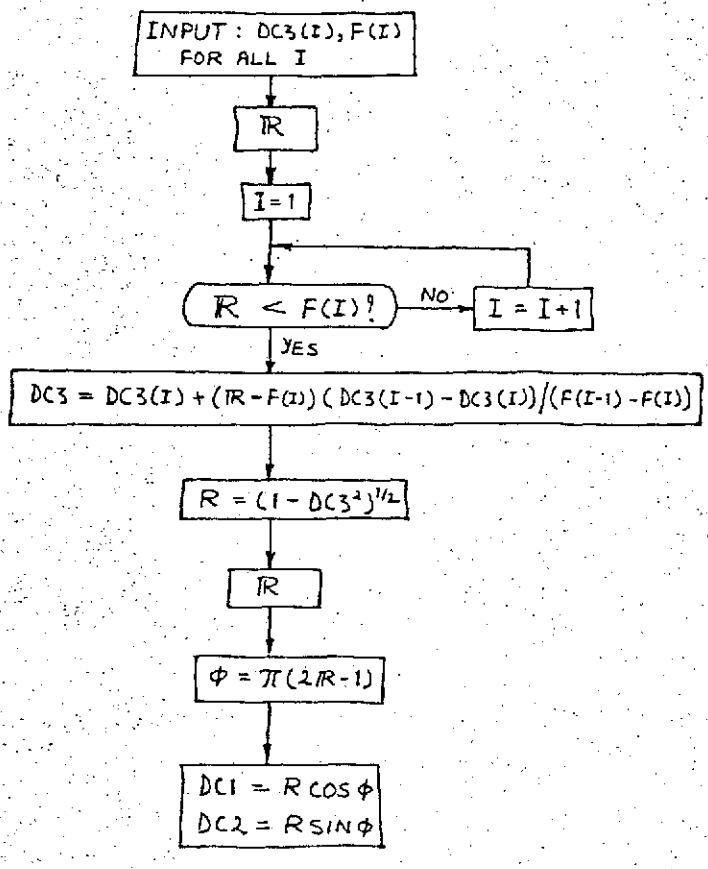

Fig. A6.6 Selection Routine for General Distribution in Upper Half Directional Space DL(3)

the range $-1 \leq DC3 \leq 1$; but more important are the directions corresponding to the range

$$-1 \leq DC3 \leq DC3P < 0 \qquad (16)$$

Here it is possible to give an equal likelihood of the ray direction on this prescribed range of Eq. 16, or its complement by assigning the respective weights (DC3P + 1), and (1 - DC3P); the total weight processed for the totality of NR ray tubes being given by

$$\tfrac{1}{2}\,NR\,(DC3P + 1) - \tfrac{1}{2}\,NR\,(DC3P - 1) = NR \qquad (17)$$

The routine for the selection with these weight factors is shown in Fig. A6.7.

RAY TUBE PROCESSING ROUTINE

The assignment of these direction coordinates, as explained in the last section, completes the initial specification of all the parameters for the processing of the ray tube. Now the machine is led from the position B to the position C of the flow diagram (Fig. A6.1). The position C forms the main core of the Monte Carlo procedure; this is a position at which the lifetime of the ray tube is processed. The technique for the processing is similar to that given in Chapter 8.

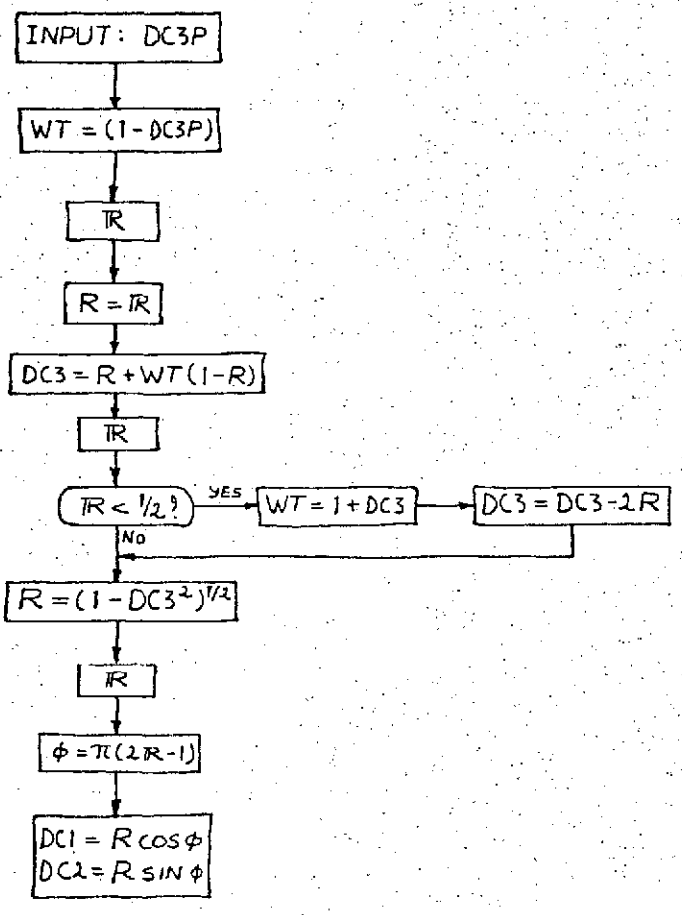

Fig. A6.7 Selection Routine for Prejudicied Directional Law DL(4)

ANALYSIS ROUTINE

The data accumulated while the ray tubes were followed are now analyzed and the results are printed. The magnitude of the statistical variability is determined by evaluating the variance and the standard deviation, as shown earlier in Chapter 8.

Appendix 7

CURVED BOUNDARY PROBLEM MONTE CARLO PROGRAMME

This appendix gives in full details the results of the application of the proposed Monte Carlo technique (Chapter 8) to a curved boundary problem that is under investigation (Chapter10). Included herein is a complete listing of the programme that was used in these calculations on the CDC 6400 of the Computing Center of the University of Virginia. The printout results accompanying this listing correspond to the pressure values shown in Fig. 65.

```
      PROGRAM  THAMEO (INPUT, OUTPUT, TAPE5=INPUT, TAPE6=OUTPUT)
000003      COMMON/CDRNLW /IRAN,RANNO,DC(4),NRA,NRC
000003      DIMENSION NDXDL(10),XS(3),XR(3),XRT(9),AI(9),AR(9),XI(9),XC(9),
     1XRA(9),XRB(9),P(250)
000003      EXTERNAL DISRAY
            C     MONTE CARLO CALCULATIONS FOR TRANSIENT ACOUSTIC FIELD INSIDE A
            C     CYLINDRICAL DUCT DUE TO A SINGLE CYCLE SINUSOIDAL SHAPE PULSE
            C     INPUT QUANTITIES
000003      READ(5,402)QQ,TP,PI,A,C,(XR(I),I=1,3),TPLS,(XS(I),I=1,3),AMN,DCTL,
     1DPHI,EPSLON,DNST $ READ(5,401)NS,NR,NRB,IRAN
            C     VARIABLES IN NONDIMENSIONAL FORM
000065      RSTR=SQRT(XR(1)**2+XR(2)**2)/A $ ZSTR=XR(3)/A $ TPSTR=C*TP/A
000077      ZTPSTR=ZSTR+TPSTR $ TPLSTR=C*TPLS/A $ JSTRT=SQRT(ZSTR**2+
     1PSTR**2)/TPLSTR     $ AOSTR=AMN/A $ X3MXSTR=DCTL/A $ DPSI=DPHI
000116      A2STR=(1.-AOSTR)/X3MXSTR $ RA=AOSTR $ RB=A2STR $ RADS2=RSTR**2
000125      FNORM=(-QQ*TPSTR*A**2)/((DNST*C**2)*(4*NR)*(TPLSTR)*((4./3.)*
     1PI*EPSLON**3))
000145      WRITE(6,500)QQ,TP,PI,A,C,TPLS,DNST,(XS(I),I=1,3),(XR(I),I=1,3),
     1AMN,DCTL,QQ,RSTR,TPSTR,ZSTR,ZTPSTR,TPLSTR,JSTRT,AOSTR,X3MXSTR,
     2A2STR,DPHI,EPSLON,FNORM $ WRITE(6,501)NS,NR,NRB,IRAN
000254      JM=0 $ DO 19 J=1,250 $ P(J)=.0
000260   19 CONTINUE $ DO 20 I=1,3 $ XS(I)=XS(I)/A
000265   20 XR(I)=XR(I)/A $ RADS2=RSTR**2 $ NSA=1 $ NRA=NRC=0
         C     RANDOM SELECTION OF THE RAY DIRECTION COSINES
000275   22 CALL DCINTL(NDXDL(NSA)) $ U=.5/SQRT(1.-DC(3)**2) $ DO 23 I=1,3
         C     DETERMINATION OF VORTICES OF THE RAY TUBE TRIANGLE AT REFERENCE PT
000306      AI(I)=DC(I) $ XI(I)=XS(I)+U*DC(I)
000313   23 CONTINUE $ XI(4)=XI(1) $ XI(5)=XI(6)=XI(2) $ XI(6)=XI(3)+DPHI
000323      XI(7)=XI(1)+DPSI $ XI(9)=XI(3) $ Y0=DISRAY(XI(4),XI(5),XI(6),XS(1)
     1,XS(2),XS(3)) $    AI(4)=(XI(4)-XS(1))/Y0 $ AI(5)=(XI(5)-XS(2))/Y0
         C     RANDOM PULSE SELECTION FROM SOURCE STRENGTH TIME HISTORY
000340      AI(6)=(XI(6)-XS(3))/Y0 $ Y0=DISRAY(XI(7),XI(8),XI(9),XS(1),XS(2),
     1XS(3)) $ AI(7)=(XI(7)-XS(1))/Y0 $ AI(8)=(XI(8)-XS(2))/Y0 $ AI(9)=(
     2XI(9)-XS(3))/Y0 $ RREF=RAYDIS=DISRAY(XI(1),XI(2),XI(3),XS(1),XS(2)
     3,XS(3)) $ CALL GRAN $ TI=RANNO*TPSTR/4. $ PREF=COS(PI*RANNO/2.)
000376      TP0=.5*TPSTR $ TI2=TP0-TI $ TI3=TP0+TI $ TI4=TPSTR-TI
         C     DETERMINATION OF REFERENCE RAY TUBE AREA ART0 FOR NORMALIZATION
000405      B0=DISRAY(XI (1),XI (2),XI (3),XI (4),XI (5),XI (6))
000411      B1=DISRAY(XI (7),XI (8),XI (9),XI (4),XI (5),XI (6))
000416      B2=DISRAY(XI (7),XI (8),XI (9),XI (1),XI (2),XI (3))
000423      B3=.5*(B0+B1+B2) $ Y1=SQRT(B3*(B3-B0)*(B3-B1)*(B3-B2)) $ ART0=Y1
000441      NCOLSN=0 $ IF(NR.LT.NRA) GO TO 110
         C     DETERMINATION OF POINT OF RAY COLLISION WITH THE DUCT SURFACE
000445   24 DO 32 J=1,7,3 $    A12=AI(J)/AI(J+1) $ A32=AI(J+2)/AI(J+1) $ A=1+
     1A12**2+(RB*A32)**2 $ B=A12*(XI(J)-A12*XI(J+1))-RB*A32*(RA+RB*(XI
     2(J+2)-A32*XI(J+1))) $ C=(RA+RB*(XI(J+2)-A32*XI(J+1)))**2-(XI(J)-
     3A12*XI(J+1))**2 $ CALL ROOT(A,B,C,UMX,UMN)
000512      IF(AI(J+1).GT.0.0)29,30
000517   29 XC(J+1)=UMX $ GO TO 31
000522   30 XC(J+1)=UMN
         C     DETERMINATION OF THE DIRECTION VECTOR OF THE REFLECTED RAY
000524   31 A22=XC(J+1)-XI(J+1) $ XC(J)=XI(J)+A12*A22 $ XC(J+2)=XI(J+2)+A32*A2
     12 $ B1=-2*XC(J) $ B2=-2*XC(J+1) $ B3=2*RB*(RA+RB*XC(J+2))
000546      ASQ=SQRT(B1**2+B2**2+B3**2) $ B1=B1/ASQ $ B2=B2/ASQ $ B3=B3/ASQ
000550      ALFACOS=-(AI(J)*B1+AI(J+1)*B2+AI(J+2)*B3) $ AR(J)=AI(J)+2*ALFACOS*
     1B1 $ AR(J+1)=AI(J+1)+2*ALFACOS*B2 $ AR(J+2)=AI(J+2)+2*ALFACOS*B3
000603   32 CONTINUE $ IF(XC(3).LT..0.OR.XC(3).GT.X3MXSTR) GO TO 22
```

```
000615          RAYDIS=RAYDIS  +DISRAY(XC(1),XC(2),XC(3),XI(1),XI(2),XI(3))
                C     THIS COMPLETES DETERMINATION OF COLLISION POINTS AND REFLECTED DCS
000623          NCOLSN=NCOLSN+1
                C     DETERMINATION OF THE NONZERO COMPONENT OF THE POINT COMMON TO
                C     RAY AND THE DUCT AXIS
000624          XRF3=XC(3)-XC(2)*AR(3)/AR(2) $ IF(ZSTR.LT.XC(3)) GO TO 42
                C     DETERMINATION OF POINT ON REFLECTED RAY BEYOND THE DUCT AXIS
000633          IF(ZSTR.LT.XRF3)52,62
000640     42   DO 46 J=1,7,3 $ A12=AR(J)/AR(J+1)
000644          A32=AR(J+2)/AR(J+1) $ A=1.0+A12**2 $ B=(XC(J)-A12*XC(J+1))*A12
000654          C=RADS2-(B/A12)**2 $ CALL ROOT(A,B,C,UMX,UMN)
000662          IF(XC(J+1).GT.0.0)43,44
000667     43   XRB(J+1)=UMN $ GO TO 45
000672     44   XRB(J+1)=UMX
000674     45   A22=XRB(J+1)-XC(J+1) $ XRB(J)=XC(J)+A12*A22 $ XRB(J+2)=XC(J+2)+
               1A32*A22
000704     46   CONTINUE
000706          B0=DISRAY(XRB(1),XRB(2),XRB(3),XRB(4),XRB(5),XRB(6))
000712          B1=DISRAY(XRB(7),XRB(8),XRB(9),XRB(4),XRB(5),XRB(6))
000717          B2=DISRAY(XRB(7),XRB(8),XRB(9),XRB(1),XRB(2),XRB(3))
000724          B3=.5*(B0+B1+B2) $ Y1=SQRT(ABS(B3*(B3-B0)*(B3-B1)*(B3-B2)))/ARTO
000743          Y2=DISRAY(XR(1),XR(2),XR(3),XRB(1),XRB(2),XRB(3)) $ GO TO 100
                C     DETERMINATION OF POINT ON REFLECTED RAY PRIOR TO DUCT AXIS
000751     52   DO 56 J=1,7,3 $ A12=AR(J)/AR(J+1)
000755          A32=AR(J+2)/AR(J+1) $ A=1.0+A12**2 $ B=(XC(J)-A12*XC(J+1))*A12
000765          C=RADS2-(B/A12)**2 $ CALL ROOT(A,B,C,UMX,UMN)
000773          IF(XC(J+1).GT.0.0)53,54
001000     53   XRA(J+1)=UMX $ GO TO 55
001003     54   XRA(J+1)=UMN
001005     55   A22=XRA(J+1)-XC(J+1) $ XRA(J)=XC(J)+A12*A22 $ XRA(J+2)=XC(J+2)+
               1A32*A22
001015     56   CONTINUE
001017          B0=DISRAY(XRA(1),XRA(2),XRA(3),XRA(4),XRA(5),XRA(6))
001023          B1=DISRAY(XRA(7),XRA(8),XRA(9),XRA(4),XRA(5),XRA(6))
001030          B2=DISRAY(XRA(7),XRA(8),XRA(9),XRA(1),XRA(2),XRA(3))
001035          B3=.5*(B0+B1+B2) $ Y1=SQRT(ABS(B3*(B3-B0)*(B3-B1)*(B3-B2)))/ARTO
001054          Y2=DISRAY(XR(1),XR(2),XR(3),XRA(1),XRA(2),XRA(3)) $ GO TO 100
001052     62   DO 63 J=1,9 $ XI(J)=XC(J) $ AI(J)=AR(J)
001067     63   CONTINUE $ GO TO 24
                C     PENETRATION IN TEST SPHERE, PRESSURE CONTRIBUTION
001071    100   IF(Y2.LT.EPSLON)105,106
001076    105   DLR=SQRT(2.*ABS((AR(3)*XRF3-(AR(1)*XR(1)+AR(2)*XR(2)+AR(3)*ZSTR))
               1**2+EPSLON**2-RADS2-(XRF3-ZSTR)**2))$ Y3=SQRT(Y1) $ Y5=RREF*Y3
001123          PR1=PREF*(Y5+DLR/2.)*DLR $ Y6=RREF+Y5
001131          J=IFIX((TI+Y6)/TPLSTR)+1-JSTRT $ IF(J.GT.JM)P(J)=P(J)+PR1
001143          J=IFIX((TI2+Y6)/TPLSTR)+1-JSTRT $ P(J)=P(J)-PR1
001152          J=IFIX((TI3+Y6)/TPLSTR)+1-JSTRT $ P(J)=P(J)-PR1
001161          J=IFIX((TI4+Y6)/TPLSTR)+1-JSTRT $ IF(J.LT. 100)P(J)=P(J)+PR1
001173    106   IF(NRA.LT.NR)22,110
001200    110   DO 115 J=1,100 $ P(J)=ENORM*P(J)
001204    115   CONTINUE $ WRITE(6,506)(J,P(J),J=1,100)
001220          WRITE(6,212)IRAN $ WRITE(6,510)ARTO
                C     FORMATS
001234    212   FORMAT(5X*IRAN =*I10)
001234    401   FORMAT(8I10)
001234    402   FORMAT(5E15.8)
001234    500   FORMAT(1H1,30X*TRANSIENT ACOUSTIC FIELD IN CYLINDRICAL DUCT*3(/)
               137X*MONTE CARLO METHOD*3(/)10X*PREASSIGNED CONSTANTS IN DIMENSIONA
```

```
     1L FORM(FPS SYSTEM)*//5X*SOURCE STRENGTH FACTOR Q0 = *E10.4,3X*SOUR
     2CE PERIOD TP = *E10.4,3X*PI = *E10.4/5X*DUCT RADIUS A = *E10.4,3X
     3*WAVE SPEED C = *E10.4,3X*ELEMENTAL TIME INTERVAL TPLS = *E10.4/
     35X*CHARACTERISTIC MASS DENSITY OF THE MEDIUM DNST = *E10.4/
     45X*SOURCE CARTESIAN COORDINATES XS(1,2,3) = *3(E10.4,2X)/
     55X*RECEIVER CARTESIAN COORDINATES XR(1,2,3) = *3(E10.4,2X)/5X*DUCT
     6 MINIMUM RADIUS AMIN = *E10.4,3X*DUCT LENGTH DCTL = *E10.4///
     710X*VARIABLES IN NONDIMENSIONAL FORM*//5X*Q0 = *E16.8,2X*RSTR = *
     8E16.8,2X*TPSTR = *E16.8/5X*ZSTR =*E16.8,2X*ZTPSTR =*E16.8,2X*TPLST
     9R = *E16.8,2X*JSTRT = *I4                /5X*A0STR = *E16.8,2X*X3MXS
     1TR = *E16.8,2X*A2STR = *E16.8,2X*DPHI=DPSI= *E16.8/5X*RADIUS OF TH
     2E TEST SPHERE EPSLON = *E16.8/5X*PRESSURE NORMALIZATION FACTOR
     3FNORM = *E16.8)
001234   501  FORMAT(5X*NS = *I2,2X*NR = *I5,2X*NRD = *I5,2X*IRAN = *I9///)
001234   506  FORMAT(20X*PRESSURE VALUES IN THE NONDIMENSIONAL FORM*/
     125X*(NOTE TIME INDEX=INDEX+JSTRT)*/(5(5X,I3,1X,E16.8)))
001234   510  FORMAT(5X*RAY TUBE AREA FOR NORMALIZATION AT REFERENCE RADIUS
     1AREF=,5  ART0 = *E27.20)
001234        STOP $ END
         C    ARITHMETIC STATEMENT FUNCTIONS
```

```
THAMED

PROGRAM LENGTH INCLUDING I/O BUFFERS
006444

FUNCTION ASSIGNMENTS

STATEMENT ASSIGNMENTS
22    - 000275   24    - 000445   29    - 000517   30    - 000522
31    - 000524   42    - 000640   43    - 000667   44    - 000672
45    - 000674   52    - 000751   53    - 001000   54    - 001003
55    - 001005   62    - 001062   100   - 001071   105   - 001076
106   - 001173   110   - 001200   212   - 001260   401   - 001263
402   - 001265   500   - 001267   501   - 001426   506   - 001435
510   - 001452

BLOCK NAMES AND LENGTHS
CORNLN - 000010

VARIABLE ASSIGNMENTS
A     - 002303   AI    - 001620   ALFACOS- 002370   AMN   - 002307
AR    - 001631   ART0  - 002357   ASQ   - 002367   A0STR - 002325
A12   - 002361   A2STR - 002330   A22   - 002366   A32   - 002362
B     - 002363   B0    - 002352   B1    - 002353   B2    - 002354
B3    - 002355   C     - 002304   DC    - 000002C01 DCTL  - 002310
DLR   - 002373   DNST  - 002313   DPHI  - 002311   DPSI  - 002327
EPSLON - 002312  FNORM - 002334   I     - 002305   IRAN  - 000000C01
J     - 002335   JM    - 002335   JSTRT - 002324   NCOLSN - 002360
NOXDL - 001567   NR    - 002315   NRA   - 000006C01 NRB   - 002316
NRC   - 000007C01 NS    - 002314   NSA   - 002337   P     - 001706
PI    - 002302   PREF  - 002345   PR1   - 002376   Q0    - 002300
R4    - 002331   RADS2 - 002333   RANNO - 000001C01 RAYDI5 - 002343
RB    - 002332   RREF  - 002342   RSTR  - 002317   TI    - 002344
TI2   - 002347   TI3   - 002350   TI4   - 002351   YP    - 002301
YPLS  - 002306   YPLSTR - 002323  YPSTR - 002321   YP0   - 002346
U     - 002340   UMN   - 002365   UMX   - 002364   XC    - 001653
XI    - 001642   XR    - 001604   XRA   - 001664   XR8   - 001675
XRF3  - 002371   XRT   - 001607   XS    - 001601   X3MXSTR- 002326
Y0    - 002341   Y1    - 002356   Y2    - 002372   Y3    - 002374
Y5    - 002375   Y6    - 002377   ZSTR  - 002320   ZYPSTR - 002322

START OF CONSTANTS
001240

START OF TEMPORARIES
001465

START OF INDIRECTS
001531

UNUSED COMPILER SPACE
020000
```

```
                FUNCTION DISRAY(X1,X2,X3,Y1,Y2,Y3)
000011          DISRAY=SQRT((Y1-X1)**2+(Y2-X2)**2+(Y3-X3)**2)
000025          RETURN $ END
          C     SUBROUTINES
```

```
DISRAY

SUBPROGRAM LENGTH
000050

FUNCTION ASSIGNMENTS

STATEMENT ASSIGNMENTS

BLOCK NAMES AND LENGTHS

VARIABLE ASSIGNMENTS
DISRAY =  003047

START OF CONSTANTS
000030

START OF TEMPORARIES
000031

START OF INDIRECTS
000047

UNUSED COMPILER SPACE
024400
```

```
                SUBROUTINE GRAN
000002          COMMON/CORNLW /IRAN,RANNO,E(6)
000002          IRAN=3125*IRAN $ I1=IRAN/67108864 $ IRAN=IRAN-I1*67108864
000011          RANNO=FLOAT(IRAN)/67108864 $ RETURN $ END
```

```
GRAN

SUBPROGRAM LENGTH
000025

FUNCTION ASSIGNMENTS

STATEMENT ASSIGNMENTS

BLOCK NAMES AND LENGTHS
CORNLW -  000010

VARIABLE ASSIGNMENTS
E      -  000002C01 IRAN   -  000000C01 I1     -  000024    RANNO  -  000001C01

START OF CONSTANTS
000016

START OF TEMPORARIES
000020

START OF INDIRECTS
000024

UNUSED COMPILER SPACE
024500
```

```
      SUBROUTINE DCINTL(NDX)
000003      COMMON/CORNLH /IRAN,RANNO,DC(4),NRA,NRC
000003      CALL GRAN
000004      DC(3)=SQRT(RANNO)
000006      RAD=SQRT(1-DC(3)**2)
000014      CALL GRAN
000015      PHI=(2*RANNO-1)*22/7
000023      DC(1)=RAD*COS(PHI)
000026      DC(2)=RAD*SIN(PHI)
000031      NRA=NRA+1
000033      NRC=NRC+1
000035      RETURN
000035      END
```

```
DCINTL

SUBPROGRAM LENGTH
000052

FUNCTION ASSIGNMENTS

STATEMENT ASSIGNMENTS

BLOCK NAMES AND LENGTHS
CORNLW -  000010

VARIABLE ASSIGNMENTS
DC     -  001002C01 NRA    -  000006C01 NRC    -  000007C01 PHI    -  000051
RAD    -  000050    RANNO  -  000001C01

START OF CONSTANTS
000037

START OF TEMPORARIES
000040

START OF INDIRECTS
000050

UNUSED COMPILER SPACE
024400
```

```
                SUBROUTINE ROOT(A,B,C,UMX,UMN)
000016          D=SQRT(B**2+A*C) $ UA=(-B+D)/A $ UB=(-B-D)/A $ UMX=AMAX1(UA,UB)
000027          UMN=AMIN1(UA,UB)
000031          RETURN $ END
```

```
ROOT

SUBPROGRAM LENGTH
000055

FUNCTION ASSIGNMENTS

STATEMENT ASSIGNMENTS

@LOCK NAMES AND LENGTHS

VARIABLE ASSIGNMENTS
D      -  000052    UA     -  000053    UB     -  000054

START OF CONSTANTS
000033

START OF TEMPORARIES
000034

START OF INDIRECTS
000052

UNUSED COMPILER SPACE
024400
```

```
CORE MAP  16.59.23.  NORMAL              CONTROL                                                  000130    014433    000000    000000
          ---TIME---LOAD MODE --L1--L2-----TYPE--------------USER-------CALL-------------FWA LOAD--LWA LOAD--BLNK COMN--LENGTH--
          FWA LOADER  054744  FWA TABLES  052770
          -PROGRAM----ADDRESS-                        --LABELED---COMMON--
          THANED      000110                                  CORNLW      000100
          DISRAY      006554
          GRAN        006624                                  CORNLW      000100
          OCINTL      006651                                  CORNLW      000100
          ROOT        006723
          SINCOS      007000
          SQRT        007077
          SYSTEM      007142                                  SCOPE2      007142
          GETBA       010254
          INPUTC      010273
          KODER       010410
          KRAKER      011652
          OUTPTC      012733
          SIOS        013025
          ----UNSATISFIED EXTERNALS-----                      REFERENCES
```

TRANSIENT ACOUSTIC FIELD IN CYLINDRICAL DUCT

MONTE CARLO METHOD

PREASSIGNED CONSTANTS IN DIMENSIONAL FORM(FPS SYSTEM)

SOURCE STRENGTH FACTOR Q0 = 1.0000E+00 SOURCE PERIOD TP = 2.0000E-03 PI = 3.1416E+00
DUCT RADIUS A = 7.5000E+00 WAVE SPEED C = 1.1000E+03 ELEMENTAL TIME INTERVAL TPLS = 5.0000E-05
CHARACTERISTIC MASS DENSITY OF THE MEDIUM DNST = 2.3780E-03
SOURCE CARTESIAN COORDINATES XS(1,2,3) = 0. 0. 0.
RECEIVER CARTESIAN COORDINATES XR(1,2,3) = 1.0000E+00 3.0000E+00 1.0000E+01
DUCT MINIMUM RADIUS AMIN = 7.5000E+00 DUCT LENGTH DCTL = 1.2000E+02

VARIABLES IN NONDIMENSIONAL FORM

Q0 = 1.00000000E+00 RSTR = 4.21637021E-01 TPSTR = 2.93333333E-01
ZSTR = 1.33333333E+00 ZTPSTR = 1.62666667E+00 TPLSTR = 7.33333333E-03 JSTRT = 190
A0STR = 1.00000000E+00 X3MXSTR = 1.60000000E+01 A2STR = 0. DPHI=DPSI= 1.00000000E-12
RADIUS OF THE TEST SPHERE EPSLON = 1.00000000E-01
PRESSURE NORMALIZATION FACTOR FNORM = -9.33397524E-03
NS = 1 NR = 5000 NR0 = 1 IRAN = 22758845

PRESSURE VALUES IN THE NONDIMENSIONAL FORM
(NOTE TIME INDEX=INDEX+JSTRT)

1	0.	2	0.	3	0.	4	0.	5	0.
6	0.	7	0.	8	0.	9	0.	10	0.
11	0.	12	0.	13	0.	14	0.	15	0.
16	0.	17	0.	18	0.	19	0.	20	0.
21	0.	22	0.	23	0.	24	0.	25	0.
26	0.	27	0.	28	0.	29	0.	30	0.
31	0.	32	0.	33	0.	34	0.	35	0.
36	0.	37	0.	38	0.	39	-1.03850833E-03	40	0.
41	-7.19264996E-04	42	-2.26885362E-03	43	-1.25847894E-03	44	-1.58043309E-03	45	-1.47552828E-03
46	-1.38178749E-03	47	-5.90468331E-04	48	-1.16271611E-03	49	-3.31580572E-04	50	-1.38739989E-04
51	3.06394004E-04	52	1.71917419E-03	53	7.61404907E-04	54	1.22018689E-03	55	0.
56	0.	57	-9.46930788E-04	58	2.76742377E-03	59	2.66128828E-03	60	0.
61	3.59776666E-04	62	3.22555296E-03	63	2.16374829E-03	64	6.38184446E-04	65	1.27556282E-03
66	1.38178749E-03	67	5.90468331E-04	68	1.16271611E-03	69	3.31580572E-04	70	1.38739989E-04
71	6.35821637E-04	72	-3.64706558E-04	73	-7.61404907E-04	74	1.54848460E-04	75	0.
76	0.	77	9.46930788E-04	78	-2.76742377E-03	79	-1.65277995E-03	80	0.
81	3.59487229E-04	82	-9.58699342E-04	83	-9.05269351E-04	84	9.42215641E-04	85	0.
86	0.	87	-1.15580914E-03	88	0.	89	0.	90	0.
91	-9.42215641E-04	92	-1.35446763E-03	93	0.	94	-1.37503536E-03	95	0.
96	0.	97	0.	98	0.	99	0.	100	0.

IRAN = 35262301
RAY TUBE AREA FOR NORMALIZATION AT REFERENCE RADIUS AREF=.5 ART0 = 4.99200647154710106399E-25

```
  05/14/72   UNIV. OF VIRGINIA SCOPE  3.3 APR 01,72 SUM 296
16.59.15.THANE96
16.59.15.THANED,M2025M,T200,CM61000. BALAKRISHNA
16.59.15.D THANEDAR AEROSPACE                    B
16.59.15.RUN(S,,,,,,THANED)
16.59.19.COMMON(THANED)
16.59.19.THANED.
16.59.23. (PFL - 014500)    CP  002.747 SEC.
16.59.23.                   PP  004.060 SEC.
16.59.23.                   IO  000.403 SEC.
17.00.01.STOP
17.00.01.CP     039.280 SEC.
17.00.01.PP     004.448 SEC.
17.00.01.IO     000.412 SEC.

                THANE96  //// END OF LIST ////  0000504 LINES
```

```
      PROGRAM VRNSTD (INPUT, OUTPUT, TAPE5 =INPUT, TAPE6 =OUTPUT)
000003      DIMENSION XR(3),XS(3),PRES(5,60),IRN(5)
000003      READ(5,401)(IRN(N),N=1,5)
000015      READ(5,402)Q0,TP,PI,A,C,(XR(I),I=1,3),TPLS,(XS(I),I=1,3),AMN,DCTL,
           1DPHI,EPSLON,DNST $ READ(5,401)NS,NR,NRB,IRAN,NRPT,JMAX
000103      PSTP=SQRT(XR(1)**2+XR(2)**2)/A $ ZSTR=XR(3)/A $ TPSTR=C*TP/A
000115      ZTPSTR=ZSTR+TPSTR $ TPLSTR=C*TPLS/A $ JSTRT=SQRT(ZSTR**2+
           1RSTR**2)/TPLSTR    $ ACSTR=AMN/A $ X3MXSTR=DCTL/A $ DPSI=DPHI
000135      A2STR=(1.-A0STR)/X3MXSTR $ RA=A0STR $ RB=A2STR
000142      FNORM=(-Q0*TPSTR*A**2)/((DNST*C**2)*(4*NR)*(TPLSTR)*((4./3.)*
           1PI*EPSLON**3))
000161      WRITE(6,500)Q0,TP,PI,A,C,TPLS,DNST,(XS(I),I=1,3),(XR(I),I=1,3),
           1AMN,DCTL,Q0,RSTR,TPSTR,ZSTR,ZTPSTR,TPLSTR,JSTRT,A0STR,X3MXSTR,
           2A2STR,DPHI,EPSLON,FNORM $ WRITE(6,501)NS,NR,NRB,NRPT
000270      DO 39 N=1,NRPT $ READ(5,402)(PRES(N,J),J=1,JMAX)
000305   39 CONTINUE $ WRITE(6,209)(IRN(N),N=1,NRPT) $ DO 40 J=1,JMAX
000324   40 WRITE(6,208)J,(PRES(N,J),N=1,NRPT)
000344      WRITE(6 ,207) $ DO 43 J=1,JMAX $ X1=X2=0.0 $ DO 41 I=1,NRPT
000354   41 X1=X1+PRES(I,J) $ X1=X1/NRPT $ DO 42 I=1, NRPT
000365   42 X2=X2+(PRES(I,J)-X1)**2 $ VRNS=X2/NRPT $ STDN=SQRT(VRNS)
000403      X1P=X1+STDN $ X1M=X1-STDN
000406   43 WRITE(6 ,208)J,X1,VRNS,STDN,X1P,X1M
      C     FORMATS
000431  207 FORMAT(30X*VARIANCE AND DEVIATION ANALYSIS*//10X*TIME INDEX*5X*MEA
           1N*14X*VARIANCE*11X*DEVIATION*7X*(MEAN)+(DEVIATION)*2X*(MEAN)-(DEVI
           2ATION)*//)
000431  208 FORMAT(12X,I3,5(4X,E16.8))
000431  209 FORMAT(10X*PRESSURE VALUES IN THE NONDIMENSIONAL FORM  SUMMARY OF
           1THE MONTE CARLO CALCULATIONS (5 RUNS)*//24X*RUN 1*,15X*RUN 2*,15X*
           2RUN 3*,15X*RUN 4*,15X*RUN 5*//10X*IRAN VALUE*,4X,I8,4(12X,I8)//)
000431  401 FORMAT(8I10)
000431  402 FORMAT(6E16.8)
000431  500 FORMAT(1H1,30X*TRANSIENT ACOUSTIC FIELD IN CYLINDRICAL DUCT*3(/)
           137X*MONTE CARLO METHOD*3(/)10X*PREASSIGNED CONSTANTS IN DIMENSIONA
           1L FORM(FPS SYSTEM)*//5X*SOURCE STRENGTH FACTOR Q0 = *E10.4,3X*SOUR
           2CE PERIOD TP = *E10.4,3X*PI = *E10.4/5X*DUCT RADIUS A = *E10.4,3X
           3*WAVE SPEED C = *E10.4,3X*ELEMENTAL TIME INTERVAL TPLS = *E10.4/
           35X*CHARACTERISTIC MASS DENSITY OF THE MEDIUM DNST = *E10.4/
           45X*SOURCE CARTESIAN COORDINATES XS(1,2,3) = *3(E10.4,2X)/
           55X*RECEIVER CARTESIAN COORDINATES XR(1,2,3) = *3(E10.4,2X)/5X*DUCT
           6 MINIMUM RADIUS AMIN = *E10.4,3X*DUCT LENGTH DCTL = *E10.4///
           710X*VARIABLES IN NONDIMENSIONAL FORM*//5X*Q0 = *E16.8,2X*RSTR = *
           8E16.8,2X*TPSTR = *E16.8/5X*ZSTR =*E16.8,2X*ZTPSTR =*E16.8,2X*TPLST
           9R = *E16.8,2X*JSTRT = *I4                /5X*A0STR = *E16.8,2X*X3MXS
           1TR = *E16.8,2X*A2STR = *E16.8,2X*DPHI=DPSI= *E16.8/5X*RADIUS OF TH
           2E TEST SPHERE EPSLON = *E16.8/5X*PRESSURE NORMALIZATION FACTOR
           3FNORM = *E16.8)
000431  501 FORMAT(5X*NS = *I2,2X*NR = *I5,2X*NRB = *I5,2X*TOTAL NUMBER OF RUN
           1S NRPT = *I2///)
000431      STOP
000433      END
```

```
VRNSTO

PROGRAM LENGTH INCLUDING I/O BUFFERS
005544

FUNCTION ASSIGNMENTS

STATEMENT ASSIGNMENTS
41      -  000354    42      -  000365    207     -  000452    208     -  000471
209     -  000475    401     -  000522    402     -  000524    500     -  000526
501     -  001655

BLOCK NAMES AND LENGTHS

VARIABLE ASSIGNMENTS
A       -  001435    AMN     -  001441    A0STR   -  001462    A2STR   -  001465
C       -  001436    DCTL    -  001442    DNST    -  001445    DPHI    -  001443
DPSI    -  001464    EPSLON  -  001444    FNORM   -  001470    I       -  001437
IRAM    -  001451    IRN     -  001424    J       -  001471    JMAX    -  001453
JSTRT   -  001461    N       -  001431    NR      -  001447    NRB     -  001450
NRPT    -  001452    NS      -  001446    PI      -  001434    PRES    -  000750
Q0      -  001432    R4      -  001466    RB      -  001467    RSTR    -  001454
STDN    -  001475    TP      -  001433    TPLS    -  001440    TPLSTR  -  001460
TPSTR   -  001456    VRNS    -  001474    XR      -  000742    XS      -  000745
X1      -  001472    X1M     -  001477    X1P     -  001476    X2      -  001473
X3MXSTR-   001463    ZSTR    -  001455    ZTPSTR  -  001457

START OF CONSTANTS
000435

START OF TEMPORARIES
000677

START OF INDIRECTS
000741

UNUSED COMPILER SPACE
002530
```

```
CORE MAP  12.25.44.  NORMAL              CONTROL                                    000100    013200    000000    000000
          ---TIME---LOAD MODE --L1--L2-----TYPE---------------USER---+---CALL-----------FWA LOAD--LWA LOAD--BLNK COMN--LENGTH--
          FWA LOADER  034744  FWA TABLES  033116
          -PROGRAM----ADDRESS-                --LABELED---COMMON--
          VPNSTD      000100
          SORT        005644
          SYSTEM      005707                          SCOPE2      005707
          GETBA       007021
          INPUTC      007040
          KODER       007155
          KRAKER      010427
          OUTPTC      011500
          SIOS        011572
          ----UNSATISFIED EXTERNALS-----              REFERENCES
```

TRANSIENT ACOUSTIC FIELD IN CYLINDRICAL DUCT

MONTE CARLO METHOD

PRESSIGNED CONSTANTS IN DIMENSIONAL FORM(FPS SYSTEM)

SOURCE STRENGTH FACTOR QO = 1.0000E+00 SOURCE PERIOD TP = 2.0000E-03 PI = 3.1416E+00
DUCT RADIUS A = 7.5000E+00 WAVE SPEED C = 1.1000E+03 ELEMENTAL TIME INTERVAL TPLS = 5.0000E-05
CHARACTERISTIC MASS DENSITY OF THE MEDIUM DNST = 2.3780E-03
SOURCE CARTESIAN COORDINATES XS(1,2,3) = 0. 0. 0.
RECEIVER CARTESIAN COORDINATES XR(1,2,3) = 1.0000E+00 3.0000E+00 1.0000E+01
DUCT MINIMUM RADIUS AMIN = 7.5000E+00 DUCT LENGTH OCTL = 1.2000E+02

VARIABLES IN NONDIMENSIONAL FORM

QO = 1.00000000E+00 RSTR = 4.21637021E-01 TPSTR = 2.93333333E-01
ZSTP = 1.33333333E+00 ZTPSTR = 1.62666667E+00 TPLSTR = 7.33333333E-03 JSTRT = 190
A1STR = 1.00000000E+00 X3MXSTR = 1.60000000E+01 A2STR = 0. DPHI=DPSI= 1.00000000E-12
RADIUS OF THE TEST SPHERE EPSLON = 1.00000000E-01
PRESSURE NORMALIZATION FACTOR FNORM = -9.33397524E-03
NS = 1 NR = 5000 NRB = 1 TOTAL NUMBER OF RUNS NRPT = 5

PRESSURE VALUES IN THE NONDIMENSIONAL FORM SUMMARY OF THE MONTE CARLO CALCULATIONS (5 RUNS)

	RUN 1	RUN 2	RUN 3	RUN 4	RUN 5
IRAN VALUE	22758845	34098429	37658337	25612063	3373511
1	-7.19254096E-04	-6.21930565E-04	0.	0.	-3.34921942E-04
2	-2.26585362E-03	-1.45231818E-03	-9.78273908E-04	-1.73863271E-03	-1.43939228E-03
3	-1.25847896E-03	-5.88822759E-03	-1.15410297E-03	-1.81477572E-03	-1.76909494E-03
4	-1.58040909E-03	-3.18109404E-03	0.	-1.94870251E-03	-9.38857579E-04
5	-1.27556282E-03	-1.06276331E-03	-3.61585190E-03	-1.19897270E-03	-1.74534145E-03
6	-1.35178749E-03	-3.01355043E-03	-1.44508435E-03	-2.00593521E-04	-6.43736124E-04
7	-5.90468331E-04	0.	-6.72021418E-04	-2.48002270E-03	-1.17447535E-03
8	-1.16271611E-03	-1.51009771E-03	1.26127104E-04	5.38301881E-04	-1.07233566E-03
9	-3.31580572E-04	6.21930565E-04	-6.95885435E-04	-4.60465875E-04	-1.13868144E-03
10	-1.38796089E-04	-5.05022058E-04	5.17793275E-04	4.76311169E-05	-2.62664168E-05
11	3.06394904E-04	-4.83516141E-04	-1.71800054E-03	2.81735851E-04	-2.58588877E-03
12	1.71917419E-03	-2.06032497E-03	1.55723819E-03	1.85389501E-04	0.
13	7.61434907E-04	8.50843967E-04	1.22054833E-03	-3.39632134E-03	1.92144616E-03
14	1.22118699E-03	1.22810741E-03	2.00173565E-03	2.89864503E-04	-8.93388665E-04
15	0.	7.96786884E-04	2.99963543E-03	-5.46479570E-04	1.17012021E-03
16	0.	-1.72831925E-03	-1.15451963E-03	2.86397477E-03	4.20366141E-03
17	-9.46930748E-04	-8.46298099E-04	0.	1.12283081E-03	3.34606471E-03
18	2.76742377E-03	2.60195217E-03	3.50049622E-04	1.90173431E-03	-1.99640986E-03
19	2.66128828E-03	3.27939530E-03	4.75478721E-03	-3.70763450E-04	3.44158198E-03
20	0.	-1.87180369E-03	2.59966569E-03	0.	1.11442963E-03
21	3.99776866E-04	1.44093833E-03	1.40785715E-04	4.16174104E-04	1.31398201E-03
22	3.22555235E-03	3.87101043E-03	2.97768013E-03	3.29321267E-03	4.03041574E-03
23	2.15374829E-03	5.99887514E-03	1.71713496E-03	3.31999728E-03	6.17253222E-04
24	6.38184446E-04	3.36582924E-03	4.24194773E-04	1.94870251E-03	2.53754555E-03
25	1.27556282E-03	1.97307783E-03	3.61585190E-03	4.06686395E-03	2.42958869E-03
26	1.35178749E-03	3.01355043E-03	1.63662312E-03	3.8673b643E-04	1.67066823E-04
27	5.90468331E-04	1.56080141E-03	3.58028065E-04	2.48002270E-03	3.07689513E-03
28	1.16271611E-03	2.66660016E-03	-6.47971701E-05	1.32443101E-03	2.76724854E-03

29	3.31583572E-04	-6.13284717E-04	7.38021489E-04	1.96694126E-03	3.22485140E-03
30	0.	9.03832097E-04	-4.18026043E-04	-4.76311159E-05	1.46596818E-04
31	6.35821637E-04	1.28058793E-03	1.88985729E-03	-2.81735851E-04	3.53936381E-03
32	-3.64716558E-04	3.04249020E-03	-1.55723819E-03	-1.85389501E-04	2.52760297E-03
33	-7.61404937E-04	-4.71836379E-04	2.52413171E-04	4.26491956E-03	-1.92144616E-03
34	1.54848460E-04	-1.09925332E-03	-2.00173565E-03	-2.89864503E-04	1.83684402E-03
35	0.	9.31532366E-04	-2.06429381E-03	5.46479570E-04	-1.53424680E-04
36	0.	5.51229216E-03	1.15451960E-03	-2.86397477E-03	-2.04879796E-03
37	9.46930758E-04	3.38090563E-03	0.	-1.12260081E-03	-2.34933391E-03
38	-2.76742377E-03	-2.60195217E-03	7.13147042E-04	0.	1.95640908E-03
39	-1.65277995E-03	-3.27939530E-03	-1.97943954E-03	9.70783450E-04	-1.35504259E-03
40	0.	2.90185945E-03	-2.59965568E-03	0.	-8.57357520E-05
41	3.59487229E-04	-1.21900777E-03	-1.40785715E-04	-4.16174108E-04	-9.78658167E-04
42	-9.58699342E-04	-2.41869224E-03	-1.99961522E-03	-1.51457996E-03	-2.59102216E-03
43	-9.05269351E-04	-1.10647550E-04	-5.63031995E-04	-1.50522156E-03	1.15264172E-03
44	9.42215641E-04	-1.84735203E-04	-4.24194773E-04	0.	-1.60668787E-03
45	0.	-9.10314519E-03	0.	-2.86789125E-03	-6.84546939E-04
46	0.	0.	-1.91733770E-04	-7.86143122E-04	4.76669301E-04
47	-1.15500914E-03	-1.56080141E-03	-2.08754843E-03	0.	-1.90194760E-03
48	0.	-1.15659247E-03	-1.55236843E-03	-1.86270289E-03	-1.69491308E-03
49	0.	-8.64584757E-06	-1.68927772E-03	-1.81709942E-03	-2.11937046E-03
50	0.	-2.21000222E-03	-9.97672327E-05	-3.70770425E-05	-1.19330391E-04
51	-9.42215641E-04	-7.97071787E-04	-1.71856744E-04	3.70770425E-05	-1.08347504E-03
52	-1.35446763E-03	-1.66852033E-03	-2.23020909E-04	3.10624043E-04	-2.52760297E-03
53	0.	-3.79007588E-04	-2.32044433E-03	-8.68598216E-04	0.
54	-1.37503536E-03	-1.28853493E-04	0.	0.	-4.29213187E-03
55	0.	-1.72831925E-03	2.23020909E-04	0.	-2.48140251E-03

VARIANCE AND DEVIATION ANALYSIS

TIME INDEX	MEAN	VARIANCE	DEVIATION	(MEAN)*(DEVIATION)	(MEAN)-(DEVIATION)
1	-3.25223321E-04	9.08875603E-08	3.01475638E-04	-3.37476827E-05	-6.36698954E-04
2	-1.57509414E-03	1.78991873E-07	4.23074311E-04	-1.15201983E-03	-1.99816845E-03
3	-2.37709603E-03	3.15199167E-06	1.77538494E-03	-6.01711097E-04	-4.15248197E-03
4	-1.52821096E-03	1.12076380E-06	1.05865133E-03	-4.69549539E-04	-2.58687219E-03
5	-1.77963844E-03	8.95610341E-07	9.46366917E-04	-8.33271519E-04	-2.72090536E-03
6	-1.33695034E-03	9.19308793E-07	9.58805920E-04	-3.78144463E-04	-2.29575051E-03
7	-9.83491935E-04	6.98999480E-07	8.36061887E-04	-1.47430108E-04	-1.81955388E-03
8	-6.16125979E-04	6.37911074E-07	7.98693354E-04	1.82567375E-04	-1.41481933E-03
9	-3.94336551E-04	3.28465760E-07	5.73113325E-04	1.78182773E-04	-9.68055878E-04
10	-2.09322144E-05	1.08637924E-07	3.29602676E-04	3.08670461E-04	-3.50534890E-04
11	-8.73855113E-04	1.30372674E-06	1.14180591E-03	3.01950794E-04	-1.98166103E-03
12	2.80295382E-04	1.69343628E-06	1.30139865E-03	1.64169403E-03	-1.08113327E-03
13	2.71644339E-04	3.53042881E-06	1.87894354E-03	2.15058793E-03	-1.60729914E-03
14	7.69295154E-04	9.85403794E-07	9.92675070E-04	1.75197022E-03	-2.23379910E-04
15	8.84024591E-04	1.47867317E-06	1.21600706E-03	2.10003165E-03	-3.31982469E-04
16	8.28153466E-04	5.34620943E-06	2.31219715E-03	3.15034662E-03	-1.47402769E-03
17	4.75127327E-04	2.20467208E-06	1.48481382E-03	1.95994115E-03	-1.00968649E-03
18	1.13294994E-03	3.11551595E-06	1.76509242E-03	2.89803236E-03	-6.32132483E-04
19	2.63325396E-03	3.71233355E-06	1.92674169E-03	4.55999556E-03	7.06512173E-04
20	3.68456406E-04	2.16500098E-05	1.47133423E-03	1.83984964E-03	-1.10293881E-03
21	8.14251316E-04	4.24396755E-07	6.51457408E-04	1.46570841E-03	1.62793597E-04
22	3.47161611E-03	1.64757174E-07	4.05902912E-04	3.87751902E-03	3.06571319E-03
23	2.76349178E-03	3.36765972E-06	1.83511845E-03	4.59852023E-03	9.28283389E-04
24	1.78289133E-03	1.25181979E-06	1.11884753E-03	2.90173883E-03	6.64043776E-04
25	2.67218838E-03	1.06675881E-06	1.03284017E-03	3.70502915E-03	1.63934881E-03
26	1.43719230E-03	8.68791228E-07	9.32389713E-04	2.36928261E-03	5.05103191E-04
27	1.61324313E-03	1.10359346E-06	1.05052056E-03	2.66376369E-03	5.62722563E-04
28	1.57123369E-03	1.10693775E-06	1.05211109E-03	2.62334479E-03	5.19122602E-04
29	1.12946210E-03	1.78313699E-06	1.33534152E-03	2.46480362E-03	-2.05879463E-04
30	1.16754349E-04	1.89393439E-07	4.35193634E-04	5.51947983E-04	-3.18439285E-04
31	1.42277896E-03	1.69142859E-05	1.30054934E-03	2.72332830E-03	1.22229623E-04
32	6.92551784E-04	3.16795089E-06	1.77987384E-03	2.47242562E-03	-1.08732216E-03
33	2.72530257E-04	4.47524259E-06	2.11547692E-03	2.38800717E-03	-1.84294666E-03
34	-2.79814203E-04	1.66109884E-05	1.28883664E-03	1.00902244E-03	-1.56867084E-03

35	-1.47941311E-04	1.06836149E-06	1.03361573E-03	8.85674418E-04	-1.18155714E-03
36	3.49807406E-04	8.70057487E-06	2.94967369E-03	3.30048149E-03	-2.59886696E-03
37	1.71140340E-04	3.79216144E-06	1.94734728E-03	2.11848762E-03	-1.77620694E-03
38	-5.39963944E-04	3.45142044E-06	1.86048930E-03	1.32052548E-03	-2.40045214E-03
39	-1.45917479E-03	1.90738033E-06	1.38107941E-03	-7.80953794E-05	-2.64025419E-03
40	4.32936036E-05	3.03539537E-06	1.74223861E-03	1.78553221E-03	-1.59044511E-03
41	-4.79027586E-04	3.23733302E-07	5.68975663E-04	8.99479738E-05	-1.34800336E-03
42	-1.83652196E-03	3.582025516-07	5.98503251E-04	-1.29802171E-03	-2.49502222E-03
43	-3.96315747E-04	7.99374947E-07	8.94077707E-04	5.07771960E-04	-1.28038345E-03
44	-2.54681441E-04	6.71794778E-07	8.19633873E-04	5.64950436E-04	-1.07431122E-03
45	-2.53111658E-03	1.19055798E-05	3.45044632E-03	9.19329642E-04	-5.98156299E-03
46	-1.00242518E-04	1.66351115E-07	4.07861637E-04	3.07619119E-04	-5.08104155E-04
47	-1.34136132E-03	5.50636602E-07	7.42048921E-04	-5.99012395E-04	-2.08311044E-03
48	-1.25331541E-03	4.47189866E-07	6.68722563E-04	-5.84592851E-04	-1.92203798E-03
49	-1.12607869E-03	8.58022075E-07	9.26294810E-04	-1.99703879E-04	-2.05237350E-03
50	-4.93235377E-04	7.38654415E-07	8.59450066E-04	3.66214688E-04	-1.35268544E-03
51	-5.75508434E-04	1.80983113E-07	4.25421101E-04	-1.50087333E-04	-1.00092953E-03
52	-1.09259756E-03	1.03693958E-06	1.01830230E-03	-7.42952547E-05	-2.11089486E-03
53	-7.13610027E-04	7.47275030E-07	8.64450710E-04	1.50840683E-04	-1.57806794E-03
54	-1.15919814E-03	2.72215245E-06	1.64989468E-03	4.90696533E-04	-2.80909242E-03
55	-7.97340170E-04	1.20308549E-06	1.09685254E-03	2.99512367E-04	-1.89419271E-03

```
 05/15/72   UNIV. OF VIRGINIA SCOPE  3.3 APR 01,72 SUM 296
12.25.37.VRNST45
12.25.37.VRNSTO,M2025W,T100,CM41000. BALAKRISHNA
12.25.37.D THANDAR AEROSPACE                    8
12.25.37.MAP(PART)
12.25.37.RUN.
12.25.40.LGO
12.25.44.  (REL - 013200)    CP  000.975 SEC.
12.25.44.                    PP  003.719 SEC.
12.25.44.                    IO  000.345 SEC.
12.25.45.STOP
12.25.45.CP     001.432 SEC.
12.25.45.PP     003.964 SEC.
12.25.45.IO     000.379 SEC.

                VRNST45  //// END OF LIST ////  0000349 LINES
```

Appendix 8

CURVED BOUNDARY PROBLEM NORMAL MODE PROGRAMME

This appendix gives in full details the results of the application of the Normal Mode solution technique (Chapter 9) to a curved boundary problem that is under investigation (Chapter10). Included herein is a complete listing of the programme that was used in these calculations on the CDC 6400 of the Computing Center of the University of Virginia.

In fact here there are two programmes. The first is just a pilot programme. As its output it shows three tables. The first table gives the characteristic values KM(K_{0j} in Chapter 9), and the expansion coefficients AM(α_{0j} in Chapter 9). These characteristic values were taken from Watson (1962, p. 748), and the expansion coefficients were then calculated using Eq. 48 of Chapter 9. The second table gives the Bessel functions of the first

kind and the zeroth order for arguments ranging from 0 to 85 at a step of 0.1, these values were taken from McClain (1962). The third table gives the different arguments that will enter in the evaluation of the integral given by Eq. 32 (Chapter 9) when the source period is divided into 40 subdivisions. Corresponding to these arguments, as required, the Bessel function values were obtained by using the method of linear interpolation in conjunction with the above tabulated values.

The subsequent programme listing corresponds to the programme in which the approximate evaluation of the definite integral was carried out by means of the Chebyshev's formula for $n = 5$. The printout results accompanying this listing correspond to the pressure values shown in Fig. 65.

```
000003          PROGRAM DUCTNRM(INPUT,OUTPUT,TAPE5=INPUT,TAPE6=OUTPUT)
000003          DIMENSION XS(3),XR(3),P(50),E(26),AM(26),AUX(10),BESLJ0(851),
               1ARGMNT(851),RGMNT(26,50),XIB(50),INDX(50)
000003          READ(5,402)Q0,TP,PI,A,C,(XR(I),I=1,3),TPLS,(XS(I),I=1,3)
000037          RSTR=SQRT(XR(1)**2+XR(2)**2)/A $ ZSTR=XR(3)/A $ TPSTR=C*TP/A
000051          ZTPSTP=ZSTR+TPSTR $ TPLSTR=C*TPLS/A $ JSTRT=ZSTR/TPLSTR
000057          JMAX=ZTPSTR/TPLSTR $ TOPITP=2.*PI/TPSTR $ JMAX1=JMAX-JSTRT
000066          WRITE(6,500)Q0,TP,PI,A,C,TPLS,(XS(I),I=1,3),(XR(I),I=1,3),Q0,RSTR,
               1TPSTR,ZSTR,ZTPSTR,TPLSTR,JMAX,JSTRT
                C     CALCULATION OF THE BESSEL-FOURIER SERIES COEFFICIENTS
000142          READ(5,402)ALPHAJ0,(E(I),I=1,26) $ WRITE(6,502)
000162          READ(5,404)(AM(I),I=1,26) $ READ(5,404)(BESLJ0(I),I=1,851)
000206          WRITE(6,503)(I,E(I),AM(I),I=1,26) $ WRITE(6,510) $ DO 28 I=1,851
000231    28    ARGMNT(I)=.1*(I-1.) $ WRITE(6,503)(I,ARGMNT(I),BESLJ0(I),I=1,851)
000253          ZSTR2=ZSTR**2 $ WRITE(6,512)
000260          XL=ZSTR $ DO 22 J=1,JMAX1 $ XL=XL+TPLSTR
000265    22    XIB(J)=SQRT(XL**2-ZSTR2) $ DO 26 M=1,26 $ EIGEN=E(M)
000301          DO 24 J=1,JMAX1 $ RGMNT(M,J)=EIGEN*XIB(J)
000311    24    CONTINUE $ WRITE(6,514)M,EIGEN
000322    26    WRITE(6,514)(J,RGMNT(M,J),J=1,JMAX1) $ WRITE(6,516)
000347          DO 28 J=1,JMAX1 $ INDX(J)=IFIX(10.*RGMNT(1,J))+1
000361    28    CONTINUE $ WRITE(6,514)(INDX(J),RGMNT(1,J),J=1,JMAX1)
                C     FORMATS
000401    402   FORMAT(5E16.8)
000401    404   FORMAT(8E10.3)
000401    500   FORMAT(1H1,30X*TRANSIENT ACOUSTIC FIELD IN CYLINDRICAL DUCT*3(/)
               137X*NORMAL MODE METHOD*3(/)10X*PREASSIGNED CONSTANTS IN DIMENSIONA
               1L FORM(FPS SYSTEM)*//5X*SOURCE STRENGTH FACTOR Q0 = *E10.4,3X*SOUR
               2CE PERIOD TP = *E10.4,3X*PI = *E10.4/5X*DUCT RADIUS A = *E10.4,3X
               3*WAVE SPEED C = *E10.4,3X*ELEMENTAL TIME INTERVAL TPLS = *E10.4/
               45X*SOURCE CARTESIAN COORDINATES XS(1,2,3) = *3(E10.4,2X)/
               55X*RECEIVER CARTESIAN COORDINATES XR(1,2,3) = *3(E10.4,2X)///
               610X*VARIABLES IN NONDIMENSIONAL FORM*//5X*Q0 = *E16.8,2X*RSTR = *
               7E16.8,2X*TPSTR = *E16.8/5X*ZSTR =*E16.8,2X*ZTPSTR =*E16.8,2X*TPLST
               8R = *E16.8,2X*JMAX = *I6,2X*JSTRT = *I4///)
000401    502   FORMAT(20X*CURVED BOUNDARY  CIRCULAR DUCT*//
               110X*TABLE 1  CHARACTERISTIC VALUES KM AND EXPANSION COEFFS. AM*/)
000401    503   FORMAT(5X,4(I3,1X,E10.3,1X,E10.3,4X))
000401    510   FORMAT(10X*TABLE 2  BESSEL FUNCTION J0(X)  (I,X,J0(X))*/)
000401    512   FORMAT(10X*TABLE 3  VALUES OF ARGUMENTS FOR THE BESSEL FUNCTIONS J
               10 IN THE INTEGRAL FOR THE PRESSURE FIELD*//)
000401    514   FORMAT(5X,8(I3,1X,E10.3,1X))
000401    516   FORMAT(10X*PILOT INDEX FOR ARGUMENTS FOR M=1*/)
000401          STOP
000403          END
```

```
DUCTNRM

PROGRAM LENGTH INCLUDING I/O BUFFERS
013150

FUNCTION ASSIGNMENTS

STATEMENT ASSIGNMENTS
402    -  000423    404    -  000425    500    -  000427    502    -  000538
503    -  000546    510    -  000553    512    -  000562    514    -  000576
516    -  000602

BLOCK NAMES AND LENGTHS

VARIABLE ASSIGNMENTS
A      -  007061    ALPHA00-  007076    AM     -  000754    ARGMNT -  002543
AUX    -  001006    BESLJ0 -  001020    C      -  007062    E      -  000722
EIGEN  -  007103    I      -  007063    INDX   -  006774    J      -  007101
JMAX   -  007073    JMAX1  -  007075    JSTRT  -  007072    M      -  007102
P      -  000640    PI     -  007060    Q0     -  007056    RGMNT  -  004266
RSTR   -  007065    TOPITP -  007074    TP     -  007057    TPLS   -  007064
TPLSTR -  007071    TPSTR  -  007067    XI0    -  006712    XL     -  007100
XR     -  000635    XS     -  000632    ZSTR   -  007066    ZSTR2  -  007077
ZTPSTR -  007070

START OF CONSTANTS
000405

START OF TEMPORARIES
000611

START OF INDIRECTS
000630

UNUSED COMPILER SPACE
022600
```

```
CORE MAP  16.36.01.  NORMAL              CONTROL                                                  000100    020604    000000    000006
---TIME---LOAD MODE --L1--L2-----TYPE--------------USER---++---CALL-------------FWA LOAD--LWA LOAD--BLNK COMN--LENGTH--
FWA LOADER  054744  FWA TABLES  053123
-PROGRAM----ADDRESS-                    --LABELED---COMMON--
OUCTNRM       000100
SQRT          013250
SYSTEM        013313                                SCOPE2       013313
GETBA         014425
INPUTC        014444
KODER         014561
KRAKER        016033
OUTPTC        017104
SIO$          017176
------UNSATISFIED EXTERNALS------                                REFERENCES
```

TRANSIENT ACOUSTIC FIELD IN CYLINDRICAL DUCT

NORMAL MODE METHOD

PREASSIGNED CONSTANTS IN DIMENSIONAL FORM(FPS SYSTEM)

SOURCE STRENGTH FACTOR Q0 = 1.0000E+00 SOURCE PERIOD TP = 2.0000E-03 PI = 3.1416E+00
DUCT RADIUS A = 7.5000E+00 WAVE SPEED C = 1.1000E+03 ELEMENTAL TIME INTERVAL TPLS = 5.0000E-05
SOURCE CARTESIAN COORDINATES XS(1,2,3) = 0. 0. 0.
RECEIVER CARTESIAN COORDINATES XR(1,2,3) = 1.0000E+00 3.0000E+00 1.0000E+01

VARIABLES IN NONDIMENSIONAL FORM

Q0 = 1.00000000E+00 RSTR = 4.21637021E-01 TPSTR = 2.93333333E-01
ZSTR = 1.33333333E+00 ZTPSTR = 1.62666667E+00 TPLSTR = 7.33333333E-03 JMAX = 221 JSTRT = 181

CURVED BOUNDARY CIRCULAR DUCT

TABLE 1 CHARACTERISTIC VALUES KM AND EXPANSION COEFFS. AM

1	3.832E+00	3.721E-04	2	7.016E+00	-1.046E-04	3	1.017E+01	-1.381E-01	4	1.332E+01	-5.556E-05
5	1.647E+01	2.635E-05	6	1.962E+01	-2.661E-05	7	2.276E+01	-1.388E-01	8	2.590E+01	-5.398E-06
9	2.905E+01	2.099E-05	10	3.219E+01	-3.437E-07	11	3.533E+01	1.739E-05	12	3.847E+01	-3.357E-06
13	4.162E+01	1.226E-05	14	4.476E+01	-6.263E-06	15	4.790E+01	1.009E-06	16	5.104E+01	-9.560E-06
17	5.419E+01	-2.304E-06	18	5.733E+01	-1.071E-05	19	6.047E+01	2.244E-06	20	6.361E+01	-6.041E-06
21	6.675E+01	4.856E-06	22	6.990E+01	4.251E-06	23	7.304E+01	6.446E-06	24	7.618E+01	2.463E-06
25	7.932E+01	6.354E-06	26	8.246E+01	-2.245E-06						

TABLE 2 BESSEL FUNCTION J0(X) (I,X,J0(X))

1	0.	1.000E+00	2	1.000E-01	9.975E-01	3	2.000E-01	9.900E-01	4	3.000E-01	9.776E-01
5	4.000E-01	9.604E-01	6	5.000E-01	9.385E-01	7	6.000E-01	9.120E-01	8	7.000E-01	8.812E-01
9	8.000E-01	8.463E-01	10	9.000E-01	8.075E-01	11	1.000E+00	7.652E-01	12	1.100E+00	7.196E-01
13	1.200E+00	6.711E-01	14	1.300E+00	6.201E-01	15	1.400E+00	5.669E-01	16	1.500E+00	5.118E-01
17	1.600E+00	4.554E-01	18	1.700E+00	3.980E-01	19	1.800E+00	3.400E-01	20	1.900E+00	2.818E-01
21	2.000E+00	2.239E-01	22	2.100E+00	1.666E-01	23	2.200E+00	1.104E-01	24	2.300E+00	5.554E-02
25	2.400E+00	2.507E-03	26	2.500E+00	-4.838E-02	27	2.600E+00	-9.681E-02	28	2.700E+00	-1.424E-01
29	2.800E+00	-1.850E-01	30	2.900E+00	-2.243E-01	31	3.000E+00	-2.601E-01	32	3.100E+00	-2.921E-01
33	3.200E+00	-3.202E-01	34	3.300E+00	-3.443E-01	35	3.400E+00	-3.643E-01	36	3.500E+00	-3.801E-01
37	3.600E+00	-3.918E-01	38	3.700E+00	-3.992E-01	39	3.800E+00	-4.026E-01	40	3.900E+00	-4.018E-01
41	4.000E+00	-3.971E-01	42	4.100E+00	-3.887E-01	43	4.200E+00	-3.766E-01	44	4.300E+00	-3.610E-01
45	4.400E+00	-3.423E-01	46	4.500E+00	-3.205E-01	47	4.600E+00	-2.961E-01	48	4.700E+00	-2.693E-01
49	4.800E+00	-2.404E-01	50	4.900E+00	-2.097E-01	51	5.000E+00	-1.776E-01	52	5.100E+00	-1.443E-01
53	5.200E+00	-1.103E-01	54	5.300E+00	-7.580E-02	55	5.400E+00	-4.121E-02	56	5.500E+00	-6.843E-03
57	5.600E+00	2.697E-02	58	5.700E+00	5.992E-02	59	5.800E+00	9.170E-02	60	5.900E+00	1.220E-01
61	6.000E+00	1.506E-01	62	6.100E+00	1.773E-01	63	6.200E+00	2.017E-01	64	6.300E+00	2.236E-01
65	6.400E+00	2.433E-01	66	6.500E+00	2.601E-01	67	6.600E+00	2.740E-01	68	6.700E+00	2.851E-01
69	6.800E+00	2.913E-01	70	6.900E+00	2.981E-01	71	7.000E+00	3.001E-01	72	7.100E+00	2.991E-01
73	7.200E+00	2.951E-01	74	7.300E+00	2.882E-01	75	7.400E+00	2.786E-01	76	7.500E+00	2.663E-01
77	7.600E+00	2.516E-01	78	7.700E+00	2.346E-01	79	7.800E+00	2.154E-01	80	7.900E+00	1.944E-01
81	8.000E+00	1.717E-01	82	8.100E+00	1.475E-01	83	8.200E+00	1.222E-01	84	8.300E+00	9.601E-02
85	8.400E+00	6.916E-02	86	8.500E+00	4.194E-02	87	8.600E+00	1.462E-02	88	8.700E+00	-1.252E-02
89	8.800E+00	-3.923E-02	90	8.900E+00	-6.525E-02	91	9.000E+00	-9.033E-02	92	9.100E+00	-1.142E-01
93	9.200E+00	-1.367E-01	94	9.300E+00	-1.577E-01	95	9.400E+00	-1.768E-01	96	9.500E+00	-1.939E-01
97	9.600E+00	-2.090E-01	98	9.700E+00	-2.218E-01	99	9.800E+00	-2.323E-01	100	9.900E+00	-2.403E-01
101	1.000E+01	-2.459E-01	102	1.010E+01	-2.490E-01	103	1.020E+01	-2.496E-01	104	1.030E+01	-2.477E-01
105	1.040E+01	-2.434E-01	106	1.050E+01	-2.366E-01	107	1.060E+01	-2.276E-01	108	1.070E+01	-2.164E-01
109	1.080E+01	-2.032E-01	110	1.090E+01	-1.881E-01	111	1.100E+01	-1.712E-01	112	1.110E+01	-1.528E-01

113	1.120E+01	-1.330E-01	114	1.130E+01	-1.121E-01	115	1.140E+01	-9.021E-02	116	1.150E+01	-6.785E-02
117	1.160E+01	-4.462E-02	118	1.170E+01	-2.133E-02	119	1.180E+01	1.967E-03	120	1.190E+01	2.505E-02
121	1.200E+01	4.769E-02	122	1.210E+01	6.967E-02	123	1.220E+01	9.077E-02	124	1.230E+01	1.108E-01
125	1.240E+01	1.296E-01	126	1.250E+01	1.469E-01	127	1.260E+01	1.626E-01	128	1.270E+01	1.766E-01
129	1.280E+01	1.887E-01	130	1.290E+01	1.989E-01	131	1.300E+01	2.069E-01	132	1.310E+01	2.129E-01
133	1.320E+01	2.167E-01	134	1.330E+01	2.183E-01	135	1.340E+01	2.177E-01	136	1.350E+01	2.150E-01
137	1.360E+01	2.101E-01	138	1.370E+01	2.032E-01	139	1.380E+01	1.943E-01	140	1.390E+01	1.836E-01
141	1.400E+01	1.711E-01	142	1.410E+01	1.570E-01	143	1.420E+01	1.414E-01	144	1.430E+01	1.245E-01
145	1.440E+01	1.065E-01	146	1.450E+01	8.754E-02	147	1.460E+01	6.786E-02	148	1.470E+01	4.764E-02
149	1.480E+01	2.708E-02	150	1.490E+01	6.391E-03	151	1.500E+01	-1.422E-02	152	1.510E+01	-3.456E-02
153	1.520E+01	-5.442E-02	154	1.530E+01	-7.361E-02	155	1.540E+01	-9.194E-02	156	1.550E+01	-1.092E-01
157	1.560E+01	-1.253E-01	158	1.570E+01	-1.401E-01	159	1.580E+01	-1.533E-01	160	1.590E+01	-1.650E-01
161	1.600E+01	-1.749E-01	162	1.610E+01	-1.830E-01	163	1.620E+01	-1.893E-01	164	1.630E+01	-1.936E-01
165	1.640E+01	-1.960E-01	166	1.650E+01	-1.964E-01	167	1.660E+01	-1.948E-01	168	1.670E+01	-1.913E-01
169	1.680E+01	-1.860E-01	170	1.690E+01	-1.788E-01	171	1.700E+01	-1.699E-01	172	1.710E+01	-1.593E-01
173	1.720E+01	-1.472E-01	174	1.730E+01	-1.337E-01	175	1.740E+01	-1.190E-01	176	1.750E+01	-1.031E-01
177	1.760E+01	-8.633E-02	178	1.770E+01	-6.870E-02	179	1.780E+01	-5.065E-02	180	1.790E+01	-3.211E-02
181	1.800E+01	-1.336E-02	182	1.810E+01	5.427E-03	183	1.820E+01	2.405E-02	184	1.830E+01	4.234E-02
185	1.840E+01	6.010E-02	186	1.850E+01	7.716E-02	187	1.860E+01	9.337E-02	188	1.870E+01	1.086E-01
189	1.880E+01	1.226E-01	190	1.890E+01	1.353E-01	191	1.900E+01	1.466E-01	192	1.910E+01	1.564E-01
193	1.920E+01	1.646E-01	194	1.930E+01	1.711E-01	195	1.940E+01	1.759E-01	196	1.950E+01	1.789E-01
197	1.960E+01	1.800E-01	198	1.970E+01	1.794E-01	199	1.980E+01	1.770E-01	200	1.990E+01	1.729E-01
201	2.000E+01	1.670E-01	202	2.010E+01	1.595E-01	203	2.020E+01	1.505E-01	204	2.030E+01	1.400E-01
205	2.040E+01	1.282E-01	206	2.050E+01	1.151E-01	207	2.060E+01	1.010E-01	208	2.070E+01	8.587E-02
209	2.080E+01	7.001E-02	210	2.090E+01	5.352E-02	211	2.100E+01	3.658E-02	212	2.110E+01	1.935E-02
213	2.120E+01	2.017E-03	214	2.130E+01	-1.526E-02	215	2.140E+01	-3.230E-02	216	2.150E+01	-4.894E-02
217	2.160E+01	-6.502E-02	218	2.170E+01	-8.037E-02	219	2.180E+01	-9.485E-02	220	2.190E+01	-1.083E-01
221	2.200E+01	-1.207E-01	222	2.210E+01	-1.317E-01	223	2.220E+01	-1.414E-01	224	2.230E+01	-1.497E-01
225	2.240E+01	-1.564E-01	226	2.250E+01	-1.615E-01	227	2.260E+01	-1.650E-01	228	2.270E+01	-1.669E-01
229	2.280E+01	-1.671E-01	230	2.290E+01	-1.656E-01	231	2.300E+01	-1.624E-01	232	2.310E+01	-1.577E-01
233	2.320E+01	-1.514E-01	234	2.330E+01	-1.436E-01	235	2.340E+01	-1.344E-01	236	2.350E+01	-1.239E-01
237	2.360E+01	-1.123E-01	238	2.370E+01	-9.952E-02	239	2.380E+01	-8.584E-02	240	2.390E+01	-7.136E-02
241	2.400E+01	-5.623E-02	242	2.410E+01	-4.060E-02	243	2.420E+01	-2.464E-02	244	2.430E+01	-8.490E-03
245	2.440E+01	7.675E-03	246	2.450E+01	2.370E-02	247	2.460E+01	3.942E-02	248	2.470E+01	5.468E-02
249	2.480E+01	6.934E-02	250	2.490E+01	8.325E-02	251	2.500E+01	9.627E-02	252	2.510E+01	1.083E-01
253	2.520E+01	1.192E-01	254	2.530E+01	1.288E-01	255	2.540E+01	1.371E-01	256	2.550E+01	1.441E-01
257	2.560E+01	1.495E-01	258	2.570E+01	1.535E-01	259	2.580E+01	1.559E-01	260	2.590E+01	1.567E-01
261	2.600E+01	1.560E-01	262	2.610E+01	1.537E-01	263	2.620E+01	1.499E-01	264	2.630E+01	1.446E-01
265	2.640E+01	1.379E-01	266	2.650E+01	1.299E-01	267	2.660E+01	1.206E-01	268	2.670E+01	1.101E-01
269	2.680E+01	9.852E-02	270	2.690E+01	8.604E-02	271	2.700E+01	7.274E-02	272	2.710E+01	5.877E-02
273	2.720E+01	4.426E-02	274	2.730E+01	2.936E-02	275	2.740E+01	1.423E-02	276	2.750E+01	-9.923E-04
277	2.760E+01	-1.615E-02	278	2.770E+01	-3.109E-02	279	2.780E+01	-4.567E-02	280	2.790E+01	-5.973E-02
281	2.800E+01	-7.316E-02	282	2.810E+01	-8.580E-02	283	2.820E+01	-9.755E-02	284	2.830E+01	-1.083E-01
285	2.840E+01	-1.179E-01	286	2.850E+01	-1.263E-01	287	2.860E+01	-1.334E-01	288	2.870E+01	-1.392E-01
289	2.880E+01	-1.435E-01	290	2.890E+01	-1.464E-01	291	2.900E+01	-1.478E-01	292	2.910E+01	-1.478E-01
293	2.920E+01	-1.463E-01	294	2.930E+01	-1.433E-01	295	2.940E+01	-1.389E-01	296	2.950E+01	-1.331E-01
297	2.960E+01	-1.261E-01	298	2.970E+01	-1.178E-01	299	2.980E+01	-1.083E-01	300	2.990E+01	-9.781E-02
301	3.000E+01	-8.637E-02	302	3.010E+01	-7.410E-02	303	3.020E+01	-6.114E-02	304	3.030E+01	-4.760E-02
305	3.040E+01	-3.364E-02	306	3.050E+01	-1.939E-02	307	3.060E+01	-4.991E-03	308	3.070E+01	9.411E-03
309	3.080E+01	2.367E-02	310	3.090E+01	3.765E-02	311	3.100E+01	5.121E-02	312	3.110E+01	6.421E-02
313	3.120E+01	7.653E-02	314	3.130E+01	8.805E-02	315	3.140E+01	9.865E-02	316	3.150E+01	1.082E-01
317	3.160E+01	1.167E-01	318	3.170E+01	1.240E-01	319	3.180E+01	1.300E-01	320	3.190E+01	1.347E-01
321	3.200E+01	1.381E-01	322	3.210E+01	1.400E-01	323	3.220E+01	1.406E-01	324	3.230E+01	1.398E-01
325	3.240E+01	1.375E-01	326	3.250E+01	1.339E-01	327	3.260E+01	1.290E-01	328	3.270E+01	1.226E-01
329	3.280E+01	1.154E-01	330	3.290E+01	1.068E-01	331	3.300E+01	9.727E-02	332	3.310E+01	8.676E-02
333	3.320E+01	7.541E-02	334	3.330E+01	6.334E-02	335	3.340E+01	5.068E-02	336	3.350E+01	3.754E-02
337	3.360E+01	2.408E-02	338	3.370E+01	1.041E-02	339	3.380E+01	-3.318E-03	340	3.390E+01	-1.697E-02
341	3.400E+01	-3.042E-02	342	3.410E+01	-4.352E-02	343	3.420E+01	-5.616E-02	344	3.430E+01	-6.819E-02
345	3.440E+01	-7.951E-02	346	3.450E+01	-9.000E-02	347	3.460E+01	-9.956E-02	348	3.470E+01	-1.081E-01
349	3.480E+01	-1.155E-01	350	3.490E+01	-1.218E-01	351	3.500E+01	-1.268E-01	352	3.510E+01	-1.306E-01
353	3.520E+01	-1.330E-01	354	3.530E+01	-1.341E-01	355	3.540E+01	-1.339E-01	356	3.550E+01	-1.323E-01
357	3.560E+01	-1.294E-01	358	3.570E+01	-1.253E-01	359	3.580E+01	-1.199E-01	360	3.590E+01	-1.133E-01
361	3.600E+01	-1.056E-01	362	3.610E+01	-9.683E-02	363	3.620E+01	-8.716E-02	364	3.630E+01	-7.664E-02
365	3.640E+01	-6.538E-02	366	3.650E+01	-5.350E-02	367	3.660E+01	-4.113E-02	368	3.670E+01	-2.837E-02
369	3.680E+01	-1.537E-02	370	3.690E+01	-2.246E-03	371	3.700E+01	1.086E-02	372	3.710E+01	2.383E-02
373	3.720E+01	3.652E-02	374	3.730E+01	4.881E-02	375	3.740E+01	6.059E-02	376	3.750E+01	7.172E-02

377	3.760E+01	8.211E-02	378	3.770E+01	9.186E-02	379	3.780E+01	1.003E-01	380	3.790E+01	1.078E-01
381	3.800E+01	1.143E-01	382	3.810E+01	1.197E-01	383	3.820E+01	1.230E-01	384	3.830E+01	1.267E-01
385	3.840E+01	1.263E-01	386	3.850E+01	1.286E-01	387	3.860E+01	1.276E-01	388	3.870E+01	1.254E-01
389	3.880E+01	1.219E-01	390	3.890E+01	1.172E-01	391	3.900E+01	1.114E-01	392	3.910E+01	1.044E-01
393	3.920E+01	9.645E-02	394	3.930E+01	8.754E-02	395	3.940E+01	7.778E-02	396	3.950E+01	6.727E-02
397	3.960E+01	5.611E-02	398	3.970E+01	4.442E-02	399	3.980E+01	3.232E-02	400	3.990E+01	1.993E-02
401	4.000E+01	7.367E-03	402	4.010E+01	-5.237E-03	403	4.020E+01	-1.776E-02	404	4.030E+01	-3.007E-02
405	4.040E+01	-4.205E-02	406	4.050E+01	-5.358E-02	407	4.060E+01	-6.456E-02	408	4.070E+01	-7.485E-02
409	4.080E+01	-8.437E-02	410	4.090E+01	-9.304E-02	411	4.100E+01	-1.007E-01	412	4.110E+01	-1.074E-01
413	4.120E+01	-1.130E-01	414	4.130E+01	-1.175E-01	415	4.140E+01	-1.208E-01	416	4.150E+01	-1.228E-01
417	4.160E+01	-1.236E-01	418	4.170E+01	-1.232E-01	419	4.180E+01	-1.216E-01	420	4.190E+01	-1.188E-01
421	4.200E+01	-1.147E-01	422	4.210E+01	-1.096E-01	423	4.220E+01	-1.033E-01	424	4.230E+01	-9.606E-02
425	4.240E+01	-8.786E-02	426	4.250E+01	-7.883E-02	427	4.260E+01	-6.901E-02	428	4.270E+01	-5.852E-02
429	4.280E+01	-4.747E-02	430	4.290E+01	-3.598E-02	431	4.300E+01	-2.415E-02	432	4.310E+01	-1.211E-02
433	4.320E+01	2.533E-05	434	4.330E+01	1.213E-02	435	4.340E+01	2.409E-02	436	4.350E+01	3.578E-02
437	4.360E+01	4.708E-02	438	4.370E+01	5.789E-02	439	4.380E+01	6.810E-02	440	4.390E+01	7.760E-02
441	4.400E+01	8.631E-02	442	4.410E+01	9.413E-02	443	4.420E+01	1.010E-01	444	4.430E+01	1.060E-01
445	4.440E+01	1.116E-01	446	4.450E+01	1.153E-01	447	4.460E+01	1.177E-01	448	4.470E+01	1.190E-01
449	4.480E+01	1.192E-01	450	4.490E+01	1.181E-01	451	4.500E+01	1.158E-01	452	4.510E+01	1.124E-01
453	4.520E+01	1.079E-01	454	4.530E+01	1.023E-01	455	4.540E+01	9.571E-02	456	4.550E+01	8.818E-02
457	4.560E+01	7.978E-02	458	4.570E+01	7.060E-02	459	4.580E+01	6.074E-02	460	4.590E+01	5.029E-02
461	4.600E+01	3.936E-02	462	4.610E+01	2.807E-02	463	4.620E+01	1.652E-02	464	4.630E+01	4.828E-03
465	4.640E+01	-6.685E-03	466	4.650E+01	-1.850E-02	467	4.660E+01	-2.991E-02	468	4.670E+01	-4.100E-02
469	4.680E+01	-5.166E-02	470	4.690E+01	-6.177E-02	471	4.700E+01	-7.125E-02	472	4.710E+01	-8.000E-02
473	4.720E+01	-8.792E-02	474	4.730E+01	-9.496E-02	475	4.740E+01	-1.010E-01	476	4.750E+01	-1.061E-01
477	4.750E+01	-1.101E-01	478	4.770E+01	-1.129E-01	479	4.780E+01	-1.147E-01	480	4.790E+01	-1.153E-01
481	4.800E+01	-1.147E-01	482	4.810E+01	-1.130E-01	483	4.820E+01	-1.102E-01	484	4.830E+01	-1.063E-01
485	4.840E+01	-1.013E-01	486	4.850E+01	-9.532E-02	487	4.860E+01	-8.840E-02	488	4.870E+01	-8.062E-02
489	4.880E+01	-7.205E-02	490	4.890E+01	-6.278E-02	491	4.900E+01	-5.290E-02	492	4.910E+01	-4.251E-02
493	4.920E+01	-3.172E-02	494	4.930E+01	-2.064E-02	495	4.940E+01	-9.367E-03	496	4.950E+01	1.972E-03
497	4.960E+01	1.327E-02	498	4.970E+01	2.441E-02	499	4.980E+01	3.529E-02	500	4.990E+01	4.579E-02
501	5.000E+01	5.581E-02	502	5.010E+01	6.526E-02	503	5.020E+01	7.404E-02	504	5.030E+01	8.206E-02
505	5.040E+01	8.924E-02	506	5.050E+01	9.552E-02	507	5.060E+01	1.008E-01	508	5.070E+01	1.051E-01
509	5.080E+01	1.084E-01	510	5.090E+01	1.105E-01	511	5.100E+01	1.116E-01	512	5.110E+01	1.115E-01
513	5.120E+01	1.103E-01	514	5.130E+01	1.080E-01	515	5.140E+01	1.047E-01	516	5.150E+01	1.003E-01
517	5.160E+01	9.488E-02	518	5.170E+01	8.856E-02	519	5.180E+01	8.136E-02	520	5.190E+01	7.337E-02
521	5.200E+01	6.465E-02	522	5.210E+01	5.531E-02	523	5.220E+01	4.544E-02	524	5.230E+01	3.513E-02
525	5.240E+01	2.449E-02	526	5.250E+01	1.363E-02	527	5.260E+01	2.646E-03	528	5.270E+01	-8.340E-03
529	5.280E+01	-1.922E-02	530	5.290E+01	-2.989E-02	531	5.300E+01	-4.024E-02	532	5.310E+01	-5.017E-02
533	5.320E+01	-5.958E-02	534	5.330E+01	-6.838E-02	535	5.340E+01	-7.647E-02	536	5.350E+01	-8.379E-02
537	5.360E+01	-9.026E-02	538	5.370E+01	-9.582E-02	539	5.380E+01	-1.004E-01	540	5.390E+01	-1.040E-01
541	5.400E+01	-1.065E-01	542	5.410E+01	-1.080E-01	543	5.420E+01	-1.084E-01	544	5.430E+01	-1.077E-01
545	5.440E+01	-1.059E-01	546	5.450E+01	-1.031E-01	547	5.460E+01	-9.923E-02	548	5.470E+01	-9.448E-02
549	5.480E+01	-8.863E-02	550	5.490E+01	-8.199E-02	551	5.500E+01	-7.455E-02	552	5.510E+01	-6.637E-02
553	5.520E+01	-5.755E-02	554	5.530E+01	-4.816E-02	555	5.540E+01	-3.832E-02	556	5.550E+01	-2.810E-02
557	5.560E+01	-1.763E-02	558	5.570E+01	-6.999E-03	559	5.580E+01	3.683E-03	560	5.590E+01	1.431E-02
561	5.600E+01	2.477E-02	562	5.610E+01	3.497E-02	563	5.620E+01	4.480E-02	564	5.630E+01	5.417E-02
565	5.640E+01	6.298E-02	566	5.650E+01	7.114E-02	567	5.660E+01	7.858E-02	568	5.670E+01	8.523E-02
569	5.680E+01	9.101E-02	570	5.690E+01	9.587E-02	571	5.700E+01	9.976E-02	572	5.710E+01	1.027E-01
573	5.720E+01	1.045E-01	574	5.730E+01	1.053E-01	575	5.740E+01	1.051E-01	576	5.750E+01	1.038E-01
577	5.760E+01	1.015E-01	578	5.770E+01	9.816E-02	579	5.780E+01	9.386E-02	580	5.790E+01	8.863E-02
581	5.800E+01	8.252E-02	582	5.810E+01	7.560E-02	583	5.820E+01	6.793E-02	584	5.830E+01	5.961E-02
585	5.840E+01	5.070E-02	586	5.850E+01	4.129E-02	587	5.860E+01	3.150E-02	588	5.870E+01	2.140E-02
589	5.880E+01	1.111E-02	590	5.890E+01	7.260E-04	591	5.900E+01	-9.648E-03	592	5.910E+01	-1.991E-02
593	5.920E+01	-2.995E-02	594	5.930E+01	-3.965E-02	595	5.940E+01	-4.900E-02	596	5.950E+01	-5.781E-02
597	5.960E+01	-6.603E-02	598	5.970E+01	-7.357E-02	599	5.980E+01	-8.037E-02	600	5.990E+01	-8.636E-02
601	6.000E+01	-9.147E-02	602	6.010E+01	-9.566E-02	603	6.020E+01	-9.889E-02	604	6.030E+01	-1.011E-01
605	6.040E+01	-1.024E-01	606	6.050E+01	-1.026E-01	607	6.060E+01	-1.017E-01	608	6.070E+01	-9.989E-02
609	6.080E+01	-9.706E-02	610	6.090E+01	-9.326E-02	611	6.100E+01	-8.854E-02	612	6.110E+01	-8.294E-02
613	6.120E+01	-7.652E-02	614	6.130E+01	-6.935E-02	615	6.140E+01	-6.150E-02	616	6.150E+01	-5.305E-02
617	6.160E+01	-4.408E-02	618	6.170E+01	-3.469E-02	619	6.180E+01	-2.496E-02	620	6.190E+01	-1.500E-02
621	6.200E+01	-4.910E-03	622	6.210E+01	5.215E-03	623	6.220E+01	1.527E-02	624	6.230E+01	2.516E-02
625	6.240E+01	3.478E-02	626	6.250E+01	4.404E-02	627	6.260E+01	5.284E-02	628	6.270E+01	6.110E-02
629	6.280E+01	6.874E-02	630	6.290E+01	7.568E-02	631	6.300E+01	8.186E-02	632	6.310E+01	8.720E-02
633	6.320E+01	9.167E-02	634	6.330E+01	9.522E-02	635	6.340E+01	9.781E-02	636	6.350E+01	9.942E-02
637	6.360E+01	1.000E-01	638	6.370E+01	9.964E-02	639	6.380E+01	9.826E-02	640	6.390E+01	9.590E-02

641	6.400E+01	9.259E-02	642	6.410E+01	8.836E-02	643	6.420E+01	8.325E-02	644	6.430E+01	7.732E-02
645	6.440E+01	7.063E-02	646	6.450E+01	6.324E-02	647	6.460E+01	5.523E-02	648	6.470E+01	4.668E-02
649	6.480E+01	3.760E-02	650	6.490E+01	2.832E-02	651	6.500E+01	1.869E-02	652	6.510E+01	8.885E-03
653	6.520E+01	-9.917E-04	654	6.530E+01	-1.084E-02	655	6.540E+01	-2.057E-02	656	6.550E+01	-3.008E-02
657	6.560E+01	-3.927E-02	658	6.570E+01	-4.806E-02	659	6.580E+01	-5.635E-02	660	6.590E+01	-6.407E-02
661	6.600E+01	-7.114E-02	662	6.610E+01	-7.748E-02	663	6.620E+01	-8.305E-02	664	6.630E+01	-8.777E-02
665	6.640E+01	-9.161E-02	666	6.650E+01	-9.453E-02	667	6.660E+01	-9.651E-02	668	6.670E+01	-9.751E-02
669	6.680E+01	-9.755E-02	670	6.690E+01	-9.660E-02	671	6.700E+01	-9.470E-02	672	6.710E+01	-9.185E-02
673	6.720E+01	-8.809E-02	674	6.730E+01	-8.345E-02	675	6.740E+01	-7.799E-02	676	6.750E+01	-7.176E-02
677	6.760E+01	-6.482E-02	678	6.770E+01	-5.725E-02	679	6.780E+01	-4.911E-02	680	6.790E+01	-4.049E-02
681	6.800E+01	-3.149E-02	682	6.810E+01	-2.218E-02	683	6.820E+01	-1.267E-02	684	6.830E+01	-3.038E-03
685	6.840E+01	6.606E-03	686	6.850E+01	1.617E-02	687	6.860E+01	2.556E-02	688	6.870E+01	3.468E-02
689	6.880E+01	4.344E-02	690	6.890E+01	5.175E-02	691	6.900E+01	5.954E-02	692	6.910E+01	6.672E-02
693	6.920E+01	7.322E-02	694	6.930E+01	7.898E-02	695	6.940E+01	8.395E-02	696	6.950E+01	8.807E-02
697	6.960E+01	9.130E-02	698	6.970E+01	9.362E-02	699	6.980E+01	9.500E-02	700	6.990E+01	9.543E-02
701	7.000E+01	9.491E-02	702	7.010E+01	9.344E-02	703	7.020E+01	9.104E-02	704	7.030E+01	8.773E-02
705	7.040E+01	8.355E-02	706	7.050E+01	7.855E-02	707	7.060E+01	7.276E-02	708	7.070E+01	6.626E-02
709	7.080E+01	5.911E-02	710	7.090E+01	5.137E-02	711	7.100E+01	4.314E-02	712	7.110E+01	3.448E-02
713	7.120E+01	2.549E-02	714	7.130E+01	1.626E-02	715	7.140E+01	6.885E-03	716	7.150E+01	-2.549E-03
717	7.160E+01	-1.195E-02	718	7.170E+01	-2.121E-02	719	7.180E+01	-3.025E-02	720	7.190E+01	-3.897E-02
721	7.200E+01	-4.729E-02	722	7.210E+01	-5.513E-02	723	7.220E+01	-6.241E-02	724	7.230E+01	-6.906E-02
725	7.240E+01	-7.500E-02	726	7.250E+01	-8.019E-02	727	7.260E+01	-8.457E-02	728	7.270E+01	-8.810E-02
729	7.280E+01	-9.075E-02	730	7.290E+01	-9.248E-02	731	7.300E+01	-9.329E-02	732	7.310E+01	-9.317E-02
733	7.320E+01	-9.212E-02	734	7.330E+01	-9.015E-02	735	7.340E+01	-8.728E-02	736	7.350E+01	-8.355E-02
737	7.360E+01	-7.898E-02	738	7.370E+01	-7.363E-02	739	7.380E+01	-6.756E-02	740	7.390E+01	-6.082E-02
741	7.400E+01	-5.348E-02	742	7.410E+01	-4.561E-02	743	7.420E+01	-3.730E-02	744	7.430E+01	-2.863E-02
745	7.440E+01	-1.969E-02	746	7.450E+01	-1.056E-02	747	7.460E+01	-1.339E-03	748	7.470E+01	7.884E-03
749	7.480E+01	1.702E-02	750	7.490E+01	2.597E-02	751	7.500E+01	3.464E-02	752	7.510E+01	4.297E-02
753	7.520E+01	5.085E-02	754	7.530E+01	5.821E-02	755	7.540E+01	6.498E-02	756	7.550E+01	7.110E-02
757	7.560E+01	7.649E-02	758	7.570E+01	8.112E-02	759	7.580E+01	8.493E-02	760	7.590E+01	8.788E-02
761	7.600E+01	8.996E-02	762	7.610E+01	9.113E-02	763	7.620E+01	9.139E-02	764	7.630E+01	9.074E-02
765	7.640E+01	8.919E-02	766	7.650E+01	8.674E-02	767	7.660E+01	8.343E-02	768	7.670E+01	7.930E-02
769	7.680E+01	7.438E-02	770	7.690E+01	6.872E-02	771	7.700E+01	6.238E-02	772	7.710E+01	5.543E-02
773	7.720E+01	4.793E-02	774	7.730E+01	3.997E-02	775	7.740E+01	3.161E-02	776	7.750E+01	2.295E-02
777	7.760E+01	1.407E-02	778	7.770E+01	5.069E-03	779	7.780E+01	-3.977E-03	780	7.790E+01	-1.297E-02
781	7.800E+01	-2.182E-02	782	7.810E+01	-3.045E-02	783	7.820E+01	-3.876E-02	784	7.830E+01	-4.667E-02
785	7.840E+01	-5.410E-02	786	7.850E+01	-6.099E-02	787	7.860E+01	-6.725E-02	788	7.870E+01	-7.284E-02
789	7.880E+01	-7.770E-02	790	7.890E+01	-8.177E-02	791	7.900E+01	-8.502E-02	792	7.910E+01	-8.741E-02
793	7.920E+01	-8.894E-02	794	7.930E+01	-8.957E-02	795	7.940E+01	-8.930E-02	796	7.950E+01	-8.815E-02
797	7.960E+01	-8.611E-02	798	7.970E+01	-8.322E-02	799	7.980E+01	-7.950E-02	800	7.990E+01	-7.499E-02
801	8.000E+01	-6.974E-02	802	8.010E+01	-6.380E-02	803	8.020E+01	-5.723E-02	804	8.030E+01	-5.010E-02
805	8.040E+01	-4.247E-02	806	8.050E+01	-3.443E-02	807	8.060E+01	-2.606E-02	808	8.070E+01	-1.743E-02
809	8.080E+01	-8.646E-03	810	8.090E+01	2.169E-04	811	8.100E+01	9.066E-03	812	8.110E+01	1.781E-02
813	8.120E+01	2.637E-02	814	8.130E+01	3.466E-02	815	8.140E+01	4.259E-02	816	8.150E+01	5.008E-02
817	8.160E+01	5.707E-02	818	8.170E+01	6.347E-02	819	8.180E+01	6.924E-02	820	8.190E+01	7.431E-02
821	8.200E+01	7.862E-02	822	8.210E+01	8.215E-02	823	8.220E+01	8.485E-02	824	8.230E+01	8.671E-02
825	8.240E+01	8.769E-02	826	8.250E+01	8.780E-02	827	8.260E+01	8.703E-02	828	8.270E+01	8.539E-02
829	8.280E+01	8.290E-02	830	8.290E+01	7.959E-02	831	8.300E+01	7.549E-02	832	8.310E+01	7.064E-02
833	8.320E+01	6.508E-02	834	8.330E+01	5.889E-02	835	8.340E+01	5.211E-02	836	8.350E+01	4.482E-02
837	8.360E+01	3.710E-02	838	8.370E+01	2.901E-02	839	8.380E+01	2.064E-02	840	8.390E+01	1.208E-02
841	8.400E+01	3.402E-03	842	8.410E+01	-5.296E-03	843	8.420E+01	-1.393E-02	844	8.430E+01	-2.242E-02
845	8.440E+01	-3.067E-02	846	8.450E+01	-3.861E-02	847	8.460E+01	-4.615E-02	848	8.470E+01	-5.322E-02
849	8.480E+01	-5.975E-02	850	8.490E+01	-6.568E-02	851	8.500E+01	-7.094E-02			

TABLE 3 VALUES OF ARGUMENTS FOR THE BESSEL FUNCTIONS J0 IN THE INTEGRAL FOR THE PRESSURE FIELD

1	3.832E+00														
1	5.366E-01	2	7.599E-01	3	9.319E-01	4	1.078E+00	5	1.206E+00	6	1.323E+00	7	1.431E+00	8	1.532E+00
9	1.627E+00	10	1.718E+00	11	1.804E+00	12	1.887E+00	13	1.966E+00	14	2.043E+00	15	2.118E+00	16	2.190E+00
17	2.260E+00	18	2.329E+00	19	2.396E+00	20	2.461E+00	21	2.525E+00	22	2.588E+00	23	2.650E+00	24	2.710E+00
25	2.770E+00	26	2.828E+00	27	2.886E+00	28	2.942E+00	29	2.998E+00	30	3.054E+00	31	3.108E+00	32	3.162E+00
33	3.215E+00	34	3.267E+00	35	3.319E+00	36	3.370E+00	37	3.421E+00	38	3.471E+00	39	3.521E+00	40	3.570E+00
2	7.016E+00														
1	9.824E-01	2	1.391E+00	3	1.706E+00	4	1.973E+00	5	2.209E+00	6	2.423E+00	7	2.621E+00	8	2.805E+00
9	2.979E+00	10	3.145E+00	11	3.303E+00	12	3.454E+00	13	3.600E+00	14	3.741E+00	15	3.877E+00	16	4.010E+00
17	4.139E+00	18	4.264E+00	19	4.387E+00	20	4.507E+00	21	4.624E+00	22	4.739E+00	23	4.852E+00	24	4.962E+00

25	5.071E+00	26	5.178E+00	27	5.284E+00	28	5.387E+00	29	5.490E+00	30	5.591E+00	31	5.690E+00	32	5.789E+00
33	5.886E+00	34	5.982E+00	35	6.077E+00	36	6.171E+00	37	6.264E+00	38	6.356E+00	39	6.447E+00	40	6.537E+00
3	1.017E+01														
1	1.425E+00	2	2.017E+00	3	2.474E+00	4	2.861E+00	5	3.203E+00	6	3.51JE+00	7	3.800E+00	8	4.068E+00
9	4.321E+00	10	4.560E+00	11	4.789E+00	12	5.009E+00	13	5.220E+00	14	5.425E+00	15	5.622E+00	16	5.815E+00
17	6.001E+00	18	6.183E+00	19	6.361E+00	20	6.535E+00	21	6.705E+00	22	6.872E+00	23	7.035E+00	24	7.196E+00
25	7.354E+00	26	7.509E+00	27	7.662E+00	28	7.813E+00	29	7.961E+00	30	8.107E+00	31	8.252E+00	32	8.394E+00
33	8.535E+00	34	8.675E+00	35	8.812E+00	36	8.949E+00	37	9.083E+00	38	9.217E+00	39	9.349E+00	40	9.480E+00
4	1.332E+01														
1	1.866E+00	2	2.642E+00	3	3.240E+00	4	3.747E+00	5	4.195E+00	6	4.601E+00	7	4.977E+00	8	5.328E+00
9	5.658E+00	10	5.972E+00	11	6.272E+00	12	6.560E+00	13	6.837E+00	14	7.104E+00	15	7.363E+00	16	7.615E+00
17	7.860E+00	18	8.098E+00	19	8.331E+00	20	8.559E+00	21	8.781E+00	22	9.000E+00	23	9.214E+00	24	9.424E+00
25	9.631E+00	26	9.834E+00	27	1.003E+01	28	1.023E+01	29	1.043E+01	30	1.062E+01	31	1.081E+01	32	1.099E+01
33	1.118E+01	34	1.136E+01	35	1.154E+01	36	1.172E+01	37	1.190E+01	38	1.207E+01	39	1.224E+01	40	1.242E+01
5	1.647E+01														
1	2.306E+00	2	3.266E+00	3	4.006E+00	4	4.632E+00	5	5.186E+00	6	5.688E+00	7	6.152E+00	8	6.586E+00
9	6.995E+00	10	7.383E+00	11	7.754E+00	12	8.109E+00	13	8.452E+00	14	8.782E+00	15	9.103E+00	16	9.414E+00
17	9.716E+00	18	1.001E+01	19	1.030E+01	20	1.058E+01	21	1.086E+01	22	1.113E+01	23	1.139E+01	24	1.165E+01
25	1.191E+01	26	1.216E+01	27	1.240E+01	28	1.265E+01	29	1.289E+01	30	1.313E+01	31	1.336E+01	32	1.359E+01
33	1.382E+01	34	1.404E+01	35	1.427E+01	36	1.449E+01	37	1.471E+01	38	1.492E+01	39	1.514E+01	40	1.535E+01
6	1.962E+01														
1	2.747E+00	2	3.890E+00	3	4.771E+00	4	5.516E+00	5	6.176E+00	6	6.774E+00	7	7.327E+00	8	7.844E+00
9	8.331E+00	10	8.793E+00	11	9.234E+00	12	9.658E+00	13	1.007E+01	14	1.046E+01	15	1.084E+01	16	1.121E+01
17	1.157E+01	18	1.192E+01	19	1.227E+01	20	1.260E+01	21	1.293E+01	22	1.325E+01	23	1.357E+01	24	1.387E+01
25	1.418E+01	26	1.448E+01	27	1.477E+01	28	1.506E+01	29	1.535E+01	30	1.563E+01	31	1.591E+01	32	1.619E+01
33	1.646E+01	34	1.673E+01	35	1.699E+01	36	1.725E+01	37	1.751E+01	38	1.777E+01	39	1.803E+01	40	1.828E+01
7	2.276E+01														
1	3.187E+00	2	4.514E+00	3	5.535E+00	4	6.401E+00	5	7.166E+00	6	7.860E+00	7	8.502E+00	8	9.101E+00
9	9.666E+00	10	1.020E+01	11	1.071E+01	12	1.121E+01	13	1.168E+01	14	1.214E+01	15	1.258E+01	16	1.301E+01
17	1.343E+01	18	1.383E+01	19	1.423E+01	20	1.462E+01	21	1.500E+01	22	1.537E+01	23	1.574E+01	24	1.610E+01
25	1.645E+01	26	1.680E+01	27	1.714E+01	28	1.748E+01	29	1.781E+01	30	1.814E+01	31	1.846E+01	32	1.878E+01
33	1.910E+01	34	1.941E+01	35	1.972E+01	36	2.002E+01	37	2.032E+01	38	2.062E+01	39	2.092E+01	40	2.121E+01
8	2.590E+01														
1	3.627E+00	2	5.137E+00	3	6.300E+00	4	7.285E+00	5	8.155E+00	6	8.946E+00	7	9.676E+00	8	1.036E+01
9	1.100E+01	10	1.161E+01	11	1.219E+01	12	1.275E+01	13	1.329E+01	14	1.381E+01	15	1.432E+01	16	1.480E+01
17	1.528E+01	18	1.574E+01	19	1.620E+01	20	1.664E+01	21	1.707E+01	22	1.750E+01	23	1.791E+01	24	1.832E+01
25	1.872E+01	26	1.912E+01	27	1.951E+01	28	1.989E+01	29	2.027E+01	30	2.064E+01	31	2.101E+01	32	2.137E+01
33	2.173E+01	34	2.209E+01	35	2.244E+01	36	2.278E+01	37	2.313E+01	38	2.347E+01	39	2.380E+01	40	2.414E+01
9	2.905E+01														
1	4.068E+00	2	5.760E+00	3	7.064E+00	4	8.168E+00	5	9.145E+00	6	1.003E+01	7	1.085E+01	8	1.161E+01
9	1.234E+01	10	1.302E+01	11	1.367E+01	12	1.430E+01	13	1.491E+01	14	1.549E+01	15	1.605E+01	16	1.660E+01
17	1.713E+01	18	1.765E+01	19	1.816E+01	20	1.866E+01	21	1.914E+01	22	1.962E+01	23	2.009E+01	24	2.055E+01
25	2.100E+01	26	2.144E+01	27	2.188E+01	28	2.231E+01	29	2.273E+01	30	2.315E+01	31	2.356E+01	32	2.397E+01
33	2.437E+01	34	2.477E+01	35	2.516E+01	36	2.555E+01	37	2.593E+01	38	2.632E+01	39	2.669E+01	40	2.707E+01
10	3.219E+01														
1	4.508E+00	2	6.383E+00	3	7.829E+00	4	9.052E+00	5	1.013E+01	6	1.112E+01	7	1.202E+01	8	1.287E+01
9	1.367E+01	10	1.443E+01	11	1.515E+01	12	1.585E+01	13	1.652E+01	14	1.716E+01	15	1.779E+01	16	1.840E+01
17	1.899E+01	18	1.956E+01	19	2.013E+01	20	2.068E+01	21	2.122E+01	22	2.174E+01	23	2.226E+01	24	2.277E+01
25	2.327E+01	26	2.376E+01	27	2.424E+01	28	2.472E+01	29	2.519E+01	30	2.565E+01	31	2.611E+01	32	2.656E+01
33	2.701E+01	34	2.745E+01	35	2.788E+01	36	2.831E+01	37	2.874E+01	38	2.916E+01	39	2.958E+01	40	2.999E+01
11	3.533E+01														
1	4.948E+00	2	7.007E+00	3	8.593E+00	4	9.936E+00	5	1.112E+01	6	1.220E+01	7	1.320E+01	8	1.413E+01
9	1.501E+01	10	1.584E+01	11	1.663E+01	12	1.740E+01	13	1.813E+01	14	1.884E+01	15	1.953E+01	16	2.019E+01
17	2.084E+01	18	2.148E+01	19	2.209E+01	20	2.270E+01	21	2.329E+01	22	2.387E+01	23	2.443E+01	24	2.499E+01
25	2.554E+01	26	2.608E+01	27	2.661E+01	28	2.713E+01	29	2.765E+01	30	2.816E+01	31	2.866E+01	32	2.915E+01
33	2.964E+01	34	3.013E+01	35	3.061E+01	36	3.108E+01	37	3.155E+01	38	3.201E+01	39	3.247E+01	40	3.292E+01
12	3.847E+01														
1	5.388E+00	2	7.630E+00	3	9.357E+00	4	1.082E+01	5	1.211E+01	6	1.329E+01	7	1.437E+01	8	1.538E+01
9	1.634E+01	10	1.725E+01	11	1.811E+01	12	1.894E+01	13	1.974E+01	14	2.052E+01	15	2.126E+01	16	2.199E+01
17	2.270E+01	18	2.339E+01	19	2.406E+01	20	2.471E+01	21	2.536E+01	22	2.599E+01	23	2.661E+01	24	2.721E+01
25	2.781E+01	26	2.840E+01	27	2.898E+01	28	2.955E+01	29	3.011E+01	30	3.066E+01	31	3.121E+01	32	3.175E+01
33	3.228E+01	34	3.281E+01	35	3.333E+01	36	3.384E+01	37	3.435E+01	38	3.486E+01	39	3.536E+01	40	3.585E+01
13	4.162E+01														
1	5.828E+00	2	8.253E+00	3	1.012E+01	4	1.170E+01	5	1.310E+01	6	1.437E+01	7	1.555E+01	8	1.664E+01
9	1.767E+01	10	1.866E+01	11	1.959E+01	12	2.049E+01	13	2.136E+01	14	2.219E+01	15	2.300E+01	16	2.379E+01
17	2.455E+01	18	2.529E+01	19	2.602E+01	20	2.673E+01	21	2.743E+01	22	2.811E+01	23	2.878E+01	24	2.944E+01

25	3.008E+01	26	3.072E+01	27	3.134E+01	28	3.196E+01	29	3.257E+01	30	3.317E+01	31	3.376E+01	32	3.434E+01				
33	3.492E+01	34	3.549E+01	35	3.605E+01	36	3.661E+01	37	3.716E+01	38	3.770E+01	39	3.824E+01	40	3.878E+01				
14	4.476E+01																		
1	6.268E+00	2	8.876E+00	3	1.089E+01	4	1.259E+01	5	1.409E+01	6	1.546E+01	7	1.672E+01	8	1.790E+01				
9	1.901E+01	10	2.006E+01	11	2.107E+01	12	2.204E+01	13	2.297E+01	14	2.387E+01	15	2.474E+01	16	2.558E+01				
17	2.640E+01	18	2.720E+01	19	2.799E+01	20	2.875E+01	21	2.950E+01	22	3.023E+01	23	3.095E+01	24	3.166E+01				
25	3.235E+01	26	3.304E+01	27	3.371E+01	28	3.437E+01	29	3.503E+01	30	3.567E+01	31	3.630E+01	32	3.693E+01				
33	3.755E+01	34	3.817E+01	35	3.877E+01	36	3.937E+01	37	3.996E+01	38	4.055E+01	39	4.113E+01	40	4.171E+01				
15	4.790E+01																		
1	6.708E+00	2	9.499E+00	3	1.165E+01	4	1.347E+01	5	1.508E+01	6	1.654E+01	7	1.789E+01	8	1.915E+01				
9	2.034E+01	10	2.147E+01	11	2.255E+01	12	2.358E+01	13	2.458E+01	14	2.554E+01	15	2.647E+01	16	2.738E+01				
17	2.826E+01	18	2.911E+01	19	2.995E+01	20	3.077E+01	21	3.157E+01	22	3.236E+01	23	3.313E+01	24	3.388E+01				
25	3.463E+01	26	3.536E+01	27	3.608E+01	28	3.678E+01	29	3.748E+01	30	3.817E+01	31	3.885E+01	32	3.953E+01				
33	4.019E+01	34	4.084E+01	35	4.149E+01	36	4.213E+01	37	4.277E+01	38	4.340E+01	39	4.402E+01	40	4.463E+01				
16	5.104E+01																		
1	7.146E+00	2	1.012E+01	3	1.241E+01	4	1.435E+01	5	1.607E+01	6	1.763E+01	7	1.907E+01	8	2.041E+01				
9	2.168E+01	10	2.288E+01	11	2.403E+01	12	2.513E+01	13	2.619E+01	14	2.722E+01	15	2.821E+01	16	2.917E+01				
17	3.011E+01	18	3.102E+01	19	3.192E+01	20	3.279E+01	21	3.364E+01	22	3.448E+01	23	3.530E+01	24	3.610E+01				
25	3.690E+01	26	3.768E+01	27	3.844E+01	28	3.920E+01	29	3.994E+01	30	4.068E+01	31	4.140E+01	32	4.212E+01				
33	4.282E+01	34	4.352E+01	35	4.421E+01	36	4.490E+01	37	4.557E+01	38	4.624E+01	39	4.691E+01	40	4.756E+01				
17	5.419E+01																		
1	7.588E+00	2	1.075E+01	3	1.318E+01	4	1.524E+01	5	1.706E+01	6	1.871E+01	7	2.024E+01	8	2.167E+01				
9	2.301E+01	10	2.429E+01	11	2.551E+01	12	2.668E+01	13	2.780E+01	14	2.889E+01	15	2.995E+01	16	3.097E+01				
17	3.196E+01	18	3.293E+01	19	3.388E+01	20	3.481E+01	21	3.571E+01	22	3.660E+01	23	3.747E+01	24	3.833E+01				
25	3.917E+01	26	3.999E+01	27	4.081E+01	28	4.161E+01	29	4.240E+01	30	4.318E+01	31	4.395E+01	32	4.471E+01				
33	4.546E+01	34	4.620E+01	35	4.694E+01	36	4.766E+01	37	4.838E+01	38	4.909E+01	39	4.979E+01	40	5.049E+01				
18	5.733E+01																		
1	8.026E+00	2	1.137E+01	3	1.394E+01	4	1.612E+01	5	1.805E+01	6	1.980E+01	7	2.141E+01	8	2.292E+01				
9	2.435E+01	10	2.570E+01	11	2.699E+01	12	2.823E+01	13	2.942E+01	14	3.057E+01	15	3.168E+01	16	3.276E+01				
17	3.382E+01	18	3.484E+01	19	3.585E+01	20	3.682E+01	21	3.778E+01	22	3.872E+01	23	3.964E+01	24	4.055E+01				
25	4.144E+01	26	4.231E+01	27	4.318E+01	28	4.402E+01	29	4.486E+01	30	4.568E+01	31	4.650E+01	32	4.730E+01				
33	4.810E+01	34	4.888E+01	35	4.966E+01	36	5.043E+01	37	5.118E+01	38	5.194E+01	39	5.268E+01	40	5.342E+01				
19	6.047E+01																		
1	8.468E+00	2	1.199E+01	3	1.471E+01	4	1.701E+01	5	1.904E+01	6	2.088E+01	7	2.259E+01	8	2.418E+01				
9	2.568E+01	10	2.711E+01	11	2.847E+01	12	2.977E+01	13	3.103E+01	14	3.224E+01	15	3.342E+01	16	3.456E+01				
17	3.567E+01	18	3.675E+01	19	3.781E+01	20	3.884E+01	21	3.985E+01	22	4.084E+01	23	4.182E+01	24	4.277E+01				
25	4.371E+01	26	4.463E+01	27	4.554E+01	28	4.644E+01	29	4.732E+01	30	4.819E+01	31	4.905E+01	32	4.990E+01				
33	5.073E+01	34	5.156E+01	35	5.238E+01	36	5.319E+01	37	5.399E+01	38	5.478E+01	39	5.557E+01	40	5.635E+01				
20	6.361E+01																		
1	8.908E+00	2	1.261E+01	3	1.547E+01	4	1.789E+01	5	2.003E+01	6	2.197E+01	7	2.376E+01	8	2.544E+01				
9	2.701E+01	10	2.851E+01	11	2.995E+01	12	3.132E+01	13	3.264E+01	14	3.392E+01	15	3.516E+01	16	3.636E+01				
17	3.752E+01	18	3.866E+01	19	3.977E+01	20	4.086E+01	21	4.192E+01	22	4.297E+01	23	4.399E+01	24	4.499E+01				
25	4.598E+01	26	4.695E+01	27	4.791E+01	28	4.885E+01	29	4.978E+01	30	5.069E+01	31	5.160E+01	32	5.249E+01				
33	5.337E+01	34	5.424E+01	35	5.510E+01	36	5.595E+01	37	5.680E+01	38	5.763E+01	39	5.846E+01	40	5.927E+01				
21	6.675E+01																		
1	9.348E+00	2	1.324E+01	3	1.623E+01	4	1.877E+01	5	2.102E+01	6	2.305E+01	7	2.493E+01	8	2.669E+01				
9	2.835E+01	10	2.992E+01	11	3.142E+01	12	3.287E+01	13	3.425E+01	14	3.559E+01	15	3.689E+01	16	3.815E+01				
17	3.938E+01	18	4.057E+01	19	4.174E+01	20	4.288E+01	21	4.400E+01	22	4.509E+01	23	4.616E+01	24	4.722E+01				
25	4.825E+01	26	4.927E+01	27	5.027E+01	28	5.126E+01	29	5.224E+01	30	5.320E+01	31	5.414E+01	32	5.508E+01				
33	5.601E+01	34	5.692E+01	35	5.782E+01	36	5.872E+01	37	5.960E+01	38	6.048E+01	39	6.134E+01	40	6.220E+01				
22	6.990E+01																		
1	9.788E+00	2	1.386E+01	3	1.700E+01	4	1.966E+01	5	2.201E+01	6	2.414E+01	7	2.611E+01	8	2.795E+01				
9	2.968E+01	10	3.133E+01	11	3.290E+01	12	3.441E+01	13	3.587E+01	14	3.727E+01	15	3.863E+01	16	3.995E+01				
17	4.123E+01	18	4.248E+01	19	4.370E+01	20	4.490E+01	21	4.607E+01	22	4.721E+01	23	4.834E+01	24	4.944E+01				
25	5.052E+01	26	5.159E+01	27	5.264E+01	28	5.367E+01	29	5.469E+01	30	5.570E+01	31	5.669E+01	32	5.767E+01				
33	5.864E+01	34	5.960E+01	35	6.054E+01	36	6.148E+01	37	6.241E+01	38	6.332E+01	39	6.423E+01	40	6.513E+01				
23	7.304E+01																		
1	1.023E+01	2	1.446E+01	3	1.776E+01	4	2.054E+01	5	2.299E+01	6	2.522E+01	7	2.728E+01	8	2.920E+01				
9	3.102E+01	10	3.274E+01	11	3.438E+01	12	3.596E+01	13	3.748E+01	14	3.894E+01	15	4.036E+01	16	4.174E+01				
17	4.308E+01	18	4.439E+01	19	4.567E+01	20	4.692E+01	21	4.814E+01	22	4.933E+01	23	5.051E+01	24	5.166E+01				
25	5.279E+01	26	5.391E+01	27	5.501E+01	28	5.609E+01	29	5.715E+01	30	5.820E+01	31	5.924E+01	32	6.027E+01				
33	6.128E+01	34	6.228E+01	35	6.327E+01	36	6.424E+01	37	6.521E+01	38	6.617E+01	39	6.712E+01	40	6.806E+01				
24	7.618E+01																		
1	1.067E+01	2	1.511E+01	3	1.853E+01	4	2.142E+01	5	2.398E+01	6	2.631E+01	7	2.845E+01	8	3.046E+01				
9	3.235E+01	10	3.415E+01	11	3.586E+01	12	3.751E+01	13	3.909E+01	14	4.062E+01	15	4.210E+01	16	4.354E+01				
17	4.494E+01	18	4.630E+01	19	4.763E+01	20	4.893E+01	21	5.021E+01	22	5.146E+01	23	5.268E+01	24	5.388E+01				

25	5.507E+01	26	5.623E+01	27	5.737E+01	28	5.850E+01	29	5.961E+01	30	6.071E+01	31	6.179E+01	32	6.286E+01
33	6.391E+01	34	6.496E+01	35	6.599E+01	36	6.701E+01	37	6.802E+01	38	6.901E+01	39	7.000E+01	40	7.098E+01
25	7.932E+01														
1	1.111E+01	2	1.573E+01	3	1.929E+01	4	2.231E+01	5	2.497E+01	6	2.739E+01	7	2.963E+01	8	3.172E+01
9	3.369E+01	10	3.556E+01	11	3.734E+01	12	3.905E+01	13	4.070E+01	14	4.229E+01	15	4.384E+01	16	4.533E+01
17	4.679E+01	18	4.821E+01	19	4.960E+01	20	5.095E+01	21	5.228E+01	22	5.358E+01	23	5.485E+01	24	5.611E+01
25	5.734E+01	26	5.855E+01	27	5.974E+01	28	6.091E+01	29	6.207E+01	30	6.321E+01	31	6.434E+01	32	6.545E+01
33	6.655E+01	34	6.763E+01	35	6.871E+01	36	6.977E+01	37	7.082E+01	38	7.186E+01	39	7.289E+01	40	7.391E+01
26	8.246E+01														
1	1.155E+01	2	1.635E+01	3	2.006E+01	4	2.319E+01	5	2.596E+01	6	2.848E+01	7	3.080E+01	8	3.297E+01
9	3.502E+01	10	3.696E+01	11	3.882E+01	12	4.060E+01	13	4.231E+01	14	4.397E+01	15	4.557E+01	16	4.713E+01
17	4.864E+01	18	5.012E+01	19	5.156E+01	20	5.297E+01	21	5.435E+01	22	5.570E+01	23	5.703E+01	24	5.833E+01
25	5.961E+01	26	6.087E+01	27	6.210E+01	28	6.333E+01	29	6.453E+01	30	6.572E+01	31	6.689E+01	32	6.804E+01
33	6.918E+01	34	7.031E+01	35	7.143E+01	36	7.253E+01	37	7.363E+01	38	7.471E+01	39	7.578E+01	40	7.684E+01

PILOT INDEX FOR ARGUMENTS FOR M=1

6	5.366E-01	8	7.599E-01	10	9.319E-01	11	1.076E+00	13	1.206E+00	14	1.323E+00	15	1.431E+00	16	1.532E+00
17	1.627E+00	18	1.718E+00	19	1.804E+00	19	1.887E+00	20	1.966E+00	21	2.043E+00	22	2.118E+00	22	2.190E+00
23	2.260E+00	24	2.329E+00	24	2.396E+00	25	2.461E+00	26	2.525E+00	26	2.588E+00	27	2.650E+00	28	2.710E+00
28	2.770E+00	29	2.828E+00	29	2.886E+00	30	2.942E+00	30	2.998E+00	31	3.054E+00	32	3.108E+00	32	3.162E+00
33	3.215E+00	33	3.267E+00	34	3.319E+00	34	3.370E+00	35	3.421E+00	35	3.471E+00	36	3.521E+00	36	3.570E+00

```
   05/04/72   UNIV. OF VIRGINIA SCOPE  3.3 APR 01,72 SUN 296
16.35.56.DUCTN48
16.35.56.DUCTNRM,M2025W,T400,CM61000. THANEDAR 8
16.35.56.D AEROSPACE                              8
16.35.56.       MAP(PART)
16.35.56.       RUN.
16.35.58.LGO
16.36.01.  (RFL - 020700)    CP  000.930 SEC.
16.36.01.                    PP  002.863 SEC.
16.36.01.                    IO  000.342 SEC.
16.36.05.STOP
16.36.05.CP     004.496 SEC.
16.36.05.PP     003.287 SEC.
16.36.05.IO     000.437 SEC.

                DUCTN48  //// END OF LIST ////  0000685 LINES
```

```
000003          PROGRAM SALUTNA(INPUT,OUTPUT,TAPE5=INPUT,TAPE6=OUTPUT)
000003          DIMENSION XS(3),XR(3),P(50),E(26),AM(25),BESLJ0(851),X(6),U(6)
000033          COMMON/FUN/TOPITP,TSTR,ZSTR,EIGEN,BESLJ0
000103          EXTERNAL FCT
000103          READ(5,402)QQ,TP,PI,A,C,(XR(I),I=1,3),TPLS,(XS(I),I=1,3)
000137          RSTR=SQRT((XR(1)**2+XR(2)**2)/A $ ZSTR=XR(3)/A $ TPSTR=C*TP/A
000251          ZTPSTR=ZSTR+TPSTR $ TPLSTR=C*TPLS/A $ JSTRT=ZSTR/TPLSTR
000357          JMAX=ZTPSTR/TPLSTR $ TOPITP=2.*PI/TPSTR $ JMAX1=JMAX-JSTRT
000656          WRITE(6,500)QQ,TP,PI,A,C,TPLS,(XS(I),I=1,3),(XR(I),I=1,3),QQ,RSTR,
                1TPSTR,ZSTR,ZTPSTR,TPLSTR,JMAX,JSTRT
                C     CALCULATION OF THE BESSEL-FOURIER SERIES COEFFICIENTS
000142          READ(5,402)ALPHA00,(E(I),I=1,26)
000166          READ(5,404)(AM(I),I=1,26) $ READ(5,404)(BESLJ0(I),I=1,851)
                C     APPROXIMATE EVALUATION OF DEFINITE INTEGRAL BY CHEBYSHEVS FORMULA
                C     COEFFICIENTS FOR N=6
000202          N=6 $ U(1)=-.8662468 $ U(2)=-.4225187 $ U(3)=-.2663E4
000207          U(4)=.2663354 $ U(5)=.4225187 $ U(6)=.8662468 $ DO 90 J=1,JMAX1
000216     90   P(J)=.0 $ DO 100 M=1,26 $ EIGEN=E(M)
000224          XL=ZSTR $ CALL FUNNY(XL,FUNXL)
000231          PKOM=EIGEN*RSTR $ J=IFIX(10.*PKOM)+1
000235          BESLR=FCT(PKOM,.1*J,BESLJ0(J),BESLJ0(J+1)) $ DO 100 JS=1,JMAX1
                C     LIMITS FOR THE DEFINITE INTEGRAL
000245          AL=XL $ BU=XL+TPLSTR
                C     ARGUMENT VALUES X(I) AND THE CORRESPONDING FUNCTION FCT
000250          FSUM=.0 $ DO 1 I=1,6 $ X(I)=(AL+BU)/2.+(BU-AL)*U(I)/2.
000262          CALL FUNNY(X(I),FXI) $ FSUM=FSUM+FXI
000266     1    CONTINUE $ FSUM=(BU-AL)*FSUM/N $ Y=AM(M)*BESLR*FSUM
000277          P(JS)=P(JS)+Y
000302     100  XL=BU $ DO 110 J=1 ,JMAX1 $ P(J)=P(J)*TOPITP
000313     110  CONTINUE $ WRITE(6,506)(J,P(J),J=1,JMAX1)
                C     FORMATS
000331     402  FORMAT(5E16.8)
000331     404  FORMAT(5E16.8)
000331     500  FORMAT(1H1,20X*TRANSIENT ACOUSTIC FIELD IN CYLINDRICAL DUCT*3(/)
                127X*NORMAL MODE METHOD*3(/)10X*PREASSIGNED CONSTANTS IN DIMENSIONA
                1L FORM(FPS SYSTEM)*//5X*SOURCE STRENGTH FACTOR QQ = *E10.4,3X*SOUR
                2CE PERIOD TP = *E10.4,3X*PI = *E10.4/5X*DUCT RADIUS A = *E10.4,3X
                3*WAVE SPEED C = *E10.4,3X*ELEMENTAL TIME INTERVAL TPLS = *E10.4/
                4*5X*SOURCE CARTESIAN COORDINATES XS(1,2,3) = *3(E10.4,2X)/
                55X*RECEIVER CARTESIAN COORDINATES XR(1,2,3) = *3(E10.4,2X)///
                613X*VARIABLES IN NONDIMENSIONAL FORM*//5X*QQ = *E16.8,2X*RSTR = *
                7E16.8,2X*TPSTR = *E16.8/5X*ZSTR =*E16.8,2X*ZTPSTR =*E16.8,2X*TPLST
                8R = *E16.8,2X*JMAX = *I4,2X*JSTRT = *I4///)
000331     506  FORMAT(20X*PRESSURE VALUES IN THE NONDIMENSIONAL FORM*/
                125X*(NOTE TIME INDEX=INDEX+JSTRT)*/(5(5X,I3,1X,E16.8)))
000331          STOP
000333          END
```

MAY 7, 1972
16.00

```
BALUTMA

PROGRAM LENGTH INCLUDING I/O BUFFERS
005015

FUNCTION ASSIGNMENTS

STATEMENT ASSIGNMENTS
90     -  000214    402    -  000361    404    -  000363    500    -  000365
506    -  000466

BLOCK NAMES AND LENGTHS
FUN    -  001527

VARIABLE ASSIGNMENTS
A      -  000720    AL     -  000744    ALPHA00-  000733    AM     -  000647
BESLJ0 -  000004C01 BESLR  -  000742    BU     -  000745    C      -  000721
E      -  000515    EIGEN  -  000003C01 FSUM   -  000746    FUNXL  -  000740
FXI    -  000747    I      -  000722    J      -  000735    JMAX   -  000731
JMAX1  -  000732    JS     -  000743    JSTRT  -  000730    M      -  000736
N      -  000734    P      -  000533    PI     -  000717    QQ     -  000715
RKON   -  000741    RSTR   -  000724    TOPTTP -  000000C01 TP     -  000716
TPLS   -  000723    TPLSTR -  000727    TPSTR  -  000725    U      -  000707
X      -  000701    XL     -  000737    XP     -  000530    XS     -  000525
Y      -  000750    ZSTR   -  000002C01 ZTPSTR -  000726

START OF CONSTANTS
000335

START OF TEMPORARIES
000504

START OF INDIRECTS
000522

UNUSED COMPILER SPACE
003000
```

```
                FUNCTION FCT(X,XLTR,YPRS,YLTR)
000707          FCT=YLTR-1A.*(XLTR-X)*(YLTR-YPRS)
000014          RETURN $ END
```

```
FCT

SUBPROGRAM LENGTH
000039

FUNCTION ASSIGNMENTS

STATEMENT ASSIGNMENTS

BLOCK NAMES AND LENGTHS

VARIABLE ASSIGNMENTS
FCT    =  000027

START OF CONSTANTS
000017

START OF TEMPORARIES
000021

START OF INDIRECTS
000027

UNUSED COMPILER SPACE
004500
```

```
      SUBROUTINE FUNNY(XI,YI)
000005 COMMON/FUN/TOPITP,TSTR,ZSTR,FIGEN,BESLJ0(851)
000005 XIC=TOPITP*(TSTR-XI) $ XIB=FIGEN*SQRT(XI**2-ZSTR**2)
000017 L=IFIX(10.*XIB)+1 $ XIB1=FCT(XIB,.1*L,BESLJ0(L),BESLJ0(L+1))
000030 YI=COS(XIC)*XIB1
000037 RETURN $ END
```

```
FUNNY

SUBPROGRAM LENGTH
000072

FUNCTION ASSIGNMENTS

STATEMENT ASSIGNMENTS

BLOCK NAMES AND LENGTHS
FUN    -  001527

VARIABLE ASSIGNMENTS
BESLJ0 -  000004C01 EIGEN  -  000003C01 L      -  000070    TOPITP -  000000C01
TSTR   -  000001C01 XIB    -  000067    XI91   -  000071    XIC    -  000066
ZSTP   -  000002C01

START OF CONSTANTS
000041

START OF TEMPORARIES
000044

START OF INDIRECTS
000064

UNUSED COMPILER SPACE
004400
```

```
 CORE MAP  16.29.40.  NORMAL              CONTROL                                    000100    014421    000021    000000
 ---TIME---LOAD MODE --L1--L2-----TYPE--------------USER-------CALL-------------FWA LOAD--LWA LOAD--RLDR_COMN--LENGTH--
          FWA LOADER  014744  FWA TABLES  013056
          -PROGRAM----ADDRESS-          --LABELS0---COMMON--
          BALUTWA     001627                        FUN         000100
          FCT         006644
          FUNNY       006674                        FUN         000100
          SINCOS      006756
          SORT        007065
          SYSTEM      007130                        SCOPE2      007130
          GETTA       010242
          INPUTC      010261
          KODER       010376
          KPAKER      011650
          OUTPTC      012721
          SIO$        013013
          ----UNSATISFIED EXTERNALS-----          REFERENCES
```

TRANSIENT ACOUSTIC FIELD IN CYLINDRICAL DUCT

NORMAL MODE METHOD

PREASSIGNED CONSTANTS IN DIMENSIONAL FORM(FPS SYSTEM)

SOURCE STRENGTH FACTOR QQ = 1.0000E+00 SOURCE PERIOD TP = 2.8000E-03 PI = 3.1416E+00
DUCT RADIUS A = 7.5000E+00 WAVE SPEED C = 1.1000E+03 ELEMENTAL TIME INTERVAL TPLS = 5.0000E-05
SOURCE CARTESIAN COORDINATES XS(1,2,3) = 0. 0. 0.
RECEIVER CARTESIAN COORDINATES XR(1,2,3) = 1.0000E+00 3.0000E+00 1.0000E+01

VARIABLES IN NONDIMENSIONAL FORM

QQ = 1.0000000E+00 RSTR = 4.21637021E-01 TPSTR = 2.93333333E-01
ZSTP = 1.7777777E+00 ZTPSTP = 1.67666667E+00 TPLSTR = 7.33333333E-03 JMAX = 221 JSTRT = 181

PRESSURE VALUES IN THE NONDIMENSIONAL FORM
(NOTE TIME INDEX=INDEX+JSTRT)

1	-5.41356675E-03	2	-1.12714460E-03	3	3.76312713E-05	4	2.35589774E-04	5	4.33991399E-04
6	6.42546727E-04	7	6.47625164E-04	8	3.44003957E-04	9	-1.88581394E-04	10	-7.55[illegible]E-04
11	-1.14268802E-03	12	-1.20330859E-03	13	-8.98261227E-04	14	-2.93262480E-04	15	4.75[illegible]E-04
16	1.24[illegible]E-03	17	1.88722892E-03	18	2.29943761E-03	19	2.45581319E-03	20	2.37865985E-03
21	2.12944935E-03	22	1.77676550E-03	23	1.41161561E-03	24	1.06504521E-03	25	7.67[illegible]E-04
26	5.22929984E-04	27	3.15452753E-04	28	1.26533386E-04	29	-5.93981013E-05	30	-2.45[illegible]E-04
31	-4.21[illegible]E-04	32	-5.63955952E-04	33	-6.43865939E-04	34	-6.33220566E-04	35	-5.17[illegible]E-04
36	-2.78922978E-04	37	5.41161494E-05	38	4.54224914E-04	39	8.77271320E-04	40	1.27[illegible]E-03

```
   05/09/72   UNIV. OF VIRGINIA SCOPE  3.3 APR 81,72 SUN 296
16.29.35.$ALUTEN
16.29.35.$ALUTHA,M2025W,T100,CM41000. THANEDAR R
16.29.35.0 APPOSPACE                                    $
16.29.35.       MAP(PART)
16.29.35.       PUN.
16.29.37.LGO
16.29.40._(PFL = 01450C)    CP   001.023 SEC.
16.29.40.                   PP   002.979 SEC.
16.29.40.                   IO   000.749 SEC.
16.29.43.STOP
16.29.43.CP     004.174 SEC.
16.29.43.PP     003.112 SEC.
16.29.43.IO     000.372 SEC.

                $ALUTEN  //// END OF LIST ////  0000297 LINES
```